The Dissertation Committee for Kimberly Dawn Myers Certifies that this is the approved version of the following dissertation:

The Microbial Ecology and Biogeochemistry of Cyanobacteria in the Arsenic-rich and Inorganic Carbon-limited Geothermal Waters of El Tatio Geyser Field, Chile

Committee:

Philip C. Bennett, Supervisor

Christopher J. Bell

Timothy M. Shanahan

Christopher R. Omelon

Christine V. Hawkes

The Microbial Ecology and Biogeochemistry of Cyanobacteria in the Arsenic-rich and Inorganic Carbon-limited Geothermal Waters of El Tatio Geyser Field, Chile

by

Kimberly Dawn Myers, A. B.

Dissertation

Presented to the Faculty of the Graduate School of

The University of Texas at Austin

in Partial Fulfillment

of the Requirements

for the Degree of

Doctor of Philosophy

The University of Texas at Austin

May 2015

Dedication

To my dearest uncle Brian, who tried very hard to get me to go skiing one morning instead of finishing my application for graduate school. You are loved and missed.

Acknowledgements

This project was supported by the US National Science Foundation grant EAR-0545336, and the Jackson School of Geosciences, the University of Texas at Austin.

I owe an incredible debt of gratitude to many UT faculty members who mentored me throughout my graduate development and dissertation work. I would like to especially thank my committee members for their help and invaluable advice. I would like to thank my advisor, Phil Bennett, for his mentorship and spectacular teaching skills. Special thanks also go to Chris Omelon, Christine Hawkes, and Kevan Moffett for their valued mentorship.

This work would not have been possible without help from the Bennett Lab Group, past and present. Special thanks to A. Engel, M. Franks, J. Santillan, L. Sydow, A. Jones, K. Gilbert, and J. Warden. Thanks also to K. Schmitz and G. Alvarez for excellent help in the lab, and R. Malin for spectacular field assistance. I would also like to thank my friends and family, especially Brianna, Matthew, Adam, Kara, Ross, and Raeanne for endless joy, love, and adventure. To Ed, your love and support has helped more than I can say with words. To my brother, Zach, aunt Sherrie, and my parents, Rich and Diane, for their unconditional love, faith, and support on this journey.

The Microbial Ecology and Biogeochemistry of Cyanobacteria in the Arsenic-rich and Inorganic Carbon-limited Geothermal Waters of El Tatio Geyser Field, Chile

Kimberly Dawn Myers, Ph.D.

The University of Texas at Austin, 2015

Supervisor: Philip C. Bennett

Geothermal settings are some of the best-known analogs for early earth environments and among the best places to investigate the impact of extreme conditions on microbial life. El Tatio Geyser Field (ETGF) is a geothermal setting located at 4,300m in the Atacama Desert region of Chile. Its high-elevation desert position leads to high UV-flux, rapid evaporation, and mineral precipitation. El Tatio geothermal waters also possess extremely limited concentrations of life-essential nutrients, such as dissolved inorganic carbon (DIC as $CO_{2(aq)}$ + HCO_3^-), contain among the highest naturally occurring concentrations of the toxic element arsenic (As as $H_3AsO_3^0$ + $H_XAsO_4^{3-X}$), and are buffered to circumneutral pH by arsenate ($H_2AsO_4^-/HAsO_4^{2-}$; $pK_a \sim 6.9$ at 25°C).

Cyanobacteria were found to be the most important primary producers supporting microbial communities in El Tatio geothermal waters. The objective of this dissertation work was to characterize the role of cyanobacteria in the ETGF microbial ecosystem, and determine the response of cyanobacteria to the high-As and low-DIC conditions present at ETGF. Field observations, geochemical analyses, and next-generation 16S rRNA gene

sequencing approaches were used to determine the geochemical controls on cyanobacterial distribution, the phylogenetic diversity of El Tatio cyanobacteria, and the corresponding microbial community structure at sites with and without cyanobacteria. Four cultured cyanobacterial strains were isolated from ETGF mat material, and experiments were performed to assess the growth and carbon-uptake response of these strains to low DIC, As^{III}, and As^{V}.

As^{III} and temperature negatively controlled the abundance and distribution of cyanobacteria in geothermal outflows throughout ETGF, whereas As^{V} positively influenced these factors. In the laboratory, As^{III} inhibited the growth of cultured strains, while As^{V} stimulated growth. Closed-system experiments showed significantly increased carbon uptake and growth in the presence of As^{V}, due to the ability of arsenate to offset the rapid upward pH shift that often occurs in mats during photosynthesis, thereby maintaining DIC in the preferred forms for cyanobacterial uptake. These results showed that As^{V} plays a positive role in the ETGF microbial ecosystem by increasing the productivity of cyanobacterial mats under low DIC and arsenate-buffered conditions.

Table of Contents

List of Tables xii

List of Figures xiv

Chapter 1: Introduction 1

Geomicrobiology of Hydrothermal Systems 1

Microbial Mat Ecology and the Cyanobacteria 2

El Tatio Geyser Field 5

Geographic Location and Geologic Setting 5

Regional Hydrology 6

Cultural Significance 8

Access and Safety concerns 9

Previous Research at El Tatio 10

Arsenic Geochemistry and Microbiology 11

Mineralogy and Microbiology 12

Primary Production in DIC-limited Microbial Mat Communities 14

Research Questions 15

General Approach 16

Sampling Locations 17

Upper Basin, between Groups U-V and U-VI 18

Middle Basin, Group M-I 19

Middle Basin, Group M-III 21

Dissertation Overview 22

Chapter 1. Tables and Figures 23

References 37

Chapter 2: The Microbial Ecology and Phylogenetic Diversity of Cyanobacteria in the Geothermal Features of El Tatio, Chile 47

Abstract 47

Introduction 48

Methods 50
Sampling and Geochemical Analysis 50
Microbial Biomass Measurements 51
Enrichment Culturing 52
DNA Extraction, Cloning, and Sequencing 52
Phylogenetic Analysis of Clone Library Sequences 54
Pyrosequencing 55
Data Processing and Statistical Analysis 56
Sequence Accessioning 56
Results 56
Environmental Clone Library Description 57
Phylogenetic Assignment of ETGF Cyanobacteria 60
Cyanobacteria Diversity through 454-pyrosequencing 61
Cyanobacteria and Community-level Properties 64
As^{III}-oxidation and Primary Producer Succession 64
Discussion 66
Chapter 2. Tables and Figures 72
References 84

Chapter 3: Morphological, phylogenetic, and physiological characterization of four cyanobacterial isolates from El Tatio, Chile 92

Abstract 92
Introduction 93
Methods 96
Cyanobacteria Culturing and Isolation 96
Microscopy 97
DNA Extraction, Cloning, and Sequencing 97
DNA Analysis and Phylogenetic Reconstruction 98
Genome Sequencing and Analysis 99
Experimental Procedures 99

Culture and Sequence Accessioning 101
Results 101
Morphological Description and Phylogenetic Affiliation 101
Physiological Characterization of Cultures 104
Growth response to temperature 105
Growth response to NaCl 105
Growth in the presence of nutrients 106
Growth in the presence of arsenite and arsenate 107
Carbon Uptake Behavior of T-025 and T-031 109
Genome Description of T-031 110
RuBisCO large subunit 111
Heterocyst differentiation 112
Discussion 112
Taxonomic Assignment of T-031 114
Physiological Comparison of Cultures 117
Chapter 3. Tables and Figures 121
References 138

Chapter 4: Arsenic Plays a Dominant Role in the Ecology of Cyanobacteria in the Geothermal Waters of El Tatio, Chile through its Impact on Carbon Uptake 143

Abstract 143
Introduction 144
Methods 148
Sample Collection and Analysis 148
Environmental DNA Extraction, Pyrosequencing, and Bioinformatics 148
Cyanobacteria Culturing, Isolation, and 16S rRNA Sequencing 149
Growth and DIC-uptake Experiments 150
In Situ Microprofiling of a Cyanobacterial Mat 151
Data Processing and Statistical Analyses 151

Strain and Nucleotide Sequence Deposition 152
Results 152
Geochemistry and Microbiology of Sample Locations 152
Arsenic Oxidation and Cyanobacteria Succession 153
In Situ Microprofile 154
Arsenic Influence on Cyanobacterial Growth 155
Impact of arsenate on DIC uptake and growth 156
Discussion 158
The Impact of Arsenate pH Buffering on Cyanobacteria Carbon Uptake 162
The Significance of CCM-buffering Through Time 165
Chapter 4. Tables and Figures 166
References 171
Chapter 5: Conclusions 181
Appendix A 184
Chapter 1 Supplement 184
Appendix B 185
Chapter 2 Supplement 185
Appendix C 195
Chapter 3 Supplement 195
Appendix D 207
Chapter 4 Supplement 207
References 212
Vita 236

List of Tables

Table 1-1: Unstable parameters from sample locations 23
Table 1-2: Major geochemical data from sample locations 24
Table 2-1: Selected geochemical data from microbial sample collection localities 72
Table 2-2: Abundances (%) of the most common bacterial phyla observed in Sanger sequencing clone libraries. 73
Table 2-3: Summary of 129 cyanobacterial clones derived from ETGF microbial mat samples 75
Table 2-4: Cyanobacterial abundance and diversity measures in pyrosequencing samples 78
Table 2-5: Linear regression analyses examining the influence of environmental parameters on cyanobacteria abundance 79
Table 2-6: Linear regression analyses show the influence of environmental parameters and cyanobacteria abundance on community-level properties 80
Table 3-1: Major geochemical data at culture collection localities 121
Table 3-2: Strain designations, culture collection ID's, and closest hits in BLAST 121
Table 4-1: Physical and chemical characteristics of sample collection localities 166
Table A-1: BG-11 (+N) media used during cyanobacterial culturing and maintenance 184
Table B-1: List of Genbank database strains, their major cyanobacterial Subsection (I-V) 185
(Table B-1, continued) 186
Table B-2: Environmental clone library Phylum level taxonomic diversity 186
Table B-3: Cyanobacterial genus-level OTUs and relative abundances 187

Table B-4: Full-length El Tatio cyanobacteria Genbank sequence database accession numbers. 188
Table B-5: List of database sequences used in *Fischerella* sp. phylogeny 191
Table B-6: Phylum level OTU table 192
Table C-1: 16S rRNA reference sequence accession 195
Table C-2: Growth response of T-025 at all concentrations of As^{III} 197
Table C-3: Growth response of T-025 at all concentrations of As^{V} 198
Table C-4: Growth response of T-039 at all concentrations of As^{III} 199
Table C-5: Growth response of T-039 at all concentrations of As^{V} 200
Table C-6: Growth response of T-045 at all concentrations of As^{III} 201
Table C-7: Growth response of T-045 at all concentrations of As^{V} 202
Table C-8: Strain ID's of organisms used to construct rbcL and hetR trees 205
Table D-1: Growth response of T-031 at all concentrations of As^{III} 210
Table D-2: Growth response of T-031 at all concentrations of As^{V} 211

List of Figures

Figure 1-1: Overview map of the ETGF basins 25
Figure 1-2: Bjerrum and Pourbaix diagrams showing $C_T(As^V)$ = 0.5 mM and 40°C, similar to conditions at ETGF 26
Figure 1-3: ESEM image of ETGF microbial filaments encased in silica 27
Figure 1-4: UV-A, -B, and PAR fluxes at ETGF 28
Figure 1-5: ETGF siliceous sinter containing cyanobacterial filaments 29
Figure 1-6: Map of geothermal feature locations throughout ETGF 30
Figure 1-7: The Great Geyser, 25 m downstream of the outflow 31
Figure 1-8: The Great Geyser, 75 m downstream of the outflow 32
Figure 1-9: Middle Basin Springs 33
Figure 1-10: The first 20 m of the New Transect 34
Figure 1-11: The Pseudomonas spring 35
Figure 1-12: The Group M-III geysers 36
Figure 2-1: Midpoint-rooted phylogenetic reconstruction of 129 cultured and culture-independent cyanobacteria clones from ETGF 74
Figure 2-2: Phylogenetic reconstruction of 129 cyanobacteria clones compared to reference sequences 76
Figure 2-3: Annotated tree of *Fischerella* 16S rRNA sequences 77
Figure 2-4: Comparison of biomass content of microbial mats in high and low-DIC features 81
Figure 2-5: Comparison of the average biomass of low and high cyanobacteria abundance sites 82
Figure 2-6: Total As, As-redox, and temperature along a 75 m section of the Great Geyser transect 83
Figure 3-1: Morphology of isolate T-025 122
Figure 3-2: Morphology of isolate T-031 123
Figure 3-3: Morphology of isolate T-039 124

Figure 3-4: Morphology of isolate T-045 124
Figure 3-5: 16S rRNA phylogenetic reconstruction of cultured isolates and environmental clones 125
Figure 3-6: 16S rRNA phylogenetic reconstruction of cultures T-025, T-039, and T-045, compared to reference sequences 126
Figure 3-7: 16S rRNA phylogeny of culture T-031 and members of cyanobacteria Subsection IV 127
Figure 3-8: Temperature growth curves 128
Figure 3-9: NaCl growth curves 129
Figure 3-10: Nutrient growth curves 130
Figure 3-11: Growth response of culture T-025 to As^{III} and As^{V} 131
Figure 3-12: Growth response of culture T-039 to As^{III} and As^{V} 132
Figure 3-13: Growth response of culture T-045 to As^{III} and As^{V} 133
Figure 3-14: DIC uptake and pH shift behavior of T-031 and T-025 134
Figure 3-15: Overview of the protein coding subsystems in T-031 135
Figure 3-16: Phylogeny of *rbc*L genes from representative Subsection I, III, IV, and V cyanobacteria 136
Figure 3-17: Phylogeny of *hetR* genes from representative Subsection III, IV, and V cyanobacteria 137
Figure 4-1: Trends of As^{III}, As^{V}, species richness, and cyanobacteria abundance along the Great Geyser transect 167
Figure 4-2: In-situ microprofiles of pH and dissolved oxygen 168
Figure 4-3: Growth curves of culture T-031 with As^{III} and As^{V} 169
Figure 4-4: Growth and DIC uptake assays of T-031 170
Figure B-1: Environmental mat sample T-05 189
Figure B-2: Environmental mat sample T075-A and T075-B 190
Figure B-3: Rarefaction curves organized by sample location 193
Figure B-4: A 16-S rRNA phylogenetic analysis of cyanobacteria 194
Figure C-1: Growth curves of cultures amended with nutrients 196

Figure C-2: Morphological comparison of *Synechocystis* sp. UTEX 2470 and T-025, T-039, and T-045 203
Figure C-3: Images of *Nostoc*, *Nodularia*, and *Anabaena* for morphological comparison to T-031 204
Figure C-4: The phylogenetic relationships of cyanobacteria from Subsections I-V inferred from 16S rRNA, *rbcL*, and *hetR* 206
Figure D-1: Cross-section of a cyanobacterially-based microbial mat at site GG-75m 207
Figure D-2: pH shift, DIC-uptake, and growth on T-031 in drift media amended with 0 mM As, 0.5 mM As^{III}, or As^{V}.....208
Figure D-3: pH shift, DIC-uptake, and growth on T-031 in drift media amended with no buffer, PO_4, or As^{V} 209

Chapter 1: Introduction

Geomicrobiology of Hydrothermal Systems

Geomicrobiology involves the study of microorganism-mineral interactions; it includes the study of microbial life in environments such as hot springs, which often exhibit dramatic physical and chemical gradients. Geothermal waters contain a variety of contaminants, such as mercury (Hg), antimony (Sb), selenium (Se), thallium (Tl), boron (B), lithium (Li), and arsenic (As) (Webster-Brown, 2000). Arsenic, a well-documented toxin, is a common constituent in both modern and ancient hydrothermal systems where its concentration often exceeds 0.01 mg/L (Thompson, 1979; Stauffer and Thompson, 1984; Ballantyne and Moore, 1988; Smedley and Kinniburgh, 2002; Webster and Nordstrom, 2003; Landrum, 2007; Landrum et al., 2009). Due to the close relationship between microorganisms and their environment, analyses of microbial genetic diversity along physical and chemical gradients in hot springs can yield insight into the diversity of microorganisms in extreme settings, their tolerance for toxins such as As, adaptations to conditions that we consider "inhospitable", and illuminate the geochemical transformations in which they participate.

Due the low solubility of oxygen at high temperature as well as the deep source of most hydrothermal waters, hot springs tend to be rich in chemically reduced substrates such as Fe^{2+}, H_2S, As^{III}, H_2, and CH_4 that provide steep geochemical gradients for chemoorgano- and chemoautotrophic microorganisms (Baross et al., 1982; Amend and Shock, 2001; Reysenbach et al., 2002; Amend et al., 2003; Budinoff and Hollibaugh,

2008; Kulp et al., 2008; Hoeft et al., 2010; Templeton, 2011). Reduced geochemical substrates are used to perform oxidation-reduction (redox) transformations, the products of which may be used as terminal electron acceptors under low-O_2 or anaerobic conditions (Widdel, 1993; Edwards et al., 2003; Canfield et al., 2006; Bethke et al., 2011).

Hydrothermal fluids were an important contributor to the composition of the early oceans, and hydrothermal systems may have served as a cradle for early biosphere evolution (Wolery and Sleep, 1976; Baross and Hoffman, 1985; Des Marais, 1998; Farmer, 2000; Reysenbach and Cady, 2001; Reysenbach and Shock, 2002). It is hypothesized that the last universal common ancestor (LUCA) of known life was thermophilic due to the deep phylogenetic position of the phylum Aquificae and the prevalence of hyperthermophiles in Domains Bacteria and Archaea (Woese, 1987; Deckert et al., 1998). Whether or not LUCA was thermophilic, modern terrestrial and marine geothermal vents are important windows into the biogeochemical processes hypothesized to play a major role in the origin and early evolution of life (Reysenbach et al., 2000; Reysenbach and Shock, 2002); modern terrestrial hot springs are among the only modern environments that resemble these ancient systems (Farmer, 2000; Rasmussen, 2000; Reysenbach and Cady, 2001).

Microbial Mat Ecology and the Cyanobacteria

Microbial mats provide a favorable habitat for microorganisms in extreme environments such as hot springs (Paerl et al., 2000). Extracellular polymeric saccharides (EPS) secreted by microorganisms provide protection from high temperature, prevent the

diffusion of toxic chemical constituents, and serve as a sticky surface for capturing nutrients, mineral electron sources, and particles that provide shielding from direct sunlight (Rambler and Margulis, 1980; Walter, 1983; Garcia-Pichel and Castenholz, 1991; Garcia-Pichel, 1998). Microbial mats are present in geothermal waters, even at high temperatures (Brock, 1978; Ward et al., 2012). Temperatures above 45°C prohibit grazing by eukaryotes, leading to the development of thick, often stratified mats; as a result geothermal environments are one of few modern environments where well-developed mats are found (Ward and Castenholz, 2000; Ward and Cohan, 2005; Ward et al., 2012).

Microbial mats in hot springs are often composed of vertically stratified consortia of photoautotrophs, chemoautotrophs, and heterotrophs, arranged both to take advantage of redox gradients and promote the exchange of metabolites such as organic carbon (Paerl et al., 2000; Stal, 2012). Photo- and chemoautotrophs are responsible for the enzymatic fixation and reduction of CO_2 into bioavailable organic carbon compounds during a process known as primary production. Primary production is often the only source of organic carbon for heterotrophic microorganisms within microbial mats, and it is therefore an essential process for the successful colonization, growth, and maintenance of microbial mat communities in hot springs (Stal et al., 1985; Stal, 2012).

Microbial mats in a variety of ecosystems are supported by way of primary production by oxygenic photosynthetic cyanobacteria (Paerl et al., 2000; Badger et al., 2006). Cyanobacteria exhibit a large amount of phylogenetic diversity in a range of extreme environments, from polar deserts to hot springs, and are among the most

important primary producers in terrestrial aquatic environments and the oceans (Whitton and Potts, 2000; Badger et al., 2006; Whitton, 2012). Though the basic building blocks of their existence are simple, cyanobacteria have acquired a diverse range of physiological strategies to deal with environmental stressors and tolerate fluctuations in the supply of water, light, and CO_2 over short to geologic timescales (Paerl et al., 2000; Badger et al., 2006). CO_2 is diffusion limited both in water and the interstitial water within microbial mats; however, all known cyanobacteria possess a CO_2-concentrating mechanism (CCM) that allows them to acclimate to limited dissolved inorganic carbon (DIC) concentrations (Giordano et al., 2005; Badger et al., 2006). In-depth reviews on the incredible physiological plasticity expressed by modern cyanobacteria and the CCM can be found elsewhere (Badger et al., 2006; Ghalambor et al., 2007).

This dissertation builds on the previous body of knowledge related to the ecology of hot spring cyanobacteria, As-biogeochemistry from previously studied geothermal areas, and As-biogeochemistry at the El Tatio Geyser Field, the field site on which my dissertation work is focused. Previous work on As at El Tatio and at other geothermal systems focused on enzymatic As transformations, the specific organisms that performed them, or on As resistance and detoxification (Cervantes et al., 1994; Gihring and Banfield, 2001; Mukhopadhyay et al., 2002; Lopez-Maury et al., 2003; Oremland and Stolz, 2003; Oremland et al., 2004; Paez-Espino et al., 2009; Bhattacharya and Pal, 2010). My work expands this view by linking As to primary production by cyanobacteria, a relationship that has not been examined prior to this work.

EL TATIO GEYSER FIELD

Geographic Location and Geologic Setting

A geochemically and geographically unique location for assessing the ecological distribution, diversity, and primary production by cyanobacteria is found in the El Tatio Geyser Field (ETGF). ETGF is a 10 km^2 geothermal field located in the Antofagasta Province, in the northern Atacama Desert region of Chile. ETGF is situated among mountain peaks at high elevation (4,320 m) in the Andean Altiplano Plateau (high plains) at 22°S latitude and 68°W longitude (Glennon and Pfaff, 2003). The geothermal field is located approximately 10 km from the Chile-Bolivia border; it is delimited on the east by a 5,500 m high volcanic chain, and on the west by the Atacama Desert basin (Lahsen and Trujillo, 1976; Lahsen, 1988).

The northern Chilean altiplano is a geologically active area, with modern occurrences of both volcanic and geothermal activity. El Tatio is one of several geothermal fields in the Tarapaca and Antofagasta regions of northern Chile (Tassi et al., 2010); it lies just west of the Altiplano-Puña Volcanic Complex (APVC), a large volcanic zone that extends slightly north and much farther south of ETGF (de Silva et al., 1994). Extensive volcanism produced regionally extensive crystal-rich dacitic ignimbrites with volumes >1000 km^3. Diapiric magmatic uprise through regional right-lateral strike-slip faults led to massive ignimbrite eruptions and subsequent formation of the calderas that comprise the APVC (de Silva, 1989). The large-scale silicic magmatism in this region is attributed to crustal thickening and heat input from subduction-related magmas. The absence of mafic volcanism led to the hypothesis that ignimbrites originated from large-

scale crustal melting that occurred when subduction-related basaltic magmas invaded the crust (de Silva, 1989).

The tectonic environment of the central Andes is dominantly compressive; however, the area hosting the APVC is characterized by neutral or extensional stresses that generated horst-graben topography. Tectonic movement during the Quaternary and Holocene produced additional normal faulting (de Silva, 1989). Thermal features are located on a north-south-oriented sunken block called the Tatio graben, and hydrothermally altered soils are present throughout the regional linear graben extending north and south of El Tatio (Glennon and Pfaff, 2003).

Regional Hydrology

El Tatio is positioned at low latitude and high elevation in the Atacama Desert, resulting in a hyper-arid climate with high evaporative flux and elevated UV-radiation relative to environments near sea level. The Atacama Desert is one of Earth's driest places. It is devoid of vegetation in many areas; however, shrubby grasses and small trees grow in wetter areas of the geyser basins. The geothermal basins at ETGF are covered in white and gray siliceous mineral sinter that precipitates from silica-supersaturated geothermal waters during evaporation.

Despite its desert location significant geothermally-driven hydrologic activity occurs at ETGF. The source of hydrothermal water is meteoric water that falls as rain in the Bolivian mountains, roughly 15-20 km east-southeast of El Tatio; the groundwater travels at an estimated rate of 1 km/year (Cusicanqui et al., 1976). On its journey west the meteoric water is heated by the Pastos Grandes and Cerro Gaucha caldera systems, part

of the APVC, located just east of ETGF (Healy and Hochstein, 1973; Lahsen and Trujillo, 1976). Sol de Mañana geothermal field lies just across the international border from El Tatio in Bolivia, and may have the same source waters as ETGF (Glennon and Pfaff, 2003). Sol de Mañana is slightly closer to the thermal source, and ETGF is at lower elevation and in a distal position (Healy and Hochstein, 1973; Lahsen and Trujillo, 1976).

The source waters are heated to 224°C in the subsurface (Giggenbach, 1978; Fournier and Potter, 1982); upon reaching El Tatio the hot water is confined to two major aquifers that are overlain by impermeable formations. The lower aquifer consists of the Puripica and Salado ignimbrites; the upper aquifer is contained within the Tucle dacite and is overlain by the impermeable Tatio ignimbrite. Geothermal waters discharge at 86.3°C, which is the local boiling point of water at the elevation of ETGF (Glennon and Pfaff, 2003). Discharge eruption heights are small compared to other geothermal sites such as Yellowstone National Park (YNP); ETGF springs attain an average height of 69 centimeters and true geyser eruptions reach an average of 76 centimeters. The causes behind the low height are unknown, but could be a function of the plumbing system, heat source, elevation, or a combination of these and other factors (Glennon and Pfaff, 2003).

With over 80 active geysers, El Tatio is the largest geyser field in the Southern Hemisphere, and the third largest geyser field in the world after YNP and Dolina Geizerov, Russia; noted geothermal features include at least 80 true geysers, 30 perpetual spouters, as well as mudpots, warm springs, solfataras, and fumaroles (Glennon and Pfaff, 2003). There are three geyser basins within ETGF, each with a different character (Figure 1-1). The Upper Geyser Basin (UB) exhibits the highest number of geothermal

features, many with low discharge and well-developed silica sinter terraces. The Middle Geyser Basin (MB) is a flat sinter plain with deep pools and fountain-type eruptions, and individual features often have higher discharge than UB features. The Group M-III features consist of springs and mudpots, and are located ~2 km east of the main MB. The Lower Geyser Basin, also known as the River Group, lies along the banks of the Río Salado, the headwaters of which are formed by geyser effluent from all three basins.

The Río Salado is a major tributary of the Río Loa, which flows west to the Pacific Ocean. Discharge from Río Salado varies seasonally, from 250 to 500 liters/second (Lahsen and Trujillo, 1976). Due to low precipitation in the desert, almost the entire Río Salado outflow originates from the ETGF drainage basin. The Río Salado and Río Loa are a major water source for the entire Antofagasta Province, and the geochemistry and mineralization of ETGF hydrothermal water has major implications for the drinking water supply of the entire region.

Cultural Significance

The name El Tatio comes from "el tata", which roughly translates to "the weeping grandfather" (Glennon and Pfaff, 2003). El Tatio's geysers are a valuable cultural resource for indigenous Chileans. The geysers are also a popular tourist attraction in the region; tours leave from San Pedro de Atacama at 4:30 am daily to allow visitors to see the geysers at dawn. The steam is most dramatic in the early morning due to colder temperatures and low wind velocity; the intense sunlight later in the day masks the effect.

Two conflicting points of view surround the cultural and economic importance of El Tatio. Members of local villages value its cultural significance and its importance for

ecotourism, and adherents to this view are focused on the preservation and protection of the site. The copper mining industry in northern Chile relies on the transport of fossil fuels from southern Chile; geothermal energy production at ETGF has been explored as an alternative power source for the region (Lahsen, 1988). There is concern that geothermal drilling and exploration may negatively impact the ecotourism value of the geysers. These debates are ongoing, and the outcome may impact the preservation of, and access to, the site in future years.

Access and Safety concerns

Although many tourists see the El Tatio geysers by way of tours from San Pedro de Atacama, its location is remote. El Tatio is 90 km northeast of San Pedro de Atacama (elevation 2,440 m; via B-245), and a 141 km drive east from Calama (elevation 2,250 m; via Rte. 21 to B-169, B-165, B-159, and B-245.) The nearest airport is in Calama; the most convenient place to stay during work is the village of San Pedro de Atacama. The geographic isolation of El Tatio necessitates extra precautions during transportation and fieldwork. There is a welcome center with public restrooms when you first arrive at El Tatio; however, no food, fuel, or potable water is available. No cell service is available at the site or surrounding area, and the nearest medical facilities will be at least a 1.5-hour drive away in San Pedro de Atacama, or 2 hours away in Calama.

No permitting is currently required to conduct sampling at the geothermal site, in contrast to the rigorous procedures required prior to sampling at Yellowstone National Park. It is considered rude to show up unannounced; advanced notice by way of letter and

email and being prepared to explain your work in both Spanish and English are highly recommended.

Previous Research at El Tatio

In the 1960s and 1970s regional geology and geochemistry studies were conducted in order to assess El Tatio's potential for geothermal electricity production; two major studies were those by Lahsen and Trujillo (1976), and Cusquicanqui et al. (1976). A large-scale inventory and description of the Tatio geysers was conducted by Glennon and Pfaff (2003); they assessed about 25% of the hydrothermal field and assigned names to individual features based on those previously mapped by Trujillo et al. (1969).

Numerous authors focused previously on the geochemical composition, isotope geochemistry, and rock/water interactions at ETGF (Ellis and Mahon, 1967; Giggenbach, 1978; Cortecci et al., 2005; Landrum, 2007; Landrum et al., 2009; Tassi et al., 2010). Others focused on silica sinter precipitation, detailed sinter mineralogy, and the morphology of sinter deposits (Jones and Renaut, 1997; Rodgers et al., 2002; Garcia-Valles et al., 2008).

Two geochemically distinct types of springs are found throughout the geyser field; chloride-rich and sulfate-rich (Cortecci et al., 2005). Oxygen and hydrogen isotopic analyses show that the composition of chloride-rich springs is controlled by magma degassing and rock-water interactions and that sulfate-rich springs are fed by steam-heated shallow meteoric water. The magmatically-derived Cl^--type waters are rich in As, B, Cs, and Li. $^{87}Sr/^{86}Sr$ ratios are uniform, consistent with values for typical Andean

central volcanic zone dacites (Cortecci et al., 2005). Sulfate-rich springs are rare; the overwhelming majority of discharging waters are moderate-salinity $Na^{+}Cl^{-}$ type waters (Tassi et al., 2010), including the waters sampled during previous work on the geomicrobiology and As-geochemistry at ETGF and the waters I sampled during my field work (Phoenix et al., 2006; Landrum, 2007; Landrum et al., 2009; Franks, 2012; Engel et al., 2013).

Arsenic Geochemistry and Microbiology

Previous authors characterized the unique As geochemistry of the waters at ETGF and the unusual emergent properties of As biogeochemistry in the system. ETGF waters contain some of the world's highest naturally occurring As and antimony (Sb) concentrations found in a surface water (Webster-Brown, 2000; Webster and Nordstrom, 2003; Landrum, 2007; Landrum et al., 2009). The exact source of As at ETGF is unknown but As is known to be especially susceptible to host-rock leaching (Ellis and Mahon, 1964, 1967); thus the high As content is probably due to leaching of volcanic host rocks by 250°C fluids as they are forced through faults toward the surface. In addition to high As, most waters have extremely low DIC found as $H_2CO_3^{*}$ and HCO_3^{-}, with almost no CO_3^{2-} (Landrum, 2007; Landrum et al., 2009; Franks, 2012).

The combination of high As and low DIC has major implications for both the geochemical dynamics of ETGF waters and the microbial ecosystem that inhabits the geothermal waters. The pH of waters at ETGF is circumneutral; it ranges from 6.8 at most discharge points and increases to ~7.1 as waters cool (Landrum, 2007; Landrum et al., 2009). Most natural waters are buffered by the carbonate system, but DIC is too low

at ETGF to contribute to pH buffering; rather, the water is strongly buffered at the pKa_2 of arsenate (Eq. 1-1, Figure 1-2) (Landrum, 2007; Landrum et al., 2009):

$$H_2AsO_4^-/HAsO_4^{2-} \quad pKa=6.94 \text{ @ } 25°C \qquad \text{(Eq. 1-1)}$$

A model ETGF geothermal feature and discharge apron known as the Great Geyser (GG) was studied previously with respect to As-biogeochemistry. Waters emerge reduced, with a 4:1 ratio of arsenite (As^{III}) to arsenate (As^{V}). Though emerging waters are found at a pH of ~6.85, close to the pKa_2 of As^{V} (Eq. 1-1), the water has low buffering capacity until the As^{III}:As^{V} ratio decreases downstream (Engel et al., 2013; Landrum et al., 2009). Within-stream As^{III}-oxidation was found to be due to microbial activity (Landrum, 2007; Landrum et al., 2009; Engel et al., 2013). DNA sequencing showed the presence of arsenite oxidase genes (*aio*A) in the GG stream, particularly genes homologous to *aio*A genes in *Chloroflexus aurantiacus* and various proteobacteria. This evidence suggests that *Chloroflexus* and proteobacteria are responsible for As^{III}-oxidation; the presence of distinct amino acid residues compared to previously sequenced *aio*A genes from other geothermal sites implies that these genes may code for novel functions (Engel et al., 2013).

Mineralogy and Microbiology

El Tatio has been identified as an analog environment for UV-inundated early Earth environments, where low atmospheric O_2 precluded UV-protective ozone formation (Berkner and Marshall, 1965; Walker et al., 1983; Kasting, 1987; Pierson et al., 1993). Fossil record examples of cyanobacteria cells and stromatolites formed by cyanobacteria 2.4 to 2.7 billion-years-ago (Ga) existed in shallow-water environments or

exposed subaerial settings that would have been subjected to high UV irradiation (Cloud, 1965; Awramik et al., 1983; Lowe, 1983) unless UV-screening mechanisms were employed (Rambler and Margulis, 1980; Walter, 1983; Garcia-Pichel and Castenholz, 1991; Phoenix et al., 2006). In the Archean phototrophic life may have existed in a protective mineral environment that can attenuate UV while still allowing photosynthetically active radiation (PAR) to penetrate (Phoenix et al., 2006).

El Tatio waters emerge supersaturated with respect to amorphous silica, leading to the precipitation of various forms of siliceous sinter known as geyserite (Rodgers et al., 2002; Fernandez-Turiel et al., 2005; Phoenix et al., 2006; Landrum, 2007; Garcia-Valles et al., 2008; Landrum et al., 2009). Virtually all microorganisms at ETGF are coated in silica; some microbial filaments resemble silica gels more than microbial biomass (Figure 1-4) (Jones and Renaut, 1997; Landrum et al., 2009). Cyanobacterial filaments were found to occupy the top one cm of porous siliceous sinter at the Terrace Geyser, a sinter terrace in the Upper Basin (Figure 1-5) (Glennon and Pfaff, 2003; Phoenix et al., 2006). ETGF cyanobacteria are encased in rapidly precipitating silica, which can shield them from UV-A, -B, and –C, while PAR can still penetrate; this combination provides a protected niche for oxygenic photosynthesis to occur (Phoenix et al., 2006).

The El Tatio geothermal system is unlike previously studied localities. The combination of low DIC and circumneutral pH conditions is unusual; low-DIC systems are typically acidic, such as Norris Geyser Basin at YNP which has low DIC similar to ETGF, but waters are between pH 2 and 3 in most Norris springs due to a lack of pH buffering capacity (Fournier, 2005; Inskeep and McDermott, 2005; Nordstrom et al.,

2005). Other arsenic-bearing systems at YNP also contain high sulfur and DIC, which leads to different microbial communities and different modes of As transformation than are expected to occur in the low-sulfur and low-DIC waters at ETGF (Connon et al., 2008; Hamamura et al., 2009).

Primary Production in DIC-limited Microbial Mat Communities

El Tatio Geyser field is an extreme environment for microorganisms due to its position at high elevation within one of the driest deserts in the world. Several key conditions at ETGF, when combined, pose an exceptional challenge for microbial life, yet the microorganisms living there may utilize unique strategies for handling environmental stress. The key conditions that I consider are high As in the form of As^{III} and As^{V}, aqueous pH buffering by arsenate, and low DIC.

Low DIC is a major stressor on microbial populations at the site, as shown by low biomass, dull coloration, and restricted microbial mat distribution in low-DIC streams; in contrast, high-DIC geothermal features contain thick and colorful mats. A major hypothesis of this dissertation is that low DIC limits the growth and long-term maintenance of microbial communities at ETGF, especially in As^{III}-rich stream regions where the lowest amounts of biomass are observed. Arsenate pH-buffering, however, improves the conditions for oxygenic photosynthetic cyanobacteria living within DIC-limited microbial mats. Enzymes used during carbon assimilation under low-DIC conditions increase the pH of the surrounding medium, which shifts the inorganic carbon speciation towards CO_3^{2-}, which is unavailable to cyanobacteria (Badger et al., 2006). Arsenate, a strong pH buffer, provides cyanobacteria with an escape from carbon

limitation induced by upward pH shifts; in this dissertation I show that this is a major reason why cyanobacteria are found only in the presence of As^V in low-DIC waters at ETGF.

The overarching goal of this work was to analyze cyanobacteria distribution at El Tatio, and to assess the role of low DIC and arsenate buffering in determining their distribution and ecological interactions. I also consider the phylogenetic diversity of cyanobacteria and compare their distribution to that of other primary producers that are important in this system, such as *Chloroflexus* sp., which performs anoxygenic photosynthesis.

Research Questions

My work is an investigation of the diversity, biogeochemistry, and microbial ecology of cyanobacteria in low-DIC geothermal streams at ETGF. Thermophilic cyanobacteria are important primary producers in geothermal environments, including El Tatio. The major upper temperature boundary on their distribution is 74°C, the upper temperature limit for photosynthesis, and they are found at temperatures as low as 20-25°C where photosynthetic eukaryotes tend to predominate (Brock, 1978; Ward et al., 2012). Within this range of temperatures, the secondary and tertiary factors that govern their distribution are less well understood, vary from system to system, and were unknown at ETGF prior to my work. The questions are:

1. What are the major physical and geochemical controls on the distribution of cyanobacteria at ETGF?

2. Are novel cyanobacterial taxa present at ETGF, and are cyanobacteria that are present at other geothermal locations also present at ETGF?
3. Is primary production by microorganisms, including cyanobacteria, inhibited by carbon limitation in low DIC springs?
4. Are cultured organisms responding to the same geochemical controls shown to influence the distribution and abundance of cyanobacteria in the field?
5. Does arsenate buffering have an impact on cyanobacteria DIC-uptake under low DIC conditions?

General Approach

In order to address these questions, three field seasons were conducted at ETGF; June 2009, May 2011, and June 2012. Water samples were collected and corresponding microbial mat samples were collected using sterile techniques. Aqueous constituents were analyzed in the Microbial Geochemistry and Q-ICP-MS Laboratories [The University of Texas at Austin (UT Austin)]. Microbial mat samples were designated for DNA, microscopy, and loss-on-ignition biomass measurement. Culturing, experimentation using cultured organisms, and clone library preparation was performed in the Microbial Geochemistry Laboratory [UT Austin]. Capillary-based sequencing was performed at the Institute of Cellular and Molecular Biology (ICMB) Core Facility [UT Austin]. Roche 454 pyrosequencing was performed at MrDNA Laboratories [Shallowater, TX].

The approaches used in this work were geared towards an interdisciplinary understanding of the questions highlighted in this dissertation. Due to the close coupling

of microorganisms and their chemical environments, geochemical analyses and classic microbial culturing techniques were used in conjunction with DNA sequencing. An in-depth assessment of microbial diversity was performed using next-generation DNA sequencing. Phylogenetic trees were made using full-length 16S rRNA genes generated by Sanger sequencing, in order to reliably place the phylogenetic diversity of ETGF sequences into the context of previously identified sequences. Four novel cyanobacterial strains were isolated from El Tatio mats in BG-11(+N) media (Appendix A). Those organisms were described, and growth responses to nutrient limitation, As, salinity, and temperature were assessed.

Sampling Locations

The sampling locations investigated during my dissertation work are described below. Numerous water and microbial mat samples were obtained in order to characterize the geochemical and microbial nature of each geothermal sampling location. Measured parameters and geochemistry from all sites within these sampling locations are listed in Tables 1-1 and 1-2. A map of sampling locations is shown in Figure 1-6. Geothermal basin nomenclature follows previous definitions set forth by Glennon and Pfaff (2003). Geothermal features refer to a discrete discharge point such as a vent, spring, geyser, or hot pool and the stream or runoff aprons that emerge from them. Water and microbial mat sampling was performed within the features described here, and where indicated multiple water and microbial samples were collected at different points within the same feature.

Individual water samples are coded by 'TAT' followed by collection year and include a unique water sample ID that represents a single water-sampling event (e.g.

TAT09-001, TAT11-001, and TAT12-001). Microbial mat samples that were collected at the same location as water samples are abbreviated using T- followed by the last two numbers of the unique water sample ID (e.g. T-31, T-34, and T-45 correspond to TAT09-031, -034, and -045, respectively). Cyanobacteria cultures are abbreviated by T- followed by 0 and the last two unique numbers of the location where they originate (e.g. T-025, originated at TAT09-025).

Upper Basin, between Groups U-V and U-VI

During the 2009 field season water and microbial mat samples were collected within a single geothermal feature in the UB. This feature was nicknamed the "Vicuña stream" due to a herd of either vicuña or guanacos that stood nearby during the sampling event. Five water samples and two microbial mat samples were collected at a series of points along a runoff stream formed by the mixing of a cool, low-DIC runoff stream (25°C), and a high-DIC stream originating at a hot, intermittently spouting vent (75°C).

Water was sampled at the spouting vent (TAT09-030), at the mixing zone of the cool low-DIC stream and the hot high-DIC vent (TAT09-031), at two points 2 m (TAT09-032) and 10 m (TAT09-033) downstream of the mixing zone, and within a high-DIC pool connected to the stream (TAT09-034) that likely had other geothermal inputs evidenced by a temperature spike. Temperature and pH measurements and DIC and As-speciation data were obtained at each location; however, full suites of analyses (major cations and anions) were only done for sample sites TAT09-032 and TAT09-034 (Tables 1-1 and 1-2). Pyrosequencing (Roche 454) data was obtained from microbial mat samples at TAT09-031 (microbial sample T-31) and TAT09-034 (microbial sample T-34). A

cyanobacterial culture organism was isolated from T-31, and is referred to as strain T-031.

Middle Basin, Group M-I

The Middle Basin (MB) is a 400 m^2 flat sinter area with about 10 true geysers, bounded on the east by a major upstream branch of the Rio Salado, and on the west by a low hill (Glennon and Pfaff, 2003). Waters in the MB are more reducing than UB or LB waters, and many discharge with more As^{III} than As^{V} (Landrum et al., 2009; Landrum, 2007). Four features were examined in the MB: the Great Geyser (GG), the Middle Basin Springs (MBS), the New Transect (NT), and the Aquificales/Pseudomonas spring (PS) (Tables 1-1 and 1-2).

The Great Geyser was the major focus of this study; extensive geochemical and microbiological sampling was conducted over the course of three field seasons. The GG is a low-DIC stream consisting of a long discharge apron with distinct geochemical facies, a steadily decreasing temperature profile, and clear microbial mat succession, making it an ideal location to study the impact of As-redox on microorganisms (Figures 1-7 and 1-8). The GG flows east-northeast for 110 m until it intersects the Group M-III discharge stream, about 20 m downstream from the MBS springs (Figure 1-9). As-geochemistry and microbial As^{III}-oxidation in this stream was described by Landrum (2007), Landrum et al. (2009), and Engel et al. (2013). Geochemical samples were collected along the discharge apron during each field season; however, my dissertation work focuses on GG results from my 2011 field season, during which the most extensive

sampling at 5 to 10 m intervals was conducted along 90 m of the transect (TAT11-001 to -012; Tables 1-1 and 1-2).

The New Transect appears to correspond to feature T92 (Glennon and Pfaff, 2003). The NT is another low-DIC stream that lies ~25 m northwest of the GG source pool, close to the low hill bounding the western portion of the MB (Figure 1-10). Geochemical sampling was done along this transect for comparison with the GG (TAT11-060 to -064; Tables 1-1 and 1-2). The NT is also a low-DIC transect with similar gradients in temperature and conductivity, and exhibits some similarities to the GG transect in microbial succession along the discharge apron. Characteristics of the NT changed visibly between 2009 and 2012. In 2009 the NT had a discrete source and an apparently higher discharge; however, during the 2011 and 2012 field seasons discharge decreased slightly, while newer, smaller springs cropped up within 20 meters of the source. Cultured organism T-039 originates from TAT09-039. Microbial samples NT-1, NT-2, and NT-3 were collected along this stream in 2012.

The Middle Basin Springs (MBS) were discussed in detail by Franks (2012). The MBS are a pair of high-DIC springs that flow into a 1 m-wide runoff stream originating in Group M-III (Figure 1-9); this stream later forms the major upstream branch of the Rio Salado and forms the eastern boundary of the main portion of the Middle Basin (Figure 1-6). Samples were collected here during all three field seasons. The most complete sampling was conducted in 2011 (TAT11-053 to -057; Tables 1-1 and 1-2); the samples corresponding to microbial samples MBS-1 and MBS-2 correspond to TAT12-040, and -

041, respectively (Tables 1-1 and 1-2, Figure 1-9). TAT09-025 corresponds to cultured organism T-025.

The Aquificales Stream was named for its pink microbial filaments resembling *Aquificales* streamers (Figure 1-11), and is believed to correspond to feature T90 (Glennon and Pfaff, 2003). These streamers were found to be composed almost entirely of *Pseudomonas* sp. through 454 pyrosequencing. This feature will not be considered further, but geochemical data can be found in Tables 1-1 and 1-2.

Middle Basin, Group M-III

Group M-III is located 2 km southeast of the main MB, but is still considered part of the MB. Group M-III is a thermal marsh with many mud pots and fumaroles, low As, and lower pH than the main MB group (Figure 1-12). Only one visit was made to these springs in 2009. This area contains some low-TDS springs; a 54°C high-DIC spring was sampled (TAT09-045). This spring was chosen due to its bright-green mats, which appeared to be different from mats in the GG, MBS, and NT features. The access road was blocked in 2011 and 2012, so no follow-up work was conducted here. Temperature, pH, and DIC were measured at both sample sites, but cations and anions were only measured at TAT09-045. Sanger sequencing and 454 pyrosequencing data were obtained from TAT09-045 (sample T-45). A unicellular cyanobacterium was cultured from mat sample T-45 (culture T-045).

Dissertation Overview

Chapter 2, "The Microbial Ecology and Phylogenetic Diversity of Cyanobacteria in the Geothermal Features of El Tatio, Chile" adds to the known distribution, diversity and ecology of geothermal cyanobacteria. Full-length 16S rRNA sequences from ETGF are compared to the known diversity of cyanobacteria. Chapter 3, "Morphological, phylogenetic, and physiological characterization of four cyanobacteria isolates from El Tatio, Chile" describes four cultured organisms that were obtained from microbial mat samples at sampling sites TAT09-025, TAT09-031, TAT09-039, and TAT09-045 (Figure 1-6). The morphology and physiology of these cyanobacterial strains are described. Chapter 4, "The Role of Arsenic During Inorganic Carbon Uptake and Primary Production by Cyanobacteria" focuses on the impact of arsenate on cyanobacterial carbon-uptake in the DIC-limited geothermal waters of El Tatio.

No previous authors have examined the impact of As on hot-spring cyanobacteria, or observed the effect of gradients of As^{III} and As^{V} on cyanobacterial distribution. The major outcome of this work is that As^{V} is indirectly beneficial to the ecosystem function within low-DIC streams at ETGF through the carbon uptake activity of cyanobacteria.

CHAPTER 1. TABLES AND FIGURES

Table 1-1: Unstable parameters from sample locations. Concentrations are expressed in μmol/L, conductivity is in mS, T°C. Missing data are indicated by a '-'. Sulfide and iron were measured using Chemetrics on a V2000 spectrophotometer.

Sample ID	Feature	Basin	T	pH	Cond	H_2S	$[Fe^{2+}]$
TAT09-025	MBS	M	66	6.0	12.0	25.8	53.8
TAT09-030	Vicuna	U	75	6.74	11.8	-	0.3
TAT09-031	Vicuna	U	26	7.11	14.3	-	-
TAT09-032	Vicuna	U	51	6.82	13.3	-	49.4
TAT09-033	Vicuna	U	52	6.78	-	-	-
TAT09-034	Vicuna	U	58	6.86	11.6	-	39.0
TAT09-039	NT	M	31	6.9	18.8	-	-
TAT09-045	Algae	M-III	54	6.0	0.5	-	-
TAT11-001	GG	M	77	6.7	18.6	15.9	-
TAT11-002	GG	M	74	6.85	-	-	-
TAT11-003	GG	M	72	6.93	19.1	21.4	-
TAT11-004	GG	M	65	6.93	-	-	-
TAT11-005	GG	M	63	6.9	19.0	1.8	-
TAT11-006	GG	M	64	6.95	-	-	-
TAT11-007	GG	M	64	6.95	18.9	4.0	-
TAT11-008	GG	M	55	7	18.6	3.1	-
TAT11-009	GG	M	45	7.05	-	-	-
TAT11-010	GG	M	43	7.1	18.2	7.0	-
TAT11-011	GG	M	37	7.1	-	-	-
TAT11-012	GG	M	34	7.15	-	0.9	-
TAT11-053	MBS	M	69	7.73	15.6	17.2	16.4
TAT11-054	MBS	M	65	6.80	10.9	19.4	5.0
TAT11-055	MBS	M	55	7.05	12.1	-	-
TAT11-056	MBS	M	46	6.54	15.4	-	-
TAT11-057	MBS	M	61	6.8	15.1	2.1	9.3
TAT11-060	NT	M	80	6.96	18.3	1.9	1.0
TAT11-061	NT	M	63	7.0	18.6	-	-
TAT11-062	NT	M	62	7.0	18.5	0.9	0.9
TAT11-063	NT	M	46	7.1	18.6	-	-
TAT11-064	NT	M	35	7.05	18.4	1.5	-
TAT11-080	PS	M	76	6.5	18.4	22.1	0.9
TAT11-081	PS	M	45	6.84	18.8	-	-
TAT12-040	MBS-1	M	60	7.0	-	-	-
TAT12-041	MBS-2	M	40	7.0	-	-	-

Table 1-2: Major geochemical data from sample locations. Concentrations are expressed in mmol/L. Missing data are indicated by a '-'.

Sample ID	[DIC]	[HCO_3^-]	[As^{III}]	[As^{V}]	[Na^+]	[Cl^-]	[NO_3^-]	[SO_4^{2-}]	[Si]
TAT09-025	2.70	0.79	0.03	0.31	103.8	122.0	0.31	1.70	4.0
TAT09-030	2.50	1.77	0.17	0.07	100.5	-	-	-	1.9
TAT09-031	0.57	0.49	0	0.42	158.8	-	-	-	2.4
TAT09-032	1.96	1.46	0	0.31	106.2	123.5	0.87	1.42	2.9
TAT09-033	2.10	1.53	-	-	-	-	-	-	-
TAT09-034	2.40	1.83	0	0.19	91.9	102.0	0.26	0.61	2.9
TAT09-039	0.24	0.19	0	0.44	171.7	-	-	-	2.6
TAT09-045	1.74	0.45	0	0.03	2.7	2.9	0.23	6.75	2.0
TAT11-001	0.47	0.33	0.39	0.1	164.0	82.7	0.01	0.51	3.5
TAT11-002	0.37	0.28	0.37	0.12	-	-	-	-	-
TAT11-003	0.43	0.34	0.37	0.12	166.3	83.7	0.04	0.63	3.5
TAT11-004	0.45	0.36	0.37	0.14	-	-	-	-	-
TAT11-005	0.39	0.31	0.37	0.13	165.0	84.1	0.01	0.59	3.5
TAT11-006	-	-	0.36	0.16	-	-	-	-	-
TAT11-007	0.36	0.29	0.31	0.20	165.9	84.2	0.02	0.58	3.3
TAT11-008	0.30	0.25	0.16	0.35	-	85.6	0.01	0.60	-
TAT11-009	0.19	0.16	-	-	-	-	-	-	-
TAT11-010	0.12	0.11	0.12	0.42	163.2	87.5	0	0.59	3.5
TAT11-011	0.13	0.11	0.07	0.46	-	-	-	-	-
TAT11-012	0.11	0.09	0.05	0.49	177.1	89.2	0	0.46	3.7
TAT11-053	3.85	3.68	0	0.45	130.9	67.9	0.02	0.56	4.3
TAT11-054	3.35	2.47	0	0.34	91.9	50.0	0.02	0.52	4.0
TAT11-055	2.10	1.75	0	0.41	121.3	61.3	0.01	0.44	2.1
TAT11-056	3.57	2.04	0	0.45	134.8	67.4	0.01	0.49	1.9
TAT11-057	3.57	2.64	0.01	0.44	130.8	67.6	0.01	0.44	4.2
TAT11-060	0.57	0.46	-	-	158.4	80.1	0.02	0.43	2.2
TAT11-061	0.46	0.37	-	-	-	-	-	-	-
TAT11-062	0.47	0.38	-	-	-	82.2	0	0.46	-
TAT11-063	0.44	0.37	-	-	-	-	-	-	-
TAT11-064	0.19	0.16	-	-	-	85.6	0.01	0.58	-
TAT11-080	0.40	0.23	0.36	0.15	167.5	83.1	0	0.42	1.9
TAT11-081	0.20	0.15	0.29	0.24	-	87.4	0	0.53	-
TAT12-040	2.89	2.36	0.25	0.11	119.8	-	-	-	2.1
TAT12-041	2.89	2.36	0	0.36	119.8	-	-	-	2.1

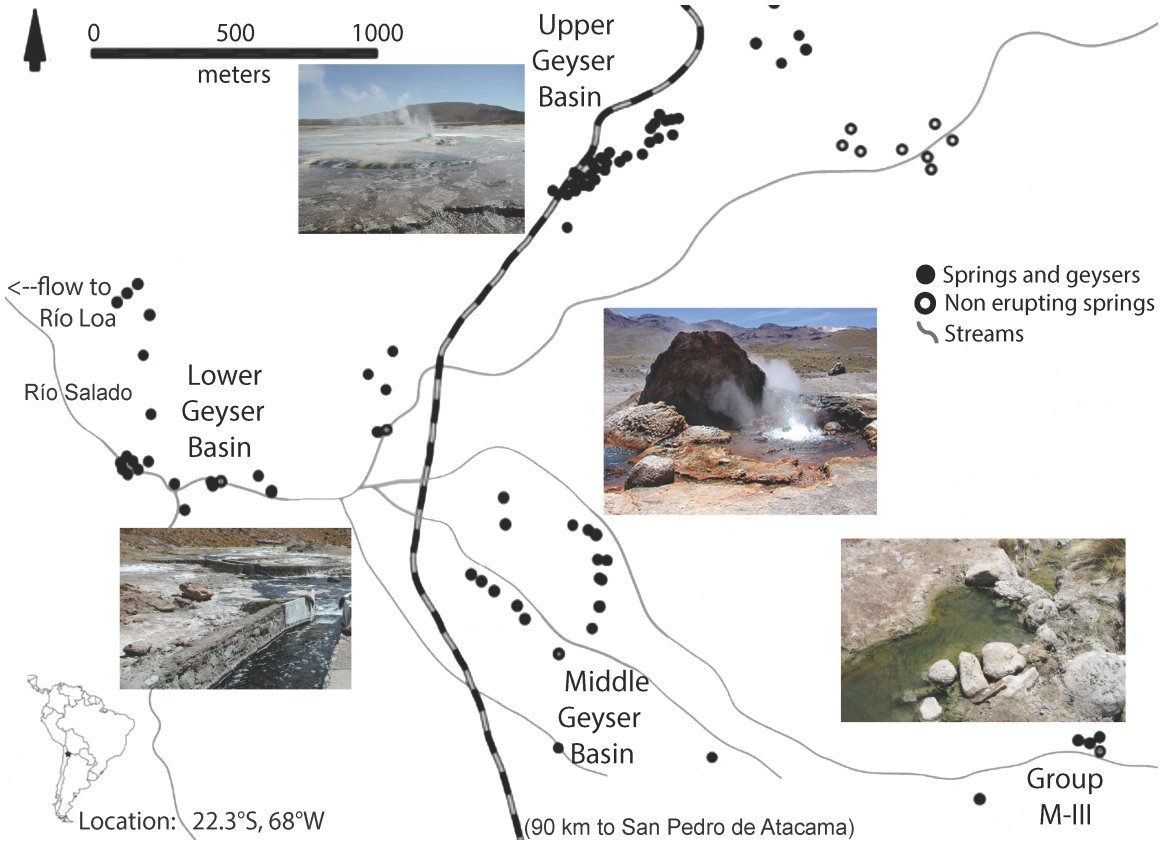

Figure 1-1: Overview map of the ETGF basins examined in this work, including the Upper Geyser Basin, Middle Geyser Basin, and Group M-III Basin. The map was modified from Glennon and Pfaff (2003).

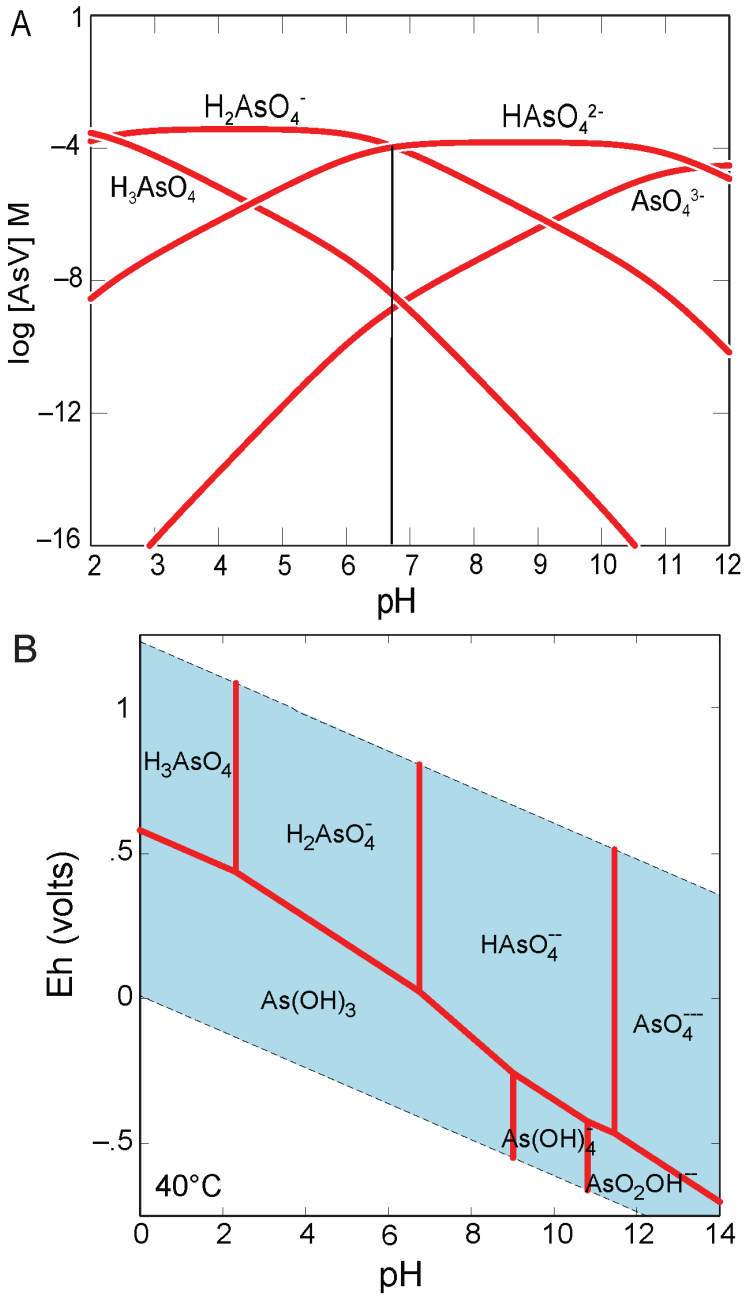

Figure 1-2: Bjerrum and Pourbaix diagrams showing $C_T(As^V)$ = 0.5 mM and 40°C, similar to conditions at ETGF (A), and the speciation of As^{III} and As^V at various pH and Eh (B). The dotted line shows the pK_a of arsenic acid (~6.9). These figures were created using the React and Act2 modules in the Geochemist's Workbench v. 10.0 (Bethke, 2008).

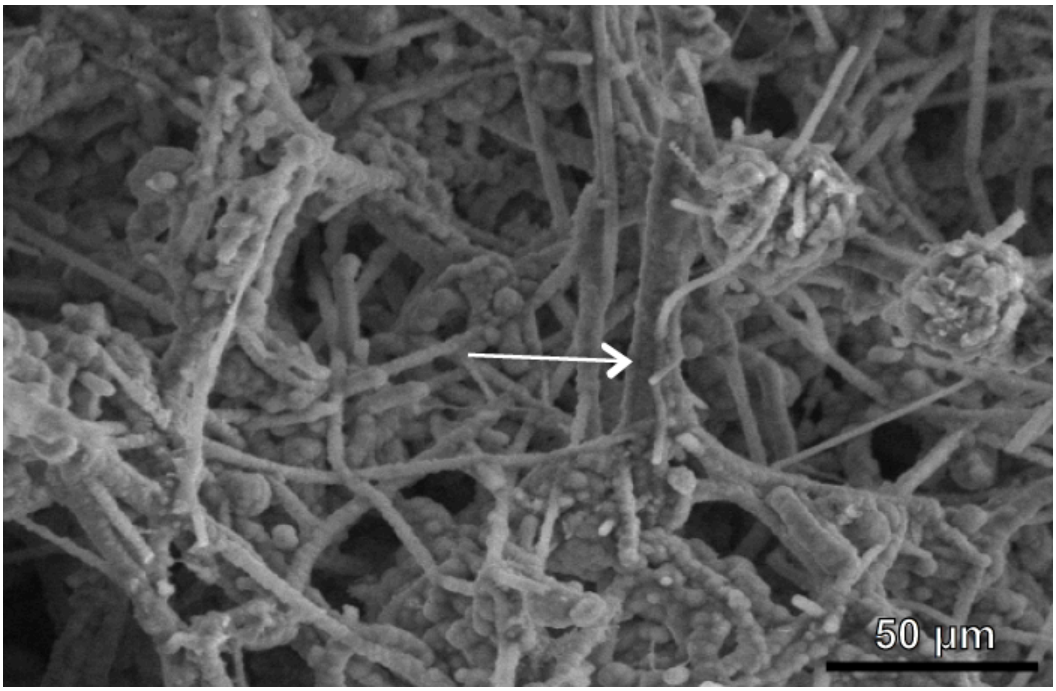

Figure 1-3: ESEM image of ETGF microbial filaments encased in silica. A cyanobacterial filament is indicated (white arrow). This image was modified from (Phoenix et al., 2006).

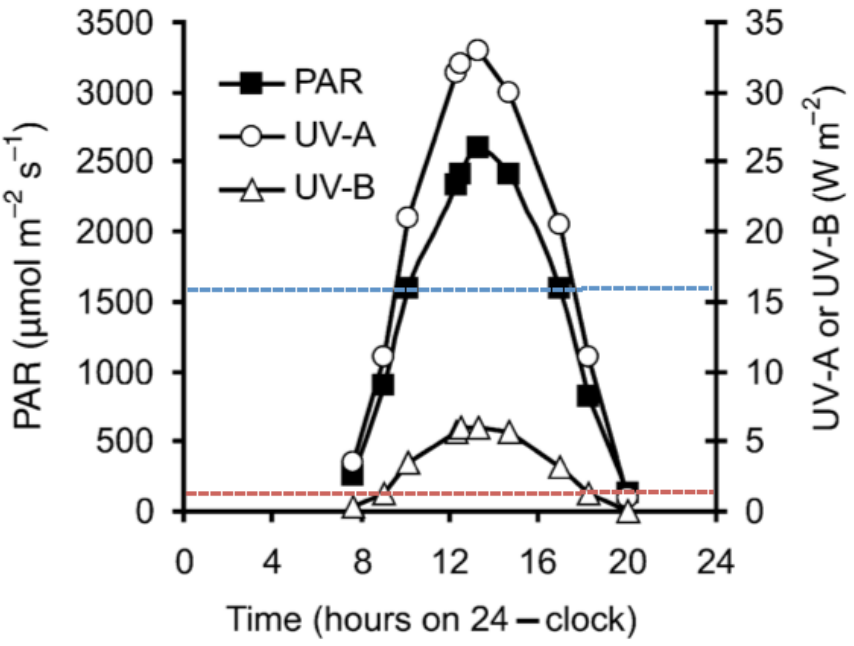

Figure 1-4: UV-A, -B, and PAR fluxes at ETGF. On average PAR is 30% higher at ETGF than at sea level (indicated by a blue dashed line). Exposure to UV-B flux at or above 1 W m^{-2} is harmful (at or above the red dashed line). This image was modified from Phoenix et al. (2006).

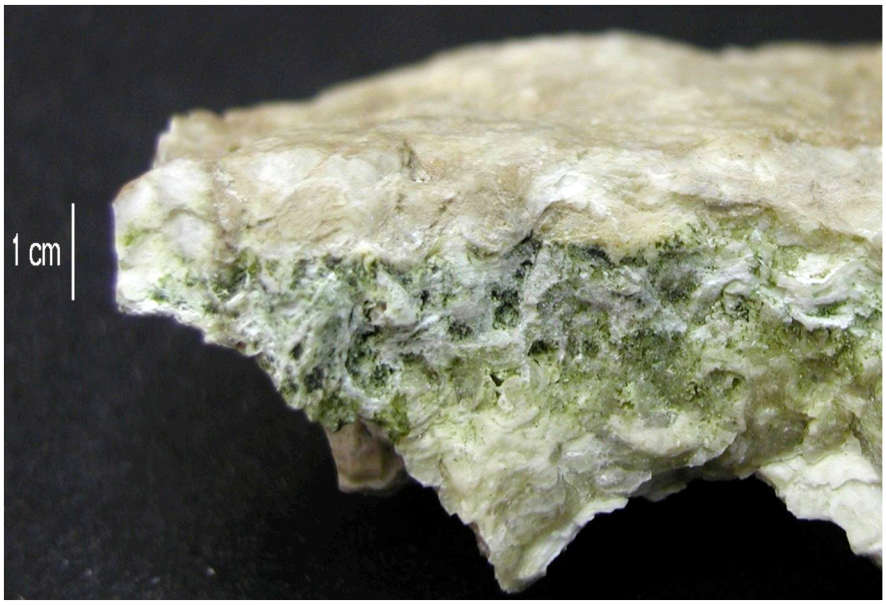

Figure 1-5: ETGF siliceous sinter containing abundant cyanobacterial filaments (dark green horizon) located up to 1 cm deep within the wavy and laminated mineral.

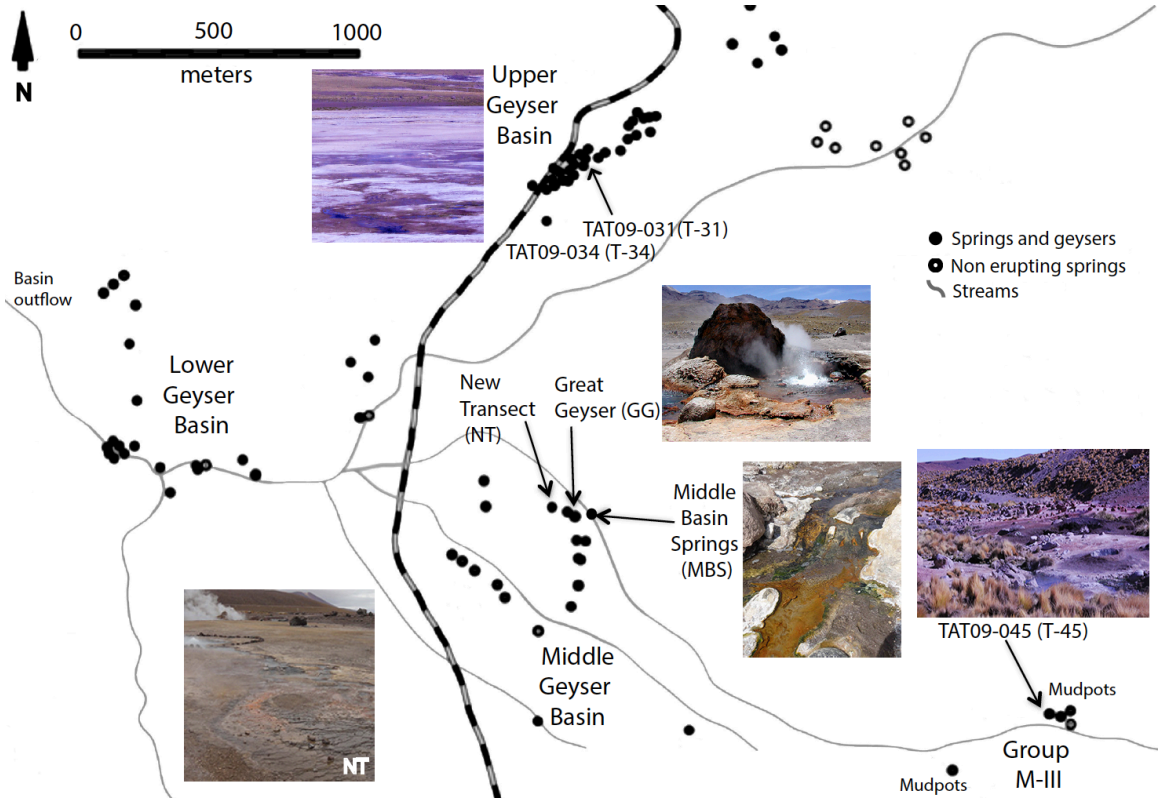

Figure 1-6: Map of geothermal feature locations throughout ETGF. Arrows indicate specific geothermal features examined in this study and the water sample ID's (TAT09-031, -034, -045) that correspond to the feature, or the abbreviated feature names (T-31, T-34, T-45, GG, NT, and MBS) that are referred to throughout this dissertation. Culture T-025 originates from the MBS. Map modified from Glennon and Pfaff (2003).

Figure 1-7: The Great Geyser, 25 m downstream of the outflow. Reddish-orange iron and silica-coated microbial streamers are located within the water, lining the bottom of the streambed. Flow direction is from the bottom to the top of the image.

Figure 1-8: The Great Geyser, 75 m downstream of the outflow. Mats at this location are green and orange in color, and more cohesive than delicate streamers found at 25 m. Flow direction is from left to right.

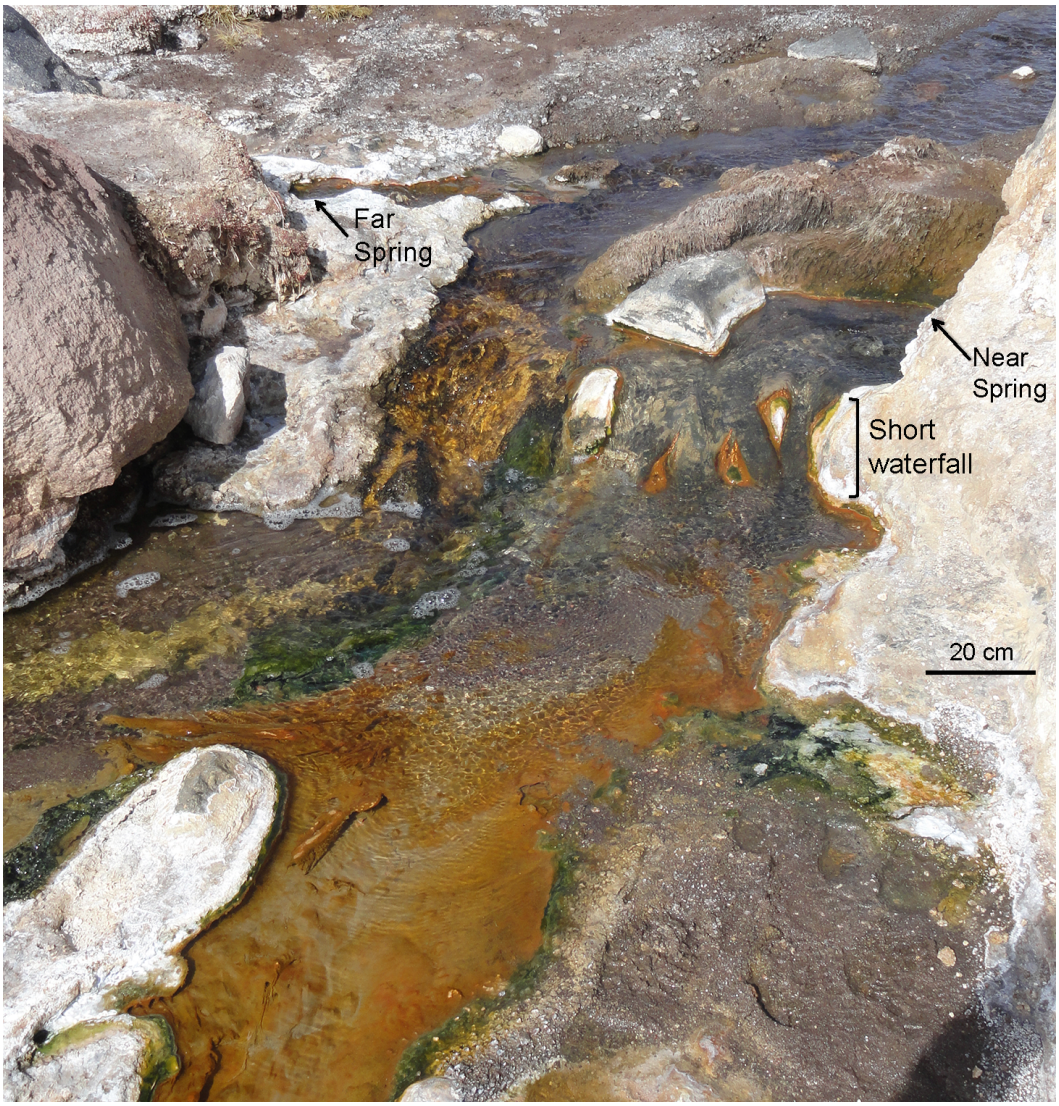

Figure 1-9: Middle Basin Springs, fed by flow from Group M-III geysers (upper right), and two springs, the near spring (right side of image, before a short waterfall), and the far spring (left side of image, also before the waterfall). Water flows from upper right to lower left of image.

Figure 1-10: The first 20 m of the New Transect. The stream is similar to the Great Geyser, which is visible in the background of the image. The NT is shorter than the GG, with sinter terraces forming in the midstream region. The mats are more colorful than mats within the Great Geyser, and additional thermal inputs are located ~19 m from the main orifice.

Figure 1-11: The Pseudomonas spring, 2 meters downstream from the outflow. This spring is located in the Middle Basin, near the New Transect (not shown in Figure 1-7).

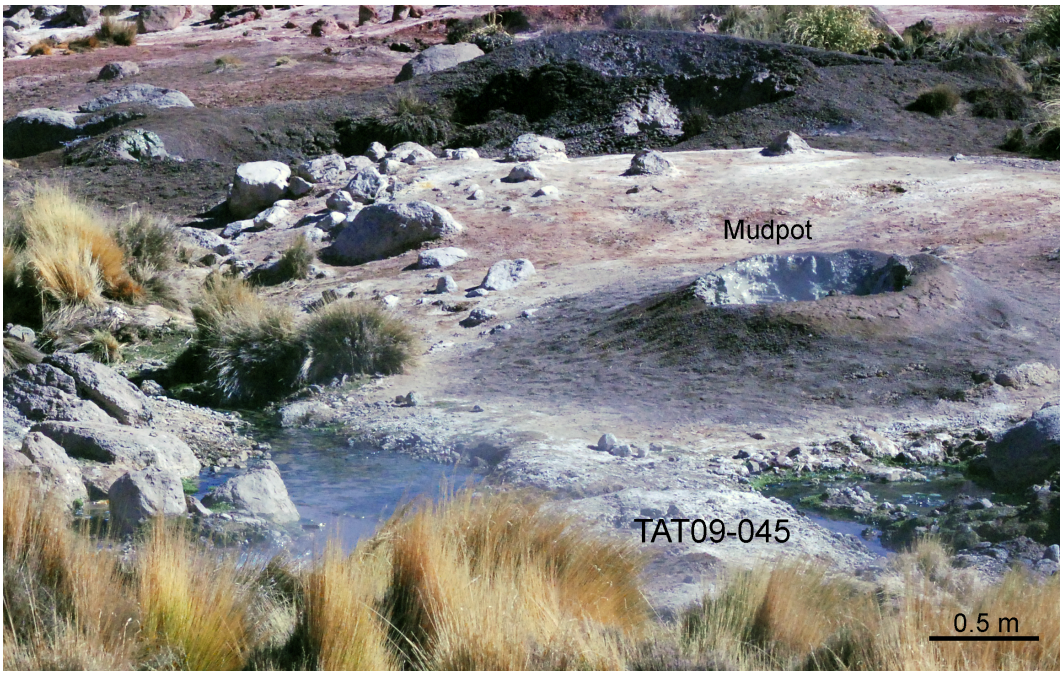

Figure 1-12: The Group M-III geysers, located ~2 km east of the main MB springs. The stream outflow where TAT09-045, -046 were sampled is in the foreground, with various mud pots visible, as well as the tall grasses found throughout the Group M-III basin.

REFERENCES

Amend, J.P., and Shock, E.L. (2001) Energetics of overall metabolic reactions of thermophilic and hyperthermophilic Archaea and Bacteria. *FEMS Microbiology Reviews* **25**: 175-243.

Amend, J.P., Rogers, K.L., Shock, E.L., Gurrieri, S., and Inguaggiato, S. (2003) Energetics of chemolithoautotrophy in the hydrothermal system of Vulcano Island, southern Italy. *Geobiology* **1**: 37-58.

Awramik, S.M., Schopf, J.W., and Walter, M.R. (1983) Filamentous fossil bacteria from the Archean of Western Australia. *Precambrian Research* **20**: 357-374.

Badger, M.R., Price, G.D., Long, B.M., and Woodger, F.J. (2006) The environmental plasticity and ecological genomics of the cyanobacterial CO_2 concentrating mechanism. *Journal of Experimental Botany* **57**: 249-265.

Ballantyne, J.M., and Moore, J.N. (1988) Arsenic geochemistry in geothermal systems. *Geochimica et Cosmochimica Acta* **52**: 475-483.

Baross, J.A., and Hoffman, S.E. (1985) Submarine hydrothermal vents and associated gradient environments as sites for the origin and evolution of life. *Origins of Life* **15**: 327-345.

Baross, J.A., Lilley, M.D., and Gordon, L.I. (1982) Is the CH_4, H_2 and CO venting from submarine hydrothermal systems produced by thermophilic bacteria? *Nature* **298**: 366-368.

Berkner, L.V., and Marshall, L.C. (1965) History of major atmospheric components. *Proceedings of the National Academy of Sciences of the United States of America* **53**: 1215-1226.

Bethke, C.M. (2008) *Geochemical and Biogeochemical Reaction Modeling*. New York, NY: Cambridge University Press.

Bethke, C.M., Sanford, R.A., Kirk, M.F., Jin, Q., and Flynn, T.M. (2011) The thermodynamic ladder in geomicrobiology. *American Journal of Science* **311**: 183-210.

Bhattacharya, P., and Pal, R. (2010) Response of cyanobacteria to arsenic toxicity. *Journal of Applied Phycology* **23**: 293-299.

Brock, T.D. (1978) Life at high temperatures. *Science* **158**: 1012-1019.

Budinoff, C.R., and Hollibaugh, J.T. (2008) Arsenite-dependent photoautotrophy by an Ectothiorhodospira-dominated consortium. *The ISME Journal* **2**: 340-343.

Canfield, D.E., Rosing, M.T., and Bjerrum, C. (2006) Early anaerobic metabolisms. *Philosophical Transactions of the Royal Society of London B Biological Sciences* **361**: 1819-1836.

Cervantes, C., Ji, G., Ramirez, J.J., and Silver, S. (1994) Resistance to arsenic compounds in microorganisms. *FEMS Microbiology Ecology* **15**: 355-367.

Cloud, P. (1965) Significance of the Gunflint (Precambrian) Microflora. *Science* **148**: 27-35.

Connon, S.A., Koski, A.K., Neal, A.L., Wood, S.A., and Magnuson, T.S. (2008) Ecophysiology and geochemistry of microbial arsenic oxidation within a high arsenic, circumneutral hot spring system of the Alvord Desert. *FEMS Microbiology Ecology* **64**: 117-128.

Cortecci, G., Boschetti, T., Mussi, M., Herrera Lameli, C., Mucchino, C., and Barbieri, M. (2005) New chemical and original isotopic data on waters from El Tatio geothermal field, northern Chile. *Geochemical Journal* **39**: 547-571.

Cusicanqui, H., Mahon, W.A.J., and Ellis, A.J. (1976) The geochemistry of the El Tatio Geothermal Field, northern Chile. In *Second United Nations Geothermal Symposium Proceedings, Lawrence Berkeley Laboratory*. Univ. of California, Berkeley, CA.

de Silva, S.L. (1989) Altiplano-Puna volcanic complex of the central Andes. *Geology* **17**: 1102-1106.

de Silva, S.L., Self, S., Francis, P.W., Drake, R.E., and Carlos, R.R. (1994) Effusive silicic volcanism in the Central Andes: The Chao dacite and other young lavas of the Altiplano-Puna Volcanic Complex. *Journal of Geophysical Research* **99**: 17805.

Deckert, G., Warren, P.V., Gaasterland, T., Young, W.G., Lenox, A.L., Graham, D.E. et al. (1998) The complete genome of the hyperthermophilic bacterium Aquifex aeolicus. *Nature* **392**: 353-358.

Des Marais, D.J. (1998) Earth's Early Biosphere. *Gravitational and Space Biology Bulletin* **11**: 23-30.

Edwards, K.J., Rogers, D.R., Wirsen, C.O., and McCollom, T.M. (2003) Isolation and Characterization of Novel Psychrophilic, Neutrophilic, Fe-Oxidizing, Chemolithoautotrophic α- and γ-Proteobacteria from the Deep Sea. *Applied and Environmental Microbiology* **69**: 2906-2913.

Ellis, A.J., and Mahon, W.A.J. (1964) Natural hydrothermal systems and experimental hot-water/rock interactions. *Geochimica et Cosmochimica Acta* **28**: 1323-1357.

Ellis, A.J., and Mahon, W.A.J. (1967) Natural hydrothermal systems and experimental hot water/rock interactions (Part II). *Geochimica et Cosmochimica Acta* **31**: 519-538.

Engel, A.S., Johnson, L.R., and Porter, M.L. (2013) Arsenite oxidase gene diversity among Chloroflexi and Proteobacteria from El Tatio Geyser Field, Chile. *FEMS Microbiology Ecology* **83**: 745-756.

Farmer, J.D. (2000) Hydrothermal systems: doorways to early biosphere evolution. *GSA Today* **10**: 1-9.

Fernandez-Turiel, J.L., Garcia-Valles, M., Gimeno-Torrente, D., Saavedra-Alonso, J., and Martinez-Manent, S. (2005) The hot spring and geyser sinters of El Tatio, Northern Chile. *Sedimentary Geology* **180**: 125-147.

Fournier, R.O. (2005) Geochemistry and Dynamics of the Yellowstone National Park Hydrothermal System. In *Geothermal Biology and Geochemistry in Yellowstone National Park*. Inskeep, W.P., and McDermott, T.R. (eds). Bozeman, MT: Thermal Biology Institute, Montana State University, pp. 3-29.

Fournier, R.O., and Potter, R.W. (1982) An equation correlating the solubility of quartz in water from 25 to 900C at pressures up to 10,000 bars. *Geochimica et Cosmochimica Acta* **46**: 1969-1973.

Franks, M.A. (2012) Archaea at the El Tatio Geyser Field: community composition, diversity, and distribution across hydrothermal features and geochemical gradients (Ph.D. Dissertation) The University of Texas at Austin.

Garcia-Pichel, F. (1998) Solar ultraviolet and the evolutionary history of cyanobacteria. *Origins of Life and Evolution of the Biosphere* **28**: 321-347.

Garcia-Pichel, F., and Castenholz, R.W. (1991) Characterization and biological implications of scytonemin, a cyanobacterial sheath pigment. *Journal of Phycology* **27**: 395-409.

Garcia-Valles, M., Fernandez-Turiel, J.L., Gimeno-Torrente, D., Saavedra-Alonso, J., and Martinez-Manent, S. (2008) Mineralogical characterization of silica sinters from the El Tatio geothermal field, Chile. *American Mineralogist* **93**: 1373-1383.

Ghalambor, C.K., McKay, J.K., Carroll, S.P., and Reznick, D.N. (2007) Adaptive versus non-adaptive phenotypic plasticity and the potential for contemporary adaptation in new environments. *Functional Ecology* **21**: 394-407.

Giggenbach, W.F. (1978) The isotopic composition of waters from the El Tatio geothermal field, Northern Chile. *Geochimica et Cosmochimica Acta* **42**: 979-988.

Gihring, T.M., and Banfield, J.F. (2001) Arsenite oxidation and arsenate respiration by a new Thermus isolate. *FEMS Microbiology Letters* **204**: 335-340.

Giordano, M., Beardall, J., and Raven, J.A. (2005) CO2 concentrating mechanisms in algae: mechanisms, environmental modulation, and evolution. *Annual Review of Plant Biology* **56**: 99-133.

Glennon, J.A., and Pfaff, R.M. (2003) The extraordinary thermal activity of El Tatio Geyser Field, Antofagasta Region, Chile. *The GOSA Transactions* **8**: 31-78.

Hamamura, N., Macur, R.E., Korf, S., Ackerman, G., Taylor, W.P., Kozubal, M. et al. (2009) Linking microbial oxidation of arsenic with detection and phylogenetic analysis of arsenite oxidase genes in diverse geothermal environments. *Environmental Microbiology* **11**: 421-431.

Healy, J., and Hochstein, M.P. (1973) Horizontal flow in hydrothermal systems. *Journal of Hydrology (NZ)* **12**: 71-82.

Hoeft, S.E., Kulp, T.R., Han, S., Lanoil, B., and Oremland, R.S. (2010) Coupled arsenotrophy in a hot spring photosynthetic biofilm at Mono Lake, California. *Applied and Environmental Microbiology* **76**: 4633-4639.

Inskeep, W.P., and McDermott, T.R. (2005) Geomicrobiology of Acid-Sulfate-Chloride Springs in Yellowstone National Park. In *Geothermal Biology and Geochemistry in Yellowstone National Park*. Inskeep, W.P., and McDermott, T.R. (eds). Bozeman, MT: Thermal Biology Institute, Montana State University, pp. 143-162.

Jones, B., and Renaut, R.W. (1997) Formation of silica oncoids around geysers and hot springs at El Tatio, northern Chile. *Sedimentology* **44**: 287-304.

Kasting, J.F. (1987) Theoretical constraints on oxygen and carbon dioxide concentrations in the Precambrian atmosphere. *Precambrian Research* **34**: 205-229.

Kulp, T.R., Hoeft, S.E., Asao, M., Madigan, M.T., Hollibaugh, J.T., Fisher, J.C. et al. (2008) Arsenic(III) fuels anoxygenic photosynthesis in hot spring biofilms from Mono Lake, California. *Science* **321**: 967-970.

Lahsen, A. (1988) Chilean geothermal resources and their possible utilization. *Geothermics* **17**: 401-410.

Lahsen, A., and Trujillo, P. (1976) El Tatio geothermal field. In *Proceedings of the 2nd United Nations Symposium on Geothermal Fields*. Berkeley, CA: pp. 157-178.

Landrum, J.T. (2007) Fate and Transport of Arsenic and Antimony in the El Tatio Geyser Field, Chile (Masters Thesis) The University of Texas at Austin.

Landrum, J.T., Bennett, P.C., Engel, A.S., Alsina, M.A., Pastén, P.A., and Milliken, K. (2009) Partitioning geochemistry of arsenic and antimony, El Tatio Geyser Field, Chile. *Applied Geochemistry* **24**: 664-676.

Lopez-Maury, L., Florencio, F.J., and Reyes, J.C. (2003) Arsenic Sensing and Resistance System in the Cyanobacterium Synechocystis sp. Strain PCC 6803. *Journal of Bacteriology* **185**: 5363-5371.

Lowe, D.R. (1983) Restricted shallow-water sedimentation of early Archean stromatolitic and evaporitic strata of the Strelley Pool Chert, Pilbara Block, Western Australia. *Precambrian Research* **19**: 239-283.

Mukhopadhyay, R., Rosen, B.P., Phung, L.T., and Silver, S. (2002) Microbial arsenic: from geocycles to genes and enzymes. *FEMS Microbiology Reviews* **26**: 311-325.

Nordstrom, D.K., Ball, J.W., and McCleskey, R.B. (2005) Ground Water to Surface Water: Chemistry of Thermal Outflows in Yellowstone National Park. In *Geothermal Biology and Geochemistry in Yellowstone National Park*. Inskeep, W.P., and McDermott, T.R. (eds). Bozeman, MT: Thermal Biology Institute, Montana State University, pp. 73-94.

Oremland, R.S., and Stolz, J.F. (2003) The ecology of arsenic. *Science* **300**: 939-944.

Oremland, R.S., Stolz, J.F., and Hollibaugh, J.T. (2004) The microbial arsenic cycle in Mono Lake, California. *FEMS Microbiology Ecology* **48**: 15-27.

Paerl, H.W., Pinckney, J.L., and Steppe, T.F. (2000) Cyanobacterial-bacterial mat consortia: examining the functional unit of microbial survival and growth in extreme environments. *Environmental Microbiology* **2**: 11-26.

Paez-Espino, D., Tamames, J., de Lorenzo, V., and Canovas, D. (2009) Microbial responses to environmental arsenic. *Biometals* **22**: 117-130.

Phoenix, V.R., Bennett, P.C., Engel, A.S., Tyler, S.W., and Ferris, F.G. (2006) Chilean high-alititude hot-spring sinters: a model system for UV screening mechanisms by early Precambrian cyanobacteria. *Geobiology* **4**: 15-28.

Pierson, B.K., Mitchell, H.K., and Ruff-Roberts, A.L. (1993) Chloroflexus aurantiacus and ultraviolet radiation: implications for Archean shallow-water stromatolites. *Origins of Life and Evolution of the Biosphere* **23**: 243-260.

Rambler, M.B., and Margulis, L. (1980) Bacterial resistance to ultraviolet irradiation under anaerobiosis: implications for pre-Phanerozoic evolution. *Science* **210**: 638-640.

Rasmussen, B. (2000) Filamentous microfossils in a 3,235-million-year-old volcanogenic massive sulphide deposit. *Nature* **405**: 676-679.

Reysenbach, A.L., and Cady, S.L. (2001) Microbiology of ancient and modern hydrothermal systems. *TRENDS in Microbiology* **9**: 79-86.

Reysenbach, A.L., and Shock, E.L. (2002) Merging genomes with geochemistry in hydrothermal ecosystems. *Science* **296**: 1077-1082.

Reysenbach, A.L., Longnecker, K., and Kirshtein, J. (2000) Novel Bacterial and Archaeal lineages from an in situ growth chamber deployed at a Mid-Atlantic Ridge hydrothermal vent. *Applied and Environmental Microbiology* **66**: 3798-3806.

Reysenbach, A.L., Gotz, D., Banta, A., Jeanthon, C., and Fouquet, Y. (2002) Expanding the distribution of the Aquificales to the deep-sea vents on Mid-Atlantic Ridge and Central Indian Ridge. *Cahiers de Biologie Marine* **43**: 425-428.

Rodgers, K.A., Greatrex, R., Hyland, M., Simmons, S.F., and Browne, P.R.L. (2002) A modern evaporitic occurrence of teruggite, $Ca_4MgB_{12}As_2O_{28}$.18H2O, and nobleite, CaB_6O_{10}.4H2O, from the El Tatio geothermal field, Antofagasta Province, Chile. *Mineralogical Magazine* **66**: 253-259.

Smedley, P.L., and Kinniburgh, D.G. (2002) A review of the source, behaviour and distribution of arsenic in natural waters. *Applied Geochemistry* **17**: 517-568.

Stal, L. (2012) Cyanobacterial Mats and Stromatolites. In *Ecology of Cyanobacteria II: Their Diversity in Space and Time*. Whitton, B.A. (ed): Springer Science+Business Media, pp. 65-125.

Stal, L.J., van Gemerden, H., and Krumbein, W.E. (1985) Structure and development of a benthic marine microbial mat. *FEMS Microbiology Ecology* **31**: 111-125.

Stauffer, R.E., and Thompson, J.M. (1984) Arsenic and antimony in geothermal waters of Yellowstone National Park, Wyoming, USA. *Geochimica et Cosmochimica Acta* **48**: 2547-2561.

Tassi, F., Aguilera, F., Darrah, T., Vaselli, O., Capaccioni, B., Poreda, R.J., and Delgado Huertas, A. (2010) Fluid geochemistry of hydrothermal systems in the Arica-Parinacota, Tarapacá and Antofagasta regions (northern Chile). *Journal of Volcanology and Geothermal Research* **192**: 1-15.

Templeton, A.S. (2011) Geomicrobiology of Iron in Extreme Environments. *Elements* **7**: 95-100.

Thompson, J.M. (1979) Arsenic and fluoride in the Upper Madison River System: Firehole and Gibbon Rivers and Their Tributaries, Yellowstone National Park, Wyoming, and Southeast Montana. *Environmental Geology* **3**: 13-21.

Walker, J.C.G., Klein, C., Schidlowski, M., Schopf, J.W., Stevenson, D.J., and Walter, M.R. (1983) Environmental evolution of the Archean-Early Proterozoic earth. In *Earth's earliest biosphere: Its origin and evolution*. Princeton, NJ: Princeton University Press, pp. 260-290.

Walter, M.R. (1983) Archean stromatolites: evidence of the Earth's earliest benthos. In *Earth's earliest biosphere: Its origin and evolution*. Schopf, J.W. (ed). Princeton, NJ: Princeton University Press, pp. 187-213.

Ward, D.M., and Castenholz, R.W. (2000) Cyanobacteria in Geothermal Habitats. In *The Ecology of Cyanobacteria: Their Diversity in Time and Space*. Whitton, B.A., and Potts, M. (eds). Netherlands: Kluwer Academic Publishers, pp. 37-59.

Ward, D.M., and Cohan, F.M. (2005) Microbial Diversity in Hot Spring Cyanobacterial Mats: Pattern and Prediction. In *Geothermal Biology and Geochemistry in Yellowstone National Park*. Inskeep, W.P., and McDermott, T.R. (eds). Bozeman, MT: Montana State University Publications, pp. 185-201.

Ward, D.M., Castenholz, R.W., and Miller, S.R. (2012) Cyanobacteria in Geothermal Habitats. In *Ecology of Cyanobacteria II: Their Diversity in Space and Time*. Whitton, B.A. (ed): Springer Science + Business Media, pp. 39-63.

Webster, J., and Nordstrom, D. (2003) Geothermal arsenic. In *Arsenic in Ground Water: Geochemistry and Occurence* Welch, A.H., and Stollenwerk, K.G. (eds). Boston: Kluwer Academic Publishers, pp. 101-126.

Webster-Brown, J.G. (2000) Chemical contaminants and their effects. In *World Geothermal Congress*. Kizuno, Japan.

Whitton, B.A. (2012) *Ecology of Cyanobacteria II: Their Diversity in Space and Time*: Springer.

Whitton, B.A., and Potts, M. (2000) Introduction to the Cyanobacteria. In *The Ecology of Cyanobacteria: Their Diversity in Time and Space*. Whitton, B.A., and Potts, M. (eds). Dordrecht, Netherlands: Kluwer Academic Publishers, pp. 1-11.

Widdel (1993) Ferrous iron oxidation by anoxygenic phototrophic bacteria. *Nature* **362**: 835-836.

Woese, C.R. (1987) Bacterial evolution. *Microbiological Reviews* **51**: 221-271.

Wolery, T.J., and Sleep, N.H. (1976) Hydrothermal circulation and geochemical flux at mid-ocean ridges. *The Journal of Geology* **84**: 249-275.

Chapter 2: The Microbial Ecology and Phylogenetic Diversity of Cyanobacteria in the Geothermal Features of El Tatio, Chile

ABSTRACT

Cyanobacteria are important primary producers for microbial mat communities in geothermal waters between 30-74°C. The phylogenetic diversity and microbial ecology of cyanobacteria were investigated within the extreme geothermal features of El Tatio Geyser Field, Chile (ETGF). El Tatio's isolated geographic location, paired with high UV-flux, high arsenic (0.4-0.6 mM As), and low dissolved inorganic carbon (0.1-0.3 mM DIC) make it a unique environmental context in which to investigate thermophilic cyanobacteria. Sanger dideoxy DNA sequencing was used to investigate the 16S rRNA diversity of El Tatio cyanobacteria. Roche 454-pyrosequencing was used to determine geochemical controls on the abundance and diversity of cyanobacterially-classified sequences and interpret the influence of cyanobacteria on microbial community diversity and function. Most cyanobacteria sequences match filamentous cyanobacteria; the most abundant and widespread organism in these springs was *Fischerella* sp., a cosmopolitan, thermophilic, N_2-fixing, and filamentous cyanobacterium. Temperature, As^{III}, and As^{V} were found to significantly influence cyanobacterial abundance and diversity throughout ETGF. Although DIC did not correlate with the abundance or diversity of cyanobacteria, higher DIC was found to contribute to cyanobacteria species dominance, higher microbial mat biomass, and increased species richness compared to low-DIC sites.

INTRODUCTION

Microbial mat communities are structurally simple yet functionally complex ecological units that promote survival in extreme environments such as hot springs (Ward et al., 1998; Paerl et al., 2000; Ward and Castenholz, 2000; Ward et al., 2012). Although many microorganisms are able to fix CO_2, primary production in geothermal microbial mats is often based on the photosynthetic activity of cyanobacteria (Ward et al., 1998; Ward and Castenholz, 2000; Ward and Cohan, 2005). The advent of DNA sequencing and next-generation sequencing techniques expanded our knowledge of cyanobacterial occurrence and distribution to far-reaching hot spring locations, making it possible to assess the effects of dispersal and local geochemical dynamics on the ecology and evolution of cyanobacteria (Papke et al., 2003; Miller, 2007; Miller et al., 2007; Ward et al., 2012).

El Tatio Geyser Field (ETGF) is a novel environmental context in which to study geothermal cyanobacteria because it possesses several key environmental differences from previously studied sites. Many previously studied systems contain high sulfide, alkaline pH, and high DIC as HCO_3^- and CO_3^{2-} (Jorgensen and Nelson, 1988; Ward and Castenholz, 2000; Connon et al., 2008; Ward et al., 2012). In contrast, El Tatio geothermal features are nonsulfidic, neutral pH, and low DIC (as $CO_{2(aq)} + HCO_3^-$). ETGF waters possess one of the highest reported naturally occurring As concentrations in a surface water (Nordstrom and Archer, 2003; Landrum, 2007; Landrum et al., 2009). Although most natural waters are buffered to circumneutral pH by the carbonate system

(Drever, 1988), ETGF waters are buffered by the arsenate oxoanion (Eq. 1-1; As^{V} as $H_xAsO_3^{3-x}$, $pK_{a2} \sim 6.94$ at 25°C) (Landrum et al., 2009; Engel et al., 2013).

Cyanobacteria are found in microbial mats in geothermal waters up to 74°C, the upper temperature limit of photosystem II; however, greater cyanobacterial diversity is found at or below 55°C (Brock, 1978; Ward et al., 2012). Cyanobacteria often dominate primary production in microbial mats due to their efficient DIC acquisition strategies (Badger et al., 2006). During primary production by cyanobacteria or other autotrophs, dissolved CO_2 is fixed enzymatically and retained in the community as biomass, or transferred to heterotrophic organisms as labile forms of organic carbon (Stal et al., 1985; Paerl et al., 2000; Stal, 2012).

Conditions present at ETGF such as high UV flux, temperatures above 30°C, and low DIC place additional pressure on carbon assimilation by cyanobacteria in the already DIC-limited waters (Badger et al., 2006). Cyanobacteria possess a CO_2-concentrating mechanism (CCM), which helps to alleviate carbon stress by concentrating CO_2 around the active site of RuBisCO, improving its carboxylation efficiency (Badger and Price, 1992; Price et al., 1998; Kaplan and Reinhold, 1999). Despite this efficient adaptation by cyanobacteria to low-DIC conditions limited biomass suggests that DIC is low enough to be considered a limiting nutrient in these waters.

Arsenic is a known toxin to multicellular organisms as well as some microorganisms; its two inorganic forms, As^{III} and As^{V} do not impact cyanobacteria equally. As^{III} is shown to negatively influence cyanobacteria by inhibiting growth at low concentrations, interfering with DNA repair mechanisms, and preventing pigment

synthesis which can result in stress to light exposure (Wang et al., 2012; Ferrari et al., 2013); however, As^{V} does not appear to impact cyanobacteria, and can lead to increased pigment synthesis and increased growth (Ferrari et al., 2013).

Here I discuss the phylogenetic diversity and microbial ecology of aquatic cyanobacteria at ETGF; the abundance and diversity of cyanobacteria were assessed along with local geochemical characteristics. Cyanobacteria appear to dominate As^{V}-rich stream regions, and are largely absent in As^{III}-rich waters. Similarly, microbial mat biomass appears greater in As^{V}-dominated stream areas that contain cyanobacteria, but greater productivity is evident in high-DIC geothermal features. Based on these observations, DIC and As-redox speciation were predicted to be important drivers of cyanobacteria abundance; by determining the distribution of primary-producing cyanobacteria As-redox speciation was predicted to determine the magnitude of primary production in microbial mats. Microbial mat community diversity and biomass abundance was hypothesized to be influenced by As and DIC; however, community-level properties also appear to depend on primary production by cyanobacteria in this DIC-limited system. Due to the isolated geographic setting and unique geochemistry of ETGF waters the recovery of novel cyanobacteria phylotypes was anticipated, as was the discovery of novel ecological strategies utilized by ETGF cyanobacteria.

METHODS

Sampling and Geochemical Analysis

Geochemical and microbiological sampling occurred in June 2009, 2011, and 2012. A total of 14 sites were sampled in six geothermal features across the Upper,

Middle, and M-III basins (Figure 1-6). pH, Eh, and temperature measurements were taken along geothermal spring discharges. Water samples were filtered to 0.2 μm and designated for various geochemical analyses. Cation samples were preserved with 3% HNO_3, and concentrations were determined using inductively coupled plasma mass spectrometry (ICP-MS) at the Laser Ablation and ICP-MS Laboratory [The University of Texas at Austin]. Anion concentrations were determined by single-column ion chromatography on a Waters HPLC (Waters Corporation, Milford, MA). Total [As], [As^{III}], and [As^{V}] were separated on a Waters HPLC with a Supelco 810 organic acid HPLC column (Supelco Analytical, Bellefonte, PA) and quantified by absorbance at 205 nm. Total DIC was measured after acidification by a non-dispersive IR detector on an Apollo 9000 Carbon Analyzer (Teledyne-Tekmar, Mason, OH).

Microbial mats were sampled aseptically at 13 locations where aqueous chemistry was characterized. Mat samples collected for DNA analysis (0.5-1.0 g) were stored in 2 mL microcentrifuge tubes and flash frozen within 2 hours of collection in a 4.1 L portable liquid nitrogen dewar (Taylor-Wharton, Theodore, AL). Samples intended for DNA sequencing were stored at -20°C until extraction. Microbial mats for biomass measurement was maintained at 4°C in the field, and stored at -20°C. Samples for enrichment culture were maintained at 4°C.

Microbial Biomass Measurements

Bulk microbial mat was dried overnight at 104°C and cooled to room temperature in a desiccation chamber. Samples were powdered, homogenized, and stored in a desiccation chamber until biomass was determined by loss on ignition (LOI) using

standard protocols (Dean, 1974). The number of replicates for biomass determination depended on the amount of available material (n = 4-12).

Enrichment Culturing

Several environmental mat samples were enriched in BG-11(+N) media without serial dilution (Appendix A) (Rippka et al., 1979). Environmental sample T-05 was collected from a subaerial mat in the splash and steam zone of a 70°C region of a stream known as the Great Geyser. Enrichment samples T075-A and T075-B were both collected from a subaqueous mat at 75m along the Great Geyser stream (GG-75; Figure 1-6). Sample T075-A was enriched in normal BG-11(+N) media, while T075-B was enriched in BG-11(+N) + 5% NaCl. Environmental samples enriched in BG-11(+N) media were examined by light microscopy on an Olympus BX41 microscope (Olympus America, Inc., Melville, NY). Images were taken at 400X, or at 1000X using an oil immersion lens, and cell size was approximated using an ocular grid.

DNA Extraction, Cloning, and Sequencing

Full-length cyanobacteria 16S rRNA sequences were obtained using a shotgun cloning and Sanger sequencing approach. Genomic DNA from microbial mats was extracted using a Power Biofilm DNA Extraction Kit (MO BIO Laboratories Inc., Carlsbad, CA). Full-length 16S rRNA gene sequences (1,450 bp) were amplified from genomic DNA by PCR in a Peltier PCT-100 thermocycler (Bio-Rad Laboratories, Hercules, CA) using universal primers 16S-8F (5'-GCYTAAAGSRICCGTAGC-3') (Nubel et al., 1997) and 16S-1492R (5'-TTMGGGGCATRCIKACCT-3') (Weisburg et

al., 1991). Each 25 μL PCR reaction contained 2-5 μl DNA (~750 ng), 0.5 mg/ml BSA, 10x PCR buffer, 0.4 μL 5 U/μL Invitrogen Taq polymerase (New England BioLabs, Ipswitch, MA), 50 mM $MgCl_2$, 10 mM dNTPs, and 10 mM of each primer. PCR conditions were 95˚C for 3 min, 35 cycles of 95˚C for 20 s, 49˚C for 15 s, 42˚C for 90 s, and a final 5 minute extension at 42˚C, modified from (Turner et al., 1999). PCR fragment length was verified on a 1.2% agarose gel containing 1.5X SYBR Safe DNA gel stain (Life Technologies Corporation, Carlsbad, CA).

PCR product was ligated onto the pCII-TOPO-TA vector transformed using competent TOP10 *E. coli* cells (Life Technologies Corporation, Carlsbad, CA), and plated on Luria-Bertani (LB) Broth (Gibco®, Grand Island, NY) agar with 100 µg/ml ampicillin sodium salt (Sigma-Aldrich Corporation, St. Louis, MO) and 50 µg/ml 5-bromo-4-chloro-3-indoyl-beta-D-galacto-pyranoside (X-GAL) (Thermo Fisher Scientific Inc., Waltham, MA) for blue/white screening. Cloning efficiency yielded 2.12 x 10^8 CFU/µg DNA. 50-100 white colonies per sample were cultured overnight in LB amended with 100 µg/ml ampicillin. Plasmid DNA was extracted using the PureLink Quick Plasmid miniprep kit (Invitrogen Life Technologies Corporation, Carlsbad, CA).

Half-length (900 bp) 16S rRNA sequences were obtained using M13(-24) reverse primers and sequenced on a 96-capillary 3730XL DNA Analyzer (LifeTech-Applied Biosystems, Foster City, CA) at the ICMB Core Facility, [The University of Texas at Austin]. Half-length sequences were similarity searched using the web-available nucleotide BLAST algorithm at www.blast.st-va.ncbi.nlm.nih.gov (Altschul et al., 1990);

sequences matching cyanobacteria were selected for full-length sequencing by also using the M13(-20) forward primer.

Forward and reverse 16S rRNA sequences were trimmed to remove ambiguous base pairs. Full-length 16S rRNA cyanobacteria sequences were constructed by ligating M13(-20) forward sequences to the reverse complements of M13(-27) reverse sequences. Reverse complements were obtained using the Sequence Manipulation Suite, a collection of online tools for analyzing and formatting DNA and protein sequences (http://bioinformatics.org/sms; ©Stothard 2000, University of Alberta, Canada). Chimera detection of full-length 16S rRNA sequences was performed using USEARCH 6.0 (Edgar et al., 2011) in the functional gene pipeline of the Ribosomal Database Project (Maidak et al., 2001). Poorly performing sequences were removed during alignment to prevent the inclusion of falsely negative chimeric sequences.

Phylogenetic Analysis of Clone Library Sequences

Full-length cyanobacteria sequences were similarity searched in BLAST. Phylogenetic reconstructions were used to determine the relative placement of unknown culture and environmental sequences with reference sequences from the GenBank database (see a full list in Table B-1). Alignment was performed in ClustalX 2.1 with a gap opening penalty of 30, and gap extension penalty of 15 (Larkin et al., 2007). Alignments were refined manually to uniform length; the alignment for all trees matched *E. coli* (J01859.1) 16S rRNA positions 105 to 1510, with a gap between positions 452 to 475. *Gloeobacter* sp. Strain PCC 7421 was used as an outgroup.

Bootstrap-supported phylogenetic trees were constructed using the Genetic Algorithm for Rapid Likelihood Inference/GARLI 2.0 web service hosted at www.molecularevolution.org (Zwickl, 2006; Bazinet et al., 2014). Cladistic analyses were performed using maximum likelihood (ML) criteria (Felsenstein, 1981), and the general time-reversible model of sequence evolution with gamma distributed rate heterogeneity and proportion of invariant sites (GTR+I+G) (Hasegawa et al., 1985; Waddell and Steel, 1997). Statistical support for each reconstruction was determined by 2000 bootstrap pseudoreplicates to ensure <1% error at a 95% confidence interval (Hedges, 1992). Bootstrap '*P*' values (*BP*) are reported as the proportion of 2000 reconstructed trees (Efron, 1979; Hedges, 1992). Majority-rule consensus trees were constructed from 2000 bootstrap replicates and nodes with <50% support were collapsed.

Pyrosequencing

High throughput next-generation sequencing was used to increase sequencing depth and maximize the discovery of cyanobacteria diversity in environmental samples. 250 to 400 bp segments of the V6 region of the 16S rRNA gene (position 939F) were sequenced on a Roche GS FLX+ platform (Roche Diagnostics Corporation, Indianapolis, IN) at MrDNA labs [Shallowater, TX]. Raw pyrosequencing reads were quality checked and OTU clustered at a 97% sequence similarity cutoff in the QIIME environment (Caporaso et al., 2010). Chimeric sequences were detected and removed using ChimeraSlayer (Haas et al., 2011). Taxonomic identification was performed with the Greengenes database paired with the RDP classifier in the QIIME environment (DeSantis et al., 2006; Wang et al., 2007; Liu et al., 2008).

Data Processing and Statistical Analysis

The significance of categorical comparisons was determined by a paired t-test of sample means, calculated in the R statistical computing package V3.0.1, http://www.R-project.org (R Core Team, 2013). Correlation between environmental variables and cyanobacteria abundance was assessed using linear regression. *P*-values were found using a two-tailed test, except where indicated. Linear regression statistics were calculated using the VassarStats online statistical computation tools (vassarstats.net; ©Richard Lowry, 1998-2014, Professor of Psychology Emeritus, Vassar College).

Sequence Accessioning

Full-length cyanobacteria 16S rRNA sequences generated during this study can be found in GenBank under accession numbers KP793972 to KP793982 (T-045), KP793944 to KP793971 (MBS-2), KP794023 to KP794047 (T-034), KP794048 to KP794052 (GG-75m), KP793983 to KP794008 (T-031), and KP794009 to KP794022 (NT-3), KP793937 to KP793943 (T-05), KP793930 to KP793936 (T075-A), and KP762335 to KP762343 (T075-B).

RESULTS

El Tatio Geyser Field waters are moderate salinity (Na:Cl) type waters, with [Cl^-] concentrations of 160-180 mM in the Upper and Middle Basins, and ~3 mM in the Group M-III springs (Table 1-2). Discharging Upper Basin (UB) and Middle Basin (MB) waters are near equilibrium with respect to amorphous silica at the source, and geyserite (silica) precipitates to form terraces or sinter cones as waters cool and evaporate. pH is near-

neutral across all sites examined, varying between 6.86 to 7.11 at most sites, and 6.1 in Group M-III (Tables 1-1, 1-2, and 2-1).

El Tatio waters can be classified either as low DIC (< 0.57 mM), or high DIC (>1.74 mM). Among the features highlighted in this study, low DIC is found in the 'Great Geyser' (GG) and 'New Transect' (NT) in the MB (0.12-0.46 mM), and TAT09-031 in the UB (0.57 mM). Discharging low DIC geyser and spring waters are reducing, with high As^{III}: As^{V} ratios (~ 4:1), but low dissolved Fe^{2+} (Tables 1-1, 2-1). Total [As] is conservative along these outflows, maintaining 0.4-0.6 mM, with the proportion of As^{V} increasing downstream. High-DIC waters, with 1.7 to 2.89 mM DIC, tend to emerge from lower discharge springs that form pools, and As^{III}-oxidation occurs over much smaller spatial scales. In the case of MBS-1 and MBS-2, dramatically different As-redox speciation is observed at sites only centimeters apart, even though other geochemical parameters are very similar (TAT12-040, -041; Table 2-1).

Environmental Clone Library Description

Microbial mats from 12 locations were assessed using culture-independent Sanger sequencing, in order to obtain full-length cyanobacterial 16S rRNA sequences. The relative abundances of taxonomic groups in clone libraries can be found in Table 2-2; total sequence counts for these and other groups not represented in the table are shown in Table B-2. Seven sites contained cyanobacteria, GG-55, GG-75, T-31, T-34, T-45, MBS-2, and NT-3, whereas no clones identified as cyanobacteria were found in GG-25, GG-40, NT-1, NT-2, or MBS-1 (Table 2-2). Temperature >50°C and [As^{III}] >0.27 mM were the conditions common to sites where no cyanobacteria 16S rRNA sequences were

recovered (Table 2-1). These mat samples also showed low cyanobacterial abundance using 454-pyrosequencing, except for GG-40 m, which contained 34% of sequences classified as cyanobacteria (Table B-3). Cyanobacteria and Chloroflexi were the most commonly identified sequence groups in clone libraries, comprising up to 73% of sequences in each sample, where present (Table 2-2). Diversity measures were not employed using the Sanger dataset because significantly greater sequencing depth was uncovered in 454 libraries.

Of the 168 full-length cyanobacteria 16S rRNA sequences, 129 total from GG-75 (5 clones), T-31 (26), T-34 (25), T-45 (11), MBS-2 (28), and NT-3 (14) passed quality control standards imposed during alignment and the NCBI database submission tools (Table B-4). Clones from three enrichment cultures were also included in the analysis. T-05 (7 clones) was collected from a subaerially-exposed mat near the outflow of the GG, exposed to periodic splash water and steam (Figure B-1); T075, collected from the same site as GG-75 was divided into T075-A (4 clones) and T075-B (9 clones) enriched in BG-11(+N) either without or with 5% NaCl (Figure B-2). GG-75 had the highest taxonomic diversity of cyanobacteria even though few clones were uncovered compared to other sites that produced more cyanobacteria clones.

Full-length cyanobacteria clones were phylogenetically analyzed to visualize major groups of El Tatio cyanobacteria, their collection location(s), close relatives, and relative abundances (Figure 2-1, Table 2-3). A midpoint-rooted ML-tree showed two major divisions of ETGF cyanobacteria. Division A (*BP* = 84) contained 21 sequences classified in 3 major groups: Group 1, Group 2, and Group 3. Group 3 was subdivided

into Subgroups 3a (*BP* = 79) and 3b (*BP* = 100). Groups 1-3 are well supported (*BP* = 96 - 100). Division B was also well supported (*BP* = 84) and contained the remaining 108 sequences, which were divided into Group 4 (9 clones) and Group 5 (99 clones). Group 5 contained Subgroups 5a, 5b, and 5c (Figure 2-1, Table 2-3).

Group 1 was strongly supported (*BP* = 100) and comprised of five sequences from enrichment cultures T-05 and T075-A. A basic-local alignment search (BLAST) revealed 99% 16S rRNA sequence similarity to *Synechocystis* sp. Strain Sai002 and *Merismopedia glauca* Strain B1448-1 (Palinska et al., 1996), and 98% similarity to *Synechocystis* sp. Strain PCC 6803 (Kaneko et al., 1996). Group 2 contained 6 clones from T-45 that clustered into three well-supported pairs (*BP* = 98-100); each showed 98% similarity to *Oscillatoria kawamurae* and *Oscillatoria duplisecta* Strain ETS-06 (Moro et al., 2007). Subgroup 3a was composed of four highly similar sequences from GG-75 m (*BP* = 86) that formed a sister group to one clone from T-31. During BLAST similarity searches no cultured or published sequences showed any similarity to Subgroup 3a; the closest match was an uncultured and unpublished sequence from hot springs in India. Subgroup 3b consisted of sequences from T-05 and T-075A, and showed 99% sequence similarity to *Leptolyngbya antarctica* Strain ANT.LACV6.1 (Taton et al., 2003; Taton et al., 2006).

Group 4 contained 9 sequences from T075-B, all forming a very well supported cluster (*BP* = 100) which likely represented the same organism due to their >99% similarity to one another. Based on their phylogenetic position with respect to other members of Nostocaceae (Subsection IV) the clones comprising Group 4 appear to

represent a novel genus, only having 97% 16S rRNA similarity to closest database matches (Table 2-3). Group 5 was the most abundant and widespread group of ETGF cyanobacteria clones with a total of 99 sequences from T075-A (1), GG-75 (1), T-31 (25), T-34 (25), T-45 (5), MBS-2 (28), and NT-3 (14). All three subgroups demonstrated 99% similarity to *Fischerella* sp., except for T075-A_6, which shows 97% similarity to the *Fischerella* sp. strains listed in Table 2-3.

Phylogenetic Assignment of ETGF Cyanobacteria

A 16S rRNA phylogenetic analysis was constructed from 33 reference sequences (Table B-1), environmental enrichment culture sequences, and 129 culture-independent sequences in order to assess the diversity and abundance of ETGF cyanobacteria. Culture-independent clones were obtained from GG-75, MBS-2, NT-3, T-31, T-34, and T-45, and a cyanobacterial sequence from previous work at ETGF (Tat-08-003-12-10) was also considered (Figure 2-2). Division A clones are found in the lower portion of the phylogenetic reconstruction along with members of Subsections I/III cyanobacteria, known as the *Oscillatoriales* (Figure 2-2). Division B clones were positioned in a monophyletic group (*BP* = 84); internal relationships were not well resolved due to the close sequence similarity of many sequences, but two well-supported groups, 4 and 5 were seen.

Group 5 ETGF clones, along with *Chlorogloeopsis fritschii* PCC 6912 and *Fischerella* sp. formed a well-supported monophyletic group (*BP* = 99). Previously sequenced and uncultured ETGF clone Tat-08-003-12-10, and Subgroups 5a-5c were 99% related to *Fischerella thermalis* Strain PCC 7521 and *Fischerella sp*. Strain MV-11

(Table 2-3). Nearly all *Fischerella* sp. clones grouped more closely to ETGF clone Tat-08-003_12_10 than to the database reference sequences used in the reconstruction (Figure 2-2).

Mastigocladus/*Fischerella* sp. clones from geothermal sites worldwide (Miller and Bebout, 2004; Miller et al., 2007; Roeselers et al., 2007; Finsinger et al., 2008; Ionescu et al., 2010; Clingenpeel et al., 2011; Engel et al., 2013) were compared to Group 5 *Fischerella* clones (Figure 2-3, Table B-5). Seven well-supported *Fischerella* groups have been identified from geothermal areas on nearly every continent (Miller et al., 2007). El Tatio *Fischerella* sequences affiliate closely with Groups 1 and 7, whereas no Group 2, or 3, and no clearly affiliated Group 4 or 6 sequences were seen. A set of 23 sequences formed a well-supported group (*BP* = 94) that did not match any previously published *Fischerella* sp. clones and only matched ETGF clone Tat-08-003_12_41 (Engel et al., 2013).

Cyanobacteria Diversity through 454-pyrosequencing

Short-read 16S rRNA sequences were generated by pyrosequencing in order to obtain a robust approximation of the breadth and depth of cyanobacterial diversity at ETGF. The most abundance organisms seen in clone libraries were also seen at high abundance in pyrosequencing libraries, but more diversity was uncovered by high-throughput sequencing allowing the quantification of species richness, evenness, and a semi-quantitative assessment of relative abundances of cyanobacteria and non-cyanobacterial OTUs (Table 2-4, Table B-6). Most sample rarefaction curves leveled off,

indicating that realized sequencing depth was sufficient to capture species richness in these samples (Figure B-3).

Phylum cyanobacteria was found to be comprised of 42 OTUs (97% cutoff) in the 13 sites examined; OTUs that were absent in the clone libraries but present in pyrosequencing libraries were *Pleurocapsa* sp., *Chlorogloeopsis* sp., and *Synechococcus* sp. (Table B-3). Similar to clone library results, *Fischerella* sp. was most abundant, comprising >50% of all cyanobacteria genera in five out of the 12 samples that contained cyanobacterially-classified OTUs. Other abundant or widely occurring genera include *Leptolyngbya* sp., *Nostoc* sp., *Oscillatoria* sp., *Pleurocapsa* sp., *Prochlorothrix* sp., and *Synechococcus* sp. (Table B-3). Cyanobacterial OTUs with >100 sequence counts at a site, in order of most to least abundant, were taxonomically identified as *Fischerella muscicola* found at 10 sites, *Nostoc punctiforme, Leptolyngbya laminosa,* and *Pleurocapsa* sp., each found at 2 locations, and *Oscillatoria* sp., *Synechococcus elongatus*, *Nostoc commune*, *Leptolyngbya frigida*, and *Arthrospira platensis*, each found at a single site. The other 33 cyanobacteria OTUs were found at low abundance (<1.5%).

Cyanobacteria abundance at the phylum level was chosen as a metric for the distribution of cyanobacteria; higher abundances of cyanobacteria sequences were assumed to indicate more favorable niches relative to sites with low cyanobacteria abundance. Linear regression showed that only a few variables significantly influenced cyanobacteria abundance and diversity throughout ETGF (Table 2-5). Temperature negatively correlated with cyanobacteria abundance ($r^2 = 0.36$, $P < 0.01$). Cyanobacteria abundance also negatively correlated to [As^{III}] ($r^2 = 0.64$, $P < 1.8 \times 10^{-4}$) and positively to

[As^{V}] (r^2 = 0.42, P < 0.026). [Na^+] and [Cl^-] were not found to influence cyanobacteria abundance, with low r^2 values and $P >> 0.05$ (Table 2-5).

DIC does not show linear relationships with cyanobacteria abundance or biomass; categorical analysis is more appropriate because DIC values are clustered below 0.5 mM and above 1.6 mM. The abundance and community dominance of cyanobacteria was possibly influenced by DIC; 80% cyanobacteria abundance was observed in the presence of high DIC, even at some of the highest temperatures (58°C). A paired t-test comparison between 24 replicates obtained from 5 low and 5 high DIC sites showed that biomass is significantly greater at high-DIC sites ($P << 0.001$, df = 23) (Figure 2-4). Although cyanobacteria abundance did not correlate to biomass, categorical comparison shows that sites with >40% cyanobacteria abundance contain significantly higher biomass compared to sites with low cyanobacteria abundance ($P << 0.001$, df = 27; Figure 2-5).

The most abundant and widely distributed cyanobacteria OTUs (97% cutoff) were also compared to environmental variables (Table 2-5). The most abundant cyanobacteria OTUs were *Fischerella* sp., *Nostoc* sp., *Oscillatoria* sp., and *Pleurocapsa* sp. Among these, only *Fischerella* correlated to environmental variables due to its occurrence at the largest number of sites. No significant correlation was observed between environmental variables and *Nostoc* sp. (GG-40), *Pleurocapsa* sp. (GG-75), and *Oscillatoria* sp. (T-45). The strongest relationship was a negative correlation between [As^{III}] and *Fischerella* abundance (r^2 = 0.46, P < 0.01). *Fischerella* also showed a significant negative relationship to temperature using a one-tailed test, but not a two-tailed test (r^2 = 0.22, P <

0.05); *Fischerella* positively correlated with [As^{V}], also using a one-tailed test ($r^2 = 0.24$, $P < 0.05$).

Cyanobacteria and Community-level Properties

The relative contribution that geochemical variables and cyanobacteria abundance played in influencing overall diversity and biomass was also investigated. [Na^{+}], [Cl^{-}], and [As^{V}] showed no correlation to species richness, however, temperature and [As^{III}] showed a significant negative correlation to richness using a one-tailed test. [DIC] showed a very strong linear relationship to species richness; high-DIC sites contained significantly greater species richness (Table 2-6). Cyanobacteria and Chloroflexi showed a strong negative relationship to each other ($r^2 = 0.57$, $P < 0.001$), the strength of which is much higher than their correlation to any variable except [As^{III}]; Chloroflexi are abundant at high-As^{III} sites, whereas cyanobacteria dominate As^{V}-rich sites and few to no Chloroflexi are seen in stream regions dominated by As^{V}. This pattern is especially evident along low-DIC and high-As stream transects such as the GG and NT (Table 2-1).

As^{III}-oxidation and Primary Producer Succession

The succession of cyanobacteria and Chloroflexi, another important primary producer in geothermal systems, was analyzed along the low-DIC Great Geyser transect with respect to As^{III}-oxidation, temperature decrease, and species richness. Geochemical data and pyrosequencing data captured the abundance and diversity of cyanobacteria, species richness, and corresponding microbial community structure at 25-, 30-, 40-, 55-, and 75 m (Table 2-1, 2-4, Figure 2-6).

GG waters were initially reducing and discharged four times more As^{III} than As^{V} at the geyser outflow. No subaqueous microbial mats were seen near the source, though a thin gray film dominated by Deinococcus-Thermus and some Chloroflexi began to appear in the first 5-10 m of the outflow (Engel et al., 2013). Bright green cyanobacterial mats were seen in a subaerial zone exposed to periodic splashes of ~55°C water and steam around the edge of the geyser pool and along the first 10-15 meters of the stream (sample T-05 (Figure B-1).

When the geyser water cooled to 60-65°C reddish-brown streamers composed of Chloroflexi (24%), Deferribacteres (13%), and Firmicutes (48%) colonized the bottom of the stream channel (Table B-6). As^{III}-oxidation occurred rapidly in the next 15-20 m stream reach (Figure 2-6). Between 30 and 40 meters As^{V} became the dominant As-species with four times more As^{V} than As^{III}; As is found as As^{V} for long distances downstream. Near the transition from As^{III} to As^{V} dominance at 40 m, microbial mats changed abruptly from streamers to an orange-green and laminated mat morphology; a significant increase in biomass also began between 40 and 55 m, continuing to 75 m where the community was dominated by Cyanobacteria (48%), Proteobacteria (30%), Chlorobi (7%), and Bacteroidetes (8%) (Table B-6). Chloroflexi dominated streamers whereas mats began to appear where cyanobacteria abundance increased which corresponded to the rapid transition to As^{V}-dominated water in this stream.

As^{III}-oxidation was the primary geochemical variable that corresponded to the pattern of Chloroflexi and cyanobacteria abundance seen along the GG stream. Chloroflexi were very abundant in the As^{III}-dominated stream region, especially between

30-40 m where As^{III}-oxidation was rapid (Figure 2-6). At 40 m, where As-redox species dominance shifted from As^{III} to As^{V}, the community shifted from Chloroflexi- to cyanobacteria-based with some overlap in their range between 40 and 55 m. The zone of cyanobacterial occupation beyond 40 m was marked by increased biomass and more cohesive mat material is seen beyond 40 m, corresponding to As^{V}-dominance and increased cyanobacteria habitation (Table 2-4). Temperature steadily decreased along the length of the stream, and the rate of decrease did not appear to influence the sudden increase in cyanobacteria abundance seen at 40 m; As^{III}-oxidation corresponded very closely. Species richness also tracked closely with cyanobacteria abundance along the GG stream and also increased at 40 m (Figure 2-6).

DISCUSSION

No springs anywhere else in the world, possess the combination of neutral pH, low DIC, and high-As seen at ETGF; previous ecological studies on thermophilic cyanobacteria have been conducted in environments with neutral to alkaline pH and high DIC (Castenholz, 1973; Brock, 1978; Garcia-Pichel and Castenholz, 1990; Ward et al., 1998; Ward and Castenholz, 2000; Ward and Cohan, 2005; Boyd et al., 2012; Ward et al., 2012). Temperature was shown to be the primary variable that controls cyanobacterial distribution and diversity in hot springs; light, aqueous chemistry, and microbial interactions (such as competition for nutrients) typically explain more localized differences among geothermal waters at similar temperatures (Ward and Castenholz, 2000; Cox et al., 2011; Boyd et al., 2012; Hamilton et al., 2012; Ward et al., 2012). In

alkaline siliceous springs at YNP, chemical factors known to influence the taxa found at different temperature ranges include pH (Brock, 1978), sulfide (Garcia-Pichel and Castenholz, 1990; Cox et al., 2011), and combined nitrogen (Ward and Castenholz, 2000). In springs with low combined nitrogen, N_2-fixing cyanobacteria should predominate; springs that contain high combined nitrogen, non-N-fixers should prevail upstream, and then be succeeded by heterocystous forms as combined nitrogen is removed downstream (Ward et al., 2012).

A combination of temperature and As, especially As-redox speciation, appear to control the realized niche occupied by cyanobacteria throughout ETGF, with clear and significant negative relationships to both increasing temperature and increasing concentrations of As^{III}. Visual characteristics of mats such as thickness, tensile strength, and color change visibly along temperature gradients. Results from the present study show that temperature plays an important organizational role for cyanobacteria abundance and diversity across sites at ETGF, yet several locations were found to lack cyanobacteria at temperatures where they would otherwise be found; this indicates that parameters other than temperature also play a role in driving the distribution of cyanobacteria at ETGF. Sharp upper boundaries to cyanobacterial occupation are seen in streams with continuous temperature gradients, a pattern that has also been observed at YNP due to sulfide and combined nitrogen.

DIC did not correlate to cyanobacteria abundance as was predicted based on the observation that cyanobacteria-dominated communities had greater biomass in DIC-rich streams; however, cyanobacteria possess a CCM that allows them to acclimate to low

carbon concentrations. DIC content is bimodal at ETGF; sites contain either low or high DIC but no intermediate concentrations were found. Although DIC does not appear to play a major role in determining the realized niche of cyanobacteria there is a complex feedback of interactions between DIC, cyanobacteria and higher community level properties such as biomass, diversity, abundance and evenness/dominance (Table 2-4). High-DIC communities appear to support a greater proportion of cyanobacteria relative to a smaller, but more diverse accompanying community of non-photosynthetic microorganisms compared to low-DIC sites. Low-DIC sites with cyanobacteria support more diverse communities than low-DIC sites without cyanobacteria, and higher-DIC sites can support higher biomass, especially when cyanobacteria are dominant community members.

The occurrence of particular microorganisms in geothermal springs is a function of physical and biological factors acting across multiple geographic scales (Papke et al., 2003; Martiny et al., 2006; Ward et al., 2012). Hot springs occur in localized areas separated by large physical distances, analogous to islands; dispersal among these locations may be limited in a similar manner (MacArthur and Wilson, 1967). On larger geographic scales, dispersal barriers may control which microorganisms are observed in certain regions (Finlay, 2002; Papke et al., 2003). There are several well-studied thermophilic cyanobacteria that have distinct global distribution patterns related to their environmental tolerances and dispersal strategy, but many thermophilic cyanobacteria exhibit a severely restricted geographic range (Ward and Castenholz, 2000).

An example of an organism with a restricted geographic range is the high temperature form of *Synechococcus* sp., which has only been confirmed in North America (Ward et al., 1998; Miller and Castenholz, 2000; Papke et al., 2003; Allewalt et al., 2006; Ward et al., 2012). Unicellular *Synechococcus* sequences were not found in clone library sequences, but were found to comprise a small part of the overall community in two pyrosequencing libraries; they were found to comprise 1% of sequences at GG 25, a high temperature and As^{III}-rich site, and as a very minor OTU in T-45, a high temperature and As-poor site (Table 2-4, Table B-3). *Synechococcus* is the predominant unicellular form at YNP; however, *Synechocystis* appears to be the dominant unicellular form to occupy ETGF springs.

No full-length ETGF clones were related to the low or high temperature forms of *Synechococcus* sp. Instead nearly 80% of culture-independent 16S rRNA sequences were identified as *Fischerella* sp. (Table 2-3). Filamentous, heterocystous, and akinete-forming *Fischerella* sp. has been described as a cosmopolitan organism, with highly similar 16S rRNA sequences distributed among hot springs found globally, although a positive correlation was shown between genetic differentiation and distance (Miller, 2007; Miller et al., 2007; Ionescu et al., 2010). Both clone library and 454-pyrosequencing-library analysis found *Fischerella*-like sequences to be the most abundant and widespread cyanobacterial genotype at ETGF, identified at many sites with a variety of temperatures and geochemical constituents (Figure 2-2, Table 2-1). A large number of ETGF *Fischerella* (25%) cluster into their own group, which does not include any previously

published sequences (Figure 2-3, Table B-5). Members of this sequence group are found in five of the six ETGF clone libraries that contain cyanobacteria.

The distribution of cyanobacteria and Chloroflexi at ETGF may be analogous to previously described relationships due to high sulfide concentration; Chloroflexi use sulfide as an electron donor for anoxygenic photosynthesis (Giovannoni et al., 1987; van der Meer et al., 2000). High sulfide prevents cyanobacterial colonization in upstream areas in some YNP streams due to its inhibitory effect on photosynthesis (Ward et al., 2012); however, sulfide decreases downstream to levels that permit their colonization downstream (van der Meer et al., 2000).

Results from this study show a similar interaction, but instead of removing sulfide, Chloroflexi remove As^{III} allowing cyanobacteria colonization downstream. The presence of As^{III}-oxidase (*aio*A) genes homologous to *Chloroflexus aurantiacus* suggests that As^{III} acts as a replacement electron donor for anoxygenic photosynthesis at ETGF in lieu of sulfide, which is extremely low. The presence of sulfide and sulfite has been shown to inhibit As^{III}-oxidation (Lieutaud et al., 2010) rendering ETGF a rare system where enzymatic As^{III}-oxidation is more likely to occur due to the absence of free sulfide.

My working model of primary producer succession along low-DIC streams at ETGF begins with primary production in the upstream microbial community dominated by microorganisms such as Chloroflexus and proteobacteria that may use As^{III} as an electron donor for anoxygenic photosynthesis (Engel et al., 2013). As^{III} oxidation results in mobile and mat-adsorbed As^{V} (Figure 2-6). Once As^{III}-oxidation nears completion *Chloroflexus* sp. decrease in abundance, presumably due to the loss of their electron

donor for anoxygenic photosynthesis in the sulfide-poor mats at ETGF. When As^{III} is depleted *Chloroflexus* sp. are outcompeted for inorganic carbon by efficient CCM-utilizing cyanobacteria.

Culture independent sequencing methods reveal that most cyanobacteria are closely related to heterocystous filamentous cyanobacteria; unicellular organisms are present but not abundant enough to detect in clone libraries unless enriched in BG-11(+N) media where they can outgrow filamentous forms. The high abundance of *Fischerella* reflects the isolated nature of ETGF at high elevation in the driest desert in the world. *Fischerella* survive periods of desiccation by forming resting cells (akinetes), can colonize nutrient-poor environments by fixing nitrogen and carbon; due to their ubiquity throughout ETGF features they must also have substantial As-tolerance

Results from this study show that cyanobacteria are abundant and ecologically important contributors to microbial communities in the carbon-limited waters of El Tatio Geyser Field. DIC is limiting at many geothermal features, shown by low biomass in low-DIC compared to high-DIC features. High DIC also positively impacts species richness; more DIC can lead to higher community function and support a higher diversity of microorganisms. Due to the unique ability of cyanobacteria to acquire sufficient carbon in spite of limitation, this negative impact is alleviated and higher biomass and species richness can be found in low DIC areas containing high cyanobacteria abundance, underscoring the vital role they play as primary producers in this carbon-starved ecosystem.

CHAPTER 2. TABLES AND FIGURES

Table 2-1: Selected geochemical data from microbial sample collection localities. All geochemical data are expressed in mmol/L. Missing data is marked as '-'. Site codes are abbreviated as follows: Great Geyser 'GG', New Transect 'NT', Middle Basin Springs 'MBS.'

Site ID	Sample ID	Basin	T°C	pH	[DIC]	[As^{III}]	[As^{V}]
GG-10 m[a]	-	Middle	71	6.86	0.43	0.37	0.12
GG-25 m	GG-25	Middle	65	6.92	0.39	0.36	0.16
GG-30 m	GG-30	Middle	62	6.92	0.39	0.36	0.14
GG-40 m	GG-40	Middle	55	6.92	0.30	0.30	0.20
GG-55 m	GG-55	Middle	46	6.96	0.24	0.13	0.41
GG-75 m	GG-75	Middle	37	7.10	0.12	0.12	0.42
TAT09-031	T-31	Upper	26	7.11	0.57	0	0.32
TAT09-034	T-34	Upper	58	6.86	2.40	0	0.27
TAT09-045	T-45	M-III	54	6.10	1.74	0	0.03
MBS-1	MBS-1	Middle	60	7.00	2.89	0.25	0.11
MBS-2	MBS-2	Middle	40	7.00	2.89	0	0.36
NT-1	NT-1	Middle	60	6.89	0.46	0.33	0.15
NT-2	NT-2	Middle	50	6.92	0.29	0.27	0.20
NT-3	NT-3	Middle	40	6.96	0.18	0	0.51

[a]No microbiological sampling was performed at this location.

Table 2-2: Abundances (%) of the most common bacterial phyla observed in Sanger sequencing clone libraries. 'Other taxa' can be found in Appendix B-1.

Sample	Cyano.	Chlorofl.	Chlorobi	Cand. OP11	Deinococc.-Thermus	Firmicutes	Proteobac.	Other taxa
GG-25	0	0	0	37.5	0	28.1	0	31.3
GG-40	0	18.8	9.4	21.9	9.4	9.4	0	12.5
GG-55	19.4	67.7	0	0	0	0	0	12.9
GG-75	17.9	0	14.9	1.5	1.5	2.3	31.3	14.9
T-31	73.2	3.6	0	1.8	0	0	10.7	5.4
T-34	65.0	10.4	0	16.7	0	4.2	0	0
T-45	67.5	0	0	0	0	0	2.5	7.5
MBS-1	0	38.7	9.7	25.8	3.2	3.2	3.2	12.9
MBS-2	73.5	0	0	6.1	4.1	0	10.2	4.1
NT-1	0	17.9	3.6	39.3	0	0	25	7.1
NT-2	0	28.1	3.1	31.3	6.3	9.4	3.1	9.4
NT-3	31.9	29.8	2.1	10.6	0	0	4.3	21.3

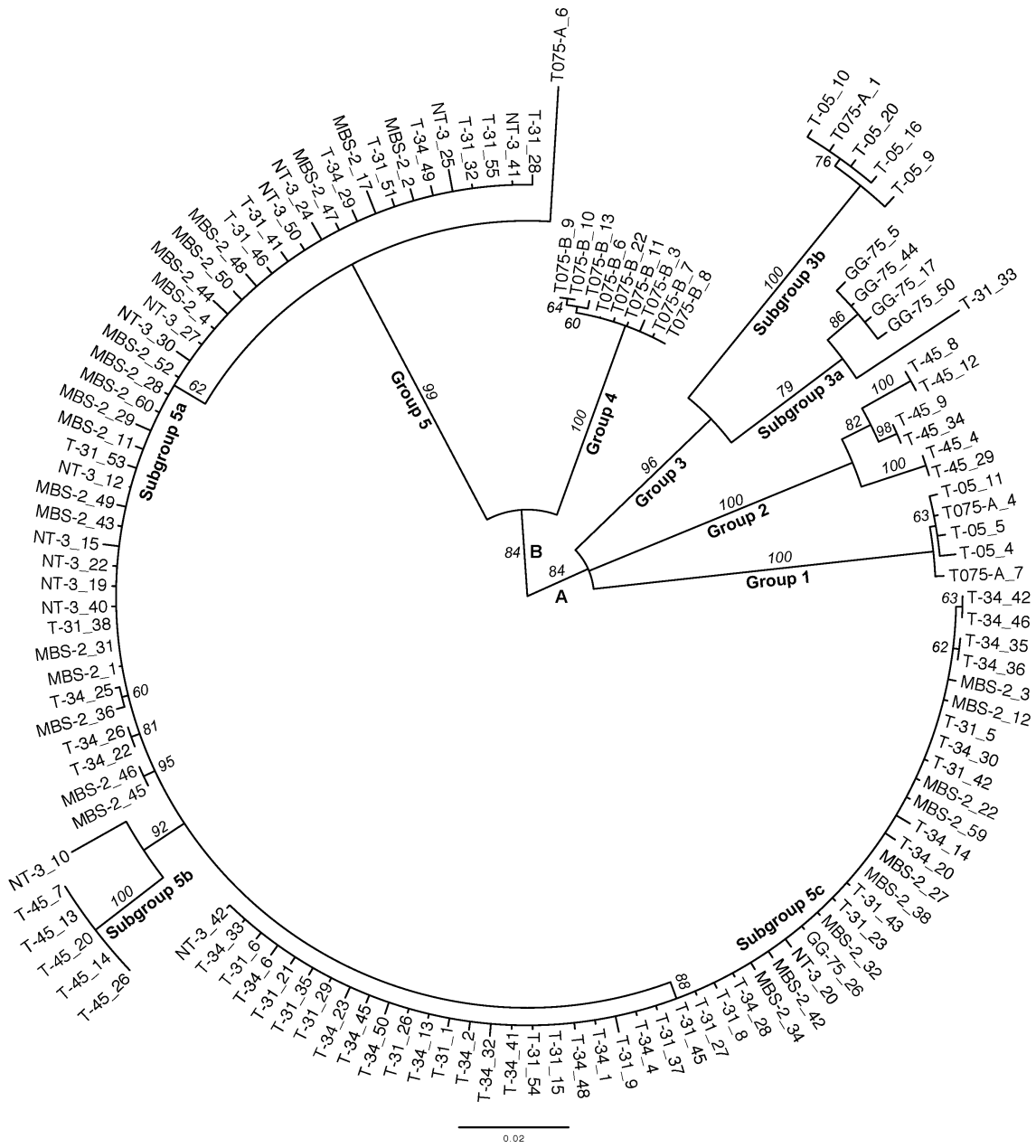

Figure 2-1: Midpoint-rooted phylogenetic reconstruction of 129 cultured and culture-independent cyanobacteria clones sequenced from ETGF. The tree was constructed under maximum likelihood criteria using GTR+I+G model with no outgroup. The scale bar reflects a genetic distance of 0.02.

Table 2-3: Summary of 129 cyanobacterial clones derived from ETGF microbial mat samples, closest NCBI database relatives, and proposed taxonomy based on closest relatives to the lowest possible taxonomic subdivision. *Gen. and sp. nov.* indicates candidate for a novel organism.

Div.	Group	Clones	#	Closest NCBI relatives to all clones in Group/Subgroup (Genbank ID)	%ID	Taxonomic hierarchy (Bacteria; Cyanobacteria; _____; _____)
A	Group 1	T075-A_4 (_7) T-05_4, _5, _11	5	*Synechocystis* sp. Strain Sai002 (GU935368) *Merismopedia glauca* Strain B1448-1 (X94705)	99 99	Oscillatoriophycideae; Chroococcales; *Synechocystis* sp.
A	Group 2	T-45_4 (_8, 9, 12, 29, 34)	6	Oscillatoria kawamurae (AB298443) Oscillatoria duplisecta ETS-06 (AM398647)	98 98	Oscillatoriophycideae; Oscillatoriales; possible *Oscillatoria* sp.
A	Group 3, Subgroup 3a	T-31_33 GG-75_5 (_17, 44, 50)	5	Uncult. Oscillatoriales cyanobacterium (HF677163)	99	Oscillatoriophycideae; unknown
A	Group 3, Subgroup 3b	T05_9, (_10, 16, 20) T075-A_1	5	Leptolyngbya antarctica ANT.LACV6.1 (AY493589)	99	Oscillatoriophycideae; Oscillatoriales; *Leptolyngbya*
B	Group 4	T075-B_3, (_6, 7, 8, 9, 10, 11, 13, 22)	9	*Cyanospira rippkae* (AY038036)	97	Nostocales; Nostocaceae; *gen. and sp. nov.*
B	Group 5, Subgroup 5a	T-31* T-34* NT-3* MBS-2*	44	Tat-08-003_12_10 (GU437365) *Fischerella* sp. MV11 (DQ786171) Uncult. Fischerella sp. Clone YL099 (HM856465) *Fischerella* sp. RV14 (DQ786172)	99 99 99 99	Stigonematales; *Fischerella*
B	Group 5, Subgroup 5b	NT-3_10 T-45_7, (_13, 14, 20, 26)	6	Tat-08-003_12_10 *Fischerella* sp. MV11 Uncult. Fischerella sp. Clone YL099 *Fischerella* sp. RV14	98 97-98 98-99 97	Stigonematales; *Fischerella*
B	Group 5, Subgroup 5c	GG-75_26 T-31* T-34* NT-3* MBS-2* T075-A_6#	49	Tat-08-003_12_10 *Fischerella* sp. MV11 Uncult. Fischerella sp. Clone YL099 (HM856465) *Fischerella* sp. RV14	99 99 99 99 #97	Stigonematales; *Fischerella*

*See Fig. 1 for complete list of clones from these sites.

T075-A_6 matched the same sequences as the rest of Subgroup 5a, but with a different %ID the first two organisms (#97).

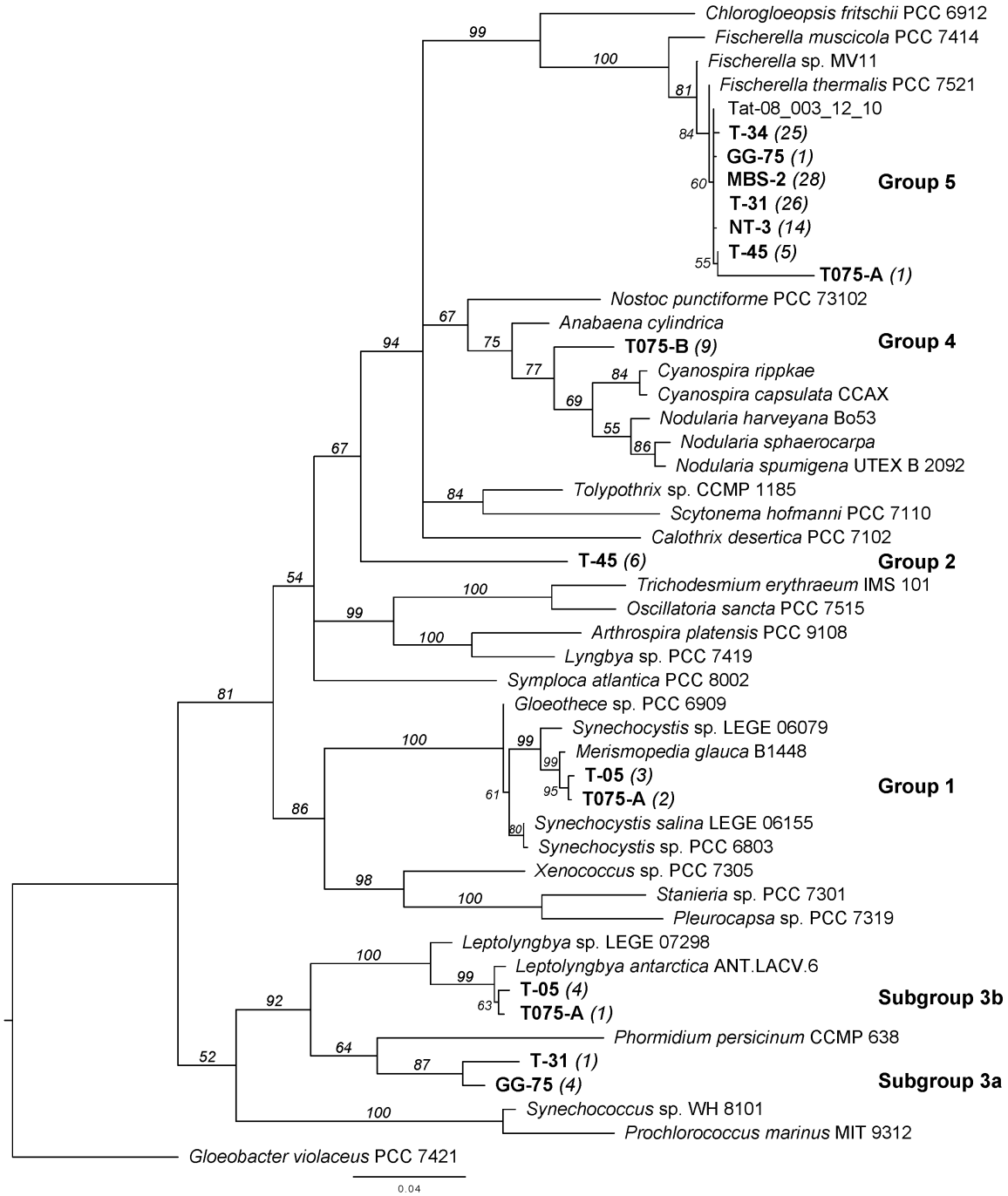

Figure 2-2: Phylogenetic reconstruction of 129 cyanobacteria clones, compared to reference sequences shows the diversity of cyanobacteria found in El Tatio geothermal features. *Gloeobacter sp*. Strain PCC 7421 was used as an outgroup. The tree was constructed under maximum likelihood criteria using the GTR+I+G model of sequence evolution.

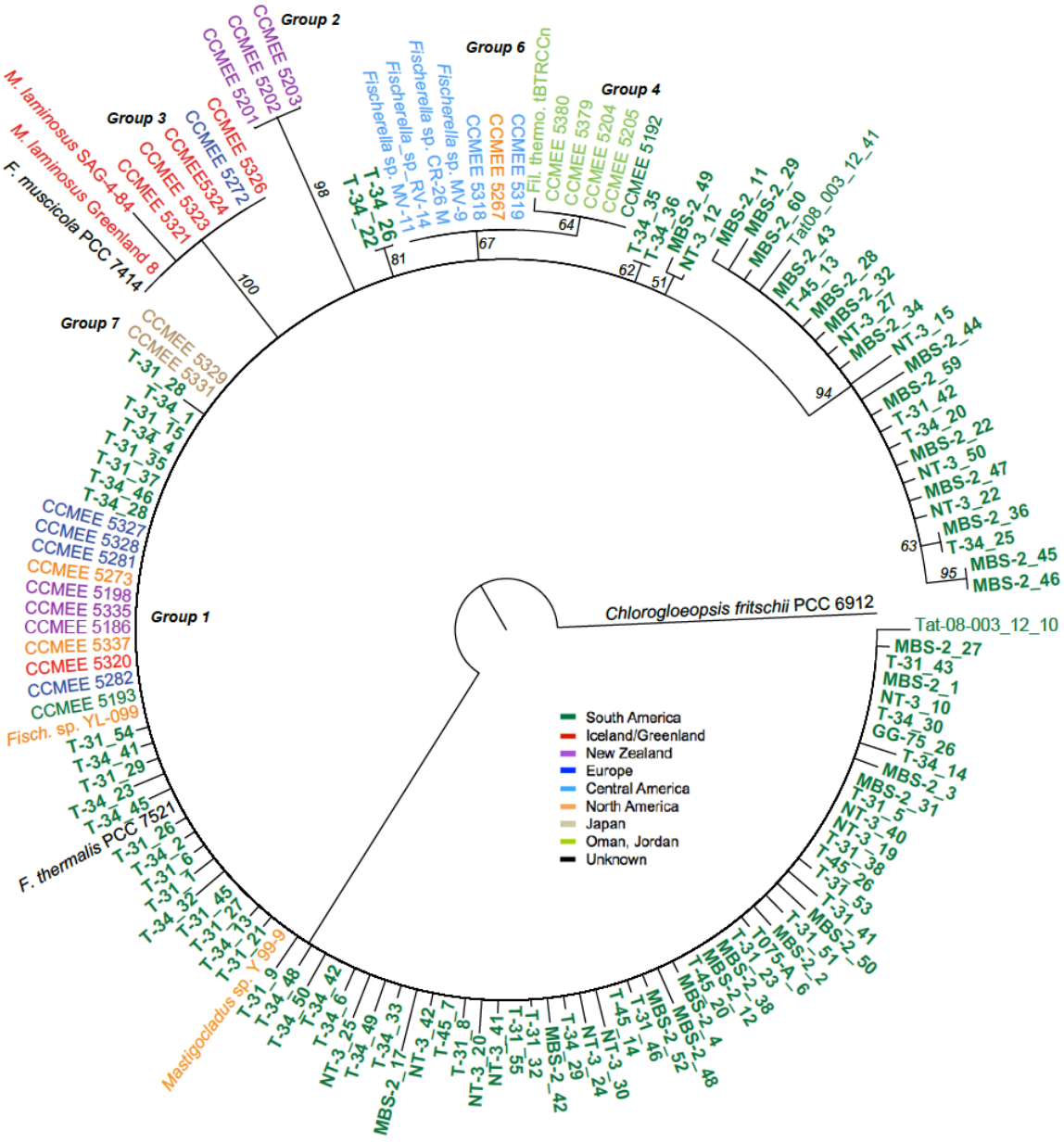

Figure 2-3: Annotated tree of *Fischerella* 16S rRNA sequences, color-coded by their geographic origin. *Chlorogloeopsis* was used as an outgroup. *Mastigocladus* (*M. laminosus*) is synonymous with *Fischerella*. El Tatio clones from this study are in bold. Genetic distances are very small (0.5 inch bar= 0.004).

Table 2-4: Cyanobacterial abundance and diversity measures in pyrosequencing samples. Cyanobacteria abundance is expressed as % abundance at the phylum level (P). All geochemical data is expressed in mmol/L. Biomass is expressed as % mass lost on ignition (LOI). Missing data is marked as '-'. Diversity measures were computed in the 'Vegan' R package on OTU tables constructed at a 97% cutoff level in the QIIME environment.

Site	% Biomass	% Cyano.[a]	Cyano. OTUs	Spp. richness	Richness-Chao1[b]	Pielou's evenness[c]	Simpson's Index (1-D)[d]	Most abundant cyano genera
GG 25	14.4 ± 1.8	1.3	5	33	37	0.58	0.23	*Synechococcus* sp. > *Chroococcidiopsis*
GG 30	-	0.2	5	30	33	0.38	0.37	*Nostoc* sp. > *Prochlorothrix* sp
GG 40	9.0 ± 2.8	33.0	11	96	99	0.73	0.06	*Nostoc* sp. >> *Prochlorothrix* sp. > *Spirulina* sp.
GG 55	16.1 ± 2.1	34.3	7	84	85	0.56	0.17	*Fischerella* sp. >>> *Prochlorococcus*
GG 75	20.7 ± 2.4	46.2	18	155	122	0.61	0.18	*Pleurocapsa* sp. >>> *Fischerella* sp. > *Leptolyngbya* sp.
T-31	16.1 ± 1.8	80.2	9	95	97	0.27	0.63	*Fischerella* >>> *Microcoleus*
T-34	43.3 ± 2.4	80.5	12	83	84	0.26	0.63	*Fischerella* >>> *Microcoleus*

[a]The proportion of Phylum Cyanobacteria sequences in the community.

[b]Species richness estimated using the Chao 1 index, to estimate hidden species.

[c]A measure of evenness among community members, with a 1 indicating similar abundances among species (show equation)

[d]Simpson's Index of Diversity, measured as 1-D (D=Simpson's Index), which is the probability that two randomly selected individuals will belong to two different categories (OTUs).

Table 2-5: Linear regression analyses examining the influence of environmental parameters on cyanobacteria abundance. The statistical significance of these correlations are reported. Values in italics are not significant at a 95% confidence interval. Italicized values marked by a '*' are significant at a 90% confidence interval, to distinguish from those that lack a trend. One-tailed tests have n-1 degrees of freedom, two-tailed tests have n-2 degrees of freedom.

Independent variable	Dependent variable	R^2 (+/-)[a]	P-value (one-tailed)	P-value (two-tailed)	n
T°C	Cyanobacteria abundance	0.50 (-)	0.004	0.007	13
$[As^{III}]$	Cyanobacteria abundance	0.86 (-)	< 0.0001	< 0.0001	13
$[As^{V}]$	Cyanobacteria abundance	0.35 (+)	0.016	0.032	13
$[Na^{+}]$	Cyanobacteria abundance	0.03	*0.28*	*0.57*	10
$[Cl^{-}]$	Cyanobacteria abundance	0.002	*0.45*	*0.91*	6

[a]Indicates a positive or negative slope to the regression relationship.

Table 2-6: Linear regression analyses show the influence of environmental parameters and cyanobacteria abundance on community-level properties such as biomass and species richness. The significance of these correlations are reported. Values in italics are not significant at a 95% confidence interval. Italicized values marked by a '*' are significant at a 90% confidence interval, to distinguish from those that lack a trend. One-tailed tests have n-1 degrees of freedom, two-tailed tests have n-2 degrees of freedom.

Independent variable	Dependent variable	R^2 (+/-)[a]	P-value (one-tailed)	P-value (two-tailed)	n
T°C	LOI weight % biomass	0.042 (-)	*0.27*	*0.54*	11
[DIC]	LOI weight % biomass	0.082 (-)	*0.20*	*0.39*	11
$[As^{III}]$	LOI weight % biomass	0.12 (-)	*0.14*	*0.29*	11
$[As^{V}]$	LOI weight % biomass	0.22 (-)	*0.075**	*0.15*	11
Cyanobacteria abundance	LOI weight % biomass	0.013 (+)	*0.37*	*0.74*	11
T°C	Species Richness	0.26 (-)	0.039	*0.078**	13
[DIC]	Species Richness	0.32 (+)	0.021	0.043	13
$[As^{III}]$	Species Richness	0.30 (-)	0.027	*0.054**	13
$[As^{V}]$	Species Richness	0.092 (+)	*0.16*	*0.31*	13
Cyanobacteria abundance	Species Richness	0.29 (+)	0.029	*0.058**	13

[a]Indicates a positive or negative slope to the regression relationship.

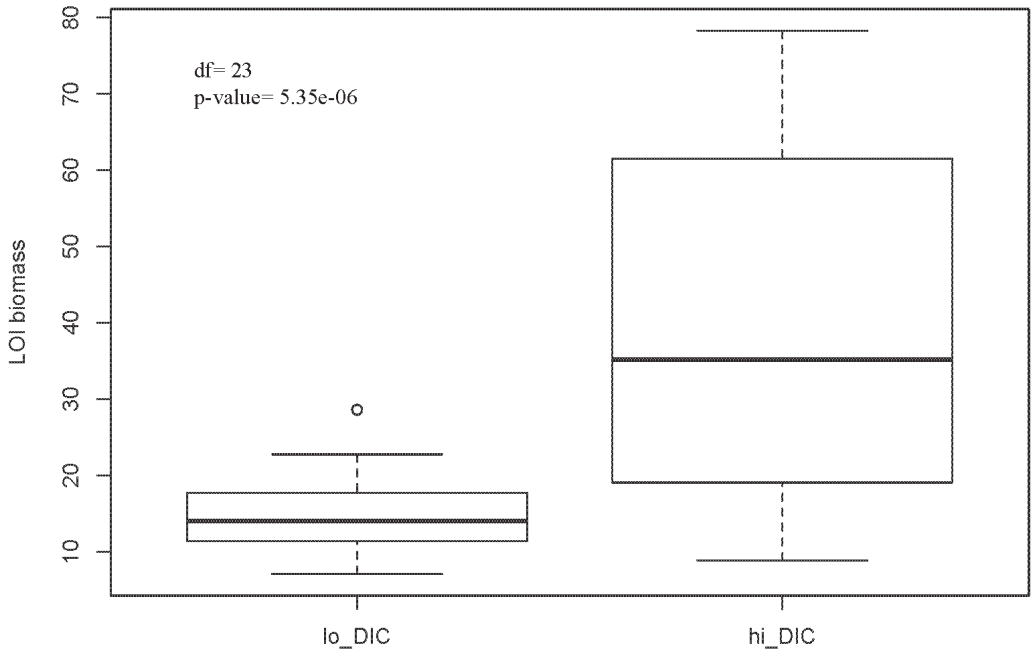

Figure 2-4: Comparison of biomass content of microbial mats in high and low-DIC features. Combustible organic content of microbial mats (LOI) is significantly higher in high [DIC] streams than in low [DIC] streams. These data combine samples from different springs, and are grouped only by [DIC].

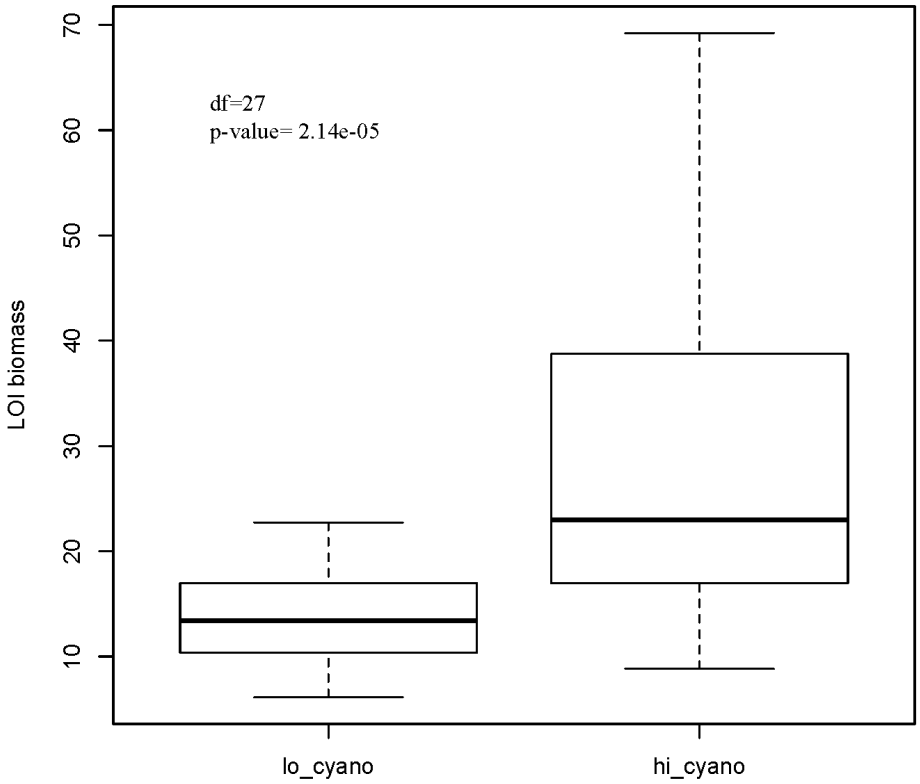

Figure 2-5: Comparison of the average biomass of low cyanobacteria (<40% abundance) and high cyanobacteria (>40% abundance) sites.

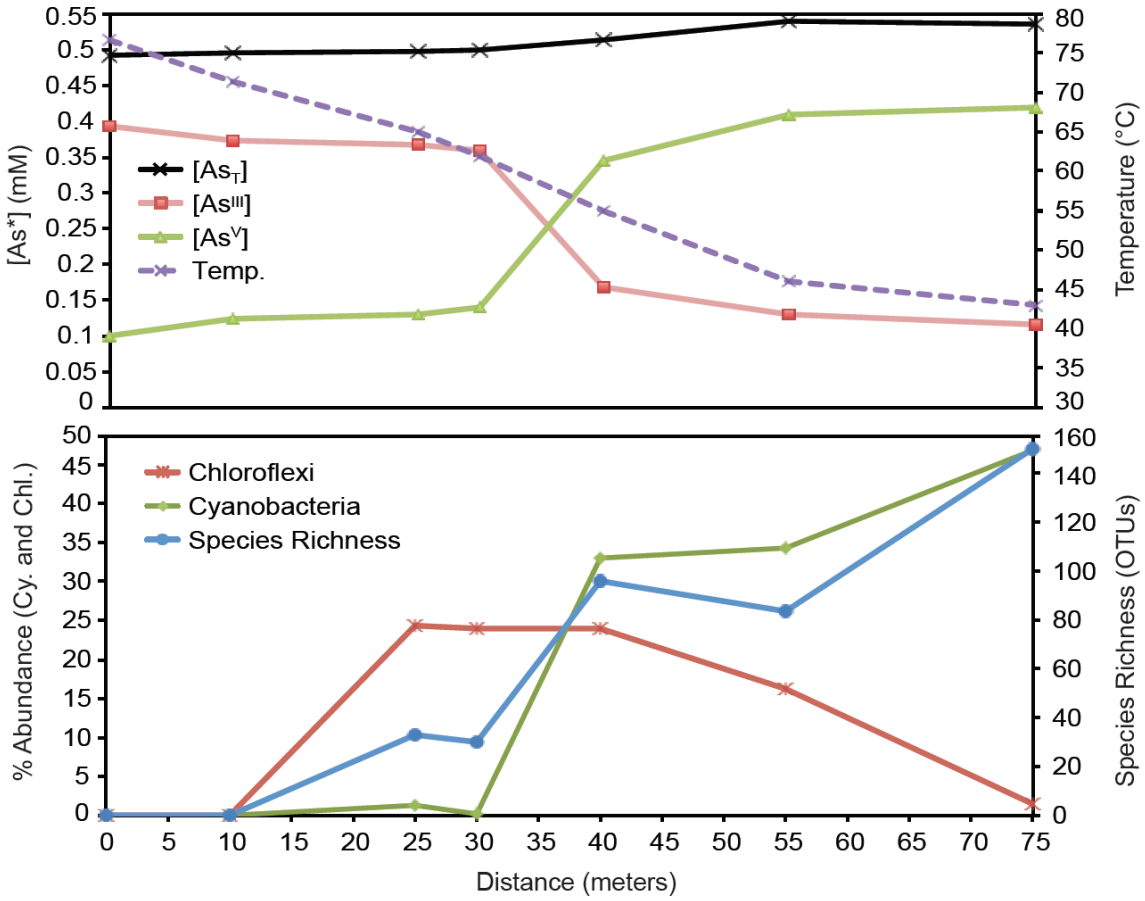

Figure 2-6: Total As, As-redox, and temperature along a 75 m section of the Great Geyser transect (A), as well as cyanobacteria and chloroflexus abundance and overall species richness (B) along the same transect.

REFERENCES

Allewalt, J.P., Bateson, M.M., Revsbech, N.P., Slack, K., and Ward, D.M. (2006) Effect of temperature and light on growth of and photosynthesis by Synechococcus isolates typical of those predominating in the octopus spring microbial mat community of Yellowstone National Park. *Applied and Environmental Microbiology* **72**: 544-550.

Altschul, S.F., Gish, W., Miller, W., Myers, E.W., and Lipman, D.J. (1990) Basic Local Alignment Search Tool. *Journal of Molecular Biology* **215**: 403-410.

Badger, M.R., and Price, G.D. (1992) The CO_2 concentrating mechanism in cyanobacteria and microalgae. *Physiologia Plantarum* **84**: 606-615.

Badger, M.R., Price, G.D., Long, B.M., and Woodger, F.J. (2006) The environmental plasticity and ecological genomics of the cyanobacterial CO_2 concentrating mechanism. *Journal of Experimental Botany* **57**: 249-265.

Bazinet, A.L., Zwickl, D.J., and Cummings, M.P. (2014) A gateway for phylogenetic analysis powered by grid computing featuring GARLI 2.0. *Systematic Biology* **63**: 812-818.

Boyd, E.S., Fecteau, K.M., Havig, J.R., Shock, E.L., and Peters, J.W. (2012) Modeling the habitat range of phototrophs in yellowstone national park: toward the development of a comprehensive fitness landscape. *Frontiers in Microbiology* **3**: 221.

Brock, T.D. (1978) Life at high temperatures. *Science* **158**: 1012-1019.

Caporaso, J.G., Kuczynski, J., Stombaugh, J., Bittinger, K., Bushman, F.D., Costello, E.K. et al. (2010) QIIME allows analysis of high-throughput community sequencing data. *Nat Methods* **7**: 335-336.

Castenholz, R.W. (1973) The possible photosynthetic use of sulfide by the filamentous phototrophic bacteria of hot springs. *Limnology and Oceanography* **18**: 863-876.

Clingenpeel, S., Macur, R.E., Kan, J., Inskeep, W.P., Lovalvo, D., Varley, J. et al. (2011) Yellowstone Lake: high-energy geochemistry and rich bacterial diversity. *Environmental Microbiology* **13**: 2172-2185.

Connon, S.A., Koski, A.K., Neal, A.L., Wood, S.A., and Magnuson, T.S. (2008) Ecophysiology and geochemistry of microbial arsenic oxidation within a high arsenic, circumneutral hot spring system of the Alvord Desert. *FEMS Microbiology Ecology* **64**: 117-128.

Cox, A., Shock, E.L., and Havig, J.R. (2011) The transition to microbial photosynthesis in hot spring ecosystems. *Chemical Geology* **280**: 344-351.

Dean, W.E. (1974) Determination of carbonate and organic matter in calcareous sediments and sedimentary rocks by loss on ignition: comparison with other methods. *Journal of Sedimentary Petrology* **44**: 242-248.

DeSantis, T.Z., Hugenholtz, P., Larsen, N., Rojas, M., Brodie, E.L., Keller, K. et al. (2006) Greengenes, a chimera-checked 16S rRNA gene database and workbench compatible with ARB. *Applied and Environmental Microbiology* **72**: 5069-5072.

Drever, J.I. (1988) *The Geochemistry of Natural Waters*. Engelwood Cliffs, NJ: Prentice-Hall.

Edgar, R.C., Haas, B.J., Clemente, J.C., Quince, C., and Knight, R. (2011) UCHIME improves sensitivity and speed of chimera detection. *Bioinformatics* **27**: 2194-2200.

Efron, B. (1979) Censored data and the bootstrap. *Journal of the American Statistical Association* **76**: 312-319.

Engel, A.S., Johnson, L.R., and Porter, M.L. (2013) Arsenite oxidase gene diversity among Chloroflexi and Proteobacteria from El Tatio Geyser Field, Chile. *FEMS Microbiology Ecology* **83**: 745-756.

Felsenstein, J. (1981) Evolutionary trees from DNA sequences: a maximum likelihood approach. *Journal of Molecular Evolution* **17**: 368-376.

Ferrari, S.G., Silva, P.G., González, D.M., Navoni, J.A., and Silva, H.J. (2013) Arsenic tolerance of cyanobacterial strains with potential use in biotechnology. *Revista Argentina de Microbiología* **45**: 174-179.

Finlay, B.J. (2002) Global dispersal of free-living microbial eukaryote species. *Science* **296**: 1061-1063.

Finsinger, K., Scholz, I., Serrano, A., Morales, S., Uribe-Lorio, L., Mora, M. et al. (2008) Characterization of true-branching cyanobacteria from geothermal sites and hot springs of Costa Rica. *Environmental Microbiology* **10**: 460-473.

Garcia-Pichel, F., and Castenholz, R.W. (1990) Comparative anoxygenic photosynthetic capacity in 7 strains of a thermophilic cyanobacterium. *Archives of Microbiology* **153**: 344-351.

Giovannoni, S.J., Revsbech, N.P., Ward, D.M., and Castenholz, R.W. (1987) Obligately phototrophic Chlororflexus: primary production in anaerobic hot spring microbial mats. *Archives of Microbiology* **147**: 80-87.

Haas, B.J., Gevers, D., Earl, A.M., Feldgarden, M., Ward, D.V., Giannoukos, G. et al. (2011) Chimeric 16S rRNA sequence formation and detection in Sanger and 454-pyrosequenced PCR amplicons. *Genome Research* **21**: 494-504.

Hamilton, T.L., Vogl, K., Bryant, D.A., Boyd, E.S., and Peters, J.W. (2012) Environmental constraints defining the distribution, composition, and evolution of chlorophototrophs in thermal features of Yellowstone National Park. *Geobiology* **10**: 236-249.

Hasegawa, M., Kishino, H., and Yano, T. (1985) Dating of the Human-Ape splitting by a molecular clock of mitochondrial DNA. *Journal of Molecular Evolution* **22**: 160-174.

Hedges, S.B. (1992) The number of replications needed for accurate estimation of the Bootstrap P value in phylogenetic studies. *Molecular Biology and Evolution* **9**: 366-369.

Ionescu, D., Hindiyeh, M., Malkawi, H., and Oren, A. (2010) Biogeography of thermophilic cyanobacteria: insights from the Zerka Ma'in hot springs (Jordan). *FEMS Microbiology Ecology* **72**: 103-113.

Jorgensen, B., and Nelson, D. (1988) Bacterial zonation, photosynthesis, and spectral light distribution in hot spring microbial mats of Iceland. *Microbial Ecology* **16**: 133-147.

Kaneko, T., Sako, S., Kotani, H., Tanaka, A., Asamizu, E., Nakamura, Y. et al. (1996) Sequence analysis of the genome of the unicellular cyanobacterium Synechocystis sp. Strain PCC6803. II. Sequence determination of the entire genome and assignment of potential protein-coding regions. *DNA Research* **3**: 109-136.

Kaplan, A., and Reinhold, L. (1999) CO_2 concentrating mechanisms in photosynthetic microorganisms. *Annual Review of Plant Physiology and Plant Molecular Biology* **50**: 539-570.

Landrum, J.T. (2007) Fate and Transport of Arsenic and Antimony in the El Tatio Geyser Field, Chile (Masters Thesis) The University of Texas at Austin.

Landrum, J.T., Bennett, P.C., Engel, A.S., Alsina, M.A., Pastén, P.A., and Milliken, K. (2009) Partitioning geochemistry of arsenic and antimony, El Tatio Geyser Field, Chile. *Applied Geochemistry* **24**: 664-676.

Larkin, M.A., Blackshields, G., Brown, N.P., Chenna, R., McGettigan, P.A., McWilliam, H. et al. (2007) Clustal W and Clustal X version 2.0. *Bioinformatics* **23**: 2947-2948.

Lieutaud, A., van Lis, R., Duval, S., Capowiez, L., Muller, D., Lebrun, R. et al. (2010) Arsenite oxidase from Ralstonia sp. 22: characterization of the enzyme and its interaction with soluble cytochromes. *The Journal of Biological Chemistry* **285**: 20433-20441.

Liu, Z., DeSantis, T.Z., Andersen, G.L., and Knight, R. (2008) Accurate taxonomy assignments from 16S rRNA sequences produced by highly parallel pyrosequencers. *Nucleic Acids Research* **36**: e120.

MacArthur, R.H., and Wilson, E.O. (1967) *The Theory of Island Biogeography*. Princeton, New Jersey: Princeton University Press.

Maidak, B.L., Cole, J.R., Lilburn, T.G., Parker Jr., C.T., Saxman, P.R., Farris, R.J. et al. (2001) The RDP-II (Ribosomal Database Project). *Nucleic Acids Research* **29**: 173-174.

Martiny, J.B., Bohannan, B.J., Brown, J.H., Colwell, R.K., Fuhrman, J.A., Green, J.L. et al. (2006) Microbial biogeography: putting microorganisms on the map. *Nature Reviews Microbiology* **4**: 102-112.

Miller, S.R. (2007) Diversity of the cosmopolitan thermophile Mastigocladus laminosus at global, regional and local scales. In *Algae and Cyanobacteria in Extreme Environments*. Seckbach, J. (ed): Springer, pp. 399-410.

Miller, S.R., and Castenholz, R.W. (2000) Evolution of thermotolerance in hot spring cyanobacteria of the genus Synechococcus. *Applied and Environmental Microbiology* **66**: 4222-4229.

Miller, S.R., and Bebout, B.M. (2004) Variation in Sulfide Tolerance of Photosystem II in Phylogenetically Diverse Cyanobacteria from Sulfidic Habitats. *Applied and Environmental Microbiology* **70**: 736-744.

Miller, S.R., Castenholz, R.W., and Pedersen, D. (2007) Phylogeography of the thermophilic cyanobacterium Mastigocladus laminosus. *Applied and Environmental Microbiology* **73**: 4751-4759.

Moro, I., Di Bella, M., Rascio, N., La Rocca, N., and Andreoli, C. (2007) Conferva duplisecta Pollini: rediscovery in Euganean Thermal Springs (Italy) and new assignment to the Oscillatoria genus. *Caryologia* **60**: 133-136.

Nordstrom, D.K., and Archer, D.G. (2003) Arsenic thermodynamic data and environmental geochemistry. In *Arsenic in Groundwater: Geochemistry and Occurrence*. Welch, A.H., and Stollenwerk, K.G. (eds). Boston: Kluwer Academic Publishers, pp. 1-25.

Nubel, U., Garcia-Pichel, F., and Muyzer, G. (1997) PCR primers to amplify 16S rRNA genes from cyanobacteria. *Applied and Environmental Microbiology* **63**: 3327-3332.

Paerl, H.W., Pinckney, J.L., and Steppe, T.F. (2000) Cyanobacterial-bacterial mat consortia: examining the functional unit of microbial survival and growth in extreme environments. *Environmental Microbiology* **2**: 11-26.

Palinska, K.A., Liesack, W., Rhiel, E., and Krumbein, W.E. (1996) Phenotype variability of identical genotypes: the need for a combined approach in cyanobacterial taxonomy demonstrated on Merismopedia-like isolates. *Archives of Microbiology* **166**: 224-233.

Papke, R.T., Ramsing, N.B., Bateson, M.M., and Ward, D.M. (2003) Geographical isolation in hot spring cyanobacteria. *Environmental Microbiology* **5**: 650-659.

Price, G.D., Sultemeyer, D., Klughammer, B., Ludwig, M., and Badger, M.R. (1998) The functioning of the CO2 concentrating mechanism in several cyanobacterial strains: a review of general physiological characteristics, genes, proteins, and recent advances. *Canadian Journal of Botany* **76**: 973-1002.

R Core Team (2013) R: A language and environment for statistical computing. In. Vienna, Austria: R Foundation for Statistical Computing.

Rippka, R., Deruelles, J., Waterbury, J.B., Herdman, M., and Stanier, R.Y. (1979) Generic assignments, strain histories and properties of pure cultures of cyanobacteria. *Journal of General Microbiology* **111**: 1-61.

Roeselers, G., Norris, T.B., Castenholz, R.W., Rysgaard, S., Glud, R.N., Kuhl, M., and Muyzer, G. (2007) Diversity of phototrophic bacteria in microbial mats from Arctic hot springs (Greenland). *Environmental Microbiology* **9**: 26-38.

Stal, L. (2012) Cyanobacterial Mats and Stromatolites. In *Ecology of Cyanobacteria II: Their Diversity in Space and Time*. Whitton, B.A. (ed): Springer Science+Business Media B.V.

Stal, L.J., van Gemerden, H., and Krumbein, W.E. (1985) Structure and development of a benthic marine microbial mat. *FEMS Microbiology Ecology* **31**: 111-125.

Taton, A., Grubisic, S., Brambilla, E., De Wit, R., and Wilmotte, A. (2003) Cyanobacterial Diversity in Natural and Artificial Microbial Mats of Lake Fryxell (McMurdo Dry Valleys, Antarctica): a Morphological and Molecular Approach. *Applied and Environmental Microbiology* **69**: 5157-5169.

Taton, A., Grubisic, S., Balthasart, P., Hodgson, D.A., Laybourn-Parry, J., and Wilmotte, A. (2006) Biogeographical distribution and ecological ranges of benthic cyanobacteria in East Antarctic lakes. *FEMS Microbiol Ecol* **57**: 272-289.

Turner, S., Pryer, K.M., Miao, V.P.W., and Palmer, J.D. (1999) Investigating deep phylogenetic relationships among Cyanobacteria and Plastids by small subunit rRNA sequence analysis. *Journal of Eukaryotic Microbiology* **46**: 327-338.

van der Meer, M.T., Schouten, S., de Leeuw, J.W., and Ward, D.M. (2000) Autotrophy of green non-sulphur bacteria in hot spring microbial mats: biological explanations for isotopically heavy organic carbon in the geological record. *Environmental Microbiology* **2**: 428-435.

Waddell, P.J., and Steel, M.A. (1997) General time-reversible distances with unequal rates across sites: mixing gamma and inverse Gaussian distributions with invariant sites. *Molecular Phylogenetics and Evolution* **8**: 398-414.

Wang, Q., Garrity, G.M., Tiedje, J.M., and Cole, J.R. (2007) Naive Bayesian classifier for rapid assignment of rRNA sequences into the new bacterial taxonomy. *Applied and Environmental Microbiology* **73**: 5261-5267.

Wang, S., Zhang, D., and Pan, X. (2012) Effects of arsenic on growth and photosystem II (PSII) activity of Microcystis aeruginosa. *Ecotoxicology and Environmental Safety* **84**: 104-111.

Ward, D.M., and Castenholz, R.W. (2000) Cyanobacteria in Geothermal Habitats. In *The Ecology of Cyanobacteria: Their Diversity in Time and Space*. Whitton, B.A., and Potts, M. (eds). Netherlands: Kluwer Academic Publishers, pp. 37-59.

Ward, D.M., and Cohan, F.M. (2005) Microbial Diversity in Hot Spring Cyanobacterial Mats: Pattern and Prediction. In *Geothermal Biology and Geochemistry in Yellowstone National Park*. Inskeep, W.P., and McDermott, T.R. (eds). Bozeman, MT: Montana State University Publications, pp. 185-201.

Ward, D.M., Castenholz, R.W., and Miller, S.R. (2012) Cyanobacteria in Geothermal Habitats. In *Ecology of Cyanobacteria II: Their Diversity in Space and Time*. Whitton, B.A. (ed): Springer Science + Business Media, pp. 39-63.

Ward, D.M., Ferris, M.J., Nold, S.C., and Bateson, M.M. (1998) A natural view of microbial biodiversity within hot spring cyanobacterial mat communities. *Microbiology and Molecular Biology Reviews* **62**: 1353-1370.

Weisburg, W.G., Barns, S.M., Pelletier, D.A., and Lane, D.J. (1991) 16S ribosomal DNA amplification for phylogenetic study. *Journal of Bacteriology* **173**: 697-703.

Zwickl, D.J. (2006) Genetic algorithm approaches for the phylogenetic analysis of large biological datasets under the maximum likelihood criterion (Ph.D. Dissertation) The University of Texas at Austin.

Chapter 3: Morphological, phylogenetic, and physiological characterization of four cyanobacterial isolates from El Tatio, Chile

ABSTRACT

Four cyanobacterial strains were isolated from microbial mat samples collected at El Tatio Geyser Field, a high As geothermal site in northern Chile. The morphology of these cultures is described, and phylogenetic placement of their 16S rRNA gene sequences is discussed. Experiments were performed to determine the growth response and physiological tolerances of cultures to temperature, salinity, nutrient amendment, As^{III}, and As^{V}. T-025, T-031, and T-039 expressed higher growth in the presence of As^{V} relative to an As^{V}-free control and sensitivity to As^{III}, whereas T-045 showed unusually high tolerance for As^{III}. T-025, T-039, and T-045 demonstrate close 16S rRNA sequence similarity to unicellular and coccoidal *Synechocystis* sp. Strain PCC 6803 (98-99%). T-031 only showed 97% similarity to the 16S rRNA sequences of filamentous and heterocystous *Nostoc* and *Nodularia*. T-031 is a candidate for a novel genus within the Subsection IV cyanobacteria because it forms a phylogenetically distinct clade compared to other genera within this group, which includes *Anabaena*, *Nostoc*, and *Nodularia*. The 6.1 Mb genome of T-031 was sequenced and described in order to further characterize the organism and its position in Subsection IV; the proposed taxonomic designation for T-031 is Candidate *Nodubaena tatiiensis* (*gen*. and *sp*. nov.)

INTRODUCTION

The morphology, 16S rRNA phylogenetic classification, and physiology of four strains of cyanobacteria cultured from El Tatio Geyser Field (ETGF) were characterized. ETGF is a geothermal environment located at 4,300 m elevation in the Atacama Desert in northern Chile. El Tatio has a number of conditions that are challenging to cyanobacteria. Its physical location leads to elevated UV flux and rapid mineral precipitation (Phoenix et al., 2006). ETGF waters have high As leading to geochemical gradients of As^{III} ($H_3AsO_3^0$) and As^V ($H_XAsO_4^{3-X}$) along geothermal outflows; As^V (pK_a ~6.9) and the waters are buffered to circumneutral pH by arsenate (Eq. 1-1, Chapter 1) (Landrum, 2007; Landrum et al., 2009). In addition to high As, ETGF waters contain limited nutrients, with dissolved inorganic carbon (DIC) found in trace amounts in most streams (Landrum et al., 2009; Engel et al., 2013).

Cyanobacteria are morphologically diverse; they are one of few prokaryotic phyla that have evolved multicellularity and the only prokaryotic phylum exhibiting cellular differentiation (Tomitani et al., 2006; Schirrmeister et al., 2011). All known members are oxygenic phototrophs and many are obligate photoautotrophs; some are able to perform respiration and fermentation, or utilize electron donors other than H_2O during facultative anoxygenic photosynthesis (Giovannoni et al., 1988; Wilmotte, 1994; Ward et al., 1998; Raven, 2012). They are unique among prokaryotes in their possession of the pigments chlorophyll (Chl) *a* and β-carotene, and also utilize phycocyanin and phycoerythrin (Stanier et al., 1971). Gloeobacteraceae, often considered a sister taxon to Phylum Cyanobacteria, is an oxygenic photosynthetic organism that uses *Chl* a, carotenoid, and

phycobiliproteins pigments characteristic of cyanobacteria, but lack thylakoid structures (Nakamura et al., 2003). Due to these important structural and molecular differences the Gloeobacteraceae are a useful outgroup for phylogenetic reconstructions of cyanobacteria (Tomitani et al., 2006).

Traditional classification schemes used morphological features to divide the cyanobacteria into five subsections (Rippka et al., 1979; Castenholz, 2001; Tomitani et al., 2006). Subsection I, the Chroococcales, is composed of unicellular forms that divide by binary fission. Subsection II, the Pleurocapsales, are also unicellular but divide by binary or multiple fission to form structures known as baeocytes (Rippka et al., 1979; Castenholz, 2001). Subsections III-V are filamentous but with varying degrees of complexity. Subsection III, the Oscillatoriales, are filamentous, non-heterocystous, and do not differentiate. Subsections IV and V are also filamentous but with the added complexity of cellular differentiation forming specialized cells known as heterocysts and akinetes. Subsection V, the Stigonematales, possess all Subsection IV characteristics as well as multiple branching (Rippka et al., 1979; Castenholz, 2001).

Phylogenetic analysis of the 16S rRNA gene sequence has allowed robust reconstructions of the evolutionary relationships among microorganisms, including the cyanobacteria. The five traditional morphological groups have largely been supported by 16S phylogenies with the modification of merging Subsections I and III into the Oscillatoriales; several reversals from multicellularity to unicellularity had occurred during the history of these groups, rendering morphology insufficient on its own for true taxonomic assignment (Tomitani et al., 2006; Schirrmeister et al., 2011).

Next-generation sequencing (NGS) technology has led to a revolution in genome sequencing; numerous cyanobacterial genomes are available for download from Genbank and other databases. Genomics is a valuable tool to investigate the metabolic capabilities of organisms. It's possible to look at groups of genes whose products are homologous to proteins with known functions; these functions are hypothetical until proven in the laboratory, but can lead to the inference of what an organism might do under certain conditions. Unicellular cyanobacteria possess genomes more similar in size to other bacteria, whereas filamentous and differentiating cyanobacteria possess genomes up to five times larger; there appears to be a correlation between genome size and morphological complexity (Herdman et al., 1979).

The distribution and abundance of cyanobacteria-classified 16S rRNA sequences in the ETGF environment are influenced more by As than by any other factor. As^{III} is a strong negative control on cyanobacteria, whereas cyanobacteria positively associate with As^{V} (Chapter 2). The growth response of four cyanobacterial cultures to As^{III}, As^{V}, and a combination of low-DIC and As^{V} were investigated. As-redox speciation was predicted to be the most prominent variables that influence the physiology of cultured cyanobacteria from ETGF. Pyrosequencing data show that cyanobacteria have low abundance in the presence of As^{III} and instead occupy As^{V}-rich regions of streams; El Tatio cultures were predicted to demonstrate low As^{III} tolerance and some measure of As^{V} tolerance based on these field observations.

METHODS

Sampling occurred in June 2009 in the Upper, Middle, and M-III Basins of ETGF (Figure 1-6). Temperature and pH were measured at locations where microbial mats were sampled, and aqueous chemistry was characterized at the locations where microbial mats were sampled. Cation, anion, As, and DIC analyses were performed using the same techniques described in Chapter 2 at the Microbial Geochemistry Laboratory [The University of Texas at Austin]. Samples designated for cyanobacteria culturing were maintained at 4°C until enrichment in media.

Cyanobacteria Culturing and Isolation

Serial dilution in BG-11(+N) media (Appendix A; Rippka et al., 1979) led to the isolation of four cyanobacteria monocultures, T-025, T-031, T-039, and T-045, from bulk microbial mat material. Cultures were maintained in BG-11(+N) at 23°C under 24 hour/day low-intensity irradiance with regular agitation to prevent biofilm formation.

Several mat samples were enriched in BG-11(+N) without serial dilution in order to assess the diversity of cyanobacteria present in selected mat locations. Environmental enrichment sample T-05 was collected from a subaerial mat in the splash and steam zone of a 70°C region of the Great Geyser stream (Figure B-1). Environmental enrichment samples T075-A and T075-B were collected from the same mat at 75 m along the Great Geyser stream (Figure B-2). Mat sample T075-A was enriched in BG-11(+N) media, while T075-B was enriched in BG-11(+N) + 5% NaCl (Appendix A).

Microscopy

Cultured organisms and environmental samples enriched in BG-11(+N) media were examined by light microscopy with an Olympus BX41 microscope (Olympus America, Inc., Melville, NY). Images were taken at 400X and at 1000X using an oil immersion lens; cell size was approximated with an ocular grid. Cell size, shape, unicellularity or filamentous morphology, filament branching, and the presence of differentiated cell types were noted for morphological identification. Identification followed the combined molecular and morphological scheme set forth in Castenholz (2001).

DNA Extraction, Cloning, and Sequencing

Full-length 16S rRNA genes were sequenced using a cloning and Sanger sequencing approach (see Chapter 2). DNA from each culture was sequenced from 10 to 20 clones using the PureLink Quick Plasmid miniprep kit (Invitrogen Life Technologies Corporation, Carlsbad, CA). Full-length 16S rRNA sequences were obtained using M13(-20) forward and M13(-24) reverse primers on a 96-capillary 3730XL DNA Analyzer (LifeTech-Applied Biosystems, Foster City, CA) at the ICMB Core Facility [The University of Texas at Austin].

Full-length 16S rRNA sequences were constructed by ligating forward sequences to reverse complements of M13(-24) reverse sequences; chimera checking was also performed as described in Chapter 2. Consensus sequences were obtained by aligning non-chimeric clones in ClustalX 2.1 (Chenna, 2003; Larkin et al., 2007). The consensus base pair at each position was selected manually. Full-length consensus sequences were

similarity searched using the web-available nucleotide BLAST algorithm at www.blast.st-va.ncbi.nlm.nih.gov (Altschul et al., 1990).

DNA Analysis and Phylogenetic Reconstruction

Phylogenetic reconstructions were used to determine how the 16S rRNA sequences of ETGF cultures relate to cultured and environmental cyanobacteria sequenced previously in other phylogenetic studies. Alignment was performed using ClustalX 2.1 with a gap opening penalty of 30, and gap extension penalty of 15 (Larkin et al., 2007). Alignments were refined manually to uniform length. The alignment used for all trees using full-length 16S rRNA sequences aligned to *E. coli* (J01859) 16S rRNA positions 131 to 1,314, with gaps between positions 198 to 212 and 458 to 479. *Gloeobacter violaceus* Strain PCC 7421 was used as an outgroup for the reconstructions of El Tatio organisms. *Oscillatoria sancta* Strain PCC 7515 was used as an outgroup for the reconstruction of T-031 relative to other Subsection IV cyanobacteria. Trees of T-031 genes *rbcL* and *hetR* were not made using an outgroup.

Statistically supported phylogenetic trees were constructed using the Genetic Algorithm for Rapid Likelihood Inference/GARLI 2.0 hosted at www.molecularevolution.org (Zwickl, 2006; Bazinet et al., 2014). Cladistic analyses were performed using maximum likelihood (ML) criteria (Felsenstein, 1981), and the general time-reversible model of sequence evolution with gamma distributed rate heterogeneity and proportion of invariant sites (GTR+I+G) (Hasegawa et al., 1985; Waddell and Steel, 1997). ML criteria were chosen in order to compare these topologies to previous ML reconstructions of cyanobacteria using similar criteria. Statistical support

for each reconstruction was determined by 2000 bootstrap replicates to ensure <1% error at 95% confidence interval (Hedges, 1992). Majority-rule consensus trees were constructed from bootstrap analyses, and nodes with <50% support were collapsed into polytomies. Reference sequences used to build phylogenetic trees with can be found along with names, taxonomic affiliation, and Genbank accession numbers (Tables B-1 and C-1).

Genome Sequencing and Analysis

The genome of T-031 was sequenced on an Illumina HiSeq platform at MrDNA laboratories [MRDNA labs, Shallowater, TX]. De novo contig assembly was performed using SeqMan Ngen software (DNASTAR, Inc.) on BaseSpace.illumina.com; annotation was done using the web available Rapid Annotation using Subsystem Technology v2.0 (RAST; rast.nmpdr.org) algorithm (Aziz et al., 2008; Overbeek et al., 2014). Visualization also occurred in RAST and reference sequences were similarity searched against the T-031 genome by using the BLAST algorithm in the RAST environment.

Experimental Procedures

Batch culture regression experiments were performed to assess the growth of cultured organisms in response to environmental variables such as salinity, As^{III}, and As^{V}. NaCl was added to BG-11(+N) at concentrations of 0, 10, 25, 50, 75, 100, 125, 150, 175, 200, 225, and 250 mM (n = 3). The Na^+/Cl^- content was considered '0' in unaltered BG-11(+N); any Na^+ and Cl^- present in the media originated from various salts containing Na^+ or Cl^- (Appendix A). Growth was monitored for six days as optical density absorbed

at 680 nm on a SMARTSpectro 2000 spectrophotometer (LaMotte Company, Chestertown, MD). Growth response to temperatures above 23°C were also assessed (*n* = 3).

Growth experiments were performed by exposing cultures T-025, T-031, T-039, and T-045 to BG-11 amended with 0, 0.5, 1.0, 1.5, 2.0, 2.5, 3.0, 3.5, or 4.0 mM As^{III} or As^{V}. Each As^{III}/As^{V}-amended treatment was titrated aseptically to pH 7 using 1N HCl or 1N NaOH. Each As^{III} or As^{V} -amended treatment group was then inoculated with one of the four cultures (*n = 3*). Cultures were maintained at 23°C under 24-hour low-intensity irradiance. Growth was monitored for 8 days by optical density (OD) at 680 nm using a SMARTSpectro 2000 spectrophotometer.

Cyanobacteria carbon uptake by cultures T-025 and T-031 was assessed in closed-system batch-culture experiments. These closed-system experiments were designed designed to mimic the diffusion-limited conditions experienced by microbial mats in the environment. 20ml aliquots of un-buffered minimal salts media (0.05 mM KCl, 1 mM NaCl, 0.15 mM $MgSO_4$, 0.25 mM $CaCl_2$, and 0.5-1.5 mM $NaHCO_3$) were dispensed into borosilicate glass tubes. Treatment groups were either un-buffered, containing no aqueous buffer except HCO_3^-, or buffered by 1.0 mM arsenate. Prior to inoculation, cells were washed three times in experimental media. All samples were titrated to pH 7 with 1N HCl, and inoculated with T-025 or T-031 (*n = 8*). Both the un-buffered control and As^{V}-amended groups started with 0.3 mM DIC (as HCO_3^-), similar to the DIC content in ETGF streams. Growth was measured daily as OD at 680nm. [DIC] was measured daily on an Apollo 9000 Carbon Analyzer (Teledyne-Tekmar, Mason,

OH). pH was measured using an IQ150 pH meter with a non-glass ISFET electrode (Hach Company, Loveland, CO). Sterile controls were used to test for pH shifts and DIC loss due to sampling methods.

Culture and Sequence Accessioning

The 16S rRNA sequences of cultured organisms were deposited in GenBank under accession numbers KP762344 (T-025), KP762334 (T-031), KP762345 (T-039), and KP762346 (T-045). Cultured strains have been accessioned into the UTEX Culture Collection of Algae [The University of Texas at Austin] under UTEX B 3001 (T-025), UTEX B 3002 (T-031), UTEX B 3003 (T-039), and UTEX B 3004 (T-045). Non-isolated enrichment culture clones can be found under KP793937 to KP793943 (T-05), KP793930 to KP793936 (T075-A), and KP762335 to KP762343 (T075-B).

RESULTS

Morphological Description and Phylogenetic Affiliation

Cyanobacterial culturing led to isolation of four new cyanobacterial strains: T-025, T-031, T-039, and T-045. T-025 was collected from a 65°C, high-DIC location in the Middle Basin Springs (MBS) with 122 mM Cl^- and 0.33 mM As, mainly as As^V (Table 3-1). Full-length 16S rRNA sequence comparison in BLAST showed 98% similarity to unicellular *Synechocystis* sp. Strain PCC 6803 (Table 3-2); however, cells were found in short filaments of 2 to 8 cells which did not match the morphology of previously described unicellular *Synechocystis* sp. (Kaneko et al., 1996; Tajima et al., 2011). Terminal cells undergo binary fission, and non-dividing cells were 3 by 4.0 μm

and ovoid in shape (Figure 3-1). T-025 cells grew rapidly when placed in fresh media and exhibited a deep blue-green color.

Culture T-031 was a filamentous cyanobacterium isolated from a 26°C, low-DIC stream in the Upper Basin, which contained ~123 mM Cl^- (measured at a site 2 meters downstream) and 0.4 mM As^V (Table 3-1). T-031 showed 96-97% 16S rRNA sequence identity to several *Nodularia* sp. strains (Moffitt et al., 2001; Lyra et al., 2005) and 97-98% similarity to *Nostoc calcicola* BDU 40302; when compared to BDU 40302 in BLAST a 98% match was found, and a 97% match when compared to T-031 in RAST (Table 3-2). T-031 performed binary cell division, and was observed to form long filaments (>20 cells) when undisturbed (Figure 3-2); the longer filaments aggregated into 0.5-1 mm clumps that adhered to the sides and bottom of the culture flask. Heterocyst formation did not occur with fixed nitrogen, but in BG-11(-N) media T-031 formed terminal and intercalary heterocysts (Figure 3-2). During long periods of undisturbed growth T-031 formed akinetes, which are oval shaped cells ~20% larger than normal vegetative cells with a more granular appearance (Figure 3-2). In bulk culture T-031 appeared bright green and grew relatively fast when frequently placed in new media.

Culture T-039 was isolated from a 31°C low-DIC location in the Middle Basin that contained ~180 mM Cl^- (measured 10 m upstream) and 0.43 mM As^V (Table 1-1). T-039 was 98% similar to *Synechocystis sp*. Strain PCC 6803 similar to T-025 (Table 3-2). Cells were also ovoid and formed short non-heterocystous filaments, similar to T-025, but cells had flatter ends than T-025 cells. T-039 appeared to undergo intercalary cell division, whereas T-025 only performed terminal cell division (Figure 3-1 and 3-3). The

T-039 16S rRNA gene sequence was >99% similar to T-025 and 98% similar to the same *Synechosystis* sp. strains as T-025.

T-045 was collected from a 58°C, high-DIC, and low-salinity location within the Group M-III geysers (Figure 1-7), which contained almost no As (0.01 mM as As^{V}) compared to other ETGF features (Table 1-1). This organism was coccoidal and did not form filaments (Figure 3-4). Its 16S gene was 99% similar to T-025 and T-039, and >98% similar to reference strains *Synechocystis* sp. and *Merismopedia glauca* (Table 3-2). Due to its unicellular and coccoidal shape it resembled previously described *Synchocystis* sp. strains more than T-025 or T-039.

A phylogenetic reconstruction was used to compare the 16S rRNA sequences of cultured isolates and enrichment culture clones to reference strains of cyanobacteria (Figure 3-5). One enrichment clone from T075-A was identified as *Fischerella* sp., but the remaining cultured isolates were placed in cyanobacteria Subsections I/III and IV based on grouping with previously described reference strains (Castenholz, 2001; Tomitani et al., 2006; Schirrmeister et al., 2011); reference sequence accession numbers are listed in Tables B-1 and C-1. Several enrichment clones demonstrated high sequence similarity to *Leptolyngbya antarctica*.

Subsection I/III cyanobacteria are found in the lower half of the phylogenetic tree, and form a reasonably well-supported sister group with Subsection II (*BP* = 72) (Figure 3-5). El Tatio sequences placed in this portion of the tree were isolates T-025, T-039, T-045, three enrichment clones from T-05, and 2 clones from T075-A; these were >99% similar to each other and *Synechocystis* sp. Strain Sai002 (*BP* = 95). These sequences are

nested in a well-supported group along with *Gloeothece* sp., several *Synechocystis* sp. strains, and *Merismopedia glauca* (*BP* = 96) (Figure 3-5). A second reconstruction confirms their placement close to Sai002, *M. glauca*, and *Synechocystis* sp. Strain LEGE 06155, but shows that they do not group as closely with several reference *Synechosystis* strains as with Sai002 (Figure 3-6).

Subsection IV cyanobacteria were positioned in the upper half of the tree in a well-supported monophyletic group (*BP* = 99) with Subsection V cyanobacteria (Figure 3-5). Culture T-031 formed a clade with T075-B (*BP* = 70), a group of nine enrichment culture clones collected from the Great Geyser outflow at 75 m. They grouped together in every phylogenetic reconstruction performed in this work, forming a distinct clade compared to other Subsection IV genera (Figures 3-5, 3-7). T-031 and T075-B show 96-98% sequence similarity to *Nostoc* sp., *Nodularia* sp., and *Cyanospira* sp. strains during BLAST searches, and 97% similarity to each another (39 base pair differences over 1,400 base pair sequence).

Physiological Characterization of Cultures

Culture physiology was examined with respect to the physical and geochemical conditions shown to influence cyanobacteria and other community-level properties at ETGF, including temperature, [DIC], [As^{III}], and [As^{V}] (Chapter 2). [Na^{+}] and [Cl^{-}] were not found to influence cyanobacteria abundance or diversity at ETGF (Chapter 2); however, salinity is known to influence the growth and physiology of many cyanobacteria and was examined during growth experiments (Oren, 2012).

Growth response to temperature

The effect of temperature on growth was examined (Table 3-1). Growth curves were measured at 25°C, 35°C, and 45°C relative to a room temperature control group (Figure 3-8). T-025, T-031, and T-045 showed more growth at 35°C compared to 25°C and room temperature. In contrast, T-031 showed a large negative growth response at 35°C relative to 25°C and room temperature; the 25°C group showed a less negative response (Figure 3-8).

Growth response to NaCl

El Tatio waters are moderately saline, with up to 200 mM [Cl^-] and 170 mM [Na^+] (Table 1-2). All four cultures exhibited a range and order of preferred salt concentrations. Culture T-025 (Figure 3-9-A) showed increased growth in the presence of all concentrations greater than baseline BG-11(+N) media (Appendix A). After 7 days, cells introduced to 50-150 mM Na^+/Cl^- grew somewhat more than cells exposed to 200-250 mM Na^+/Cl^-. All treatments amended with Na^+/Cl^- showed significantly greater growth than the control; however, the differences in growth (plus error) were not large enough to distinguish a distinct range of preferred salt content. Culture T-039 (Figure 3-9-B) showed a negative growth response to increasing Na^+/Cl^- ($r^2 = 0.97$, $P < 0.0001$). Culture T-031 (Figure 3-9-C) showed a positive growth response to increasing Na^+/Cl^- ($r^2 = 0.87$, $P < 0.0001$), although not until the second half of the experiment when the order of preference switched from low to high Na^+/Cl^-. Due to cell clumping in response to salt, error with T-031 was higher than observed with the other three cultures. Culture T-045 (Figure 3-9-D) also showed a positive response to increasing Na^+/Cl^- ($r^2 = 0.82$, $P <$

0.0001). The magnitude of the difference in T-045's response between treatments was low, resembling T-025 more than T-031 or T-039.

Growth in the presence of nutrients

Many of the ETGF waters sampled during this study contain low [DIC] as HCO_3^-, low combined nitrogen as NH_4^+ or NO_3^-, and unknown but probably trace [PO_4^{3-}] (Table 1-2). Cultures were grown in normal BG-11(+N) media until reaching stationary phase then supplied with fresh BG-11(+N) spiked with nutrients (1.0 mM HCO_3^-, NO_3^-, or PO_4^{3-}) to determine whether they significantly affect growth. Growth curves were recorded for 14 days (Figure C-1); the relative magnitude of growth in the presence of each nutrient is shown after 8 days (Figure 3-10).

When supplied with additional DIC T-025 showed the most positive growth response relative to the control and other treatments (Figure 3-10-A). T-025 grew in the presence of extra PO_4^{3-}, but it did not positively affect growth relative to the control; growth with PO_4^{3-} mirrored growth in the control until day 7, where it decreased for the remainder of the experiment (Figure C-1-A). T-025 showed a negative response to NO_3^-, with almost no growth after 8 days and an initial seven-day period of low OD in excess of 5% below the starting measurement (Figure 3-10, Figure C-1-A).

T-039 did not exhibit a notable response to any nutrient (Figure 3-10-B). Growth with HCO_3^- was similar to the control for 12 days, after which additional HCO_3^- appeared to aid growth (Figure C-1-B). Growth was similar with NO_3^- and PO_4^{3-} throughout the experiment with small variations between days 3 and 8. Culture T-045 experienced low %OD changes compared to T-025 and T-039, but elevated growth with NO_3^- and HCO_3^-

relative to the control for the entire experiment, and more growth with PO_4^{3-} for 11 days (Figures 3-10-D, C-1-D).

T-031 showed no difference among the control and nutrient-amended groups until day 4, when growth with NO_3^- ceased; by day 8 growth with NO_3^- was significantly lower than the other three groups (Figure 3-10-C, Figure C-1-C). Between days 4 and 8 growth leveled off in the control, HCO_3^-, and PO_4^{3-} groups; however, at day 9 growth in the control group began to increase while it decreased slightly in the other two (Figure C-1-C).

Growth in the presence of arsenite and arsenate

Growth was monitored during exposure to 0.5 mM increments of As^{III} and As^{V}, up to 4 mM As^{III}. The growth curves for T-025, T-039, and T-045 are described here (Figure 3-11); the curves for T-031 are discussed thoroughly in Chapter 4 (Figure 4-3). Only data for 0, 0.5, 1, 2, 3, and 4 mM are shown here for ease of visualization; full data sets are available in Tables C-2, C-3, and C-4.

T-025 exhibited a strong negative correlation to As^{III} ($r^2 = 0.72$, $P < 0.01$) and growth was limited during exposure to all tested As^{III} concentrations relative to the As-free control (Figure 3-11-A). The upper As^{III}-tolerance of this strain appears to be 1.0-1.5 mM; the 1.5 mM As^{III} treatment experienced significant pigment bleaching and cell death within the first 24 hours of the experiment; 0.5 and 1.0 mM treatments experienced slight bleaching, but not significant cell death. Exposure to all tested As^{V} concentrations resulted in increased growth relative to the control, especially at 0.5 mM As^{V} (Figure 3-

11-B). Growth appeared to be stimulated during the first 48 hours of As^{V} exposure at all concentrations relative to the control (Figure 3-11).

T-039 also exhibited a negative correlation to As^{III} ($r^2 = 48$, $P < 0.05$). Growth with As^{III} was stimulated in the first 48 hours at all concentrations, and after this point all As^{III} treatments exhibited the same rate of %OD decline for the remainder of the experiment (Figure 3-12-A). Growth was 30% greater in the control than at 1.0 mM As^{III}, which grew 8% in total, and lowest at 4 mM As^{III}, which experienced a net 1% decrease relative to starting OD. Similar to T-025, T-039 experienced a positive response to As^{V} exposure, but only cells in 0.5 mM As^{V} experienced higher growth relative to the control over the duration of the experiment. The lowest overall growth was observed at 1.0 and 2.0 mM As^{V} (Figure 3-12-B). T-039 did not show a direct correlation to As^{V}, similar to T-025.

T-045 expressed unexpectedly high growth response to 0.5 to 1.0 mM As^{III} relative to the control, but growth decreased when exposed to 2.0 mM As^{III} (Figure 3-13-A). Growth at 0.5 and 1.0 mM As^{III} was sustained throughout the 8-day experiment, and no pigment bleaching was observed in these cells, which appeared bright green and healthy. By the end of the 8 day experiment T-045 did not show a preference for any concentration of As^{V} relative to the control; although, all concentrations of As^{V} stimulated a 20-25% OD increase during the first 24 hours of the experiment (Figure 3-13-B). The correlation between T-045 growth and increasing As^{III} was not diagnostic of the trend observed in the growth chart, as T-045 showed a strong negative correlation with As^{III} ($r^2 = 0.80$, $P < 0.01$).

Carbon Uptake Behavior of T-025 and T-031

Carbon uptake by T-025 and T-031 was compared under closed-system, DIC-limited conditions, with and without 0.5 mM arsenate acting as a pH buffer. Both organisms elevate the pH of the growth media in the absence of a pH buffer; (Figure 3-14). Under unbuffered conditions T-031 removed 75% of available DIC and increased the pH reached 10.1 and after that point no additional DIC uptake was observed (Figure 3-14-A, B). When the same experiment was performed on a high DIC culture, T-025, the unbuffered treatment group experienced an upward pH shift to 9.5, after which no carbon was assimilated (Figure 3-14-D). The increase to maximum pH occurred in only 24 hours in T-031, as opposed to 48 hours in T-025 (Figure 3-14-A, D).

Under unbuffered conditions DIC removal was more constant and gradual in T-025 compared to T-031 (Figure 3-14-B, E). Both unbuffered groups exhibited 75% DIC removed over the course of the experiment, but the rate of DIC removal differed between T-025 and T-031 (Figure 3-14-B, E). Growth in the unbuffered groups of T-031 and T-025 also differed (Figure 3-14-C, F). Growth did not increase significantly in T-031 until 24 to 72 hours, and reached a maximum on day five (Figure 3-14-C); T-025 grew 60-70% within 24 hours, and growth only increased slightly in the following days (Figure 3-14-F).

Arsenate had a dramatic effect on pH, DIC-uptake, and growth in both cultures. pH only increased from 7 to 7.4 over the course of the experiment in the presence of arsenate (Figure 3-14-A, D). T-031 achieved significantly greater growth in the presence of arsenate compared to unbuffered conditions; the difference was maintained in

subsequent days although it did not continue to increase (Figure 3-14-B). During the first 24 hours arsenate-buffered T-025 showed significantly greater DIC uptake than the unbuffered group (Figure 3-14-E). Both cultures showed 25% greater DIC uptake in the presence of arsenate relative to controls, although DIC removal by T-025 was more gradual than DIC removal by T-031 (Figure 3-14-E). T-031 grew more in the presence of arsenate, whereas T-025 showed similar growth in both the unbuffered and arsenate-buffered groups (Figure 3-14-F). Sterile controls were subjected to sample removal throughout the experiment; no shifts in pH, [DIC], or OD were observed.

Genome Description of T-031

The genome of culture T-031 was annotated and described. The genome was a single circular chromosome 6,123,027 base pairs in length, with an average GC content of 46%. The chromosome contains 6,143 regions identified as protein-encoding groups (PEGs) on 74 contigs. Comparison to previously annotated organisms show that 30% of the PEGs can be placed within 400 known subsystems, which are comprised of PEGs that work together to perform known cellular functions. The remaining 70% of PEGs show sequence similarity to genes with hypothetical functions or no known functions. When compared to other genomes available in RAST, close relatives to T-031, in order of similarity, are *Nostoc punctiforme* Strain PCC 73102, *Nostoc* sp. Strain PCC 7120, Anabaena variabilis Strain ATCC 29413, and *Nodularia spumigena* Strain CCY 9414. These matches are similar to those determined in BLAST and through phylogenetic analysis of the 16S rRNA gene, although not identical; *Nostoc* was not among the most similar sequences found during 16S rRNA analysis (Table 3-2, Figure 3-7).

PEGs are organized into functional gene subsystems (Figure 3-15). The 3 largest subsystems in T-031 are "cofactors, vitamins, prosthetic groups, and pigments" (307 features), "amino acids and derivatives" (347 features), and "carbohydrates" (321 features) (Figure 3-15). The carbohydrates subsystem contains 119 features related to the metabolism of organic carbon compounds; these include the TCA cycle, gluconeogenesis, acetogenesis, glycolysis, the pentose phosphate pathway, and the Entner-Doudoroff pathway. Features are also present that function in glycerate and glycogen metabolism, as well as fermentation. Genes related to CO_2-fixation comprise 25% of all carbohydrate subsystem features (78 total), and include CO_2-uptake and carboxysome construction (38 features), photorespiration (20 features), and the Calvin-Benson cycle (20 features).

RuBisCO large subunit

All cyanobacteria possess the gene encoding the large subunit of the Ribulose-1,5-Bisphosphate Carboxylase Oxygenase (RuBisCO) enzyme (*rbcL*). The portion of the *rbcL* gene used for phylogenetic analysis was found on contig 3 between positions 494,217 to 495,647. A bootstrap-supported ML phylogeny was constructed using *rbcL* encoding genes from Subsections I, -III, -IV, and -V cyanobacteria (Figure 3-16). No outgroup was used during this reconstruction; Subsections I/III cyanobacteria occupy the most basal region of the tree, and Subsections IV and -V are positioned further up in a well-supported monophyletic group (*BP* = 78). *Fischerella rbcL* genes form cluster A, while the majority of Subsection IV cyanobacteria fall into cluster B. T-031 *rbcL* is positioned in cluster B, most closely associated with *Nostoc* sp. Strain PCC 7906 *rbcL*

and *Anabaena* WH *rbcL*, and showed 91% and 89% sequence similarity to those genes, respectively.

Heterocyst differentiation

T-031 forms terminal and intercalary heterocysts for N_2-fixation (Figure 3-2). The gene for heterocyst differentiation (*hetR*) was compared to *hetR* genes from heterocyst-forming members of Subsections IV and V cyanobacteria, as well as homologous sequences from several non-heterocystous Subsection III cyanobacteria (Figure 3-17). The portion of the *hetR* gene used for phylogenetic analysis was found on contig 3 between base pair positions 156,901 to 157,793.

The Subsections IV and V *hetR* gene group is reasonably well supported (*BP* = 71), although the relationships among Subsections IV and V are poorly resolved. All Subsection V cyanobacteria are grouped together with good support (*BP* = 91), and Subsection IV cyanobacteria are distributed among the other 5 groups. T-031 was placed in a well-supported subgroup containing two *Nodularia hetR* sequences (*BP* = 96); relationships among subgroups in this portion of the tree are less well resolved (*BP* = 53, 59). The % sequence similarity between T-031 *hetR* and other sequence groups are shown; the closest matches are *Nodularia* sp. Strain KAC17, *Nodularia spumigena* (90%) and *Nostoc* sp. Strain PCC 7107 (83%) (Figure 3-17).

DISCUSSION

Widespread use of culture-independent DNA sequencing has broadened our understanding of the diversity and ecology of microorganisms in environments such as

hot springs (Ward et al., 1998). Culture-independent approaches show that the majority of 16S rRNA sequences classified as cyanobacteria at ETGF, a high-As geothermal system, are most similar to filamentous and heterocystous *Fischerella* sp. Most areas at ETGF with high cyanobacteria abundance contain As^{V}; cyanobacteria exhibit a significant negative correlation to As^{III} in ETGF streams (Chapter 2). Although culture-independent methods can inform which microorganisms occupy an environment, culture-dependent investigations are still the most important way to test hypotheses about the functional role of microorganisms in the environment and assess their response to environmental conditions.

Four strains of cyanobacteria were isolated from microbial mats originating in geochemically distinct locations at El Tatio Geyser Field. Cultures T-025, T-039, and T-031 originate in settings with high As^{V}, while T-045 originates in a low As site (Table 3-1). T-031 and T-039 originate in low temperature and low-DIC environments, whereas T-025 and T-045 originate from high temperature and high DIC environments. *Fischerella* sp. was seldom seen in enrichment culture; unicellular and filamentous non-heterocystous forms such as *Synechocystis* sp., and *Leptolyngbya* sp. comprised the majority of environmental cultures. The lack of these sequences in culture-independent clone libraries indicates that unicellular and non-heterocystous filamentous cyanobacteria are present in the environment but not abundant; this suggests that significant culture bias was introduced during laboratory growth conditions, largely due to the goal of obtaining organisms amenable to optical density analysis and by the use of BG-11(+N) media for enrichment and isolation.

Non-heterocystous and coccoidal strain T-045 and filamentous strain T-025 and T-039, showed >99% 16S rRNA sequence similarity to each other, and >98% similarity to several *Synechocystis* sp. strains and other members of the order Chroococcales (Castenholz, 2001). Only T-045 morphologically resembles previously studied *Synechocystis* strains; cultures T-025 and T-039, despite possessing species level 16S rRNA sequence similarity (99%) are filamentous and do not resemble the morphology of any known Chroococcales strains that group in this portion the tree, such as *Gleothece*, *Merismopedia*, and *Synechocystis* (Figure 3-5) (Stanier et al., 1971; Komarek, 1976; Rippka et al., 1979). The reason for this is unknown at this time.

Taxonomic Assignment of T-031

Filamentous and heterocystous strain T-031 can be placed firmly within the Nostocaceae (*Cyanobacteria; Nostocales; Nostocaceae)*, due to 16S rRNA sequence similarity to *Nostoc*, *Anabaena*, and *Nodularia* and consistent placement with these organisms during phylogenetic analysis; genome-wide comparison showed similarity to *Nostoc* sp. Strain PCC 73102 and *Anabaena* sp. Strain PCC 7122; however, generic level assignment of T-031 among *Nostoc*, *Anabaena*, and *Nodularia* is not clear based solely on phylogenetic and genomic analysis.

The combined assessment of 16S rRNA sequence similarity and its phylogenetic placement among *Nostoc*, *Anabaena*, and *Nodularia* shows that T-031 is a new genus. Phylogenetic analyses place T-031 nearest to *Nodularia* but T-031 always forms a distinct sister clade with *Nodularia* but never within it (Figure 3-5). T-031 always groups more closely with El Tatio enrichment clones T075-B than with other Nostocaceae; no

other sequences were found to group closely with them in these phylogenies. Cultured and rigorously identified members of *Nodularia*, *Nostoc*, and *Anabaena* show that members of each genus are >98% similar to one another on the basis of 16S rRNA similarity, whereas T-031 is a maximum of 97% similar to *Nodularia*, and even less similar to *Anabaena* and Nostoc (96%). *Nostoc calcicola* BDU 40302 appears to be misidentified and is probably *Nodularia*, due to its close grouping with *Nodularia* in reconstructions (Figure 3-7). Similarly, *Cyanospira*, which were previously identified as a novel genus (Florenzano et al., 1985) are also probably *Nodularia* based on my phylogenetic analyses (Figure 3-7).

Morphological features were examined to compare T-031 to other Nostocaceae to clarify its taxonomic placement. *Anabaena, Nostoc*, and *Nodularia* images were compared to T-031, and no exact matches were found through certain features of T-031 resembled aspects of these other genera (Figure C-3). Inclusion within the current definition of *Nodularia* may be ruled out on the basis of morphology; *Nodularia* sp. possess disk-shaped cells whose width always exceed length (Rippka et al., 1979). T-031 has oval to barrel shaped cells, which fit more closely to descriptions of *Nostoc* and *Anabaena*; however, there is substantial convergent morphology among *Nostoc* and *Anabaena* and many features appear indistinguishable between these genera. T-031 heterocysts, which are spherical and more translucent than vegetative cells, resemble those of various species of *Nostoc* (Figure 3-2, Figure C-3). A developmental character that can help distinguish *Nostoc* and *Anabaena,* known as hormogonia, are absent in mature cyanobacterial trichomes (Rippka et al., 1979) so genomic evidence was used.

Known *Nostoc* sp. have a narrow range of mol % GC (39-45%), as do *Anabaena* (38-44%) and *Nodularia* (~41%) (Herdman et al., 1979; Rippka et al., 1979; Kaneko et al., 2001). T-031 possesses 46% GC content, most similar to *Nostoc*, but slightly above the range defined in Herdman et al. (1979) which caps at 45%. Only 30% of T-031 genome fits into known subsystems. This leaves 70% of genes with either unknown or hypothetical function, a significantly greater proportion of unknown genes compared to the genome of *Anabaena* sp. Strain PCC 7120, which only contained 50% of genes with unknown or hypothetical functions (Kaneko et al., 2001).

A large proportion of T-031 genome subsystems are involved in carbon and carbohydrate metabolism, many of which have to do with photorespiration, organic carbon metabolism, and fermentation. T-031 has 20 subsystem features related to photorespiration, known as the oxidative C2 cycle (Eisenhut et al., 2006; Reumann and Weber, 2006). T-031 originates in an extremely DIC-limited environment at ETGF, and it follows that the organism would possess mechanisms for recovering carbon that would otherwise be lost without photorespiration. This also provides evidence for exclusion of T-031 from *Anabaena*, all of which are obligate photoautotrophs; and shows more similarity to *Nostoc* which is known to perform photoheterotrophy using sucrose, glucose, and fructose (Rippka et al., 1979). Although T-031 possesses the machinery for photorespiration, no evidence for photorespiration was seen in carbon uptake experiments, which would result in DIC increase. Once DIC was removed from the experimental media it remained within cells; DIC did not increase in the media even weeks after introduction to the closed-system batch culture experiments.

T-031 *rbcL* and *hetR* gene trees expressed similar relationships to reference sequences to those observed using the more highly conserved 16S rRNA trees, although differences were observed in the grouping and order of node placement among the Nostocaceae (Figure 3-16, 3-17). The ordering of relationships among functional genes in Subsection IV cyanobacteria is different in these trees than what is seen in 16S rRNA trees; these genes can undergo rapid and unconstrained sequence evolution compared to the vital and highly conserved 16S rRNA gene. The relationships of *hetR* and *rbcL* to 16S rRNA phylogenies of heterocystous cyanobacteria were investigated previously (Figure C-4); the *rbcL* relationships shown here agree with the *rbcL* reconstruction by Tomitani et al. (2006).

Some additional data are needed to confirm that T-031 represents a previously undescribed taxon at the genus level, but there are sufficient differences between T-031, *Nodularia*, *Anabaena*, and *Nostoc* to warrant assignment to a new genus. Morphologically T-031 appears similar to both *Anabaena* and *Nostoc*, bearing little resemblance to *Nodularia*. Phylogenetically, T-031 is placed more closely with *Nodularia* than with *Anabaena* or *Nostoc*. The proposed generic name for T-031 is Candidate genus *Nodubaena*, combining the names *Nodularia* and *Anabaena* due to the phylogenetic and superficial morphological similarity to these genera, respectively. A proposed specific name is *tatiiensis*, after El Tatio Geyser Field.

Physiological Comparison of Cultures

The results from growth experiments show that three closely related organisms, T-025, T-039, and T-045 show differences in growth response to varied experimental

conditions. Variability in the response of different *Synechocystis* strains, indicate that genetically similar *Synechocystis* sp. can exhibit different responses to environmental stimuli (Tajima et al., 2011). Although light was not examined here, the responses to salt, temperature, As^{III}, and As^{V} indicates that the high similarity between 16S rRNA strands (>99%) of T-025, T-039, and T-045 does not translate to high similarity in their environmental preferences or their morphology.

T-025 and T-045 were obtained from high-DIC environments and responded positively to added carbon. T-039, collected in a low-DIC environment, did not demonstrate higher growth in the C-amended group relative to the control, suggesting more efficient DIC-scavenging by this organism compared to T-025 and T-045. The other low-DIC culture, T-031, also showed no response to added carbon. NO_3^- had the most variable effect on growth among the *Synechocystis* group, severely inhibiting growth by T-025, and having almost no affect to T-039, and a small positive affect to T-045.

Growth temperature optima often reflect the temperature of the collection environment; members of the same species can adapt to different temperature niches within the same geothermal feature or even the same microbial mat (Ward et al., 2012). T-025, T-039, and T-045 prefer growth conditions 10-20°C above room temperature, shown by more rapid growth, and increased biomass. This is consistent with the temperature at their collection sites which ranged from 31 to 65°C. T-031, collected in a 26°C environment prefers room temperature conditions.

Cyanobacteria abundance and diversity did not correlate with salinity at ETGF (Chapter 2); however, salinity is known to play an important role in maintaining osmotic equilibrium (Oren, 2012). Na^+ is also known to influence energy dependent DIC uptake across cell membranes in some cyanobacteria (Badger et al., 2006). ETGF is a moderately saline environment with [Cl^-] in the 150-200 mM range (Tables 1-2, 2-1). When cultures were exposed to 0-250 mM Na^+/Cl^- in order to determine their preferred salinity range, any positive or negative linear response to Na^+/Cl^-, and whether these preferences reflect their environment of origin (Table 3-2). T-045 showed a positive response to higher salt despite originating in a low-salinity environment in the Group M-III geysers (Table 3-2). ETGF cultures did not show a preference for the Na^+/Cl^- concentrations in their environment of origin. Based on these results, these organisms can be classified as 'euryhaline' due to their ability to tolerate a broad range of salinities (Oren, 2012).

T-025 and T-039 had a similar response to As^{III} and AsV, although T-025 appears to have a higher tolerance to As^{III} than T-039 (1-1.5 mM versus 0-0.5 mM). These organisms also exhibit similar responses to As^V. T-025 shows an affinity for all tested As^V concentrations relative to the control, and T-039 also shows elevated growth at all As^V concentrations. T-025 and T-031 grew more in response to As^V, especially 0.5 mM, which is similar to the As^V concentration in ETGF waters (Landrum et al., 2009).

T-045 exhibited a distinct response to As compared to the other three cultures that had low As^{III} tolerance. Instead, T-045 experienced a positive growth response up to 1.5 mM to As^{III}; visual examination showed that growth at these concentrations continued

long after the conclusion of the experiment, although cell death and pigment bleaching was observed at concentrations higher than 1.5 mM As^{III}. T-045 did not show increased growth relative to the control on exposure to As^{V}. The reason for T-045 preference for As^{III} is speculated to have to do with its low-As environment of origin; an organism originating in a low-As environment may benefit from a detoxification response to As^{III} using the ars operon. When cyanobacteria cannot avoid As, they seem to accumulate As^{V} within their biomass (my unpublished observations) or form less toxic organoarsenical compounds (Yin et al., 2011). Experiments on T-025 and T-031 show that 0.5-1 mM As^{V} can benefit cells under DIC-limited conditions. In the perpetually DIC-limited environment at ETGF cells appear to benefit from As^{V} exposure, an unusual response to an element that can be considered a potent environmental toxin.

CHAPTER 3. TABLES AND FIGURES

Table 3-1: Major geochemical data at culture collection localities at ETGF. Concentrations were measured at a site 2 meters downstream of collections locality. Cl^- values were estimated for TAT09-031 and TAT09-039. [Cl^-]=123.0 was measured 2 meters downstream from the TAT09-031 collection locality. [Cl^-]=180.5 was measured 20 meters upstream of TAT09-039, and a second site 20 meters downstream of TAT09-039 measured 180.8 mM.

Site	Strain	T°C	pH	[DIC]	[As^{III}]	[As^{V}]	[Na^+]	[Cl^-]
TAT09-025	T-025	65.5	6.1	2.7	0.03	0.31	103.8	122.2
TAT09-031	T-031	25.8	7.1	0.57	0	0.42	158.9	123.7
TAT09-039	T-039	30.9	7.0	0.24	0	0.44	171.7	180.5
TAT09-045	T-039	53.9	6.1	1.7	0	0.04	2.7	2.9

Table 3-2: Strain designations, culture collection ID's, and closest hits in BLAST and their % sequence similarity to the cultured ETGF strain (Altschul et al. 1990). Taxonomy represents that of similar database sequences, not the taxonomy of the culture organisms.

Culture	UTEX ID	Close BLAST Hits	%ID	Taxonomy of BLAST relatives
T-025	UTEX B 3001	*Synechocystis* sp. LEGE 06079 (HM217076) *Synechocystis* sp. Sai002 (GU935368)	99 99	Oscillatoriophycideae; Chroococcales; *Synechocystis* " "
T-031	UTEX B 3002	*Nostoc calcicola* strain BDU 40302 (KC883980) *Nodularia harveyana* strain Bo53 (AJ781143)	98 96	Nostocales; Nostocaceae; *Nostoc* Nostocales; Nostocaceae; *Nodularia*
T-039	UTEX B 3003	*Synechocystis* sp. LEGE 06079 (HM217076.1) *Synechocystis* sp. Sai002 (GU935368)	99 99	Oscillatoriophycideae; Chroococcales; *Synechocystis* " "
T-045	UTEX B 3004	*Synechocystis* sp. Sai002 (GU935368) Merismopedia glauca strain B1448-1 (X94705)	99 99	Oscillatoriophycideae; Chroococcales; *Synechocystis* Oscillatoriophycideae; Chroococcales; *Merismopedia*

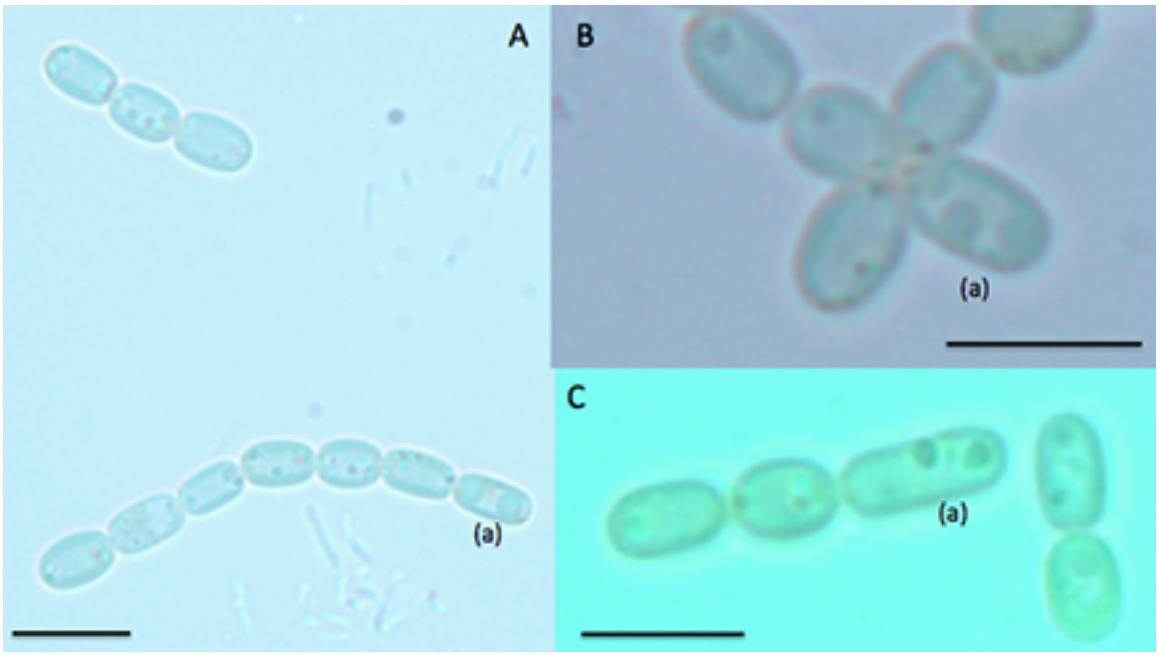

Figure 3-1: Morphology of isolate T-025. Images are shown at 1000X (A), and zoomed in, also at 1000X (B, C). Cells are cylindrical with rounded ends, approximately 4 x 3.5 µm in size. Short filaments of cells are connected end to end, and appear to divide at the terminal cells (a). Scale bars in each image are 10 µm.

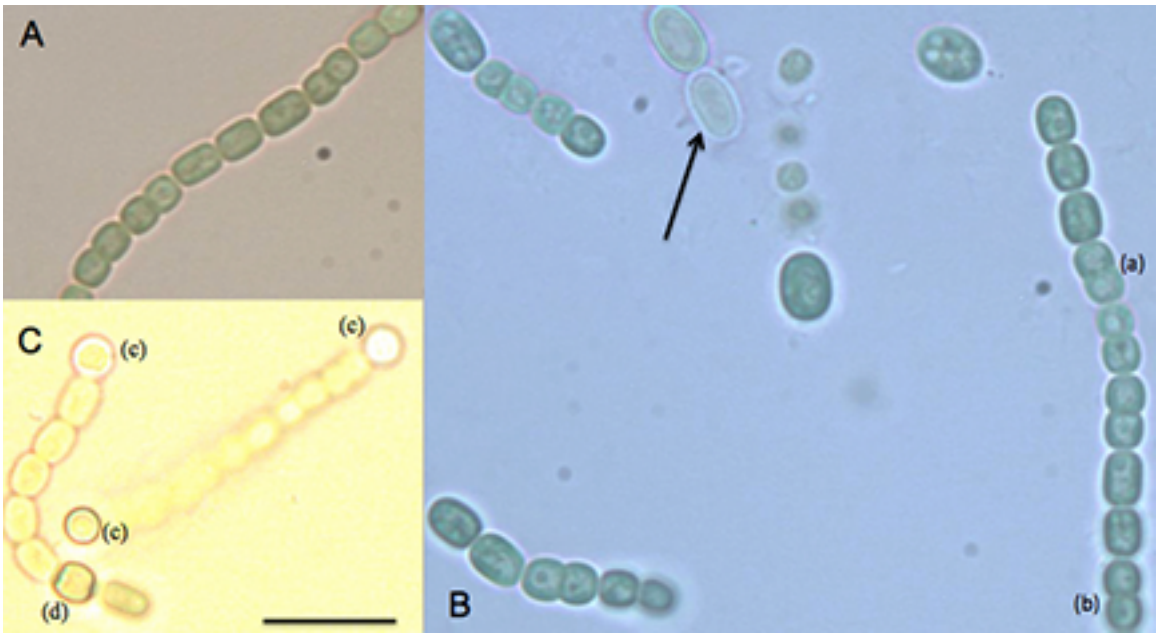

Figure 3-2: Morphology of isolate T-031. Images are shown at 1000x magnification. Cells are cylindrical with rounded ends, approximately 3 x 4 µm in size. Short filaments of cells are connected end to end, and appear to undergo intercalary division (a) and terminal cell division (b). Larger and more translucent cells are akinetes (arrow). No heterocysts are visible in (A) and (B), due to growth in nitrogen rich media, but are visible when grown in BG-11(-N), where terminal (c) and intercalary (d) heterocysts are visible (C). Scale bar in (C) is 10 µm and applies to all images.

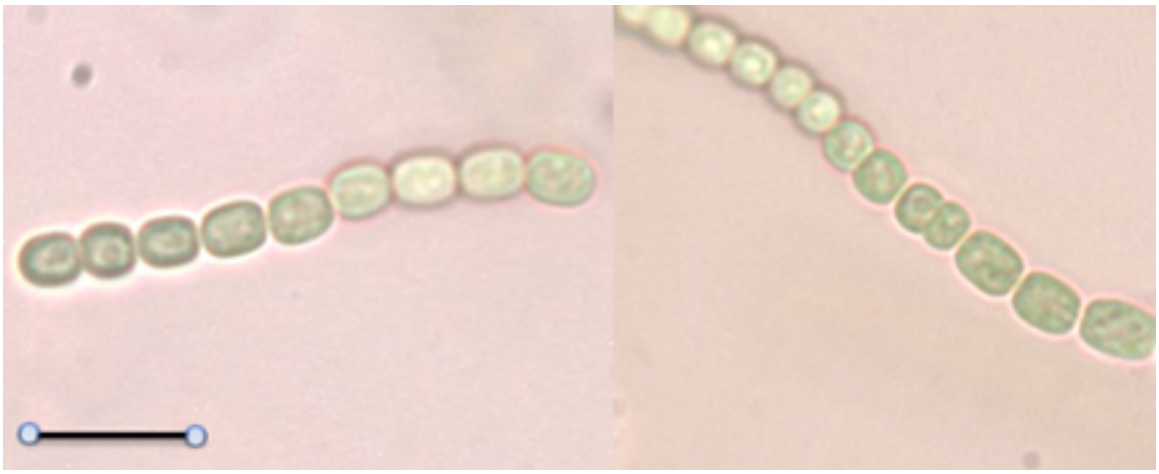

Figure 3-3: Cultured isolate T-039. Images are shown at 1000X magnification. Cells are in short filaments, oval in shape, and binary cell division appears to occur in the center of the filament (image on right). Scale bar is 10 μm for both images.

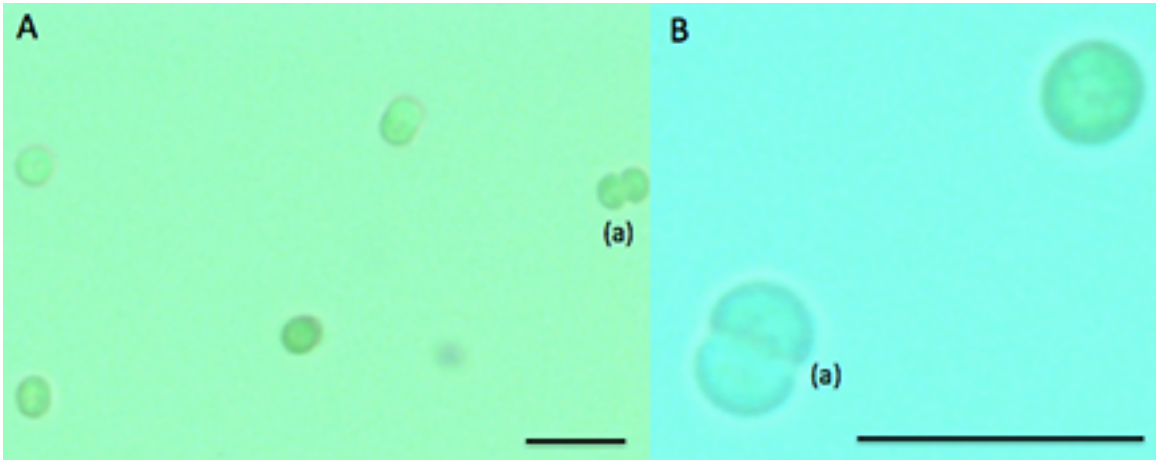

Figure 3-4: Cultured isolate T-045 morphology. Images are shown at 1000x (A), and zoomed in at 1000x (B) magnification. Cells are spherical, approximately 2-3 μm in diameter, and undergo binary fission (a). Scale bars in each image are 10 μm.

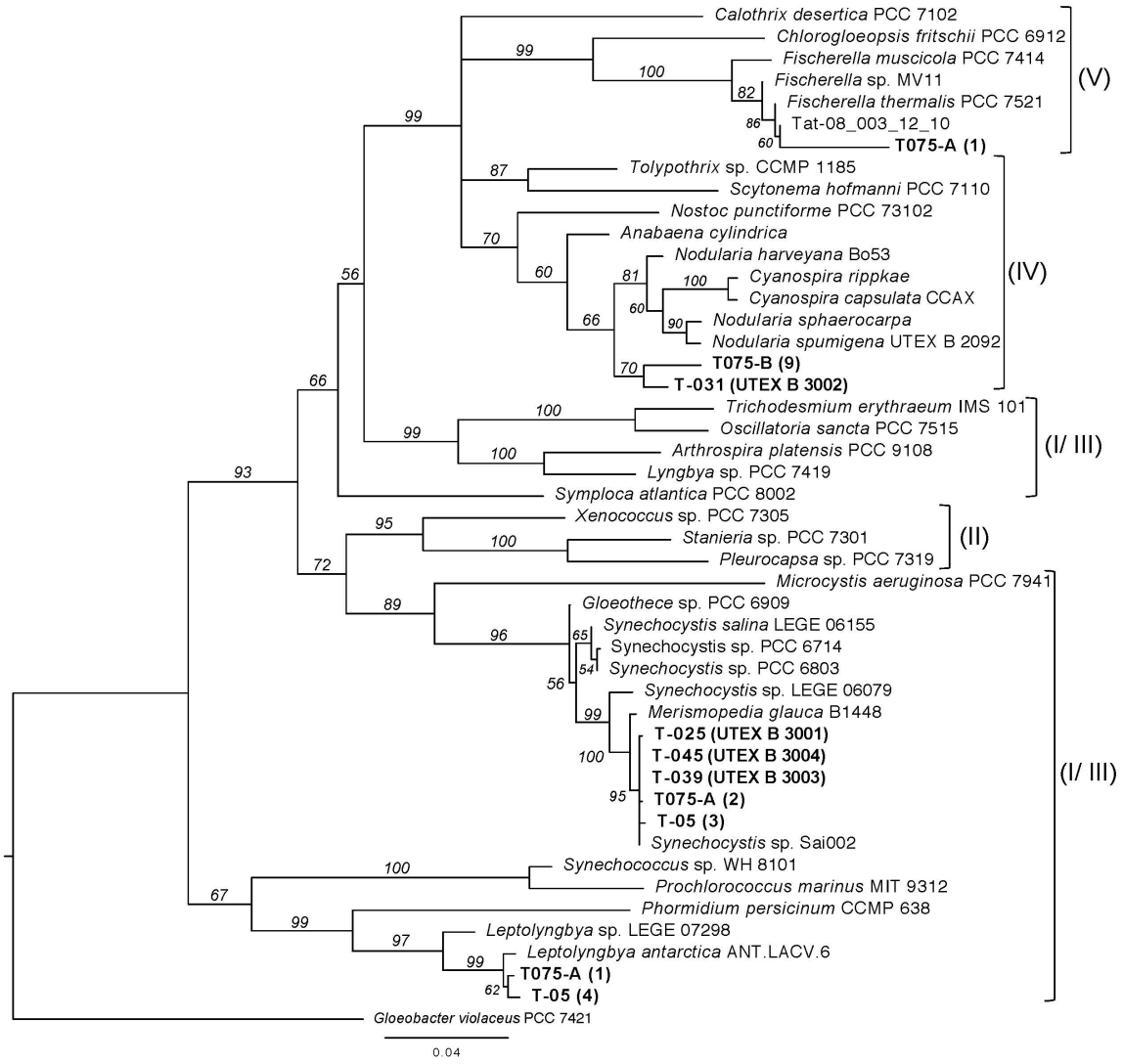

Figure 3-5: 16S rRNA phylogenetic reconstruction of cultured isolates and environmental clones, and selected database sequences shows the diversity of cyanobacteria found in El Tatio geothermal features. *Gloeobacter* PCC 7421 was used as an outgroup. The tree was constructed under maximum likelihood criteria using GTR+G+I model of sequence evolution. UTEX ID's of cultured El Tatio strains are in parentheses. The Subsection of each portion of the tree is bracketed and labeled I-V. Subsections I and III have been combined in this analysis.

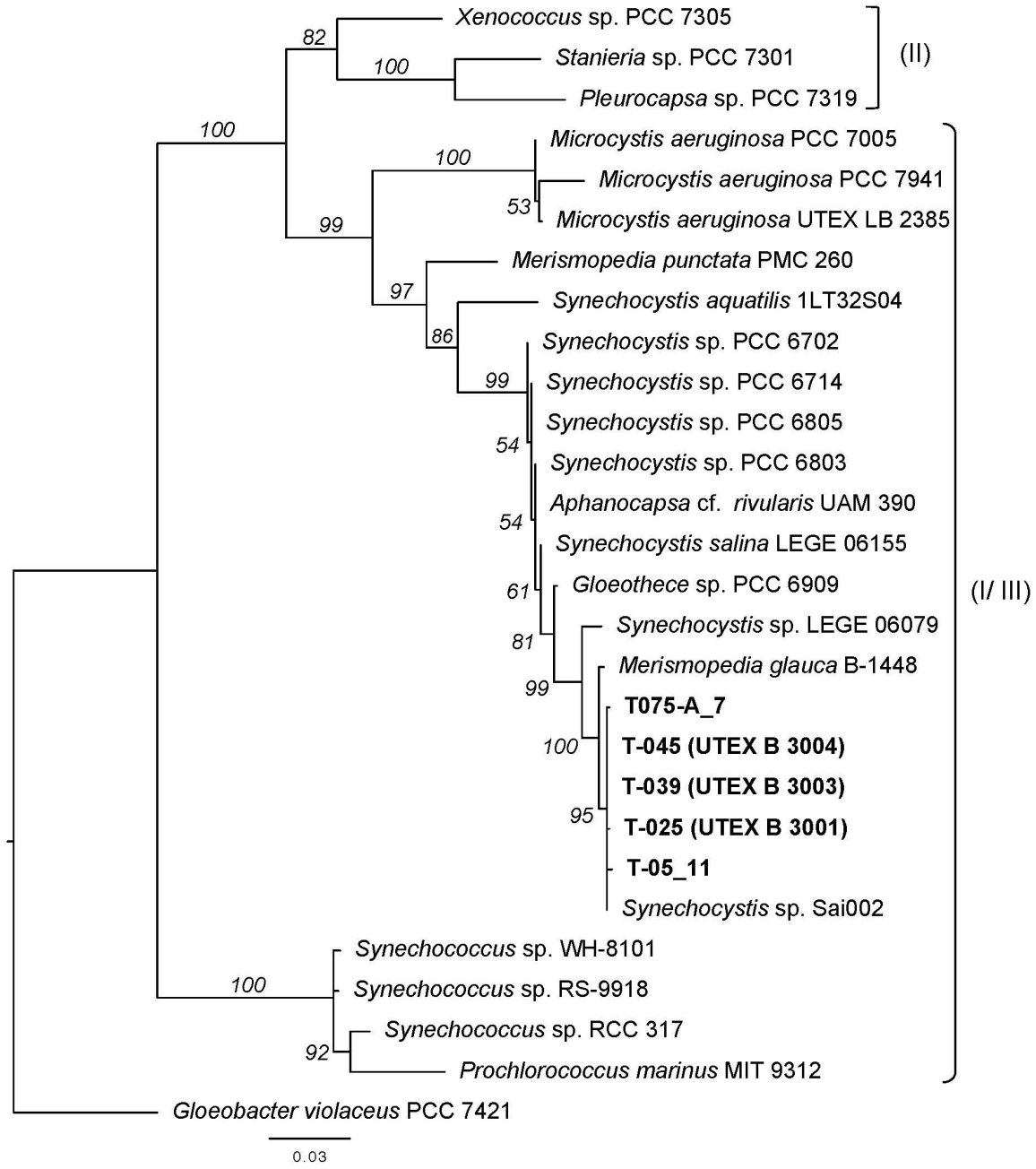

Figure 3-6: 16S rRNA phylogenetic reconstruction of cultures T-025, -039, and -045, compared to database sequences shows the diversity of Subsection I cyanobacteria in El Tatio geothermal features. *Gloeobacter* PCC 7421 was used as an outgroup. The tree was constructed under maximum likelihood criteria using GTR+G+I model.

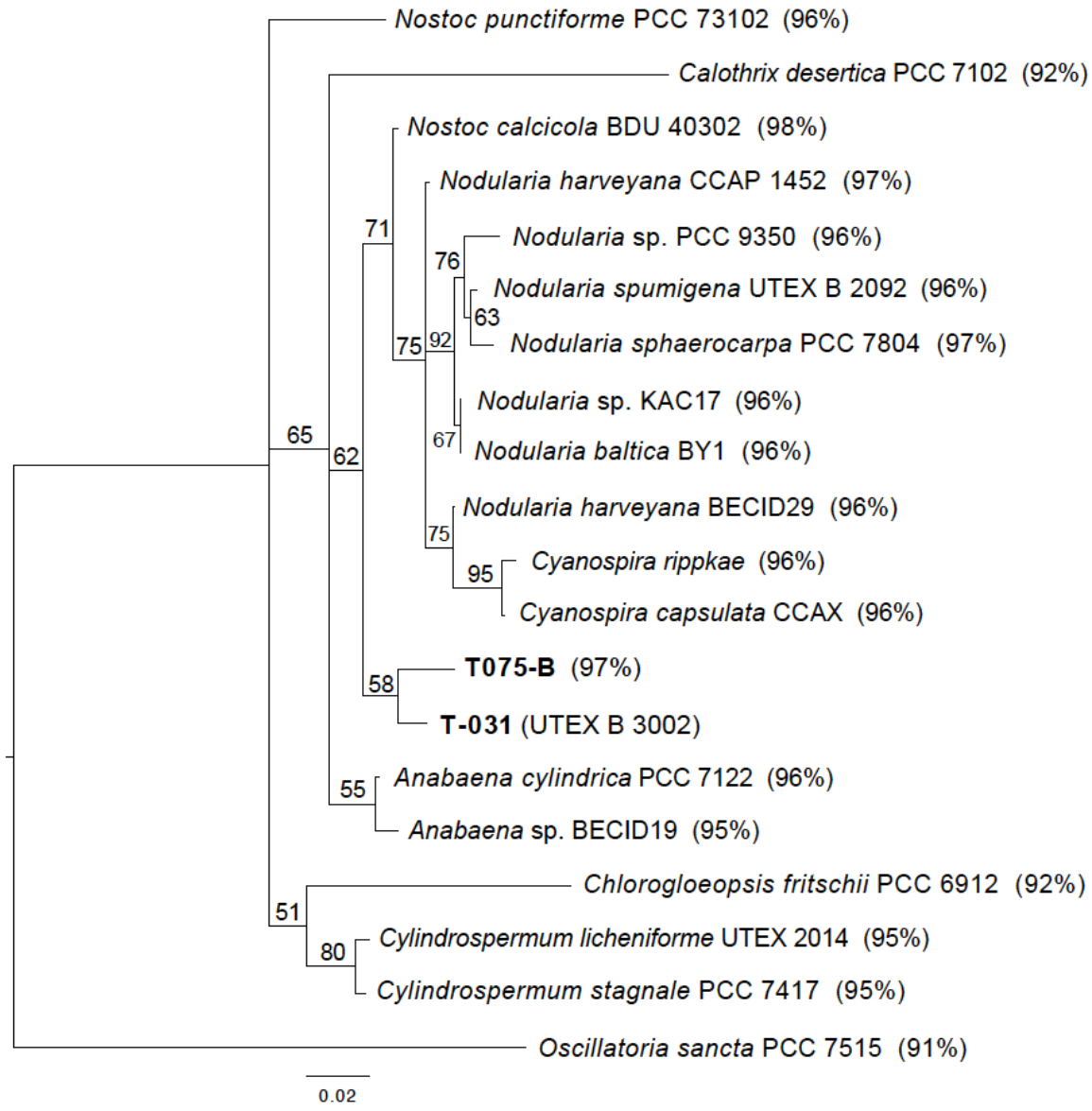

Figure 3-7: 16S rRNA phylogeny of culture T-031 and members of cyanobacteria Subsection IV. Constructed using maximum likelihood criteria under the GTR+G+I model. Subsection III cyanobacterium *Oscillatoria* PCC 7515 was used as an outgroup.

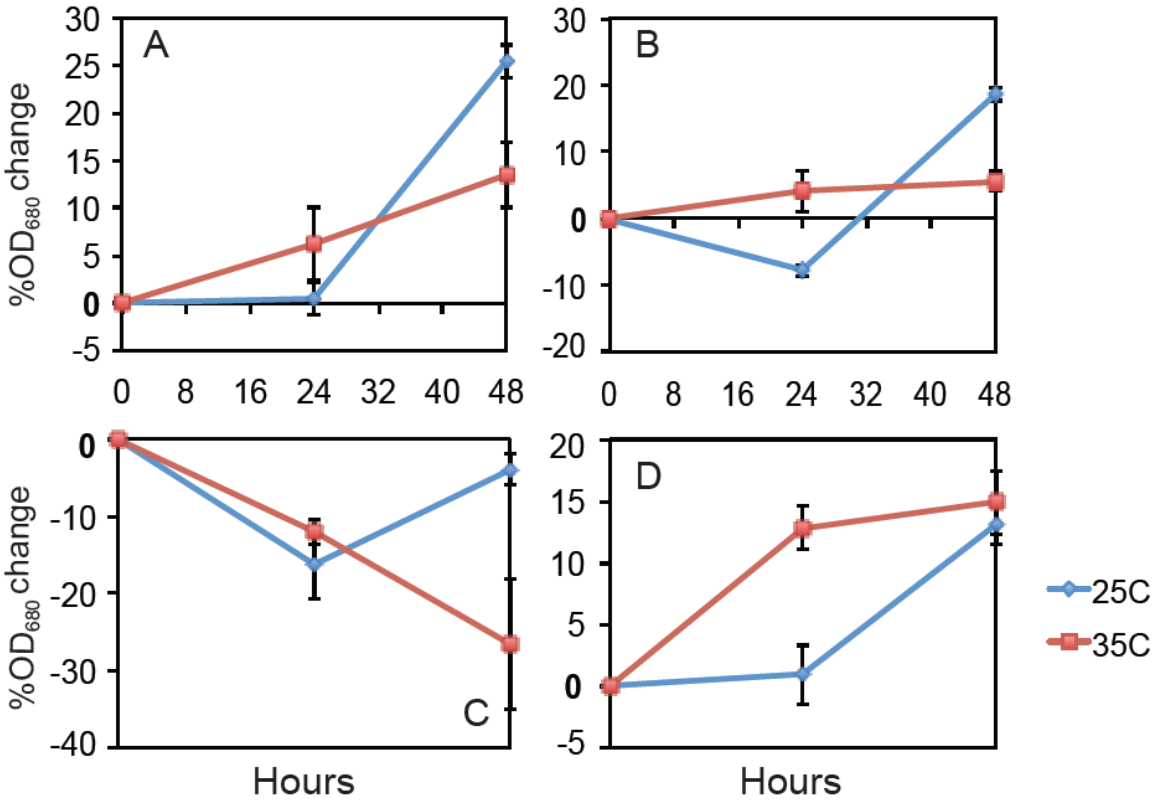

Figure 3-8: Temperature growth curves at 25°C, and 35°C relative to growth at room temperature (23°C) of T-025 (A), T-039 (B), T-031 (C) and T-045 (D). (*n* = 3).

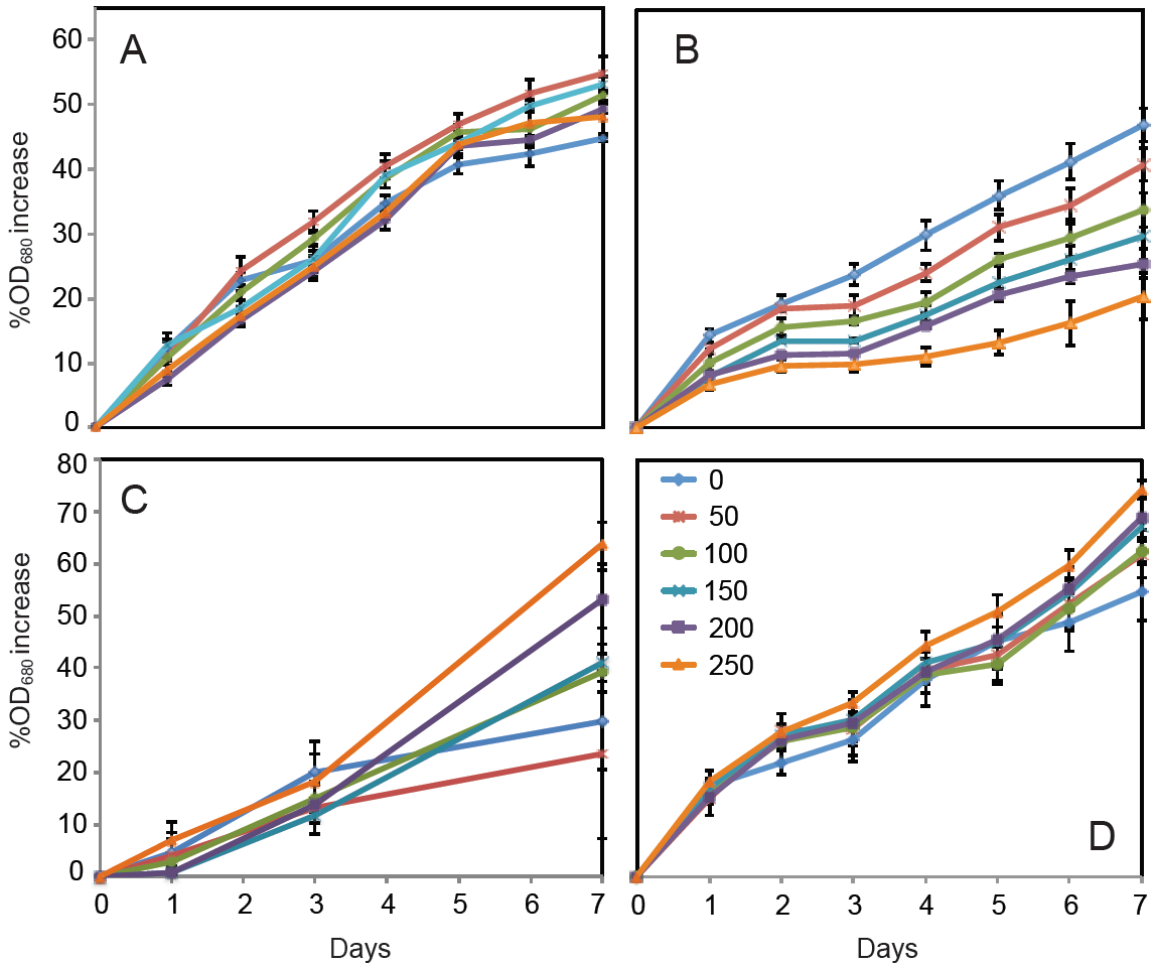

Figure 3-9: Growth of culture T-025 (A), T-039 (B), T-031 (C), and T-045 (D) in 0, 50, 100, 150, 200, or 250 mM [NaCl] added to normal BG11(+N) media (n = 3).

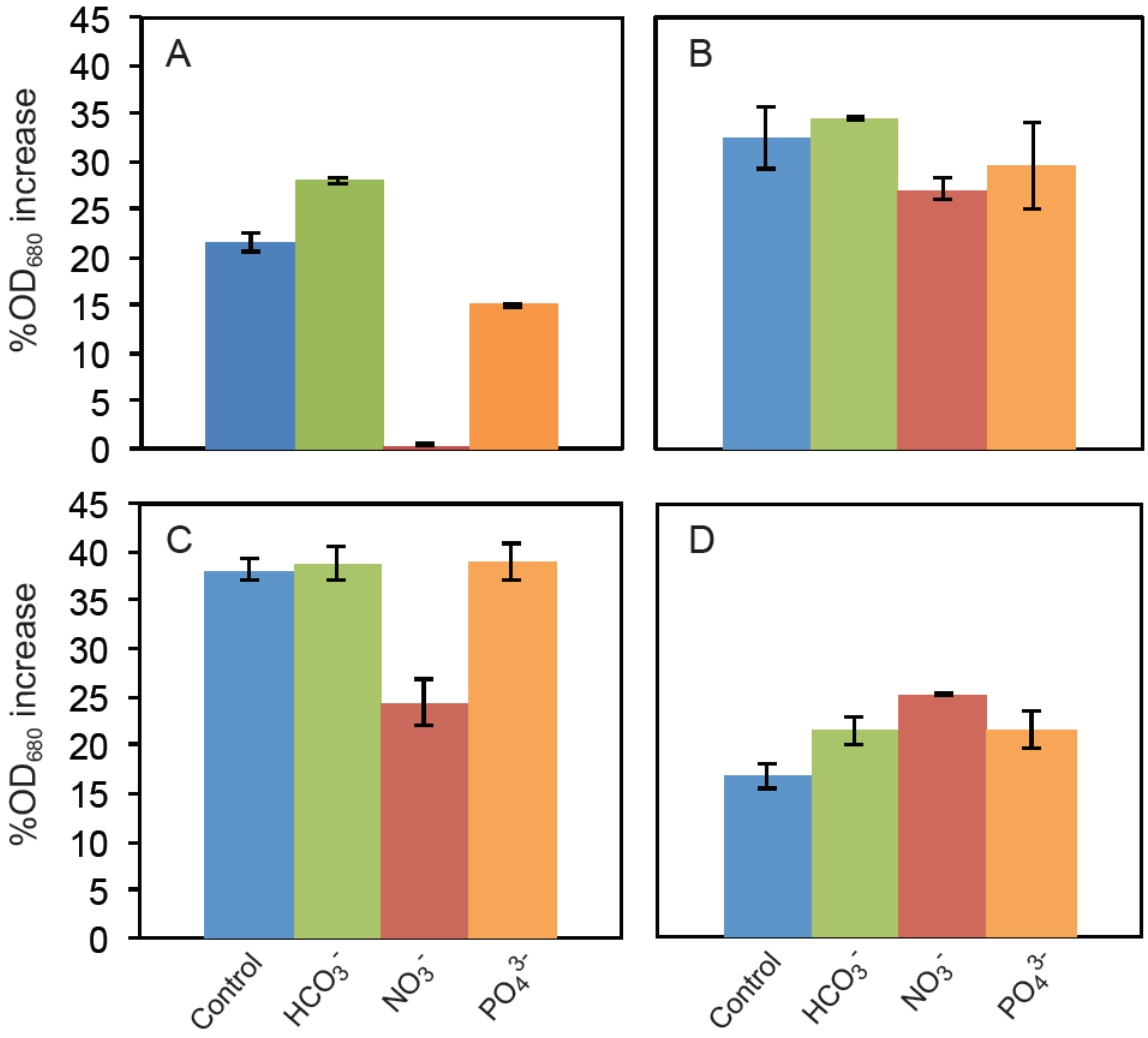

Figure 3-10: Growth of cultures (A) T-025, (B) T-039, (C) T-031, and (D) T-045 after 8 days in BG-11(+N) amended with no additional nutrients (control), 1 mM HCO_3^-, 1 mM NO_3^-, or 1 mM PO_4^{3-}. Cells were placed in dilute BG-11(+N) one week prior to experiment to "starve" cells. Error is reported as standard error of the mean (n = 2).

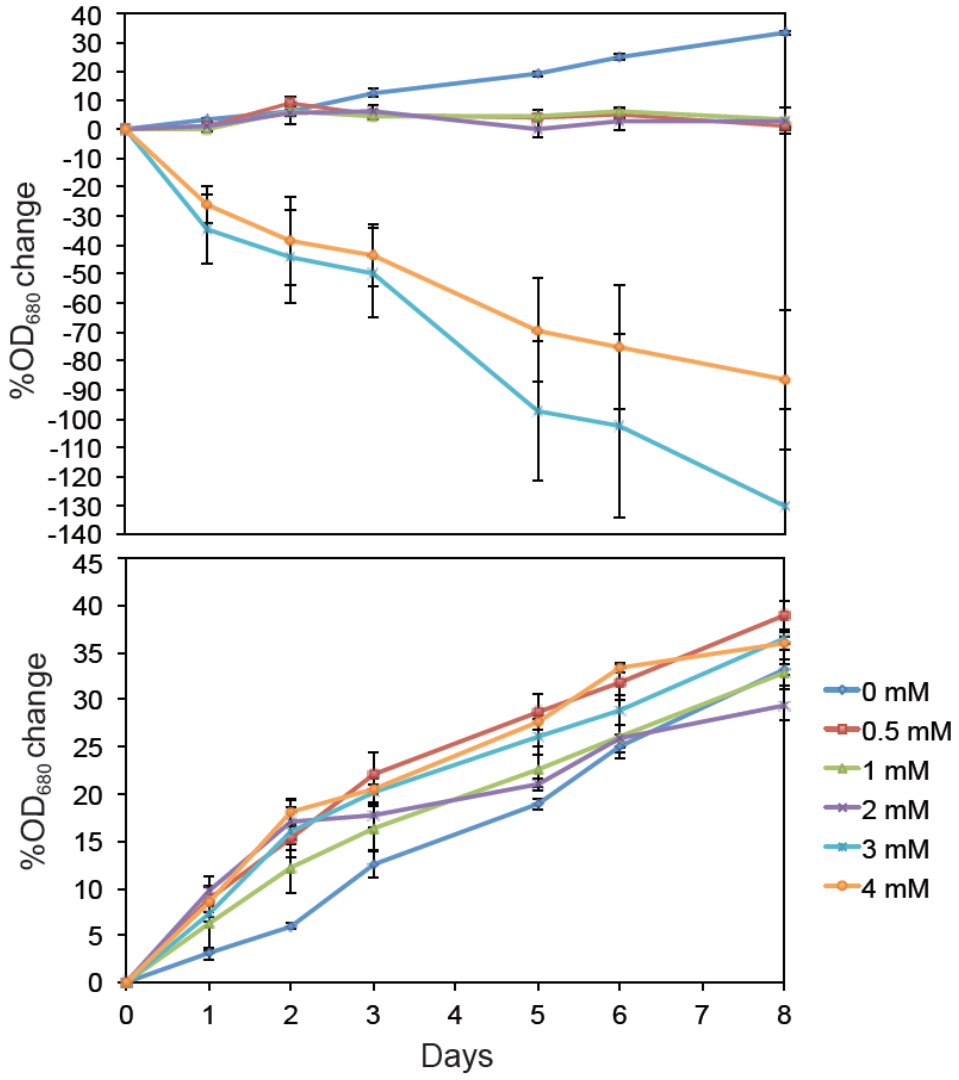

Figure 3-11: Growth response, measured as daily change in optical density at 680 nm, of culture T-025 when exposed to 0-4.0 mM As^{III} (A), or 0-4 mM As^{V} (B). Error bars represent standard error of the mean (n = 3).

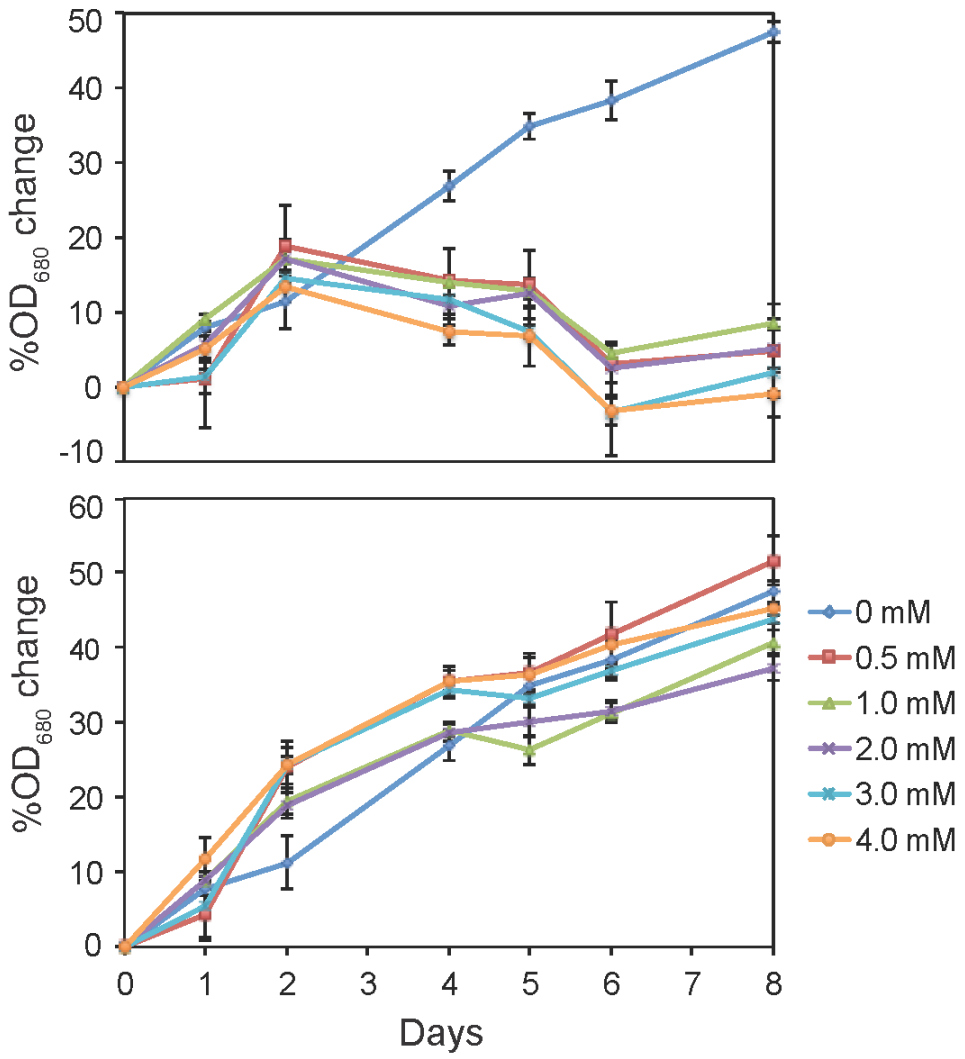

Figure 3-12: Growth response, measured as daily change in optical density at 680 nm, of culture T-039 when exposed to 0-4.0 mM As^{III} (A), or 0-4 mM As^{V} (B). Error bars represent standard error of the mean (n = 3).

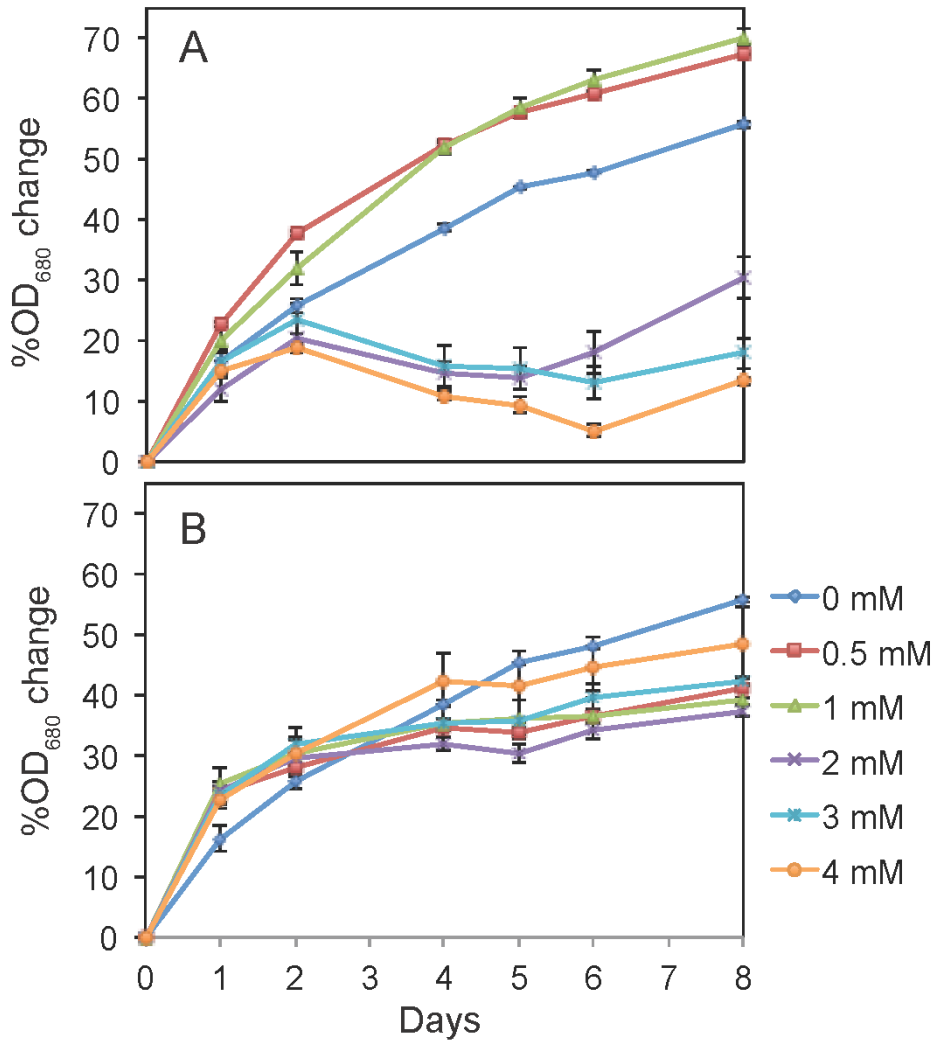

Figure 3-13: Growth response, measured as daily change in optical density at 680 nm, of culture T-045 when exposed to 0-4.0 mM As^{III} (A), or 0-4 mM As^{V} (B). Error bars represent standard error of the mean (n = 3).

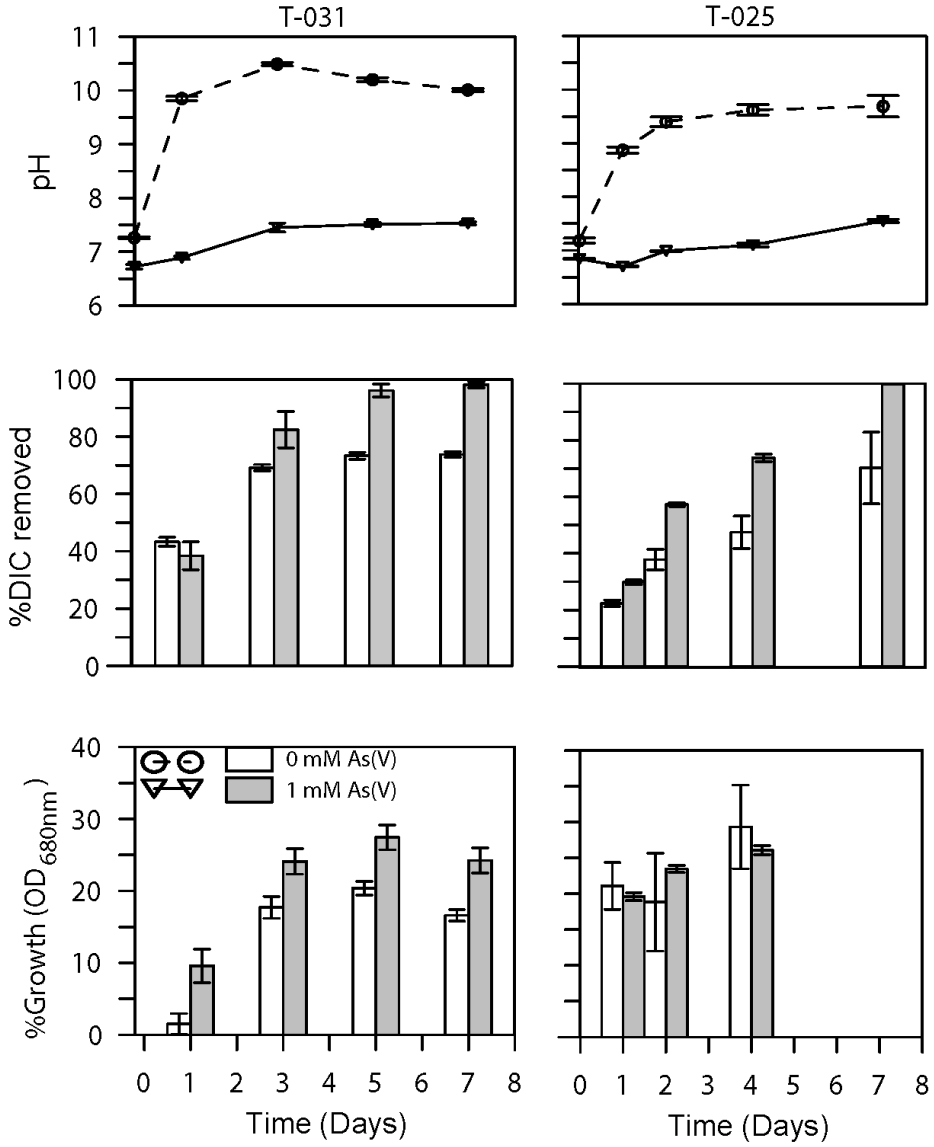

Figure 3-14: A comparison of the DIC uptake and pH shift behavior of T-031 and T-025, with and without 1 mM As^V. Error bars represent standard error of the mean (n = 8, T-031; n = 10, T-025).

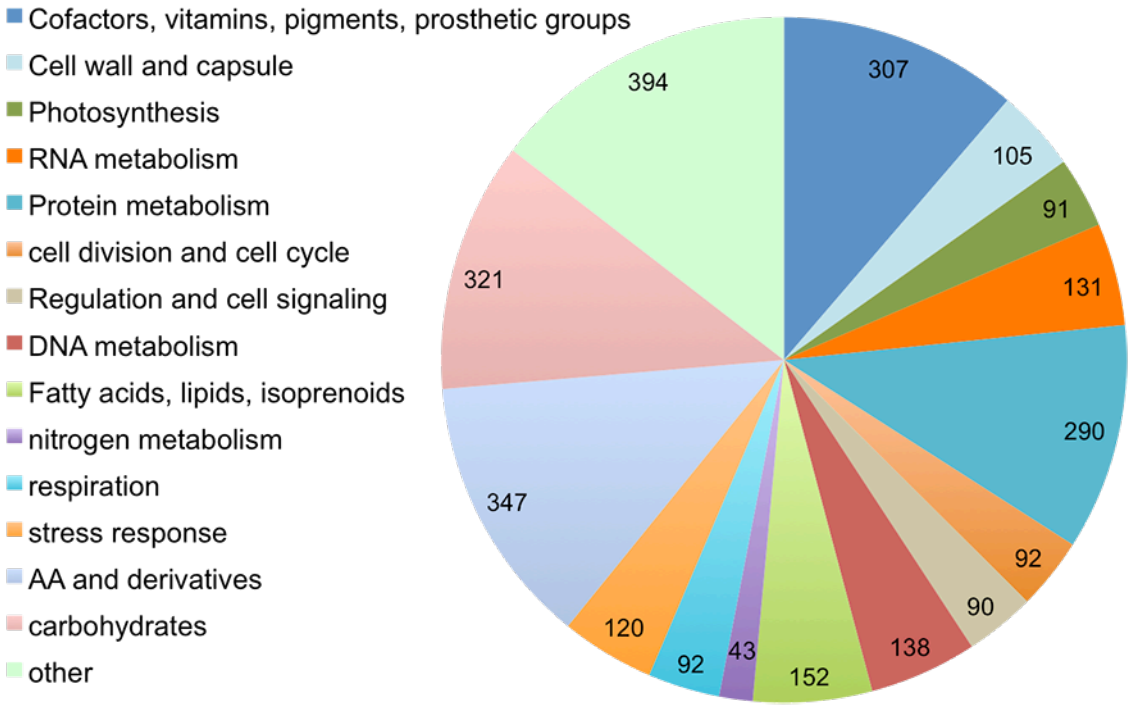

Figure 3-15: Overview of the metabolic and protein coding subsystems in the genome of T-031 (UTEX B 3002). Only 30% of the entire genome fits within known subsystems (1,833 hypothetical and non-hypothetical protein coding regions), while 70% of the genome contains putative protein coding regions that do not fall within known subsystems. A total of 2,713 subsystem features are represented here.

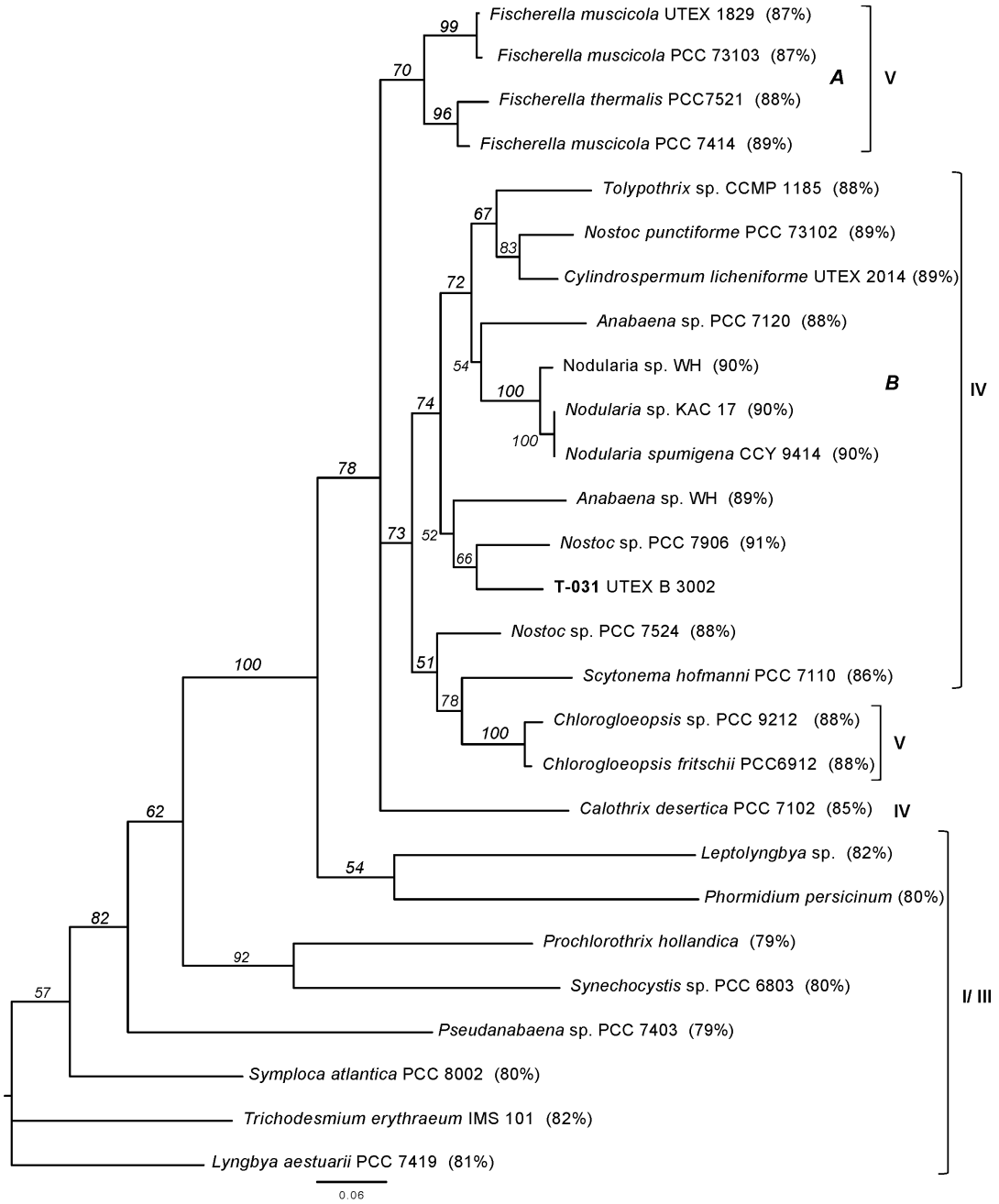

Figure 3-16: Phylogeny of *rbc*L genes from representative Subsection I, III, IV, and V cyanobacteria compared to the *rbc*L gene of T-031. Sequences for two major groups, A, composed mainly of *Fischerella* sp., and B, composed mainly of Nostocales and other Subsection IV organisms. No outgroup was used in this reconstruction. % sequence similarity of each sequence to T-031 *rbcL* is indicated in parentheses.

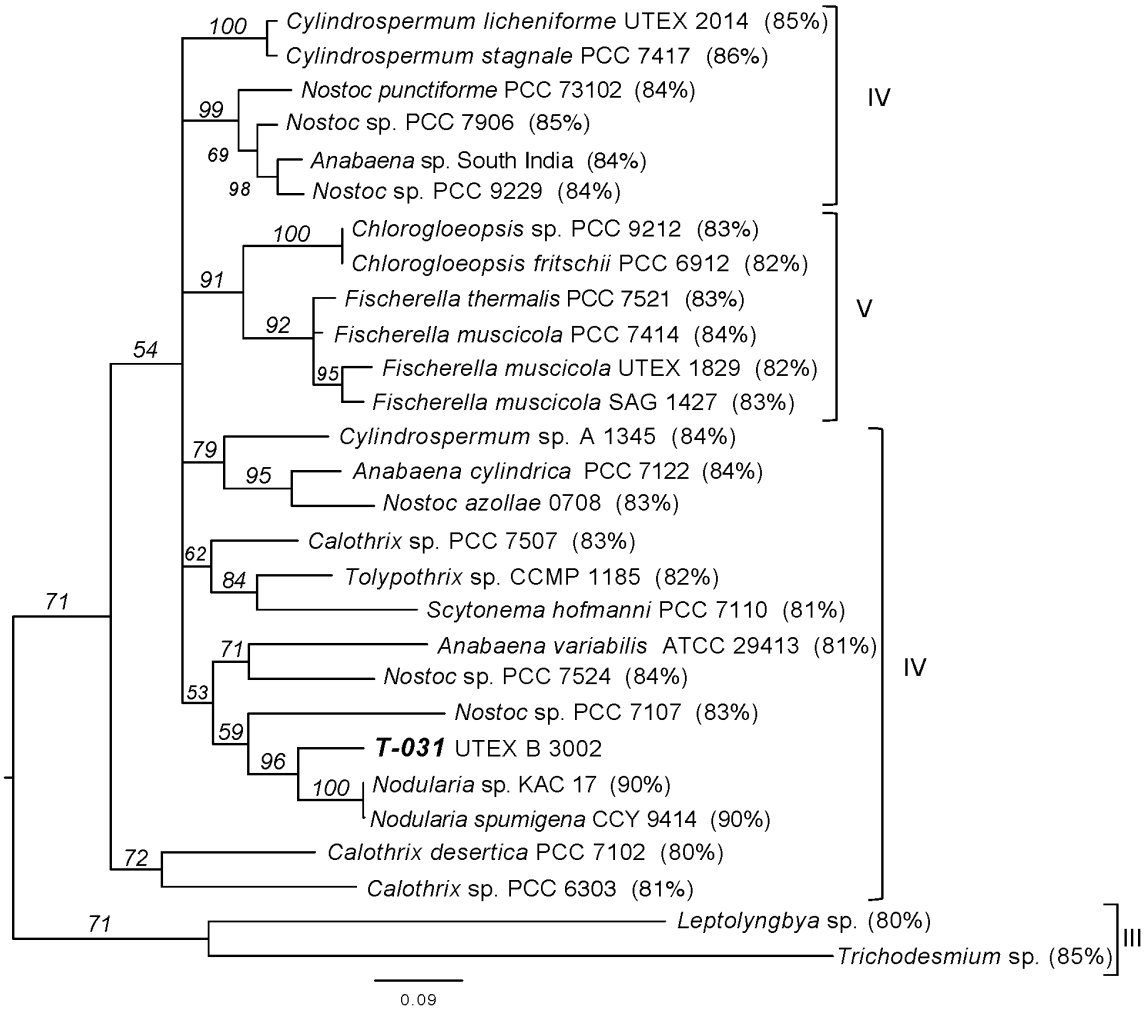

Figure 3-17: Phylogeny of *hetR* genes from representative Subsection III, IV, and V cyanobacteria compared to the *hetR* gene of T-031. No outgroup was used in this reconstruction.

REFERENCES

Altschul, S.F., Gish, W., Miller, W., Myers, E.W., and Lipman, D.J. (1990) Basic Local Alignment Search Tool. *Journal of Molecular Biology* **215**: 403-410.

Aziz, R.K., Bartels, D., Best, A.A., DeJongh, M., Disz, T., Edwards, R.A. et al. (2008) The RAST Server: rapid annotations using subsystems technology. *BMC Genomics* **9**: 75.

Badger, M.R., Price, G.D., Long, B.M., and Woodger, F.J. (2006) The environmental plasticity and ecological genomics of the cyanobacterial CO_2 concentrating mechanism. *Journal of Experimental Botany* **57**: 249-265.

Bazinet, A.L., Zwickl, D.J., and Cummings, M.P. (2014) A gateway for phylogenetic analysis powered by grid computing featuring GARLI 2.0. *Systematic Biology* **63**: 812-818.

Castenholz, R.W. (2001) Phylum BX. Cyanobacteria. In *Bergey's Manual*.

Chenna, R. (2003) Multiple sequence alignment with the Clustal series of programs. *Nucleic Acids Research* **31**: 3497-3500.

Eisenhut, M., Kahlon, S., Hasse, D., Ewald, R., Lieman-Hurwitz, J., Ogawa, T. et al. (2006) The plant-like C2 glycolate cycle and the bacterial-like glycerate pathway cooperate in phosphoglycolate metabolism in cyanobacteria. *Plant Physiology* **142**: 333-342.

Engel, A.S., Johnson, L.R., and Porter, M.L. (2013) Arsenite oxidase gene diversity among Chloroflexi and Proteobacteria from El Tatio Geyser Field, Chile. *FEMS Microbiology Ecology* **83**: 745-756.

Felsenstein, J. (1981) Evolutionary trees from DNA sequences: a maximum likelihood approach. *Journal of Molecular Evolution* **17**: 368-376.

Florenzano, G., Sili, C., Pelosi, E., and Vincenzini, M. (1985) Cyanospira rippkae and Cyanospira capsulata (gen. nov. and spp. nov.): new filamentous heterocystous cyanobacteria from Magadi lake (Kenya). *Archives of Microbiology* **140**: 301-306.

Giovannoni, S.J., Turner, S., Olsen, G.J., Barns, S., Lane, D.J., and Pace, N.R. (1988) Evolutionary relationships among cyanobacteria and green chloroplasts. *Journal of Bacteriology* **170**: 3584-3592.

Hasegawa, M., Kishino, H., and Yano, T. (1985) Dating of the Human-Ape splitting by a molecular clock of mitochondrial DNA. *Journal of Molecular Evolution* **22**: 160-174.

Hedges, S.B. (1992) The number of replications needed for accurate estimation of the Bootstrap P value in phylogenetic studies. *Molecular Biology and Evolution* **9**: 366-369.

Herdman, M., Janvier, M., Rippka, R., and Stanier, R.Y. (1979) Genome size of cyanobacteria. *Journal of General Microbiology* **111**: 73-85.

Kaneko, T., Nakamura, Y., Wolk, C.P., Kuritz, T., Sasamoto, S., Watanabe, A. et al. (2001) Complete genomic sequence of the filamentous nitrogen-fixing cyanobacterium Anabaena sp. Strain PCC 7120. *DNA Research* **8**: 205-213.

Kaneko, T., Sako, S., Kotani, H., Tanaka, A., Asamizu, E., Nakamura, Y. et al. (1996) Sequence analysis of the genome of the unicellular cyanobacterium Synechocystis sp. Strain PCC6803. II. Sequence determination of the entire genome and assignment of potential protein-coding regions. *DNA Research* **3**: 109-136.

Komarek, J. (1976) Taxonomic review of the genera Synechocystis Sauv. 1892, Synechococcus Nag. 1849, and Cyanothece gen. nov. (Cyanophyceae). *Archiv fur Protistenkunde*: 119-179.

Landrum, J.T. (2007) Fate and Transport of Arsenic and Antimony in the El Tatio Geyser Field, Chile (Masters Thesis) The University of Texas at Austin.

Landrum, J.T., Bennett, P.C., Engel, A.S., Alsina, M.A., Pastén, P.A., and Milliken, K. (2009) Partitioning geochemistry of arsenic and antimony, El Tatio Geyser Field, Chile. *Applied Geochemistry* **24**: 664-676.

Larkin, M.A., Blackshields, G., Brown, N.P., Chenna, R., McGettigan, P.A., McWilliam, H. et al. (2007) Clustal W and Clustal X version 2.0. *Bioinformatics* **23**: 2947-2948.

Lyra, C., Laamanen, M., Lehtimaki, J.M., Surakka, A., and Sivonen, K. (2005) Benthic cyanobacteria of the genus Nodularia are non-toxic, without gas vacuoles, able to glide and genetically more diverse than planktonic Nodularia. *International Journal of Systematic and Evolutionary Microbiology* **55**: 555-568.

Moffitt, M.C., Blackburn, S.I., and Neilan, B.A. (2001) rRNA sequences reflect the ecophysiology and define the toxic cyanobacteria of the genus Nodularia. *International Journal of Systematic and Evolutionary Microbiology* **51**: 505-512.

Nakamura, K., Kaneko, T., Sato, S., Mimuro, M., Miyashita, H., Tsuchiya, T. et al. (2003) Complete genome structure of Gloeobacter violaceus PCC 7421, a cyanobacterium that lacks thylakoids. *DNA Research* **10**: 137-145.

Oren, A. (2012) Salts and Brines. In *Ecology of Cyanobacteria II: Their Diversity in Space and Time*. Whitton, B.A. (ed): Springer Science+Business Media, pp. 401-426.

Overbeek, R., Olson, R., Pusch, G.D., Olsen, G.J., Davis, J.J., Disz, T. et al. (2014) The SEED and the Rapid Annotation of microbial genomes using Subsystems Technology (RAST). *Nucleic Acids Research* **42**: D206-214.

Phoenix, V.R., Bennett, P.C., Engel, A.S., Tyler, S.W., and Ferris, F.G. (2006) Chilean high-alititude hot-spring sinters: a model system for UV screening mechanisms by early Precambrian cyanobacteria. *Geobiology* **4**: 15-28.

Raven, J.A. (2012) Carbon. In *The Ecology of Cyanobacteria II: Their Diversity in Time and Space*. Whitton, B.A. (ed). New York, NY: Springer Science+Business Media, pp. 443-460.

Reumann, S., and Weber, A.P. (2006) Plant peroxisomes respire in the light: some gaps of the photorespiratory C2 cycle have become filled--others remain. *Biochimica et Biophysica Acta* **1763**: 1496-1510.

Rippka, R., Deruelles, J., Waterbury, J.B., Herdman, M., and Stanier, R.Y. (1979) Generic assignments, strain histories and properties of pure cultures of cyanobacteria. *Journal of General Microbiology* **111**: 1-61.

Schirrmeister, B.E., Antonelli, A., and Bagheri, H.C. (2011) The origin of multicellularity in cyanobacteria. *BMC Evolutionary Biology* **11**: 45.

Stanier, R.Y., Kunisawa, R., Mandel, M., and Cohen-Bazire, G. (1971) Purification and properties of unicellular blue-green algae (Order Chroococcales). *Bacteriological Reviews* **35**: 171-205.

Tajima, N., Sato, S., Maruyama, F., Kaneko, T., Sasaki, N.V., Kurokawa, K. et al. (2011) Genomic structure of the cyanobacterium Synechocystis sp. PCC 6803 strain GT-S. *DNA Research* **18**: 393-399.

Tomitani, A., Knoll, A.H., Cavanaugh, C.M., and Ohno, T. (2006) The evolutionary diversification of cyanobacteria: molecular-phylogenetic and paleontological perspectives. *Proceedings of the National Academy of Sciences of the United States of America* **103**: 5442-5447.

Waddell, P.J., and Steel, M.A. (1997) General time-reversible distances with unequal rates across sites: mixing gamma and inverse Gaussian distributions with invariant sites. *Molecular Phylogenetics and Evolution* **8**: 398-414.

Ward, D.M., Castenholz, R.W., and Miller, S.R. (2012) Cyanobacteria in Geothermal Habitats. In *Ecology of Cyanobacteria II: Their Diversity in Space and Time*. Whitton, B.A. (ed): Springer Science + Business Media, pp. 39-63.

Ward, D.M., Ferris, M.J., Nold, S.C., and Bateson, M.M. (1998) A natural view of microbial biodiversity within hot spring cyanobacterial mat communities. *Microbiology and Molecular Biology Reviews* **62**: 1353-1370.

Wilmotte, A. (1994) Molecular evolution and taxonomy of the Cyanobacteria. In *The Molecular Biology of Cyanobacteria*. Bryant, D.A. (ed). Dordrecht, Netherlands: Springer Science + Business Media, pp. 1-25.

Yin, X.X., Chen, J., Qin, J., Sun, G.X., Rosen, B.P., and Zhu, Y.G. (2011) Biotransformation and volatilization of arsenic by three photosynthetic cyanobacteria. *Plant Physiology* **156**: 1631-1638.

Zwickl, D.J. (2006) Genetic algorithm approaches for the phylogenetic analysis of large biological datasets under the maximum likelihood criterion (Ph.D. Dissertation) The University of Texas at Austin.

Chapter 4: Arsenic Plays a Dominant Role in the Ecology of Cyanobacteria in the Geothermal Waters of El Tatio, Chile through its Impact on Carbon Uptake

ABSTRACT

The circumneutral geothermal waters of El Tatio Geyser Field, northern Chile contain high arsenic (0.4-0.6 mM As_T), limited dissolved inorganic carbon (0.1-0.3 mM DIC), and are buffered by arsenate (As^V). The distribution and productivity of cyanobacteria appear to be strongly influenced by the lack of DIC coupled to As redox speciation. Geochemical analyses, 16S rRNA pyrosequencing, and laboratory experiments were used to assess the impact of As concentration and speciation on the environmental distribution, DIC uptake, and growth of El Tatio cyanobacteria. Results show that cyanobacteria are abundant in As^V-dominated areas, but largely absent in As^{III}-dominated areas of DIC-limited streams. A novel cyanobacterial strain isolated from El Tatio demonstrated greater photosynthetic DIC uptake and higher subsequent biomass increase in the presence of As^V compared to As-free controls, whereas As^{III} limited survival and growth. Given that As^V (as $H_2AsO_4/HAsO_4^{2-}$) buffers pH, the presence of even low concentrations of As^V can be advantageous by mitigating biologically induced pH shifts, thereby maintaining DIC as HCO_3^- for photosynthesis. We propose that pH buffering by arsenate is central to the long-term survival of cyanobacteria-based microbial mats in DIC-limited streams at El Tatio, allowing them to allocate maximum assimilated DIC towards growth.

INTRODUCTION

Hot springs are extreme environments characterized by both high and highly variable temperatures with wide-ranging chemical conditions and nutrient compositions, while often containing toxic elements such as arsenic (As) (Ellis and Mahon, 1964; Ellis and Mahon, 1967, 1977; Stauffer et al., 1980; Webster and Nordstrom, 2003). In spite of these stressors, geothermal waters can support microbial mats dominated by Bacteria and Archaea (Paerl, 1996; Paerl et al., 2000; Ward and Cohan, 2005; Stal, 2012), and the membership and diversity of these communities is strongly influenced by physical and geochemical gradients at various spatial scales (Ward et al., 2012). Cyanobacteria often act as the dominant primary producers for hot spring microbial mat communities by fixing dissolved inorganic carbon (DIC) and providing organic carbon for heterotrophic and chemoorganotrophic prokaryotes (Ward and Castenholz, 2000; Stal, 2012).

El Tatio Geyser Field (ETGF) is an extreme environment, even among hydrothermal spring complexes. Located at ~4,300 m elevation in the Atacama Desert Region of northern Chile, the climate is hyper-arid and experiences high UV radiation flux (Phoenix et al., 2006). Numerous springs, geysers, and boiling pools discharge reduced, nonsulfidic, circumneutral, and moderate salinity (Na:Cl type) waters near the local boiling point of 86°C (Lahsen and Trujillo, 1976; Giggenbach, 1978; Glennon and Pfaff, 2003; Cortecci et al., 2005; Tassi et al., 2005). These waters contain some of the highest reported naturally occurring total inorganic As concentrations in the world ($[As_T]$=0.4-0.6mM) (Ellis and Mahon, 1977; Ballantyne and Moore, 1988; Webster and Nordstrom, 2003; Landrum et al., 2009; Engel et al., 2013).

Emerging waters at ETGF contain high concentrations of arsenite (As^{III} as $H_3AsO_3^0$) that is rapidly oxidized to arsenate (As^V as $H_xAsO_4^{3-x}$) in association with microbial mats (Landrum et al., 2009), likely due to the activity of *Chloroflexus* sp. and various Proteobacteria (Engel et al., 2013). Once oxidized, arsenic persists as As^V, eventually reaching the regionally important Rio Loa, the major surface water resource in Region II, Chile (Smedley and Kinniburgh, 2002; Romero et al., 2003; Landrum et al., 2009; Alsina et al., 2013; Leiva et al., 2014).

Most geothermal waters at ETGF have low [DIC] (0.1-0.3 mM C, primarily as HCO_3^-) (Landrum et al., 2009), which is low enough to pose a challenge to photoautotrophic carbon fixation. Cyanobacteria possess a CO_2 concentrating mechanism (CCM) that improves the carbon fixation efficiency of RuBisCO during acclimation to low DIC environments (Price et al., 1998; Kaplan and Reinhold, 1999; Badger et al., 2002; Badger and Price, 2003; Raven, 2003; Giordano et al., 2005; Badger et al., 2006; Price et al., 2008); however, the CCM is meant to function as a short-term stress response mechanism, and has not been linked to sustained long-term growth. Furthermore, ETGF possesses an additional suite of stressors known to negatively impact RuBisCO's affinity for CO_2, such as high temperature and high light intensity (Badger, 1980; Woodger et al., 2003; McGinn et al., 2004; Badger et al., 2006). Additionally, within diffusion limited microbial mat environments, the dehydration step of carbonic anhydrase (CA) enzyme activity can elevate pH conditions and further deplete cells' access to CO_2 (Purcell, 1977; Badger et al., 2006).

While natural waters are commonly pH buffered by the carbonate system (Greenfield and Baker, 1920; Drever, 1988), most streams at ETGF have DIC concentrations that are too low to effectively buffer pH to the observed circumneutral range. Low DIC waters throughout El Tatio are instead buffered by arsenate (As^V), a multi-protic weak acid with a strong pH buffering capacity at 6.94, the pK_{a2} of the arsenic acid system at 25°C ($H_2AsO_4^-/HAsO_4^{2-}$) (Landrum et al., 2009). In contrast, other documented examples of low-DIC hydrothermal systems are acidic, such as the acid-sulfate and acid-sulfate-chloride waters found in the Norris Geyser Basin of Yellowstone (Stauffer et al., 1980; Langner et al., 2001; Nordstrom et al., 2005). As^V is also the primary redox buffer in ETGF waters (Landrum et al., 2009), but only the pH buffering effect of arsenate will be discussed further.

The importance of external pH buffering for efficient inorganic carbon uptake by photosynthetic organisms during CCM activity has been documented in higher DIC environments such as the ocean (~2 mM DIC as HCO_3^-, pH 8.3) (Badger et al., 2006). Proton buffering by biosilica and silicic acid has been reported to improve DIC uptake in diatoms by aiding proton transfer during CA activity; as a result, CCM buffering indirectly plays a crucial role in the ocean's biogeochemical carbon cycle (Lindskog and Coleman, 1973; Milligan and Morel, 2002). Due to the importance of pH buffering for CCM-utilizing organisms in high-DIC environments, we predicted that pH buffering by arsenate should play an important role for cyanobacteria in the DIC-limited waters at ETGF.

Prokaryotic As metabolism and As biogeochemical cycling has been reviewed extensively elsewhere and is beyond the scope of this report (e.g. (Mukhopadhyay et al., 2002; Oremland et al., 2004; Silver and Phung, 2005; Lloyd and Oremland, 2006; Oremland et al., 2009)). Though cyanobacteria are not known to participate in energy conserving As metabolism, unicellular strains have shown a detoxification response to As^{V} by expression of the *ars* gene cluster, which reduces As^{V} to As^{III} and subsequently pumps the more toxic As^{III} out of the cytoplasm (Lopez-Maury et al., 2003). Other research using cultured filamentous cyanobacteria found evidence that As^{V} is sequestered in their biomass (Bhattacharya and Pal, 2011), or that it may even enhance growth (Maeda et al., 1987; Thiel, 1988; Ferrari et al., 2013); however, no clear ecophysiological explanations have been proposed for these latter cases.

The As-rich and DIC-poor geothermal waters at ETGF provide an ideal setting in which to explore the previously undescribed relationship between arsenic, carbon, and primary productivity by cyanobacteria. This work aims to characterize environmental cyanobacterial distribution in relation to As^{III} and As^{V}, as well as explain the apparent positive influence of the pH buffering capacity of arsenate on cyanobacterial carbon assimilation and growth in the laboratory, especially under carbon limitation. We hypothesize that pH buffering by arsenate permits long-term scavenging of DIC by El Tatio cyanobacteria by preventing the CCM-induced pH shift usually observed in microbial mats during photosynthetic activity, allowing these important primary-producing microorganisms to form extensive microbial mats in the face of limited inorganic carbon availability.

METHODS

Sample Collection and Analysis

Geochemical and microbiological sampling took place in June 2009, 2011, and 2012 across 6 distinct geothermal features in the Upper and Middle Basins of ETGF. pH, Eh, and T(°C) were measured at time of sampling, and microbial mats were sampled aseptically. Water was filtered to 0.2 μm and analyzed for major cations, anions, arsenic species, and DIC using previously reported methods (Landrum et al., 2009). Samples collected for DNA sequencing were flash frozen and stored in a portable dry nitrogen dewar (Taylor-Wharton, Theodore, AL) until transport to the lab, and stored at -20°C until extraction. Samples intended for culturing were stored at 4°C.

Environmental DNA Extraction, Pyrosequencing, and Bioinformatics

Genomic DNA was extracted from microbial mat samples using a Power Biofilm DNA Extraction Kit (MO BIO Laboratories, Inc., Carlsbad, CA). DNA concentration and quality were verified using a NanoDrop Spectrometer (Fisher Scientific-USA, Pittsburgh, PA). The V6 region (position 939F) of the 16S rRNA gene was 454-pyrosequenced on a Roche GS FLX+ platform (Roche Diagnostics Corporation, Indianapolis, IN). Raw pyrosequencing reads were quality checked and OTU clustered at a 97% sequence similarity cutoff in the QIIME environment (Caporaso et al., 2010). Chimeric sequences were detected and removed using ChimeraSlayer (Haas et al., 2011). Taxonomic identification was performed using the Greengenes database and the RDP classifier in the QIIME environment (DeSantis et al., 2006; Wang et al., 2007; Liu et al., 2008).

Cyanobacteria Culturing, Isolation, and 16S rRNA Sequencing

Cyanobacterial strain T-031 was cultured from microbial mat sample TAT09-031 by enrichment in liquid BG-11(+N) media (Rippka et al., 1979). Cells were initially maintained at 23°C under low-intensity 12h/day irradiance for ~6 months, after which they were moved to 24h/day irradiance at 23°C. Four to six transfers to fresh media resulted in the isolation of monoculture T-031, confirmed by bright field and phase-contrast microscopy using an Olympus BX41 microscope (Olympus America, Inc., Melville, NY) and full-length 16S rRNA sequencing.

Full-length 16S rRNA gene sequences were amplified from genomic DNA from T-031 and DNA from site GG-75m (T075-B) by PCR in a Peltier PCT-100 thermocycler (Bio-Rad Laboratories, Hercules, CA) with cyanobacterial primers 16S-8F (5'-GCYTAAAGSRICCGTAGC-3') (Nubel et al., 1997) and 16S-1492R (5'-TTMGGGGCATRCIKACCT-3') (Weisburg et al., 1991). Each 25 μL PCR reaction contained 2-5 μl DNA (~750 ng), 0.5 mg/ml BSA, 10x PCR buffer, 0.4 μL 5 U/μL Invitrogen Taq polymerase (New England BioLabs, Ipswitch, MA), 50 mM $MgCl_2$, 10 mM dNTPs, and 10 mM of each primer. PCR conditions were 95˚C for 3 min, 35 cycles of 95˚C for 20 s, 49˚C for 15 s, 42˚C for 90 s, and a final 5 minute extension at 42˚C, protocol modified from (Turner et al., 1999). Amplified 16S rRNA genes were cloned using a TOPO® TA kit and pCR®II-TOPO® vector (Life Technologies, Grand Island, NY) following all manufacturer instructions, followed by capillary-based sequencing on a 3730XL platform (LifeTech-Applied Biosystems, Foster City, CA) at The University of Texas at Austin's ICMB DNA sequencing Core facility.

Growth and DIC-uptake Experiments

Growth experiments were performed by exposing T-031 to varying concentrations of As^{III} and As^{V}. Aliquots of BG-11 were dispensed into borosilicate glass culture tubes with 0, 0.5, 1.0, 1.5, 2.0, 2.5, 3.0, 3.5, or 4.0 mM As^{III} or As^{V}. Each As^{III} or As^{V}-amended treatment was titrated aseptically to pH 7 using 1N HCl or 1N NaOH. Each As^{III} or As^{V} -amended treatment group was then inoculated with T-031 (*n = 3*). Cultures were maintained at 23°C under 24-hour low-intensity irradiance the experiment. Growth was monitored for 8 days by optical density (OD) at 600 nm using a SMARTSpectro 2000 spectrophotometer (LaMotte Company, Chestertown, MD).

Cyanobacteria carbon uptake was assessed in closed system batch culture experiments designed to mimic the diffusion-limited conditions of microbial mats during photosynthesis. 20ml aliquots of un-buffered minimal salts media (0.05 mM KCl, 1 mM NaCl, 0.15 mM $MgSO_4$, 0.25 mM $CaCl_2$, and 0.5mM $NaHCO_3$) were dispensed into borosilicate glass tubes. Treatment groups were un-buffered, containing no aqueous buffer other than the limited nutrient HCO_3^-, or buffered by 1 mM As^{V}. Prior to inoculation, cells were washed three times in experimental media to remove residual BG11(+N). All samples were titrated to an initial pH of 7 with 1N HCl, and then inoculated with cyanobacteria harvested from culture T-031 (*n = 8*). Both the un-buffered control and As^{V}-amended groups began with [DIC]=0.3 mM (as HCO_3^-), similar to the [DIC] found in low-DIC streams at ETGF. Growth was measured daily as OD at 680nm. [DIC] was determined daily using an Apollo 9000 Carbon Analyzer (Teledyne-Tekmar, Mason, OH), and pH was measured with an IQ150 pH meter with a non-glass electrode

ISFET probe (Hach Company, Loveland, CO). Sterile controls were done to test for pH shifts or DIC removal due to sampling methods.

In Situ Microprofiling of a Cyanobacterial Mat

Measurements of dissolved oxygen (O_2) and pH were collected along a vertical profile extending from the water column down through the cyanobacteria-dominated top layer of a microbial mat in the Great Geyser (site GG-75m, Table 4-1, Figure D-1). O_2 and pH microsensors (Unisense A/S, Aarhus, Denmark) with ~500 μm tip diameters were calibrated following the manufacturer's instructions using a microsensor multimeter. O_2 was measured with a microsensor attached to a micromanipulator/stand assembly positioned adjacent to the stream, and concentrations were recorded over a 1000 μm vertical range by manual adjustment at 50-100 μm increments. Measurements were monitored and recorded when they reached stable values corresponding to re-equilibrated conditions within the mat using SensorTrace PRO software (Unisense A/S, Aarhus, Denmark). This identical procedure was repeated for pH in the same location as O_2.

Data Processing and Statistical Analyses

Significance of categorical comparisons and responses of experimental treatments were determined by a paired t-test of sample means, calculated in the R statistical computing package V3.0.1, at http://www.R-project.org (R Core Team, 2013). Experimental carbon uptake and growth were normalized as %DIC removed, or %OD increase during measurement intervals. Strength of correlation between environmental variables and %Cyanobacteria were measured using linear regression. All *P* values were

found using a two-tailed test, except where indicated. Linear regression statistics were calculated using the VassarStats Statistical Computation online tools (©Richard Lowry, 1998-2014, Professor of Psychology Emeritus, Vassar College [vassarstats.net]).

Strain and Nucleotide Sequence Deposition

Strain T-031 was deposited in the UTEX Culture Collection of Algae under accession number UTEX B 3002. The sequence for this strain has been submitted to the GenBank database (KP762334)**.** Nine clones from site GG-75m were deposited to GenBank (KP762335 to KP762343), with the sample ID heading "T075-B".

RESULTS

Geochemistry and Microbiology of Sample Locations

Most features throughout ETGF are low DIC (Landrum et al., 2009), discharging geothermal water at a source pool, which flows into long discharge aprons ranging from 25-100 m in length. High-DIC springs are present but rare, and due to low discharge volumes tend to form small pools rather than streams. Variation in As-redox speciation was observed along geyser outflows and within high-DIC pools. Low DIC waters discharge at ~86°C and are geochemically reduced, containing dissolved Fe^{2+} and 4: 1 As^{III}: As^{V}. Arsenic was found only as inorganic As^{III} and As^{V}; methyl arsenates and trimethylarsenic were not detected in any aqueous samples.

Cyanobacterial abundance (%Cyanobacteria) was compared across sites in order to determine which parameters (temperature, [DIC], [As^{III}], and [As^{V}]) influence the presence, absence, and abundance of cyanobacteria throughout ETGF (Table 4-1). pH is

6.8-7.2 at all sites and therefore was excluded from the analysis as a potential controlling variable. A significant negative correlation was observed between temperature and %Cyanobacteria (r^2=0.46, $P < 0.05$); however, a highly significant negative correlation was observed between [As^{III}] and %Cyanobacteria (r^2=0.84, $P < 0.0001$). When both low and high DIC sites were considered, [As^{V}] correlated positively with %Cyanobacteria but was only significant at >95% CI using a one-tailed test (r^2=0.29, $P < 0.05$). When only low DIC sites are considered the positive correlation is highly significant (r^2=0.80, $P < 0.005$), similar to the negative correlation observed between As^{III} and %Cyanobacteria. [DIC] showed no correlation with cyanobacteria abundance in linear regression due to clustered DIC values below 0.5 mM or above 1.6 mM. High DIC springs are observed to support more biomass (Chapter 2, this dissertation) and a higher abundance of cyanobacteria 16S rRNA sequences than low DIC streams (Table 4-1), but were not the main focus of this study.

Arsenic Oxidation and Cyanobacteria Succession

Cyanobacteria succession was examined along a 75 m section of a model transect known as the Great Geyser (GG) (Table 4-1, Figure 4-1), studied previously with respect to microbial As^{III}-oxidation and As-biogeochemistry (Landrum et al., 2009; Engel et al., 2013). The GG stream discharges water as short cycle (~5 min) eruptions near local boiling temperature (86°C), forming a deep pool, splash zone, and 1.5 m siliceous sinter tower. Microbial mats were not observed in the pool and proximal outflow channel (~80°C) until water temperatures were near 70°C, where a thin biofilm dominated by *Thermus sp*. can be found (A. Engel, [University of Tennessee, Knoxville] personal

communication). Waters discharge 4 times more As^{III} than As^{V}, and As^{III} remains constant for the first 15 m, suggesting little to no oxidation by biotic or abiotic mechanisms (Figure 4-1). Reddish-brown microbial streamers containing opal-A silica and hydrous ferric oxides (Landrum et al., 2009) were observed in waters with temperatures ranging from 60-65°C, starting at 25 m and extending downstream to ~40 m.

Observations of As^{III} oxidation began at ~25 m with a rapid transition from As^{III}- to As^{V}-dominated waters between 25 and 40 m (Figure 4-1). Cyanobacteria were not observed in microbial biomass collected in the As^{III}-dominated waters but were present by 40 meters (~55°C) where a sudden transition in arsenic-redox from As^{III} to As^{V} also occurs. Cyanobacteria were observed in increasing abundance downstream of 40 m, forming extensive mats downstream of 55 m (46°C) that also contained abundant silica (Figure 4-1, Figure D-1).

In Situ Microprofile

Microscale vertical profiles of pH and O_2 recorded within a cyanobacteria-dominated mat at site GG-75 m confirmed oxygenic photosynthesis (Figure 4-2). Dissolved [O_2] increased sharply by 0.3 mmol/L between the water (0 μm) and a depth of 100 μm, remaining at 0.65 mmol/L until 400 μm depth, below which it decreased to nearly half the concentration observed in the overlying water (0.4 mmol/L). These elevated O_2 levels corresponded with a bright green-pigmented layer of filamentous cyanobacteria within the mat (Figure D-1). Atmospheric saturation of O_2 at the in-situ temperature of 37°C is 0.70 mmol/L, indicating that the mat remains slightly

undersaturated with O_2 during photosynthesis, though approaches saturation in the peak photosynthetic zone. Changes in pH with depth did not show the same trend within the photosynthetic zone; pH decreased from 7.05 to 6.7 within the first 150 μm and remained at 6.7 throughout the same zone that had elevated O_2 levels relative to stream water. pH then decreased at the same depth where O_2 decreased, reaching 6.4 in the deepest measured part of the mat. We were unable to obtain a comparative profile at an As^{III}-dominated location, due to the friable and non-laminated character of the iron- and silica-rich streamers.

Arsenic Influence on Cyanobacterial Growth

A new cyanobacterial strain was cultured from a microbial mat sample collected at site TAT09-031 the Upper Basin in June 2009 (Table 4-1). Strain T-031 (UTEX B 3002) is a filamentous and heterocystous morphotype when grown without fixed nitrogen, and when grown in BG11(+N) cells form short, non-heterocystous filaments (Figure C-3). Phylogenetic analysis placed T-031 within the Subsection IV cyanobacteria, also known as the Nostocales (Figure 3-5) (Castenholz, 2001).

Experiments showed different growth responses when T-031 was exposed to varying concentrations of As^{III} and As^{V} relative to the 0 mM $As^{III/V}$ control groups (Figure 4-3). T-031 was exposed to 0-4 mM As^{III}- and As^{V} at 0.5 mM increments, however, only the data from 0, 0.5, 1.0, 2.0, 3.0, and 4.0 mM treatments are shown for ease of visualization. No changes in %OD were observed in sterile controls over the course of the experiment. Growth data for all concentrations are shown in (Tables D-1, D-2).

Cyanobacteria exposed to 0.5, 1.0, 2.0, and 4.0 mM As^{III} showed an average of 10% greater growth over the control during the first 24 hours, however this growth either leveled off (0.5, 2.0 mM) or decreased sharply (1.0, 4.0 mM) between 24 and 48 hours (Figure 4-3, A). Growth in 0.5 mM As^{III} stabilized near 18% relative to starting OD, and growth decreased steadily throughout the remainder of the experiment in all treatment groups with >0.5 mM As^{III}. Pigment bleaching was observed within 1-3 weeks in all treatments ≥1.0 mM As^{III}, and to a small extent at 0.5 mM, indicating that under nutrient-rich conditions T-031 can tolerate up to 0.5 mM As^{III}, though only for a short time.

In contrast, in the presence of 0.5-4.0 mM As^{V} T-031 showed increased growth above that in the control over the first 2-3 days (Figure 4-3, B). By day 4, growth in the control was comparable to all but that with 0.5 mM As^{V}, which was significantly higher throughout the entire experiment. In general, T-031 exhibited less overall growth in the presence of all concentrations of As^{III} compared to the 0 mM As^{III} control group, whereas 0.5 mM As^{V} significantly enhanced growth through the duration of the experiment, and probably beyond, based on the trajectory of the growth curve. Though it cannot necessarily be concluded that all tested concentrations of As^{V} are beneficial for growth compared to the control, 0.5 mM As^{V} (equivalent to the average As^{V} at ETGF) does appear to be beneficial, and appears to enhance long-term growth in addition to stimulating growth on the first 2 days of the experiment.

Impact of arsenate on DIC uptake and growth

Experiments examining the role of pH buffering by arsenate on DIC uptake and pH shift showed a considerable difference between unbuffered conditions and those

buffered by arsenate (Figure 4). In the unbuffered treatment group pH increased from 7.2 to 10.1 in the first 24 hours post-inoculation, and remained at or above 10 for the duration of the experiment (Figure 4-4, A). In contrast, pH only increased 0.1 pH units in the arsenate buffered group during the first 24 hours, and over the following 6 days reached a maximum of 7.4. After 24 hours (post inoculation), both groups had removed 40% of the available carbon from the media; however, by day 3 the rate of DIC removal slowed in the unbuffered treatment, leveling off when 75% of the available carbon was removed (Figure 4-4, B). Between 24 and 72 hours the arsenate buffered treatment continued to remove DIC at approximately the same rate as on day 1, and 80% of initial DIC supply was removed by this point. While the unbuffered group did not assimilate any additional carbon after day 3, the arsenate buffered group continued to remove DIC until 98% (±0.94%) of the initial DIC supply was removed from the media (Figure 4-4, B). The difference in carbon uptake between the two groups beyond day 3 is highly significant ($P < 1 \times 10^{-6}$, paired t-test).

Overall, cyanobacteria in the arsenate buffered media acquired 25% more carbon than the unbuffered group. The increased magnitude of carbon uptake in the arsenate buffered group resulted in 5 times greater biomass during the first 24 hours; 10% in the arsenate buffered group, compared to 1-2% (Figure 4-4, C). This difference in growth was maintained throughout the experiment, and overall, the arsenate buffered group was able to divert more of the carbon that they assimilated to growth. The difference in mean growth of the two groups was highly significant ($P < 0.001$, paired t-test). No pH, DIC, or OD changes were observed in sterile controls throughout the experiment.

When closed experiments were exposed to 0.5 mM As^{III} under moderately DIC-limited starting conditions (0.76 mM C) pH shifted more than in the arsenate buffered group, and As^{III} exposed cells took up less DIC (51% of the total supply) than the unbuffered and arsenate buffered groups (57% and 68% of the total supply, respectively) (Figure D-2, A and B). Though DIC uptake in the As^{III} group was not much different than the unbuffered group, growth was more negatively affected, with only 2.5% in the As^{III} group, compared to 5% and 9% in the unbuffered and arsenate groups, respectively (Figure D-2, C).

Buffering by 0.5 mM phosphate (pK_{a2} = 7.2 at 25°C) was tested under similar conditions due to its similar pH buffering and chemical behavior to arsenate (pK_{a2} = 6.94). pH change was larger than expected for buffered groups, but both maintained much lower pH than the unbuffered group (Figure D-3, A). Though there was not a large different in DIC uptake among all of the groups phosphate and arsenate followed similar growth curves until day 2, when growth with arsenate continued to increase but growth with phosphate leveled off (Figure D-3, B and C). No pH, DIC, or OD changes were observed in sterile controls during the latter two experiments.

DISCUSSION

Thermal and geochemical dynamics are known to drive the distribution and abundance of microorganisms in hot springs. Temperature tends to be the primary control on the occurrence of cyanobacterial taxa along geothermal outflows, while other parameters such as light and geochemical constituents typically play a secondary role

(Ward and Castenholz, 2000; Sompong et al., 2005; Cox et al., 2011; Boyd et al., 2012; Ward et al., 2012). Here we described a system in which cyanobacteria presence, absence and abundance is influenced primarily by As-redox speciation, and to a lesser extent by temperature. A novel El Tatio organism was cultured and used to characterize the influence of As^{III} and As^{V} on growth and photosynthetic DIC-uptake of cyanobacteria in the DIC-limited and As-rich ETGF system.

Although some thermophilic cyanobacteria can tolerate temperatures up to 74°C, many filamentous thermophilic cyanobacteria occupy a preferred temperature range below 55°C (Ward and Castenholz, 2000; Ward et al., 2012). Temperature does play a role in microbial mat succession at ETGF, similar to previously studied geothermal settings. Linear regression analysis demonstrates a significant negative correlation between temperature and cyanobacteria abundance. In the model low DIC transect cyanobacteria increase in abundance where temperatures fall below 55°C, consistent with observations at other geothermal locations. However, abundant cyanobacteria were observed at TAT09-034 (80% of the total community), a 58°C site containing 0 mM As^{III}, and only 2.2% cyanobacteria were observed at NT-2, a 50°C site containing 0.27 mM As^{III} (Table 4-1). These two examples, alongside the trend of cyanobacteria succession with As^{III}-oxidation in the model GG transect (Figure 4-1), exemplify why factors other than temperature need to be considered to explain cyanobacteria distribution at ETGF.

Arsenic redox speciation, especially As^{III}, has a strong influence on the presence and abundance of cyanobacteria at ETGF, especially in low-DIC streams. Cyanobacteria were not observed to comprise more than 2% of the microbial the community at any site

containing > 0.15 mM As^{III}; this concentration appears to be the cutoff between rare (0-2.2%) and abundant (18-80%) cyanobacteria at all sites considered, regardless of other geochemical parameters (Table 4-1). The relationship between cyanobacteria abundance and As^{V} was positive, yet not as direct as the negative association between cyanobacteria and As^{III}. When both low- and high-DIC sites were considered, a positive association is observed between As^{V} and cyanobacteria abundance, but when only low-DIC sites were considered, the positive association was highly significant, demonstrating that a more easily defined environmental link exists between cyanobacterial abundance and As^{V} in low-DIC streams.

Strain T-031 responded differently to As^{III} and As^{V} in laboratory experiments, with severe growth inhibition at and above 1 mM As^{III} compared to enhanced growth with 0.5 mM As^{V} (Figure 4-3). While growth was not fully impacted at 0.5 mM, the concentration of As^{III} most similar to those naturally occurring at ETGF (0.3-0.4 mM), additional factors can explain the absence of cyanobacteria in waters containing > 0.15 mM As^{III}. The most notable among these are the high levels of UV radiation experienced in the high elevation ETGF system (Phoenix et al., 2006). UV can induce frequent DNA mutations (van der Leun and de Gruijl, 1993) and inhibits the activity of photosystem II, which is essential for O_2-evolution during cyanobacterial photosynthesis. As^{III} interferes with the production of the UV-protecting pigments that cyanobacteria use to shield themselves from the negative effects of UV exposure (Wang et al., 2012), and resulting declines in pigment production lead to photoinhibition and damage to protein synthesis (Donkor and Hader, 1991; Jeffery et al., 1996). While our experiments did not consider

the effects of UV, observations of pigment bleaching at 0.5 mM As^{III} suggests that light sensitivity may be a major factor contributing to their absence in stream areas that possess > 0.15 mM As^{III}.

Cyanobacteria As^{V} tolerance has been reported previously; exposure of *Anabaena variabilis* to 100mM As^{V} showed no significant impact on growth, and it was suggested that As^{V} accumulated to high concentrations within cells (Thiel, 1988). *Phormidium* sp., a cyanobacterial genus known to be present in geothermal outflows, has also been shown to grow in the presence of high As^{V} (Maeda et al., 1987). Consistent with previous findings, T-031 demonstrated significantly greater growth at all tested concentrations of As^{V} in the first 48 hours compared to the control, and the 0.5 mM As^{V} treatment showed sustained increased growth relative to the control.

Preliminary work examining the fate of arsenic in experiments with cultured ETGF organisms show that As^{V} accumulates in cells, even when exposed to As^{V} for as little as 24 hours (our unpublished results). The physiological reasons for this are unknown at this time, and we speculate that there could be inactivation of one or more components of the *ars* arsenic resistance operon, allowing As^{V} to accumulate within cells rather than be excreted from cells. In the DIC-limited ETGF waters, As^{V} accumulation in biomass is hypothesized to serve a dual function: (a) help cells avoid pigment bleaching through As^{III} exposure caused by *ars* reductase activity, and (b) help cells maintain biomass by buffering detrimental pH shifts that occur during CCM activity, discussed in the following section.

The Impact of Arsenate pH Buffering on Cyanobacteria Carbon Uptake

While concentrations of $CO_{2(aq)}$ are normally low in natural waters, DIC scavenging is further complicated in settings like ETGF due to inherent inefficiencies of the RuBisCO enzyme at high UV, elevated $[O_{2(aq)}]$, and temperatures above 30°C (Kaplan et al., 1994; Badger et al., 2006). Cyanobacteria possess a CCM, which actively increases the cell's internal HCO_3^- pool which involves: (i) transport proteins to bring extracellular HCO_3^- across the cell membrane (Omata et al., 1999; Maeda et al., 2002; Price et al., 2002; Shibata et al., 2002; Badger and Price, 2003; Price et al., 2004; Zhang et al., 2004); (ii) utilization of carbonic anhydrase (CA), an enzyme that dehydrates HCO_3^- to CO_2 and OH^- (Eq. 4-1) (Fukuzawa et al., 1992; Price et al., 1992; Yu et al., 1992; Badger and Price, 1994);

$$HCO_{3\,(cell)}^- \leftrightarrow CO_{2(cell)} + OH^- \quad \text{via CA (reversible)} \qquad \text{(Eq. 4-1)}$$

and (iii) a protein compartment known as the carboxysome which helps concentrate CO_2 around the RuBisCO active site (Price et al., 1998; Kaplan and Reinhold, 1999; Badger et al., 2002; Price et al., 2002). The CCM generates substantial hydroxyl ion (Eq. 4-1), which results in an increase in pH of the extracellular medium in poorly-buffered or HCO_3^--buffered waters and exacerbates the difficulty of taking up carbon for RuBisCO (Goldman et al., 1981; Azov, 1982; Aizawa and Miyachi, 1986; Badger et al., 2006).

The ability to assimilate DIC under high pH conditions depends on the flexibility of the CCM, which can vary among cyanobacteria from different environments. Cyanobacteria from low-DIC environments, or estuarine settings where pH and [DIC] change rapidly, possess aggressive CCMs that act rapidly and induce a dramatic pH

increase (Eq. 4-1) (Badger et al., 2006; Carrasco et al., 2008) similar to the pH increase experienced by T-031 in unbuffered conditions (Figure 4-4, A). In contrast, cyanobacteria originating from high-DIC environments, or environments with a continuous DIC supply such as the ocean (~2 mM, pH 8.3), tend not to exhibit an aggressive CCM response (Kaplan et al., 1980; McGinn et al., 2003; Woodger et al., 2003).

T-031 showed greater carbon uptake in the presence of arsenate compared to the unbuffered control. When buffered with 1 mM As^V, 99% of the available carbon was removed, while the pH only increased from 7-7.5 (Figure 4-4, A and B). Growth in the arsenate buffered treatments continued throughout the entire period, suggesting that more of the assimilated carbon was diverted to growth than in the unbuffered group. These results suggest that both the magnitude of carbon uptake and growth is positively influenced by the presence of dissolved As^V under low-DIC conditions. In contrast, only 75% of available DIC was removed in unbuffered experiments, which also underwent a dramatic pH increase to 10.1, which appears to be the pH at which the organism no longer assimilated carbon based on the all three experiments reported here (Figure 4-4, Figure D-2, and Figure D-3). Growth in the unbuffered control was suppressed during the first 24 hours, suggesting that aggressive action by the CCM forced the cells to divert assimilated carbon towards future carbon acquisition, rather than growth. Increased DIC uptake also occurred in the presence of phosphate, although the positive impact on growth was less than with arsenate indicating that other pH buffers can have a positive impact on growth in DIC-limited conditions, although arsenate appears to perform better than phosphate for reasons that are unknown at this time (Figure D-3).

Even in well-buffered systems, microbial mats are reported to experience a shift of 2-3 pH units during peak photosynthesis due to the combined effects of carbon depletion and CCM-induced pH shift (Revsbech and Ward, 1984), exacerbated by the diffusion limited microbial mat environment (Badger et al., 2006). Even when DIC supply is sufficient, pH increase shifts the equilibrium away from CO_2 toward less energetically convenient forms such as HCO_3^- and CO_3^{2-}. While CO_2 passes easily through cell membranes, charged HCO_3^- requires energy intensive transport into the cell (McGinn et al., 2003; Woodger et al., 2003; McGinn et al., 2004). Above pH 8.4, an increasingly significant fraction of DIC is present as CO_3^{2-}, which is unavailable for cellular transport due to its strong negative charge. Arsenate pH buffering maximizes DIC uptake by removing a daily upper limit on carbon availability imposed by typical CCM-induced pH shift. Arsenate pH buffering may be enough to make a significant difference in DIC uptake within a single photoperiod in the DIC-limited cyanobacterial mats at ETGF, which may explain why thicker microbial mats are found in As^V-dominated areas of low DIC streams than in areas that contain As^{III}, which was observed to negatively impact DIC uptake and growth.

In situ microelectrode profiling of pH and O_2 confirmed no detectable increase in bulk water or within-mat pH during daylight periods despite O_2 production associated with cyanobacterial photosynthesis, and in fact pH decreased from 7.1 to 6.7 in this zone (Figure 4-2). Two buffering mechanisms could contribute to this observation, related to either the substantial fraction of solid amorphous silica or As^V in the aqueous phase: (i) silica that dissolves in the presence of hydroxide (Eq. 4-2):

$$H_4SiO_{4(opal\text{-}A)} + OH^- \rightarrow H_3SiO_4^- + H_2O \quad \text{(Eq. 4-2)}$$

and; (ii) $H_2AsO_4^-$ donating protons to neutralize hydroxyl ion production:

$$H_2AsO_4^- + OH^- \leftrightarrow HAsO_4^{2-} + H_2O \quad \text{(Eq. 4-3)}$$

The net result of Eq. 4-2 and 4-3 is pH buffering in the photosynthetically active zone of the mat, maintaining a favorable pH range for cyanobacterial uptake of CO_2 and HCO_3^-.

The Significance of CCM-buffering Through Time

Cyanobacteria have formed the basis of microbial mat communities for at least 2.5 Ga and probably much longer (Paerl, 1996; Brocks, 1999; Paerl et al., 2000; Giordano et al., 2005; Buick, 2008) and have had a profound impact on Earth's evolution through oxygenic photosynthesis. Previous work showed that biologically precipitated silica increases DIC uptake in diatoms by buffering both the rate limiting step of the CA enzyme and the pH shift induced by OH^- production (Milligan and Morel, 2002). Similarly, the observed effect of arsenate pH buffering on cyanobacteria CCM activity and growth, paired with As^V-resistance in many different cyanobacteria and algae (Maeda et al., 1987; Thiel, 1988; Lopez-Maury et al., 2003) suggests that the evolution of the cyanobacterial CCM was influenced by the presence of inorganic buffers such as arsenate, and that this process may have played a significant role in carbon cycling throughout the evolutionary history of cyanobacteria. The precise combination of low-DIC, high [As], and pH buffering by arsenate may be unique to the ETGF system; however, the proposed ability of cyanobacteria to adapt to and utilize aqueous and mineral buffers to assimilate carbon underscores one of many reasons why this group has been so successful in time and space.

CHAPTER 4. TABLES AND FIGURES

Table 4-1: Physical and chemical characteristics of sample collection localities. TAT09-031 is the collection locality of strain T-031. 'GG' represents a low-DIC stream known as the 'Great Geyser', 'MBS' denotes a site downstream of two high DIC springs known as the 'Middle Basin Springs', and 'NT' refers to the 'New Transect'.

Site code[a]	Geyser Basin[b]	T°C	pH	[DIC][c] mM C	[As^{III}] mM	[As^{V}] mM	%Cyano abundance[d]
GG-10m	Middle	71	6.9	0.37	0.37	0.12	-
GG-25m	Middle	65	6.9	0.34	0.36	0.16	1.3
GG-30m	Middle	62	6.9	0.39	0.35	0.14	0.2
GG-40m	Middle	55	6.9	0.29	0.16	0.35	18.1
GG-55m	Middle	46	7.0	0.24	0.13	0.41	34.3
GG-75m	Middle	37	7.1	0.15	0.12	0.42	48.2
TAT09-031	Upper	26	7.1	0.57	0	0.32	80.2
TAT09-034	Upper	58	6.9	2.4	0	0.27	80.5
TAT09-045	M-III	54	6.1	1.74	0	0.03	41.9
MBS-1	Middle	60	7.0	2.89	0.25	0.11	0.4
MBS-2	Middle	40	7.0	2.54	0	0.36	80.0
NT-1	Middle	60	6.9	0.46	0.33	0.15	0
NT-2	Middle	50	6.9	0.29	0.27	0.20	2.2
NT-3	Middle	40	7.0	0.18	0	0.51	58.5

[a]Site codes correspond to discrete sample locations.
[b]Follows ETGF naming conventions from Glennon and Pfaff (2003).
[c]Measured [DIC] = $H_2CO_3^*$ + HCO_3^- + CO_3^{2-} measured as mM C. CO_3^{2-} is negligible in this system.
[d]Proportional abundance of cyanobacteria obtained from 454-pyrosequencing data.

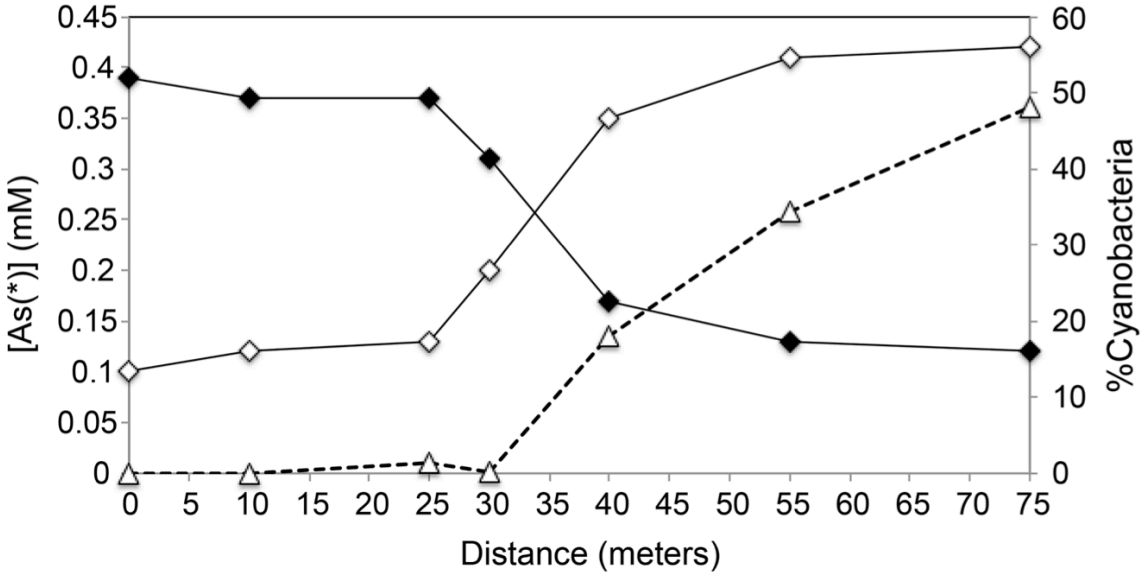

Figure 4-1: Trends of [As^{III}], mM (◆), [As^{V}], mM (◇), and phylum cyanobacteria % community abundance quantified by 454-pyrosequencing (Δ) along a 75m reach of the model high arsenic low-DIC Great Geyser transect.

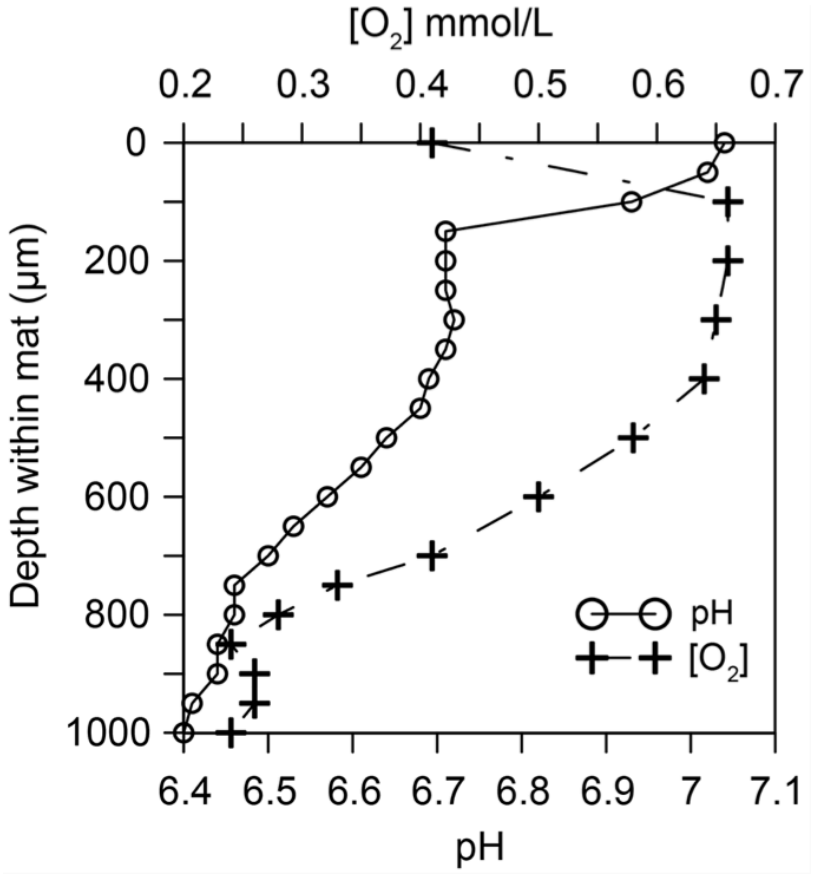

Figure 4-2: In-situ microprofiles of pH (O) and dissolved oxygen concentration [O_2] mmol/L (+) of the top 1mm of a microbial mat at 75m along the Great Geyser transect, corresponding to site GG-75m (Table 4-1). Depth of 0 µm represents the water-microbial mat interface. Dashed lines on the photograph mark the upper 1 mm of a slice of a corresponding section of the sampled mat.

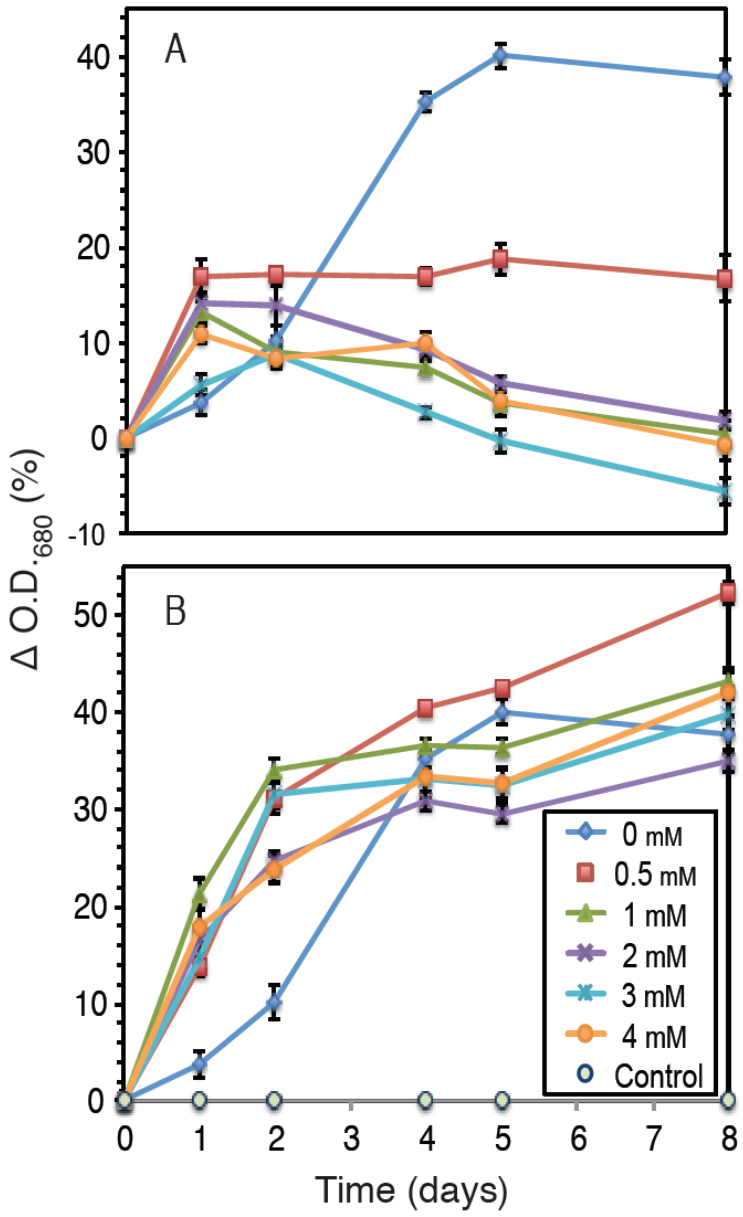

Figure 4-3: Growth curves of culture T-031 on exposure to 0-4 mM As^{III} (A), and 0-4 mM As^{V} (B). %OD indicates the optical density change relative to day 0. Error bars represent standard error of the mean (*n = 3*).

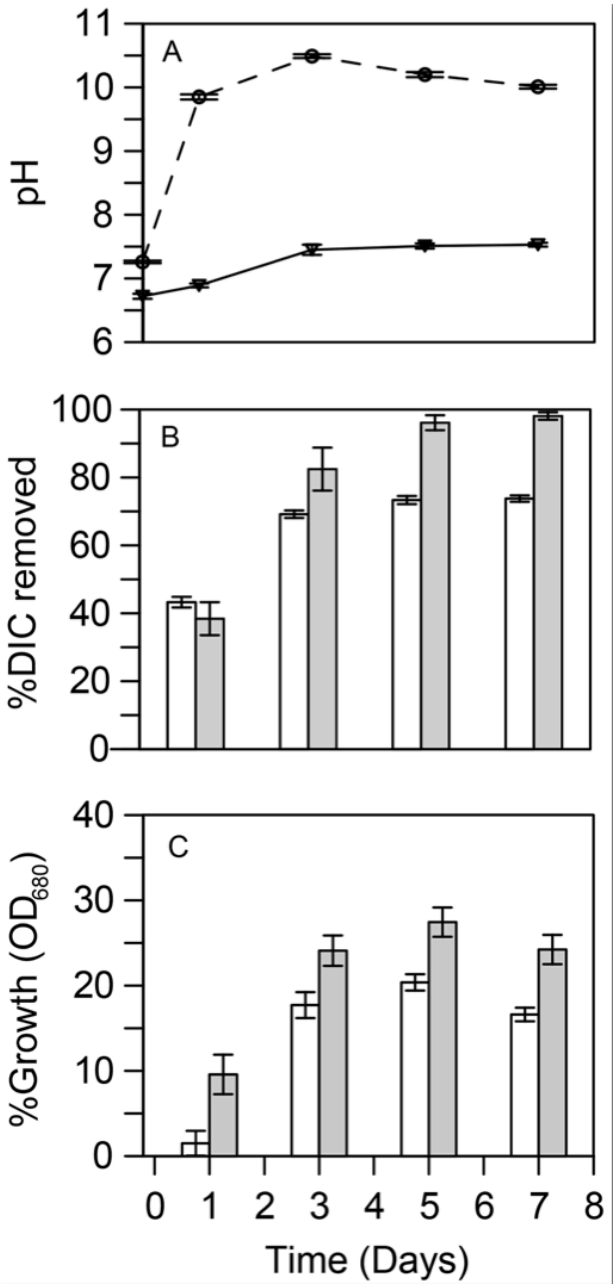

Figure 4-4: Growth and DIC uptake assays were performed with low-DIC culture T-031 in unbuffered (0 mM As(V)) conditions (O, white bars), or conditions buffered by 1 mM As(V) (▽, gray bars). pH change (A), the percent of DIC removed from the medium (B) and cell growth as %OD change relative to day 0 (C) were measured daily, or every other day. Error bars reported as standard error of the mean ($n = 8$).

REFERENCES

Aizawa, K., and Miyachi, S. (1986) Carbonic anhydrase and CO_2 concentrating mechanisms in microalgae and cyanobacteria. *FEMS Microbiology Reviews* **39**: 215-233.

Alsina, M.A., Zanella, L., Hoel, C., Pizarro, G.E., Gaillard, J.-F., and Pasten, P.A. (2013) Arsenic speciation in sinter mineralization from a hydrothermal channel of El Tatio geothermal field, Chile. *Journal of Hydrology* **in press**.

Azov, Y. (1982) Effect of pH on inorganic carbon uptake in algal cultures. *Applied and Environmental Microbiology* **43**: 1300-1306.

Badger, M.R. (1980) Kinetic properties of ribulose 1,5-bisphosphate carboxylase/oxygenase from Anabaena variabilis. *Archives of Biochemistry and Biophysics* **201**: 247-254.

Badger, M.R., and Price, G.D. (1994) The role of carbonic anhydrase in photosynthesis. *Annual Review of Plant Physiology and Plant Molecular Biology* **45**: 369-392.

Badger, M.R., and Price, G.D. (2003) CO_2 concentrating mechanisms in cyanobacteria: molecular components, their diversity and evolution. *Journal of Experimental Botany* **54**: 609-622.

Badger, M.R., Hanson, D., and Price, G.D. (2002) Evolution and diversity of CO_2 concentrating mechanisms in cyanobacteria. *Functional Plant Biology* **29**: 161-173.

Badger, M.R., Price, G.D., Long, B.M., and Woodger, F.J. (2006) The environmental plasticity and ecological genomics of the cyanobacterial CO_2 concentrating mechanism. *Journal of Experimental Botany* **57**: 249-265.

Ballantyne, J.M., and Moore, J.N. (1988) Arsenic Geochemistry in Geothermal Systems. *Geochimica et Cosmochimica Acta* **52**: 475-483.

Bhattacharya, P., and Pal, R. (2010) Response of cyanobacteria to arsenic toxicity. *Journal of Applied Phycology* **23**: 293-299.

Boyd, E.S., Fecteau, K.M., Havig, J.R., Shock, E.L., and Peters, J.W. (2012) Modeling the habitat range of phototrophs in yellowstone national park: toward the development of a comprehensive fitness landscape. *Frontiers in Microbiology* **3**: 221.

Brocks, J.J. (1999) Archean Molecular Fossils and the Early Rise of Eukaryotes. *Science* **285**: 1033-1036.

Buick, R. (2008) When did oxygenic photosynthesis evolve? *Philosophical Transactions of the Royal Society of London B Biological Sciences* **363**: 2731-2743.

Caporaso, J.G., Kuczynski, J., Stombaugh, J., Bittinger, K., Bushman, F.D., Costello, E.K. et al. (2010) QIIME allows analysis of high-throughput community sequencing data. *Nature Methods* **7**: 335-336.

Carrasco, M., Mercado, J.M., and Niell, F.X. (2008) Diversity of inorganic carbon acquisition mechanisms by intact microbial mats of Microcoleus chthonoplastes (Cyanobacteriae, Oscillatoriaceae). *Physiolia Plantarum* **133**: 49-58.

Castenholz, R.W. (2001) Phylum BX. Cyanobacteria. In *Bergey's Manual*.

Cortecci, G., Boschetti, T., Mussi, M., Lameli, C.H., Mucchino, C., and Barbieri, M. (2005) New chemical and original isotopic data on waters from El Tatio geothermal field, northern Chile. *Geochemical Journal* **39**: 547-571.

Cox, A., Shock, E.L., and Havig, J.R. (2011) The transition to microbial photosynthesis in hot spring ecosystems. *Chemical Geology* **280**: 344-351.

DeSantis, T.Z., Hugenholtz, P., Larsen, N., Rojas, M., Brodie, E.L., Keller, K. et al. (2006) Greengenes, a chimera-checked 16S rRNA gene database and workbench compatible with ARB. *Applied and Environmental Microbiology* **72**: 5069-5072.

Donkor, V., and Hader, D.-P. (1991) Effects of solar and ultraviolet radiation on motility, photomovement, and pigmentation in filamentous gliding cyanobacteria. *FEMS Microbiology Ecology* **86**: 159-168.

Drever, J.I. (1988) *The Geochemistry of Natural Waters*. Engelwood Cliffs, NJ: Prentice-Hall.

Ellis, A.J., and Mahon, W.A.J. (1964) Natural hydrothermal systems and experimental hot-water/rock interactions. *Geochimica et Cosmochimica Acta* **28**: 1323-1357.

Ellis, A.J., and Mahon, W.A.J. (1967) Natural hydrothermal systems and experimental hot-water/rock interactions (Part II). *Geochimica et Cosmochimica Acta* **31**: 519–538.

Ellis, A.J., and Mahon, W.A.J. (1977) *Chemistry and Geothermal Systems*. New York: Academic Press.

Engel, A.S., Johnson, L.R., and Porter, M.L. (2013) Arsenite oxidase gene diversity among *Chloroflexi* and *Proteobacteria* from El Tatio Geyser Field, Chile. *FEMS Microbiology Ecology* **83**: 745-756.

Ferrari, S.G., Silva, P.G., González, D.M., Navoni, J.A., and Silva, H.J. (2013) Arsenic tolerance of cyanobacterial strains with potential use in biotechnology. *Revista Argentina de Microbiología* **45**: 174-179.

Fukuzawa, H., Suzuki, E., Komukai, Y., and Miyachi, S. (1992) A gene homologous to chloroplast carbonic anhydrase (icfA) is essential to photosynthetic carbon dioxide fixation by Synechococcus PCC7942. *Proceedings of the National Academy of Sciences of the United States of America* **89**: 4437-4441.

Giggenbach, W.F. (1978) The isotopic composition of waters from the El Tatio geothermal field, Northern Chile. *Geochimica et Cosmochimica Acta* **42**: 979-988.

Giordano, M., Beardall, J., and Raven, J.A. (2005) CO_2 concentrating mechanisms in algae: mechanisms, environmental modulation, and evolution. *Annual Review of Plant Biology* **56**: 99-133.

Glennon, J.A., and Pfaff, R.M. (2003) The extraordinary thermal activity of El Tatio Geyser Field, Antofogasta Region, Chile. *The GOSA Transactions* **8**: 31-78.

Goldman, J.C., Dennett, M.R., and Riley, C.B. (1981) Inorganic carbon sources and biomass regulation in intensive microalgal cultures. *Biotechnology and Bioengineering* **23**: 995-1014.

Greenfield, R.E., and Baker, G.C. (1920) Relationship of hydrogen-ion concentration of natural waters to carbon dioxide content. *The Journal of Industrial and Engineering Chemistry* **12**: 989-991.

Haas, B.J., Gevers, D., Earl, A.M., Feldgarden, M., Ward, D.V., Giannoukos, G. et al. (2011) Chimeric 16S rRNA sequence formation and detection in Sanger and 454-pyrosequenced PCR amplicons. *Genome Research* **21**: 494-504.

Jeffery, W.H., Aas, P., Lyons, M.M., Coffin, R.B., Ralph, J.P., and Mitchell, D.L. (1996) Ambient solar radiation-induced photodamage in marine bacterioplankton. *Photochemistry and Photobiology* **64**: 419-427.

Kaplan, A., and Reinhold, L. (1999) CO_2 concentrating mechanisms in photosynthetic microorganisms. *Annual Review of Plant Physiology and Plant Molecular Biology* **50**: 539-570.

Kaplan, A., Badger, M.R., and Berry, J.A. (1980) Photosynthesis and the intracellular inorganic carbon pool in the bluegreen alga Anabaena variabilis: response to external CO_2 concentration. *Planta* **149**: 219-226.

Kaplan, A., Schwarz, R., Lieman-Hurwitz, J., Ronen-Tarazi, M., and Reinhold, L. (1994) Physiological and Molecular Studies on the Response of Cyanobacteria to Changes in the Ambient Inorganic Carbon Concentration. In *The Molecular Biology of Cyanobacteria*. Bryant, D.A. (ed): Kluwer Academic Publishers, pp. 469-485.

Lahsen, A., and Trujillo, P. (1976) El Tatio Geothermal Field. In *Proceedings of the 2nd United Nations Symposium on Geothermal Fields*. Berkeley, CA, pp. 157-178.

Landrum, J.T., Bennett, P.C., Engel, A.S., Alsina, M.A., Pastén, P.A., and Milliken, K. (2009) Paritioning geochemistry of arsenic and antimony, El Tatio Geyser Field, Chile. *Applied Geochemistry* **24**: 664-676.

Langner, H.W., Jackson, C.R., McDermott, T.R., and Inskeep, W.P. (2001) Rapid oxidation of arsenite in a hot spring ecosystem, Yellowstone National Park. *Environmental Science and Technology* **35**: 3302-3309.

Leiva, E.D., Ramila, C., Vargas, I.T., Escauriaza, C.R., Bonilla, C.A., Pizarro, G.E. et al. (2014) Natural attenuation process via microbial oxidation of arsenic in a high Andean watershed. *Science of the Total Environment* **466-467**: 490-502.

Lindskog, S., and Coleman, J.E. (1973) The catalytic mechanism of carbonic anhydrase. *Proceedings of the National Academy of Sciences of the United States of America* **70**: 2505-2508.

Liu, Z., DeSantis, T.Z., Andersen, G.L., and Knight, R. (2008) Accurate taxonomy assignments from 16S rRNA sequences produced by highly parallel pyrosequencers. *Nucleic Acids Research* **36**: e120.

Lloyd, J.R., and Oremland, R.S. (2006) Microbial transformations of arsenic in the environment: from soda lakes to aquifers. *Elements* **2**: 85-90.

Lopez-Maury, L., Florencio, F.J., and Reyes, J.C. (2003) Arsenic sensing and resistance system in the cyanobacterium Synechocystis sp. Strain PCC 6803. *Journal of Bacteriology* **185**: 5363-5371.

Maeda, S., Badger, M.R., and Price, G.D. (2002) Novel gene products associated with NdhD3/D4-containing NDH-1 complexes are involved in photosynthetic CO_2 hydration in the cyanobacterium, Synechococcus sp. PCC7942. *Molecular Microbiology* **43**: 425-435.

Maeda, S., Wada, H., Kumeda, K., Onoue, M., Ohki, A., Higashi, S., and Takeshita, T. (1987) Methylation of inorganic arsenic by arsenic-tolerant freshwater algae. *Applied Organomettalic Chemistry* **1**: 465-472.

McGinn, P.J., Price, G.D., and Badger, M.R. (2004) High light enhances the expression of low-CO_2-inducible transcripts involved in the CO_2-concentrating mechanisms in Synechocystis sp. PCC6803. *Plant, Cell and Environment* **27**: 615-626.

McGinn, P.J., Price, G.D., Maleszka, R., and Badger, M.R. (2003) Inorganic carbon limitation and light control the expression of transcripts related to the CO_2-concentrating mechanism in the cyanobacterium Synechocystis sp. strain PCC6803. *Plant Physiology* **132**: 218-229.

Milligan, A.J., and Morel, F.M.M. (2002) A proton buffering role for silica in diatoms. *Science* **297**: 1848-1850.

Mukhopadhyay, R., Rosen, B.P., Pung, L.T., and Silver, S. (2002) Microbial arsenic: from geocycles to genes and enzymes. *FEMS Microbiology Reviews* **26**: 311-325.

Nordstrom, K.D., Ball, J.W., and McCleskey, R.B. (2005) Ground Water to Surface Water: Chemistry of Thermal Outflows in Yellowstone National Park. In *Geothermal Biology and Geochemistry in Yellowstone National Park*. Inskeep, W.P., and McDermett, T.R. (eds). Bozeman, MT: Thermal Biology Institute, Montana State University, pp. 73-94.

Nubel, U., Garcia-Pichel, F., and Muyzer, G. (1997) PCR primers to amplify 16S rRNA genes from cyanobacteria. *Applied and Environmental Microbiology* **63**: 3327-3332.

Omata, T., Price, G.D., Badger, M.R., Okamura, M., Gohta, S., and Ogawa, T. (1999) Identification of an ATP-binding cassette transporter involved in bicarbonate uptake in the cyanobacterium Synechococcus sp. strain PCC 7942. *Proceedings of the National Academy of Sciences of the United States of America* **96**: 13571-13576.

Oremland, R.S., Stolz, J.F., and Hollibaugh, J.T. (2004) The microbial arsenic cycle in Mono Lake, California. *FEMS Microbiology Ecology* **48**: 15-27.

Oremland, R.S., Saltikov, C.W., Wolfe-Simon, F., and Stolz, J.F. (2009) Arsenic in the evolution of earth and extraterrestrial ecosystems. *Geomicrobiology Journal* **26**: 522-536.

Paerl, H. (1996) Microscale physiological and ecological studies of aquatic cyanobacteria: macroscale implications. *Microscopy Research and Technique* **33**: 47-72.

Paerl, H.W., Pinckney, J.L., and Steppe, T.F. (2000) Cyanobacterial-bacterial mat consortia: examining the functional unit of microbial survival and growth in extreme environments. *Environmental Microbiology* **2**: 11-26.

Phoenix, V.R., Bennett, P.C., Engel, A.S., Tyler, S.W., and Ferris, F.G. (2006) Chilean high-altitude hot-spring sinters: a model system for UV screening mechanisms by early Precambrian cyanobacteria. *Geobiology* **4**: 15-28.

Price, G.D., Coleman, J.R., and Badger, M.R. (1992) Association of carbonic anhydrase activity with carboxysomes isolated from the cyanobacterium Synechococcus PCC7942. *Plant Physiology* **100**: 784-793.

Price, G.D., Maeda, S., Omata, T., and Badger, M.R. (2002) Modes of active inorganic carbon uptake in the cyanobacterium, Synechococcus sp. PCC7942. *Functional Plant Biology* **29**: 131-149.

Price, G.D., Badger, M.R., Woodger, F.J., and Long, B.M. (2008) Advances in understanding the cyanobacterial CO_2-concentrating-mechanism (CCM): functional components, Ci transporters, diversity, genetic regulation and prospects for engineering into plants. *Journal of Experimental Botany* **59**: 1441-1461.

Price, G.D., Sultemeyer, D., Klughammer, B., Ludwig, M., and Badger, M.R. (1998) The functioning of the CO_2 concentrating mechanism in several cyanobacterial strains: a review of general physiological characteristics, genes, proteins, and recent advances. *Canadian Journal of Botany* **76**: 973-1002.

Price, G.D., Woodger, F.J., Badger, M.R., Howitt, S.M., and Tucker, L. (2004) Identification of a SulP-type bicarbonate transporter in marine cyanobacteria.

Proceedings of the National Academy of Sciences of the United States of America **101**: 18228-18233.

Purcell, E. (1977) Life at low Reynolds number. *American Journal of Physics* **45**: 3-11.

Raven, J.A. (2003) Inorganic carbon concentrating mechanisms in relation to the biology of algae. *Photosynthesis Research* **77**: 155-171.

Revsbech, N., and Ward, D. (1984) Microelectrode studies of interstitial water chemistry and photosynthetic activity in a hot spring microbial mat. *Applied and Environmental Microbiology* **48**: 270-275.

R Core Team (2013) R: A language and environment for statistical computing. In. Vienna, Austria: R Foundation for Statistical Computing.

Rippka, R., Deruelles, J., Waterbury, J.B., Herdman, M., and Stainer, R.Y. (1979) Generic assignments, strain histories and properties of pure cultures of cyanobacteria. *Journal of General Microbiology* **111**: 1-61.

Romero, L., Alonso, H., Campano, P., Fanfani, L., Cidu, R., Dadea, C. et al. (2003) Arsenic enrichment in waters and sediments of the Rio Loa (Second Region, Chile). *Applied Geochemistry* **18**: 1399-1416.

Shibata, M., Ohkawa, H., Katoh, H., Shimoyama, M., and Ogawa, T. (2002) Two CO_2 uptake systems in cyanobacteria: four systems for inorganic carbon acquisition in Synechocystis sp. strain PCC6803. *Functional Plant Biology* **29**: 123-129.

Silver, S., and Phung, L.T. (2005) Genes and enzymes involved in bacterial oxidation and reduction of inorganic arsenic. *Applied and Environmental Microbiology* **71**: 599-608.

Smedley, P.L., and Kinniburgh, D.G. (2002) A review of the source, behaviour and distribution of arsenic in natural waters. *Applied Geochemistry* **17**: 517-568.

Sompong, U., Hawkins, P.R., Besley, C., and Peerapornpisal, Y. (2005) The distribution of cyanobacteria across physical and chemical gradients in hot springs in northern Thailand. *FEMS Microbiology Ecology* **52**: 365-376.

Stal, L. (2012) Cyanobacterial Mats and Stromatolites. In *Ecology of Cyanobacteria II: Their Diversity in Space and Time*. Whitton, B.A. (ed): Springer Science+Business Media, pp. 65-125.

Stauffer, R.E., Jenne, E.A., and Ball, J.W. (1980) Chemical studies of selected trace elements in hot-spring drainages of Yellowstone National Park. In. United States Department of the Interior, G.S. (ed). Washington: United States Government Printing Office, pp. 1-20.

Tassi, F., Martinez, C., Vaselli, O., Capaccioni, B., and Viramonte, J. (2005) Light hydrocarbons as redox and temperature indicators in the geothermal field of El Tatio (northern Chile). *Applied Geochemistry* **20**: 2049-2062.

Thiel, T. (1988) Phosphate transport and arsenate resistance in the cyanobacterium Anabaena variabilis. *Journal of Bacteriology* **170**: 1143-1147.

Turner, S., Pryer, K.M., Miao, V.P.W., and Palmer, J.D. (1999) Investigating deep phylogenetic relationships among Cyanobacteria and Plastids by small subunit rRNA sequence analysis. *Journal of Eukaryotic Microbiology* **46**: 327-338.

van der Leun, J.C., and de Gruijl, F.R. (1993) Influences of ozone depletion on human and animal health. In *UV-B radiation and ozone depletion: Effects on humans, animals, plants, microorganisms, and materials*. Tevini, M. (ed). Ann Arbor, MI: Lewis Publishers.

Wang, Q., Garrity, G.M., Tiedje, J.M., and Cole, J.R. (2007) Naive Bayesian classifier for rapid assignment of rRNA sequences into the new bacterial taxonomy. *Applied and Environmental Microbiology* **73**: 5261-5267.

Wang, S., Zhang, D., and Pan, X. (2012) Effects of arsenic on growth and photosystem II (PSII) activity of Microcystis aeruginosa. *Ecotoxicology and Environmental Safety* **84**: 104-111.

Ward, D.M., and Castenholz, R.W. (2000) Cyanobacteria in Geothermal Habitats. In *The Ecology of Cyanobacteria*. Whitton, B.A., and Potts, M. (eds). Netherlands: Kluwer Academic Publishers, pp. 37-59.

Ward, D.M., and Cohan, F.M. (2005) Microbial Diversity in Hot Spring Cyanobacterial Mats: Pattern and Prediction. In *Geothermal Biology and Geochemistry in Yellowstone National Park*. Inskeep, W.P., and McDermott, T.R. (eds). Bozeman, MT: Montana State University Publications, pp. 185-201.

Ward, D.M., Castenholz, R.W., and Miller, S.R. (2012) Cyanobacteria in Geothermal Habitats. In *Ecology of Cyanobacteria II, Their Diversity in Space and Time*. Whitton, B.A. (ed): Springer Science+Business Media, pp. 39-63.

Webster, J.G., and Nordstrom, D.K. (2003) Geothermal Arsenic. In *Arsenic in Groundwater: Geochemistry and Occurence*. Welch, A.H., and Stollenwerk, K.G. (eds). Boston: Kluwer Academic Publishers, pp. 101-125.

Weisburg, W.G., Barns, S.M., Pelletier, D.A., and Lane, D.J. (1991) 16S ribosomal DNA amplification for phylogenetic study. *Journal of Bacteriology* **173**: 697-703.

Woodger, F.J., Badger, M.R., and Price, G.D. (2003) Inorganic carbon limitation induces transcripts encoding components of the CO_2-concentrating mechanism in Synechococcus sp. PCC7942 through a redox-independent pathway. *Plant Physiology* **133**: 2069-2080.

Yu, J., Price, G.D., Song, L., and Badger, M.R. (1992) Isolation of a putative carboxysomal carbonic anhydrase gene from the cyanobacterium Synechococcus PCC7942. *Plant Physiology* **100**: 794-800.

Zhang, P., Battchikova, N., Jansen, T., Appel, J., Ogawa, T., and Aro, E.M. (2004) Expression and functional roles of the two distinct NDH-1 complexes and the carbon acquisition complex NdhD3/NdhF3/CupA/Sll1735 in Synechocystis sp PCC 6803. *The Plant Cell* **16**: 3326-3340.

Chapter 5: Conclusions

Cyanobacteria are important primary producers in hot spring microbial mat communities. The phylogenetic diversity and microbial ecology of cyanobacteria was investigated within the extreme geothermal features of El Tatio Geyser Field, Chile (ETGF) in order to determine their diversity, the controls on their distribution, and the adaptive mechanisms utilized to alleviate stress in the extreme ETGF environment. El Tatio's isolated geographic location, paired with high UV-flux, high arsenic (0.4-0.6 mM), and extremely low dissolved inorganic carbon (0.1-0.3 mM) make it a unique environmental context in which to investigate the phylogenetic diversity and ecology of cyanobacteria.

This dissertation (i) expands the known geographic and phylogenetic diversity of geothermal cyanobacteria, (ii) describes the geochemical controls on cyanobacteria and microbial community properties in a novel geochemical context, and (iii) provides a new context in which to consider the impact of arsenic on microbial ecosystems through the primary productive capacity of cyanobacteria. Though the effects of As^{III} and As^{V} on cyanobacteria growth and physiology have been considered in the past, this is the first study that links cyanobacterial distribution to gradients of As^{III} and As^{V} in a natural setting. Additionally, four novel cultured cyanobacterial strains were described and submitted to the UTEX Culture Collection of Algae where they will be maintained and made available for future work. Cultures T-025, T-039, and T-045 are closely related to previously described unicellular and coccoidal *Synechocystis*. Culture T-031 is only 97% similar to the 16S rRNA sequences of previously cultured and described filamentous and

heterocystous Nostocaceae, and is a candidate for a novel genus within the Subsection IV cyanobacteria. Most cyanobacteria 16S rRNA sequences match filamentous cyanobacteria, and the most abundant and widespread organism in these springs was *Fischerella*, a cosmopolitan N-fixing filamentous cyanobacterium found in other geothermal locations.

El Tatio cyanobacteria have to assimilate life essential carbon in an environment where nearly every condition is working against that goal. El Tatio's position at high elevation leads to high UV flux. High UV and temperatures above 30°C in thermal water lead to decreased efficiency by the enzyme RuBisCO, beyond what cyanobacteria typically experience in a microbial mat. These factors add to carbon stress already experienced by cyanobacteria surviving in the face of carbon limitation. The effect of carbon limitation in this ecosystem is evidenced by visual comparison of mats in low and high-DIC streams, but was also confirmed by a quantitative comparison that shows that biomass is significantly lower in low-DIC streams compared to high-DIC streams.

Low DIC locations that are dominated by As^{V} host mats with significantly more abundant cyanobacteria than locations dominated by As^{III}, and cyanobacteria abundance shows a very significant negative relationship to [As^{III}] throughout the geothermal field. When cultured isolates were exposed to increasing [As^{III}] in the laboratory, an overall negative response was observed, confirming these field observations. It should be noted however, that their tolerance for As^{III} in the lab (0.5-1.0 mM) exceeded their apparent upper limit in the field (~0.15 mM), indicating that other environmental factors also

influence their successful colonization and survival at El Tatio, and that these factors, such as temperature or UV, have an antagonistic effect in combination with As^{III}.

While [DIC] did not correlate with the abundance or diversity of cyanobacteria, higher DIC did contribute to cyanobacteria species dominance, higher biomass, and higher microbial community diversity compared to low-DIC sites. It is not surprising that DIC concentration did not affect cyanobacteria abundance, because cyanobacteria possess a CO_2-concentrating mechanism (CCM) to alleviate the effects carbon limitation. The most exciting emergent property in this system is the effect of the combination of low DIC and As^{V} on cyanobacteria abundance and biomass. In the laboratory, when cyanobacteria were exposed to closed and carbon limited conditions similar to those experienced in a diffusion limited microbial mat within a low-DIC stream, arsenate buffered cells removed up to 25% more carbon from the media and maintain higher biomass than cells in unbuffered media. This was attributed to the pH buffering capacity of arsenate, which has the ability to prevent an upward pH shift that occurs during cyanobacterial CCM activity. Even at peak daylight, El Tatio mats are strongly buffered to pH 6.7 throughout the photosynthetic zone, allowing carbon to remain in the forms of CO_2 and HCO_3^-, their preferred forms for assimilation. This phenomenon appears to be especially important to filamentous cyanobacteria, which are anchored within microbial mats and cannot escape diffusion-limited conditions within the mat. pH buffering by arsenate is central to the long-term survival of cyanobacteria-based microbial mats in DIC-limited streams at El Tatio, by allowing them to allocate more carbon towards growth, and less carbon and energy toward 'expensive' CCM machinery.

Appendix A

CHAPTER 1 SUPPLEMENT

Table A-1: BG-11 (+N) media used during cyanobacterial culturing and maintenance. This recipe was obtained from the UTEX Culture Collection of Algae website (www.utex.org). BG-11 (+N) amended with 5 g/L NaCl was used in some cases. BG-11 (-N) follows the same recipe, minus the addition of $NaNO_3$.

Component	Amount	Stock Solution Concentration	Final Concentration
$NaNO_3$	10 mL/L	30 g/200 mL dH_2O	17.6 mM
K_2HPO_4	10 mL/L	0.8 g/200 mL dH_2O	0.23 mM
$MgSO_4 \cdot 7H_2O$	10 mL/L	1.5 g/200 mL dH_2O	0.3 mM
$CaCl_2 \cdot 2H_2O$	10 mL/L	0.72 g/200 mL dH_2O	0.24 mM
Citric acid $\cdot H_2O$	10 mL/L	0.12 g/200 mL H_2O	0.031 mM
Ferric ammonium citrate	10 mL/L	0.12 g/200 mL H_2O	0.021 mM
$Na_2EDTA \cdot 2H_2O$	10 mL/L	0.02 g/200 mL H_2O	0.0027 mM
$NaHCO_3$	10 mL/L	0.4 g/200 mL H_2O	0.19 mM
BG-11 Trace Metals Solution	1 mL/L		
BG-11 Trace Metals Solution			
H_3BO_3	2.86 g/L		46 mM
$MnCl_2 \cdot 4H_2O$	1.81 g/L		9 mM
$ZnSO_4 \cdot 7H_2O$	0.22 g/L		0.7 mM
$Na_2MoO_4 \cdot 2H_2O$	0.39 g/L		1.6 mM
$CuSO_4 \cdot 5H_2O$	0.079 g/L		0.3 mM
$Co(NO_3)_2 \cdot 6H_2O$	49.4 g/L		0.17 mM

Appendix B

CHAPTER 2 SUPPLEMENT

Table B-1: List of Genbank database strains, their major cyanobacterial Subsection (I-V) (Tomitani et al., 2006), and taxonomic classification. 'Classification' follows as (Bacteria; Cyanobacteria; class; family/order, if relevant; *genus*). Gloeobacter violaceus PCC 7421 (NR_074282.1) can be considered a basal member of Subsection I (Cyanobacteria; Gloeobacteria; Gloeobacterales; *Gloeobacter*).

Genbank ID	*Genus sp.*	Strain ID	Subsection	Classification
AF001480	*Synechococcus sp.*	WH 8101	I	Oscillatoriophycideae; Chroococcales; *Synechococcus*
AF053398	*Prochlorococcus marinus*	MIT 9312	I	Prochlorales; Prochlorococcaceae; *Prochlorococcus*
U40340	*Microcystis aeruginosa*	PCC 7941	I	Oscillatoriophycideae; Chroococcales; *Microcystis*
NR_074311	*Synechocystis sp.*	PCC 6803	I	Oscillatoriophycideae; Chroococcales; *Synechocystis*
HM217076	*Synechocystis sp.*	LEGE 06079	I	Oscillatoriophycideae; Chroococcales; *Synechocystis*
HQ832911	*Synechocystis salina*	LEGE 06155	I	Oscillatoriophycideae; Chroococcales; *Synechocystis*
X94705	*Merismopedia glauca*	B1448-1	I	Oscillatoriophycideae; Chroococcales; *Merismopedia*
HE975009	*Gleothece sp.*	PCC 6909	I	Oscillatoriophycideae; Chroococcales; *Gleothece*
AF132783	*Xenococcus sp.*	PCC 7305	II	Pleurocapsales; *Xenococcus*
AB039009	*Staniera sp.*	PCC 7301	II	Pleurocapsales; *Staniera*
AB039006	*Pleurocapsa sp.*	PCC 7319	II	Pleurocapsales; *Pleurocapsa*
AB075994	*Phormidium persicinum*	CCMP 638	III	Oscillatoriophycideae; Oscillatoriales; *Pseudanabaena*
AB075997	*Symploca atlantica*	PCC 8002	III	Oscillatoriophycideae; Oscillatoriales; *Symploca*
AJ000714	*Lyngbya sp.*	PCC 7419	III	Oscillatoriophycideae; Oscillatoriales; *Lyngbya*
NR_074275	*Trichodesmium erythraem*	IMS 101	III	Oscillatoriophycideae; Oscillatoriales; *Trichodesmium*
NR_114511	*Oscillatoria sancta*	PCC 7515	III	Oscillatoriophycideae; Oscillatoriales; *Oscillatoria*
AY493589	*Leptolyngbya antarctica*	ANT.LACV6.1	III	Oscillatoriophycideae; Oscillatoriales; *Leptolyngbya*
HM217044	*Leptolyngbya sp.*	LEGE 07298	III	Oscillatoriophycideae; Oscillatoriales; *Leptolyngbya*
DQ393284	*Arthrospira platensis*	PCC 9108	III	Oscillatoriophycideae; Oscillatoriales; *Arthrospira*
AB075998	*Tolypothrix sp.*	CCMP1185	IV	Nostocales; Microchaetaceae; *Tolypothrix*
NR_112175	*Calothrix desertica*	PCC 7102	IV	Nostocales; Rivulariaceae; *Calothrix*

(Table B-1, continued)

AB075996	*Scytonema hofmanni*	PCC 7110	IV	Nostocales; Scytonemataceae; *Scytonema*
NR_102457	*Anabaena cylindrica*	PCC 7122	IV	Nostocales; Nostocaceae; *Anabaena*
AF268022	*Nodularia spumigena*	UTEX B 2092	IV	Nostocales; Nostocaceae; *Nodularia*
AJ781143	*Nodularia harveyana*	Bo53	IV	Nostocales; Nostocaceae; *Nodularia*
KM019930	*Nodularia sphaerocarpa*	PCC 7804	IV	Nostocales; Nostocaceae; *Nodularia*
AY038036	*Cyanospira rippkae*	PCC 9501	IV	Nostocales; Nostocaceae; *Cyanospira*
FR774775	*Cyanospira capsulata*	CCAX/CC87E	IV	Nostocales; Nostocaceae; *Cyanospira*
NR_074317	*Nostoc punctiforme*	PCC 73102	IV	Nostocales; Nostocaceae; *Nostoc*
AB075981	*Chlorogloeopsis fritschii*	PCC 6912	V	Stigonematales; *Chlorogloeopsis*
DQ786171	*Fischerella sp.*	MV-11	V	Stigonematales; *Fischerella*
AB075897	*Fischerella thermalis*	PCC 7521	V	Stigonematales; *Fischerella*
AB075986	*Fischerella muscicola*	PCC 7414	V	Stigonematales; *Fischerella*

Table B-2: Environmental clone library Phylum level taxonomic diversity, presented as the number of sequences per clone library.

Phylum	GG-25	GG-40	GG-55	GG-75	T-31	T-34	T-45	MBS-1	MBS-2	NT-1	NT-2	NT-3
Acidobacteria	0	0	0	3	2	0	0	0	1	0	0	2
Aquificae	6	2	0	0	0	0	0	0	0	1	0	0
Bacteroidetes	1	6	0	8	3	2	9	1	1	2	3	0
Caldiserica	0	0	0	0	0	0	0	1	0	0	0	0
Chlorobi	0	3	0	10	0	0	0	3	0	1	1	1
Chloroflexi	0	6	21	2	2	5	0	12	0	5	9	14
Cyanobacteria	0	0	6	12	41	31	27	0	36	0	0	15
Cand. OP 1	0	0	0	0	0	0	0	0	0	1	0	0
Cand. OP 8	0	0	0	0	0	0	0	1	0	0	0	0
Cand. OP 10	1	1	0	0	0	0	0	0	0	0	1	1
Cand. OP 11	12	7	0	1	1	8	0	8	3	11	10	5
Deferribacteres	2	0	4	0	0	0	0	0	0	0	0	2
Deinococcus-Thermus	0	3	0	1	0	0	0	1	2	0	2	0
Firmicutes	9	3	0	2	0	2	0	1	0	0	3	0
Ignavibacteriae	0	0	0	1	0	0	0	0	0	0	1	1
Nitrospirae	0	0	0	0	0	0	0	2	0	0	0	0
Planktomycetales	0	0	0	1	0	0	1	0	0	0	0	0
Proteobacteria	0	0	0	1	0	0	0	0	0	0	0	2
Spirochaetes	0	0	0	4	0	0	2	0	1	0	1	0
Verrucomicrobia	0	0	0	4	0	0	2	0	1	0	1	0
Unclassified	1	1	0	0	1	0	0	0	0	0	0	2

Table B-3: Cyanobacterial genus-level OTUs and relative abundances (%) of cyanobacteria sequences relative to all phyla in the community, generated by 454-pyrosequencing. These numbers reflect the % of total community composition, since cyanobacterial abundances differ among samples.

Cyanobacteria *Genera*	GG-25	GG-30	GG-40	GG-55	GG-75	T-31	T-34	T-45	MBS-1	MBS-2	NT-1	NT-2	NT-3
Anabaena	0	0	0	0	0.1	2	0	0	0	1	0	0	2
Arthrospira	0	0	0.1	0.1	0.8	0	0	0	0	0	1	0	0
Calothrix	0	0	0	0	0	3	2	9	1	1	2	3	0
Chamaesiphon	0	0	0	0	0	0	0	0	1	0	0	0	0
Chroococcidiopsis	0.3	0	0	0	0.2	0	0	0	3	0	1	1	1
Cyanobacterium	0	0	0	0	0.2	2	5	0	12	0	5	9	14
Fischerella	0.1	0	0	33.0	4.0	41	31	27	0	36	0	0	15
Leptolyngbya	0	0	1.8	0	2.1	0	0	0	0	0	1	0	0
Limnothrix	0	0	0	0	0	0	0	0	1	0	0	0	0
Lyngbya	0	0	0	0	0	0	0	0	0	0	0	1	1
Microcoleus	0	0	0	0.2	0	1	8	0	8	3	11	10	5
Microcystis	0	0	0	0.2	0	0	0	0	0	0	0	0	2
Nodularia	0.1	0	0	0	0	0	0	0	1	2	0	2	0
Nostoc	0	0.2	20.5	0.1	0.2	0	2	0	1	0	0	3	0
Oscillatoria	0	0	0	0	0	0	0	0	0	0	0	1	1
Phormidium	0	0	0	0	0	0	0	0	2	0	0	0	0
Planktothricoides	0	0	0	0	0	0	0	1	0	0	0	0	0
Planktothrix	0	0	0	0.1	0	0	0	0	0	0	0	0	2
Pleurocapsa	0	0	0	0	40.1	0	0	2	0	1	0	1	0
Prochlorococcus	0	0	0	0.4	0	0	0	0	0	0	0	0	0
Prochlorothrix	0	0	10.1	0	0.1	0	0	0	0	0	0	0	0
Pseudanabaena	0	0	0.2	0	0	0	0	0	0	0	0	0	0
Rivularia	0	0	0	0	0.1	0	0	0	0	0	0	0	0
Scytonema	0	0	0	0	0	0	0	0.5	0	0	0	0	0
Spirulina	0	0	1.0	0	0.1	0	0	0	0	0.1	0	0	0
Synechococcus	0.9	0	0	0	0.1	0	0	1.0	0	0	0	0	0
Thermosynechococcus	0	0	0	0	0.1	0	0	0	0	0	0	0	0

Table B-4: Full-length El Tatio cyanobacteria Genbank sequence database accession numbers.

Sequence ID	Genbank Acc. No.	Sequence ID	Genbank Acc. No.	Sequence ID	Genbank Acc. No.
T-31_1	KP793983	T-34_41	KP794041	NT-3_30	KP794018
T-31_5	KP793984	T-34_42	KP794042	NT-3_40	KP794019
T-31_6	KP793985	T-34_45	KP794043	NT-3_41	KP794020
T-31_8	KP793986	T-34_46	KP794044	NT-3_42	KP794021
T-31_9	KP793987	T-34_48	KP794045	NT-3_50	KP794022
T-31_15	KP793988	T-34_49	KP794046	GG-75_5	KP794048
T-31_21	KP793989	T-34_50	KP794047	GG-75_17	KP794049
T-31_23	KP793990	MBS-2_1	KP793944	GG-75_26	KP794050
T-31_26	KP793991	MBS-2_2	KP793945	GG-75_44	KP794051
T-31_27	KP793992	MBS-2_3	KP793946	GG-75_50	KP794052
T-31_28	KP793993	MBS-2_4	KP793947	T-45_4	KP793972
T-31_29	KP793994	MBS-2_11	KP793948	T-45_7	KP793973
T-31_32	KP793995	MBS-2_12	KP793949	T-45_8	KP793974
T-31_33	KP793996	MBS-2_17	KP793950	T-45_9	KP793975
T-31_35	KP793997	MBS-2_22	KP793951	T-45_12	KP793976
T-31_37	KP793998	MBS-2_27	KP793952	T-45_13	KP793977
T-31_38	KP793999	MBS-2_28	KP793953	T-45_14	KP793978
T-31_41	KP794000	MBS-2_29	KP793954	T-45_20	KP793979
T-31_42	KP794001	MBS-2_31	KP793955	T-45_26	KP793980
T-31_43	KP794002	MBS-2_32	KP793956	T-45_29	KP793981
T-31_45	KP794003	MBS-2_34	KP793957	T-45_34	KP793982
T-31_46	KP794004	MBS-2_36	KP793958	T-05_4	KP793937
T-31_51	KP794005	MBS-2_38	KP793959	T-05_5	KP793938
T-31_53	KP794006	MBS-2_42	KP793960	T-05_9	KP793939
T-31_54	KP794007	MBS-2_43	KP793961	T-05_10	KP793940
T-31_55	KP794008	MBS-2_44	KP793962	T-05_11	KP793941
T-34_1	KP794023	MBS-2_45	KP793963	T-05_16	KP793942
T-34_2	KP794024	MBS-2_46	KP793964	T-05_20	KP793943
T-34_4	KP794025	MBS-2_47	KP793965	T075-A_1	KP793930
T-34_6	KP794026	MBS-2_48	KP793966	T075-A_3	KP793931
T-34_13	KP794027	MBS-2_49	KP793967	T075-A_4	KP793932
T-34_14	KP794028	MBS-2_50	KP793968	T075-A_6	KP793933
T-34_20	KP794029	MBS-2_52	KP793969	T075-A_7	KP793934
T-34_22	KP794030	MBS-2_59	KP793970	T075-A_10	KP793935
T-34_23	KP794031	MBS-2_60	KP793971	T075-A_11	KP793936
T-34_25	KP794032	NT-3_10	KP794009	T075-B_3	KP762335
T-34_26	KP794033	NT-3_12	KP794010	T075-B_6	KP762336
T-34_28	KP794034	NT-3_15	KP794011	T075-B_7	KP762337
T-34_29	KP794035	NT-3_19	KP794012	T075-B_8	KP762338
T-34_30	KP794036	NT-3_20	KP794013	T075-B_9	KP762339
T-34_32	KP794037	NT-3_22	KP794014	T075-B_10	KP762340
T-34_33	KP794038	NT-3_24	KP794015	T075-B_11	KP762341
T-34_35	KP794039	NT-3_25	KP794016	T075-B_13	KP762342
T-34_36	KP794040	NT-3_27	KP794017	T075-B_22	KP762343

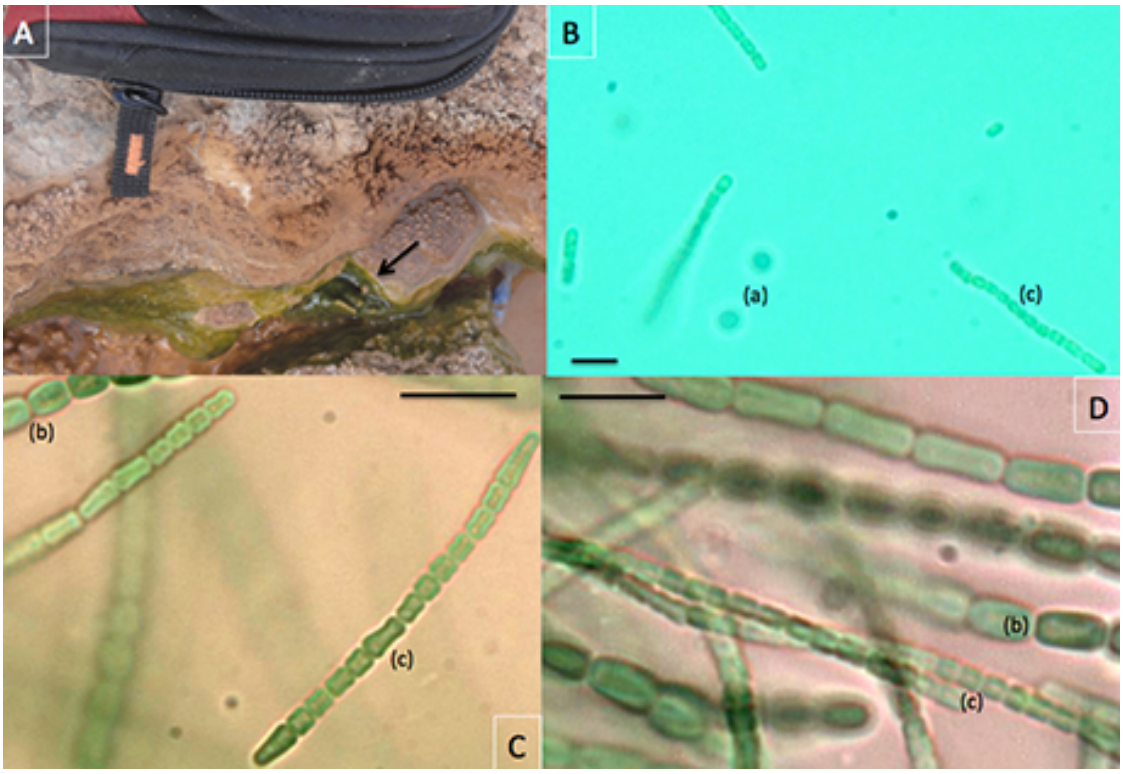

Figure B-1: Environmental mat sample T-05 enriched in BG11(+N) media without transfer. The original sample was collected from a subaerial mat (A, arrow) exposed to steam and splash water of ~50-55°C. Microscopic images are shown at 1000X magnification (B) some zoomed in (C, D). Several morphotypes are present, a unicellular form (a), a filamentous form with large barrel-shaped cells 8-9 μm) (b), and a filamentous form with small square shaped cells (2-3 μm) (c). No cells shown here appear heterocystous due to enrichment in BG-11(+N) media. Scale bar is 10 μm.

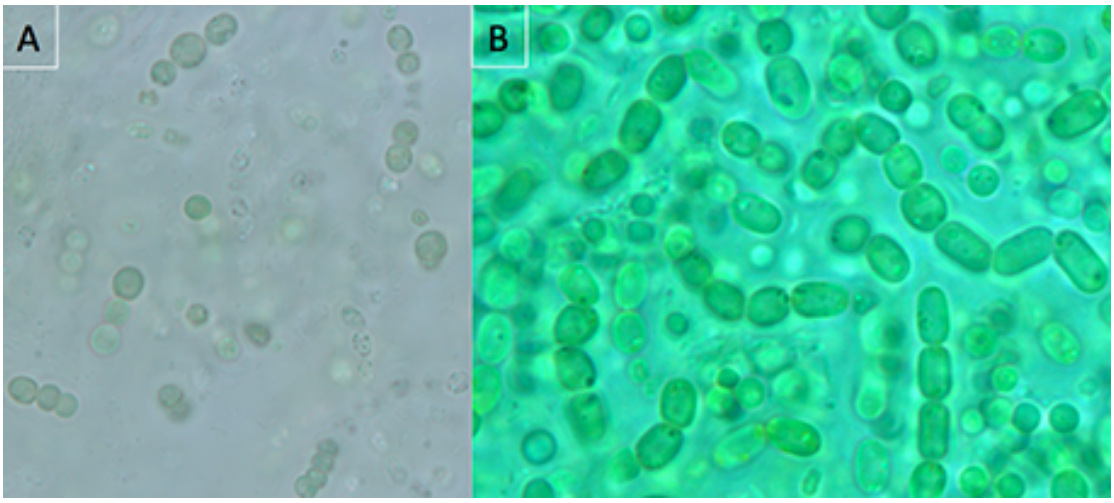

Figure B-2: Environmental enrichment culture T075-A (A), and T075-B (B) at 1,000X magnification.

Table B-5: List of database sequences used in *Fischerella* sp. reconstruction, along with references.

Sequence ID	NCBI Acc. No.	Country of Origin	Group (Miller et al. 2007)	Reference
CCMEE5327	EF566834	Italy	Group 1	Miller et al., 2007
CCMEE5328	EF566835	Italy	Group 1	Miller et al., 2007
CCMEE5337	EF566836	OR	Group 1	Miller et al., 2007
CCMEE5320	EF566837	Iceland	Group 1	Miller et al., 2007
CCMEE5273	EF566838	BC	Group 1	Miller et al., 2007
CCMEE5198	EF566839	NZ	Group 1	Miller et al., 2007
CCMEE5186	EF566840	NZ	Group 1	Miller et al., 2007
CCMEE5335	EF566841	NZ	Group 1	Miller et al., 2007
CCMEE5281	EF566842	Slovakia	Group 1	Miller et al., 2007
CCMEE5282	EF566843	Slovakia	Group 1	Miller et al., 2007
CCMEE5193	EF566844	Puheohe Springs, Chile	Group 1	Miller et al., 2007
CCMEE5201	EF566845	NZ	Group 2	Miller et al., 2007
CCMEE5202	EF566846	NZ	Group 2	Miller et al., 2007
CCMEE5203	EF566847	NZ	Group 2	Miller et al., 2007
CCMEE5323	EF566848	Iceland	Group 3	Miller et al., 2007
CCMEE5321	EF566849	Iceland	Group 3	Miller et al., 2007
CCMEE5324	EF566850	Iceland	Group 3	Miller et al., 2007
CCMEE5326	EF566851	Iceland	Group 3	Miller et al., 2007
CCMEE5272	EF566852	Portugal	Group 3	Miller et al., 2007
CCMEE5192	EF566854	Chile	Group 4	Miller et al., 2007
CCMEE5204	EF566855	Oman	Group 4	Miller et al., 2007
CCMEE5205	EF566856	Oman	Group 4	Miller et al., 2007
CCMEE5379	EF566857	Oman	Group 4	Miller et al., 2007
CCMEE5380	EF566858	Oman	Group 4	Miller et al., 2007
CCMEE5319	EF566860	Guatemala	Group 6	Miller et al., 2007
CCMEE5267	EF566861	AK	Group 6	Miller et al., 2007
CCMEE5318	EF566862	El Salvador	Group 6	Miller et al., 2007
CCMEE5329	EF566863	Japan	Group 7	Miller et al., 2007
CCMEE5331	EF566864	Japan	Group 7	Miller et al., 2007
Thermophil. cyano. tBTRCCn 403	DQ471444	Zerka Ma'in, Jordan	Group 4	Ionescu et al., 2010
M laminosus Greenland_8	DQ431003	Greenland	Group 3	Roeselers et al., 2007
Fischerella sp. MV-11	DQ786171	Costa Rica	Group 6	Finsinger et al., 2008
Fischerella sp. RV-14	DQ786173	Costa Rica	Group 6	Finsinger et al., 2008
Fischerella sp CR-26 M	EF545613	Costa Rica	Group 6	Unpublished
Fischerella sp. MV-9	DQ786169	Costa Rica	Group 6	Finsinger et al., 2008
M laminosus SAG 4.84	EU116035	Iceland	Group 3	Kastovsky and Johansen 2008
M laminosus Y-99-9	AY426547	YNP	Group 1	Miller and Bebout 2004
Fischerella sp clone YL099	HM856465	YNP	Group 1	Clingenpeel et al., 2011
Tat-08-003_12_41	GU437321	ETGF, Chile	Unassigned	Engel et al., 2013
Tat08_003_12_10	GU437365	ETGF, Chile	Group 1	Engel et al., 2013

Table B-6: Phylum level OTU table, with abundances of phyla relative to the total sequences per sample (%). Phyla with < 1% are grouped into 'other'.

Phylum	GG-25	GG-30	GG-40	GG-55	GG-75	T-31	T-34	T-45	MBS-1	MBS-2	NT-1	NT-2	NT-3
Acidobacteria	0	0	0	0	3.0	1.3	0	0	0	0	0	1.4	2.0
Actinobacteria	1.1	0	0	0	0	0	0	0	1.1	0	1.3	0	0
Bacteroidetes	6.7	0	31.4	3.7	8.0	1.4	5.4	14.5	2.0	0	6.6	5.6	3.1
Chlorobi	0	0	5.4	0	6.7	1.1	5.1	1.1	0	0	0	3.5	11.4
Chloroflexi	24.3	0	1.3	16.3	1.6	4.1	5.3	0	19.2	0	51.1	55.2	12.7
Cyanobacteria	1.3	0	33.7	34.3	48.2	80.2	80.5	41.9	0	80.0	0	2.2	58.5
Deferribacteres	12.5	0	0	14.1	0	0	0	0	9.5	0	14.0	0	6.4
Deinococcus-Thermus	0	0	0	1.2	0	0	0	0	3.6	0	6.5	2.3	0
Firmicutes	47.9	0	0	0	0	1.1	1.2	10.4	2.2	0	0	0	0
Nitrospirae	1.8	0	0	0	0	0	0	0	33.6	0	0	0	0
OP 1 (Cand.)	0	0	6.2	11.8	0	0	0	0	0	0	2.6	0	0
OP 8 (Cand.)	0	0	0	0	0	0	0	0	1.4	0	0	0	0
Proteobacteria	3.2	97.7	18.1	10.6	29.7	9.6	1.7	28.4	23.9	17.2	15.7	27.1	5.4
Spirochaetes	0	0	0	1.3	0	0	0	0	0	0	0	0	0
Ws3 (Cand.)	0	0	0	2.8	0	0	0	0	0	0	0	0	0
other	1.3	2.3	4.1	4.1	2.8	1.4	0.8	3.8	3.4	2.8	2.2	2.7	0.6
Total sequences	11,942	7,854	4,144	7,032	14,124	10,355	8,888	4,391	23,915	40,703	8,731	11,452	12,129

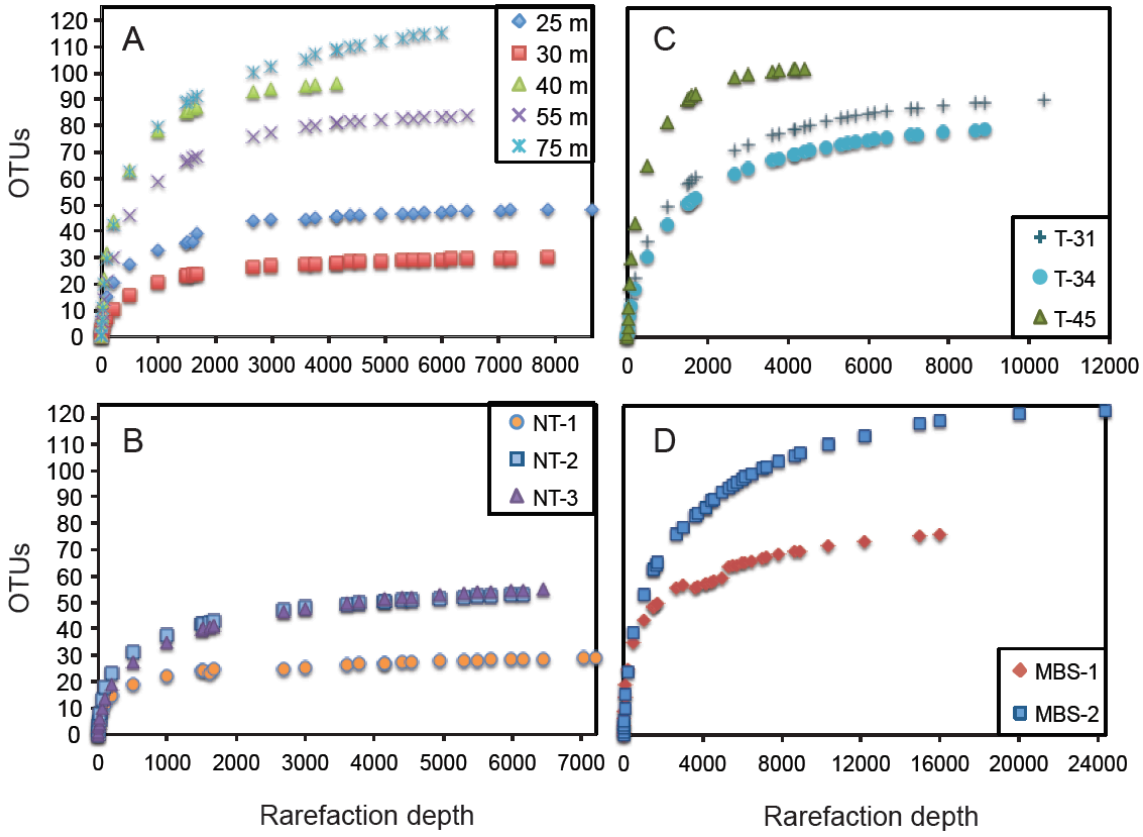

Figure B-3: Rarefaction curves constructed from each pyrosequencing sample, organized by sample location. Five Great Geyser samples (A) and three New Transect samples, from the Middle Basin. Two samples from the Upper Basin, plus T-45 from group M-III springs (C), and two samples from the Middle Basin Springs (D). Rarefaction depth, as the number of sequences randomly subsampled from the entire sequence pool, and the resulting number of OTUs discovered at each random subsample, show that sampling depth was adequate to show the relative species richness (OTUs) at each site. Rarefaction data were generated in the 'Vegan 2.0-3' R package (Oksanen, Guillaume et al. 2015).

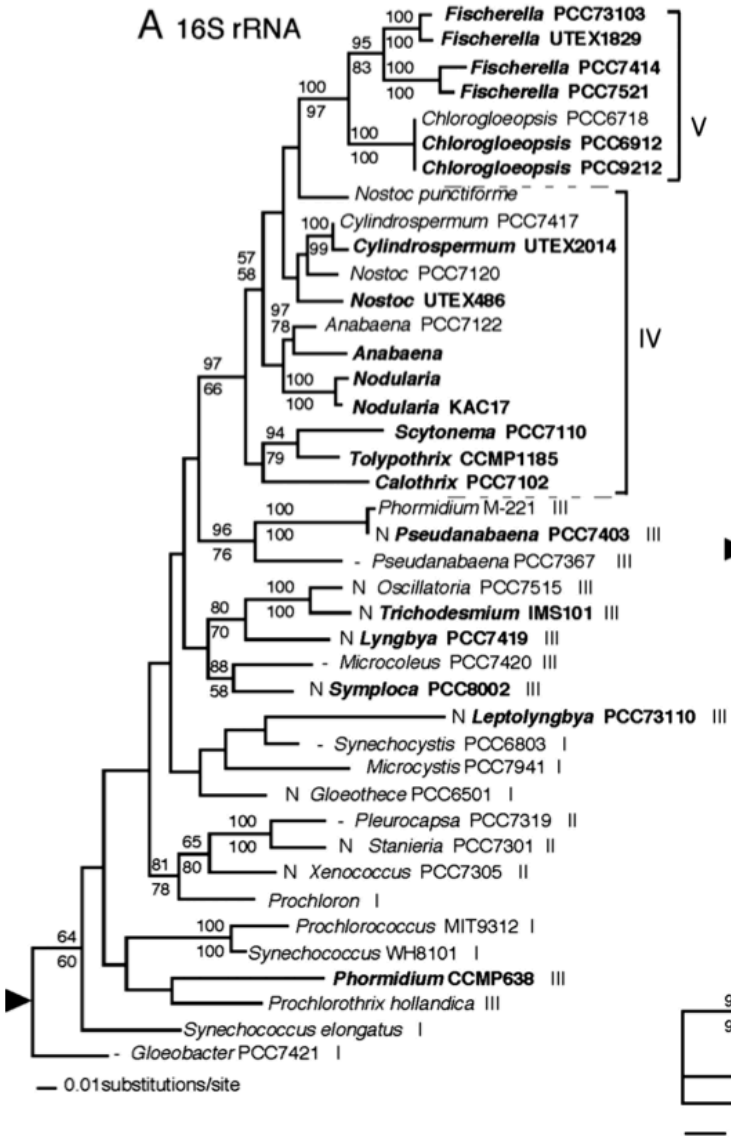

Figure B-4: A 16-S rRNA phylogenetic analysis of cyanobacteria. This phylogeny was constructed using maximum likelihood criteria in PAUP v4.0b (Swofford) modified from Tomitani et al. (2006). The arrow represents the position of the root with outgroup *Gloeobacter* PCC 7421. Cyanobacteria Subsections IV and V are monophyletic groups in this reconstruction. Numbers above and below nodes represent bootstrap proportions for 1,000 replicate trees calculated by Neigbor Joining and Maximum Parsimony methods, respectively.

Appendix C

CHAPTER 3 SUPPLEMENT

Table C-1: 16S rRNA reference sequence accession numbers and affiliated taxonomy of reference organisms used to construct the phylogenies in Figures 3-5, 3-6, and 3-7. Reference sequences that do not appear in this table can be found in Table B-1.

Genbank ID	*Genus sp.*	Strain ID	Subsection	Classification
JQ070058	*Aphanocapsa cf. rivularis*	UAM 380	I	Oscillatoriophycideae; Chroococcales; *Aphanocapsa*
GQ859638	*Merismopedia punctata*	PMC 260	I	Oscillatoriophycideae; Chroococcales; *Merismopedia*
KM019996	*Microcystis aeruginosa*	PCC 7005	I	Oscillatoriophycideae; Chroococcales; *Microcystis*
HF678505	*Microcystis aeruginosa*	UTEX LB 2385	I	Oscillatoriophycideae; Chroococcales; *Microcystis*
AY172828	*Synechococcus sp.*	RS-9918	I	Oscillatoriophycideae; Chroococcales; *Synechococcus*
JF306684	*Synechococcus sp.*	RCC 317	I	Oscillatoriophycideae; Chroococcales; *Synechococcus*
FM177503	*Synechocystis aquatilis*	1LT332S04	I	Oscillatoriophycideae; Chroococcales; *Synechocystis*
CP007542	*Synechocystis sp.*	PCC 6714	I	Oscillatoriophycideae; Chroococcales; *Synechocystis*
GU935368	*Synechocystis sp.*	Sai002	I	Oscillatoriophycideae; Chroococcales; *Synechocystis*
AB041936	*Synechocystis sp.*	PCC 6702	I	Oscillatoriophycideae; Chroococcales; *Synechocystis*
AB041937	*Synechocystis sp.*	PCC 6714	I	Oscillatoriophycideae; Chroococcales; *Synechocystis*
AB041938	*Synechocystis sp.*	PCC 6805	I	Oscillatoriophycideae; Chroococcales; *Synechocystis*
EF583857	*Anabaena sp.*	BECID19	IV	Nostocales; Nostocaceae; *Anabaena*
AB075983	*Cylindrospermum licheniforme*	UTEX 2014	IV	Nostocales; Nostocaceae; *Cylindrospermum*
NR_102462	*Cylindrospermum stagnale*	PCC 7417	IV	Nostocales; Nostocaceae; *Cylindrospermum*
AJ781146	*Nodularia harveyana*	BECID29	IV	Nostocales; Nostocaceae; *Nodularia*
KC912772	*Nodularia harveyana*	CCAP 1452	IV	Nostocales; Nostocaceae; *Nodularia*
AJ133177	*Nodularia baltica*	BY1	IV	Nostocales; Nostocaceae; *Nodularia*
AY038034	*Nodularia sp.*	PCC 9350	IV	Nostocales; Nostocaceae; *Nodularia*
AB075991	*Nodularia sp.*	KAC17	IV	Nostocales; Nostocaceae; *Nodularia*
KC883980	*Nostoc calcicola*	BDU 40302	IV	Nostocales; Nostocaceae; *Nostoc*

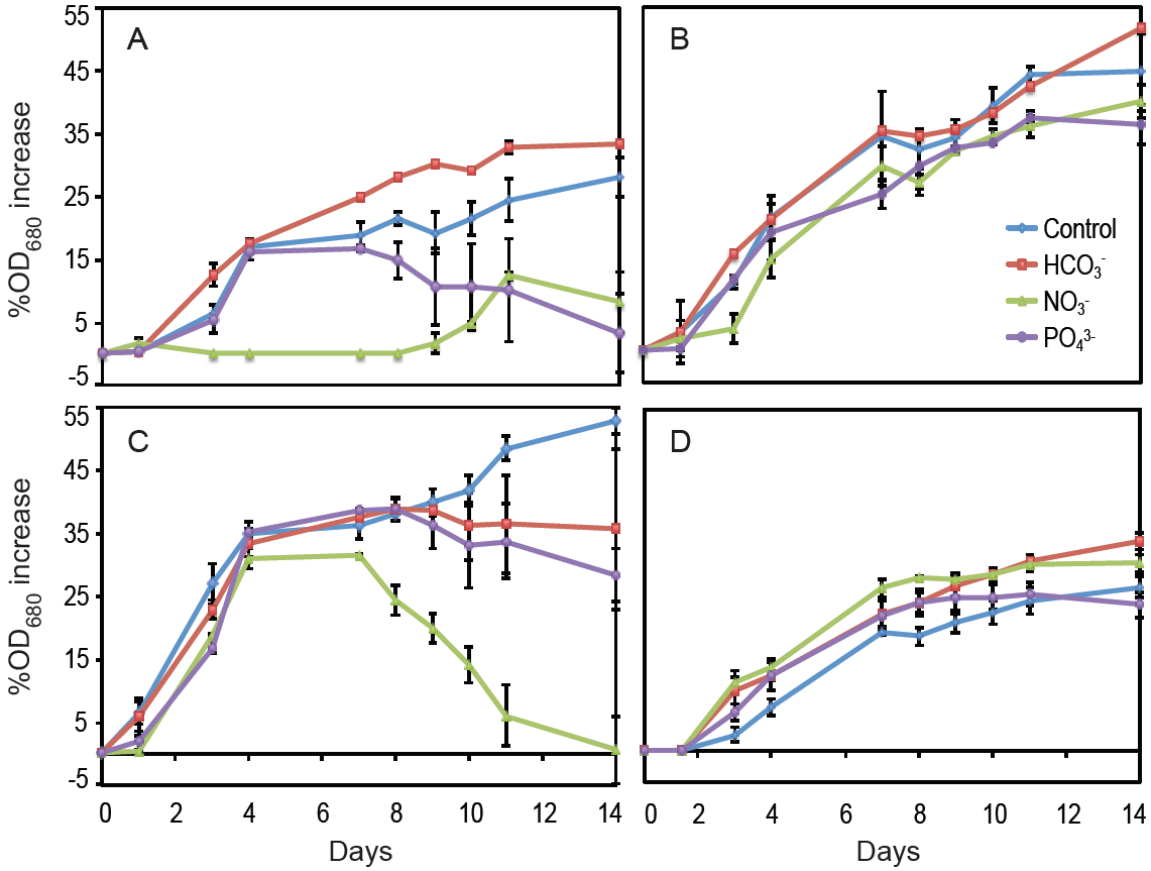

Figure C-1: Growth curves of cultures (A) T-025, (B) T-039, (C) T-031, and (D) T-045 over a 14 day experiment in BG-11(+N) amended with no additional nutrients (control), 1 mM HCO_3^-, 1 mM NO_3^-, or 1 mM PO_4^{3-}. Cells were placed in dilute BG-11(+N) one week prior to experiment to "starve" cells. Day 8 of this chart corresponds to Figure 3-10. Error is reported as standard error of the mean (n = 2). Days 3-7 in (A) were below -5%, and were artificially placed at 0 to aid visualization. The actual values are: -7.28 (± 1.39), -6.13 (± 2.10), and -5.04 (± 1.43) on days 3, 4, and 7, respectively.

Table C-2: Growth response of T-025 at all concentrations of As^{III} (0, 0.5, 1.0, 1.5, 2.0, 2.5, 3.0, 3.5, and 4.0 mM) and standard error of the mean (n = 3). Values represent %OD change from starting OD measurement (Day 0).

%OD	1	2	3	5	6	8
0	3.07	5.95	12.57	18.89	24.99	33.14
0.5	1.10	8.94	5.08	3.62	5.09	0.88
1	0.17	6.07	4.23	4.42	5.92	3.46
1.5	-13.92	-10.67	-12.07	-32.37	-33.34	-50.10
2	1.34	5.39	5.88	0.21	3.04	2.76
2.5	-19.86	-22.28	-21.11	-46.23	-50.20	-47.61
3	-34.55	-44.01	-49.62	-97.34	-102.50	-130.23
3.5	-24.40	-26.34	-26.82	-44.57	-43.99	-57.95
4	-26.27	-38.56	-43.63	-69.48	-75.19	-86.44
	Std. Error					
0	0.61	0.26	1.41	0.59	1.25	0.58
0.5	1.92	2.37	1.65	3.05	1.43	0.33
1	0.53	1.69	0.32	0.43	1.57	3.99
1.5	4.17	5.72	8.25	7.16	11.90	8.09
2	1.32	3.56	2.36	3.24	3.41	4.26
2.5	12.12	15.94	15.79	24.09	31.44	33.56
3	15.52	14.63	18.69	13.10	11.26	16.38
3.5	11.40	11.20	12.90	23.54	21.38	10.79
4	6.17	15.46	10.76	17.77	21.62	24.26

*Same blank (control) used for both As^{III} and As^{V} treatment groups, and recorded as raw absorbance data.

Table C-3: Growth response of T-025 at all concentrations of As^V (0, 0.5, 1.0, 1.5, 2.0, 2.5, 3.0, 3.5, and 4.0 mM) and standard error of the mean (n = 3). Values represent %OD change from starting OD measurement (Day 0).

%OD	1	2	3	5	6	8
0	3.07	5.95	12.57	18.89	24.99	33.14
0.5	8.81	15.26	22.11	28.69	31.79	38.87
1	6.34	12.25	16.40	22.66	26.10	32.81
1.5	7.77	15.68	17.98	21.49	28.11	30.81
2	9.70	16.96	17.77	21.07	25.88	29.39
2.5	9.27	12.67	15.37	20.70	24.31	29.46
3	7.40	15.97	20.08	26.11	28.87	36.53
3.5	6.58	15.29	20.48	26.33	30.74	35.07
4	8.49	18.14	20.58	27.57	33.28	35.89
	Std. Error					
0	0.61	0.26	1.41	0.59	1.25	0.58
0.5	1.40	1.20	2.18	1.94	1.84	1.55
1	2.95	2.82	2.38	2.41	1.26	1.34
1.5	0.78	0.78	1.26	3.13	1.64	1.29
2	1.65	2.33	1.37	0.42	1.48	1.64
2.5	2.05	0.52	0.38	0.84	1.03	0.85
3	1.02	2.67	1.40	1.94	1.53	0.68
3.5	3.45	2.67	1.54	0.87	1.68	1.80
4	1.57	1.37	0.43	0.84	0.51	0.68

Table C-4: Growth response of T-039 at all concentrations of As^{III} (0, 0.5, 1.0, 1.5, 2.0, 2.5, 3.0, 3.5, and 4.0 mM) and standard error of the mean (n = 3). Values represent %OD change from starting OD measurement (Day 0).

%OD	1	2	3	5	6	8
0	7.83	11.30	26.85	34.88	38.27	47.29
0.5	0.95	18.74	14.12	13.71	3.06	4.88
1	9.07	17.09	14.00	12.92	4.53	8.44
1.5	1.41	8.63	5.35	5.52	-3.99	0.10
2	5.59	17.20	10.91	12.41	2.40	5.02
2.5	-2.00	13.88	7.54	9.40	-3.04	1.17
3	1.29	14.69	11.56	7.29	-3.39	2.06
3.5	1.58	13.29	5.82	4.79	-4.32	2.07
4	5.00	13.35	7.33	6.81	-3.33	-1.06
	Std. Error					
0	1.02	3.54	2.05	1.73	2.62	1.36
0.5	6.54	5.46	4.39	4.69	2.52	6.25
1	0.64	1.74	0.35	1.18	1.10	0.59
1.5	4.00	4.30	4.47	3.93	4.51	6.51
2	1.82	2.42	2.80	2.00	3.49	2.63
2.5	0.18	0.57	0.27	2.14	3.12	3.15
3	2.15	0.90	0.65	0.89	1.73	2.66
3.5	3.12	2.53	3.08	4.27	5.20	1.65
4	2.65	2.10	1.78	4.05	5.92	2.98

Table C-5: Growth response of T-039 at all concentrations of As^V (0, 0.5, 1.0, 1.5, 2.0, 2.5, 3.0, 3.5, and 4.0 mM) and standard error of the mean (n = 3). Values represent %OD change from starting OD measurement (Day 0).

%OD	1	2	4	5	6	8
0	7.83	11.30	26.85	34.88	38.27	47.29
0.5	4.24	24.13	35.63	36.82	41.71	51.67
1	8.93	19.52	29.09	26.27	31.34	40.79
1.5	8.23	21.71	32.56	31.50	34.99	41.66
2	8.89	18.97	28.69	30.15	31.66	37.30
2.5	3.85	22.91	31.42	30.05	35.96	40.17
3	5.41	24.29	34.39	33.19	36.85	43.79
3.5	9.87	23.17	32.18	33.99	35.07	43.89
4	11.72	24.31	35.44	36.32	40.31	45.19
	Std. Error					
0	1.02	3.54	2.05	1.73	2.62	1.36
0.5	3.40	2.42	1.39	2.51	4.42	3.26
1	1.19	1.76	1.13	1.94	1.26	1.64
1.5	2.62	0.88	0.74	0.95	1.48	2.21
2	5.21	2.92	3.86	3.99	4.23	1.88
2.5	1.56	2.80	2.12	2.56	1.87	3.70
3	4.17	1.13	0.82	0.91	0.88	0.61
3.5	1.22	1.34	3.04	3.46	1.25	1.86
4	2.97	3.18	2.12	2.47	2.18	0.79

Table C-6: Growth response of T-045 at all concentrations of As^{III} (0, 0.5, 1.0, 1.5, 2.0, 2.5, 3.0, 3.5, and 4.0 mM) and standard error of the mean (n = 3). Values represent %OD change from starting OD measurement (Day 0).

%OD	1	2	4	5	6	8
0	16.36	25.74	38.68	45.27	47.95	55.70
0.5	22.60	37.62	52.38	57.85	60.83	67.45
1	19.87	31.88	51.98	58.47	63.09	70.28
1.5	17.69	22.20	28.04	40.58	49.43	60.57
2	11.85	20.49	14.43	13.66	17.91	30.36
2.5	17.90	22.39	17.11	16.40	15.05	19.96
3	16.41	23.58	15.69	15.45	13.12	17.93
3.5	15.47	18.17	9.46	10.11	9.27	14.88
4	14.89	18.67	10.75	9.39	5.08	13.29
	Std. Error					
0	2.17	1.12	0.66	0.31	0.36	0.42
0.5	0.32	0.44	0.26	0.44	0.34	0.12
1	3.20	2.63	1.30	1.63	1.70	1.26
1.5	1.45	0.36	0.35	0.48	0.73	0.43
2	1.96	0.76	2.08	1.91	3.47	3.38
2.5	1.91	3.43	2.92	4.10	1.44	2.54
3	1.80	2.42	3.66	3.49	2.78	2.63
3.5	1.45	1.45	3.56	3.47	2.82	2.81
4	0.53	0.59	0.60	1.52	1.07	0.63

Table C-7: Growth response of T-045 at all concentrations of As^V (0, 0.5, 1.0, 1.5, 2.0, 2.5, 3.0, 3.5, and 4.0 mM) and standard error of the mean (n = 3). Values represent %OD change from starting OD measurement (Day 0).

%OD	1	2	4	5	6	8
0	16.36	25.74	38.68	45.27	47.95	55.70
0.5	23.88	28.02	34.55	34.01	36.59	41.20
1	25.29	30.40	35.35	36.03	36.73	39.10
1.5	26.86	33.61	36.65	36.38	39.65	41.03
2	24.08	29.72	32.10	30.38	34.12	37.53
2.5	25.02	30.51	33.66	33.18	35.25	38.44
3	23.60	32.01	35.34	35.90	39.70	42.45
3.5	24.15	29.77	36.53	38.14	41.16	43.17
4	22.73	30.61	42.42	41.46	44.73	48.63
	Std. Error					
0	2.17	1.12	0.66	0.31	0.36	0.42
0.5	1.98	0.61	0.46	0.66	0.09	1.63
1	2.92	2.51	3.31	3.19	3.95	2.66
1.5	4.87	5.19	3.71	4.81	4.46	4.16
2	1.86	0.84	1.18	1.55	1.34	1.13
2.5	1.23	0.49	0.47	1.22	0.96	0.58
3	1.47	1.22	0.82	0.32	2.14	0.51
3.5	1.20	1.12	1.12	0.49	1.50	0.33
4	1.38	4.11	4.46	5.77	5.09	5.90

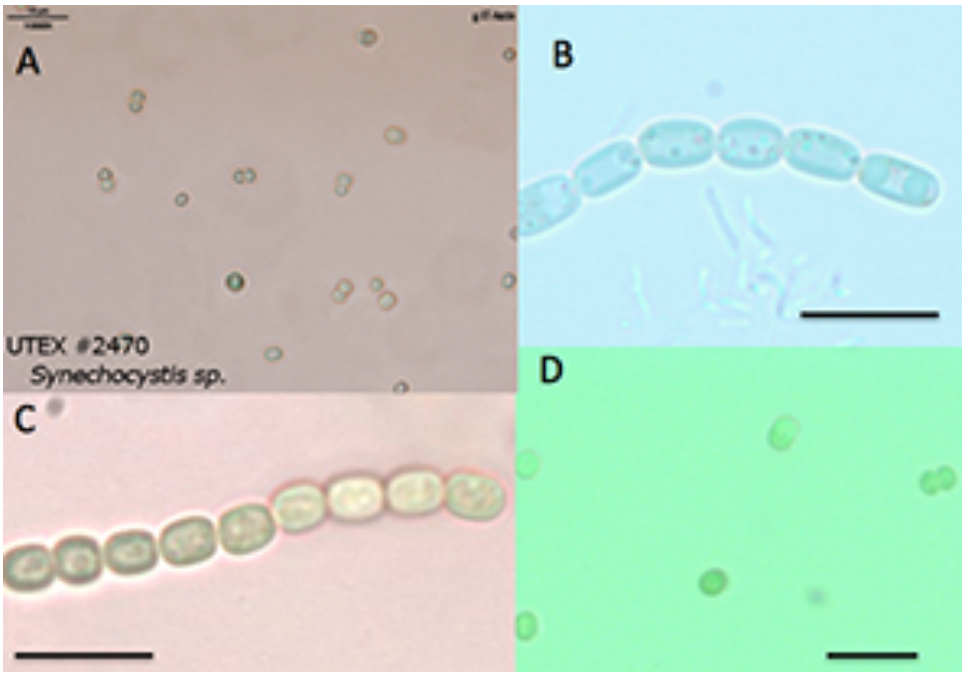

Figure C-2: Morphological comparison of *Synechocystis* sp. UTEX 2470 (A), and cultures T-025 (B), T-039 (C), and T-045 (D), all classified as *Synechocystis* using the 16S rRNA gene sequence. Scale bars in each image are 10 μm.

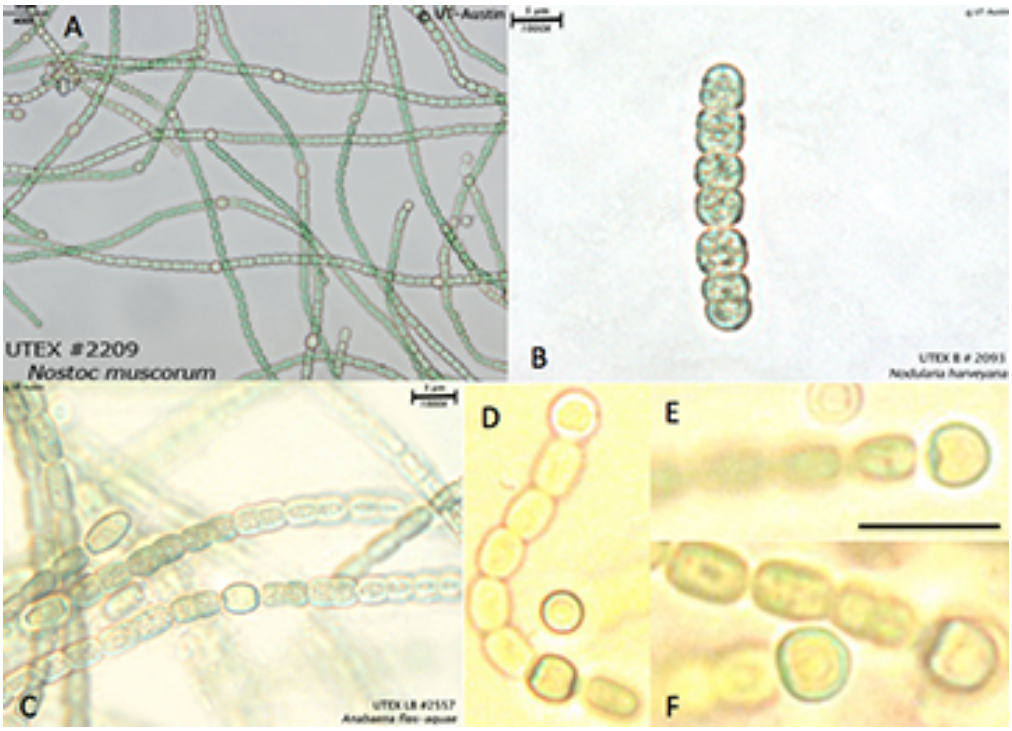

Figure C-3: Images of *Nostoc* at 400X, scale bar 20 µm (A), *Nodularia* at 1000X, scale bar 5 µm (B), and *Anabaena* at 1000X, scale bar 5 µm (C), for morphological comparison to T-031 at 1000X (D, E, F). Scale bar in (E) is 10 µm, (F) is slightly zoomed in relative to (D, E). Images A-C obtained from utex.org.

Table C-8: Strain ID's of organisms used to construct rbcL and hetR trees, along with Genbank accession numbers for rbcL and/or hetR genes for each strain. If an accession number is marked by '-' it indicates that the gene for that organism not used in the reconstruction, or is not possessed by the organism.

Genus sp.	Strain ID	Subsection	Genbank Acc. No. (rbcL)	Genbank Acc. No. (hetR)
Synechocystis sp.	PCC 6803	I	D64000	-
Phormidium persicinum	CCMP 638	III	AB075918	-
Prochlorothrix hollandica		III	X57359	-
Symploca atlantica	PCC 8002	III	AB075921	-
Lyngbya aestuarii	PCC 7419	III	AB075915	-
Trichodesmium erythraem	IMS 101	III	AB075924	AF410432
Pseudanabaena sp.	PCC 7403	III	AB075920	-
Leptolyngbya sp.	PCC 73110	III	AB075914	AF410433
Tolypothrix sp.	CCMP 1185	IV	AB075923	AB075818
Calothrix desertica	PCC 7102	IV	AB075906	AB075807
Calothrix sp.	PCC 7507	IV	-	CP003943
Calothrix sp.	PCC 6303	IV	-	CP003610
Scytonema hofmanni	PCC 7110	IV	AB075921	AB075817
Anabaena sp.	PCC 7120	IV	L02522	-
Anabaena sp.	WH	IV	AB075905	-
Anabaena sp. South India		IV	-	DQ439539
Anabaena cylindrica	PCC 7122	IV	-	CP003659
Anabaena variabilis	ATCC 29413	IV	-	CP000117
Nodularia spumigena	CCY 9414	IV	CP007203	CP007203
Nodularia sp.	KAC 17	IV	AB075917	AB075815
Nodularia sp.	WH	IV	AB075916	-
Nostoc azollae	0708	IV	-	CP002059
Nostoc punctiforme	PCC 73102	IV	CP001037	AF318069
Nostoc sp.	PCC 7524	IV	CP003552	CP003552
Nostoc sp.	PCC 7906	IV	AB075918	AB075816
Nostoc sp.	PCC 7102	IV	-	M37779
Cylindrospermum licheniforme	UTEX 2014	IV	AB075909	AB075810
Cylindrospermum stagnale	PCC 7417	IV	-	CP003642
Cylindrospermum sp.	A 1345	IV	-	DQ439538
Chlorogloeopsis sp.	PCC 9212	V	AB075908	AB075809
Chlorogloeopsis fritschii	PCC 6912	V	AB075907	AB075808
Fischerella muscicola	UTEX 1829	V	AB075910	AB075814
Fischerella muscicola	PCC 73103/ SAG 1427	V	AB075911	AB075811
Fischerella muscicola	PCC 7414	V	AB075912	AB075812
Fischerella thermalis	PCC 7521	V	AB075913	AB075813

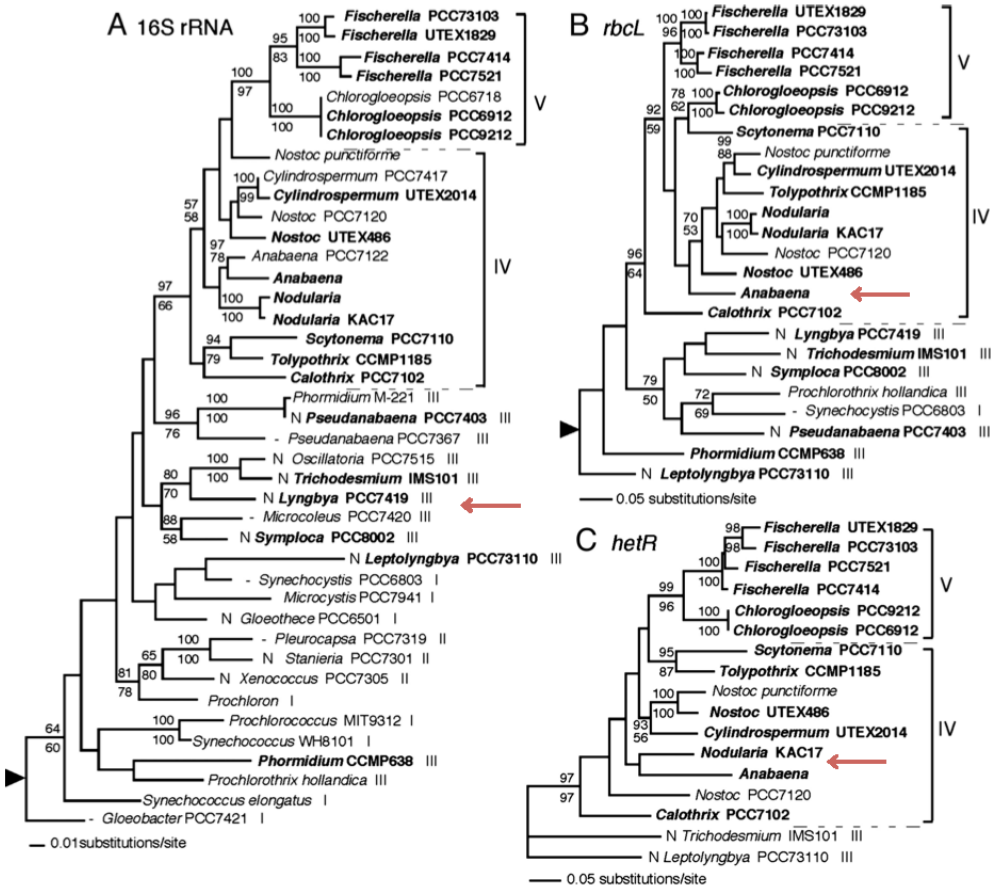

Figure C-4: The phylogenetic relationships of cyanobacteria from Subsections I-V inferred from 16S rRNA (A), *rbcL* (B), and *hetR* (C) using ML methods; the approximate position of T-031 is indicated relative to the reconstruction (modified from Tomitani et al., 2006).

Appendix D

CHAPTER 4 SUPPLEMENT

Figure D-1: Cross-section of a cyanobacterially-based microbial mat at site GG-75m. *In situ* microprofiles of pH and dissolved [O_2] mmol/L were recorded within the top 1 mm of this mat prior to cutting this cross section (Figure 4-2).

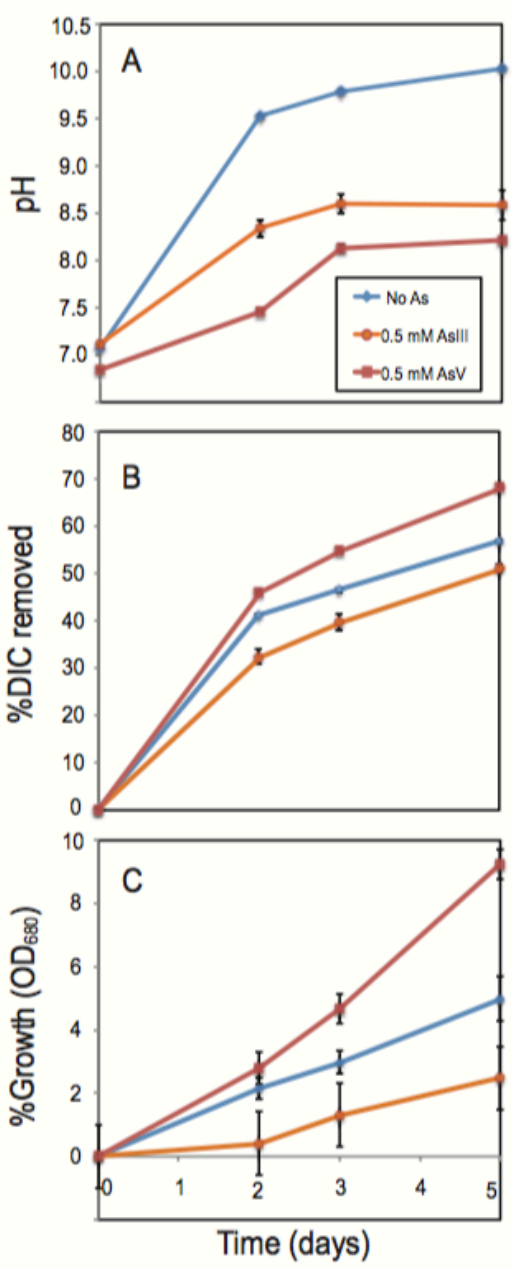

Figure D-2: pH shift (A), DIC-uptake (B), and growth (C) assays were performed on T-031 in drift media amended with 0 mM As (No As), 0.5 mM arsenite (As^{III}), or 0.5 mM arsenate (As^{V}). %DIC is the proportion of DIC removed relative to the initial amount (0.76 mM C), and %OD is the proportion of growth relative to starting conditions, measured by optical density at 680nm. Error bars represent standard error of the mean, and are smaller than the data symbol, where absent (*n = 10*).

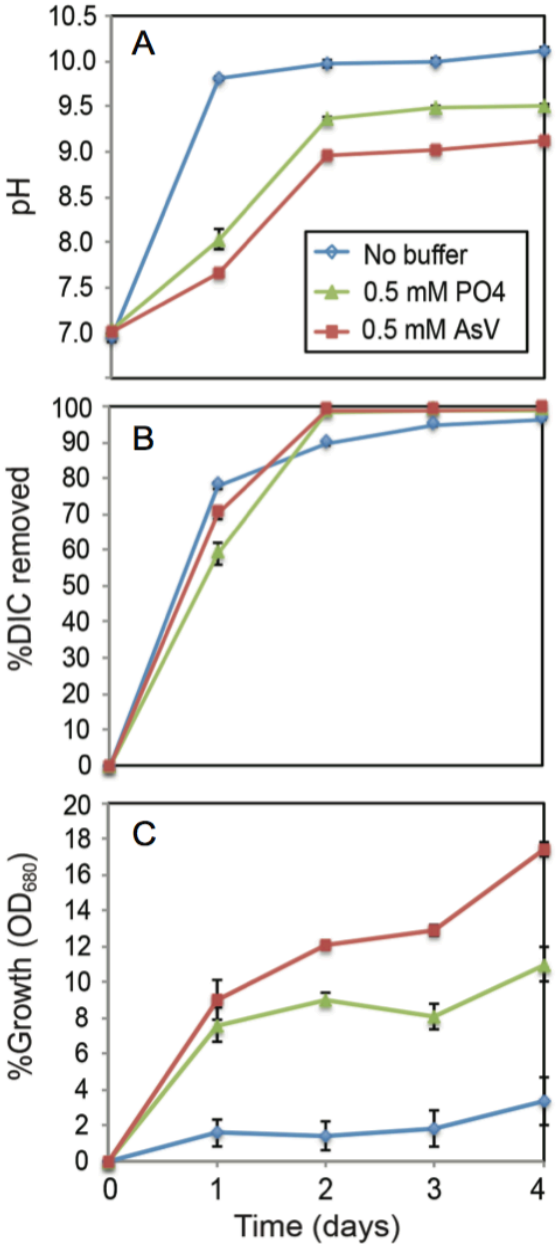

Figure D-3: pH shift (A), DIC-uptake (B), and growth (C) assays were performed on T-031 in drift media amended with no buffer, or buffered by 0.5 mM phosphate (PO_4), or 0.5 mM arsenate (As^V). %DIC is the proportion of DIC removed relative to the initial amount (0.4 mM C), and %OD is the proportion of growth relative to starting conditions, measured by optical density at 680nm. Error bars represent standard error of the mean, and are smaller than the data symbol, where absent (*n = 3*).

Table D-1: Growth response of T-031 at all concentrations of As^{III} (0, 0.5, 1.0, 1.5, 2.0, 2.5, 3.0, 3.5, and 4.0 mM) and standard error of the mean (n = 3). Values represent %OD change from starting OD measurement (Day 0).

%OD	1	2	4	5	8
0	3.70	10.13	35.21	40.04	37.80
0.5	16.81	17.24	17.02	18.70	16.79
1	13.24	9.03	7.46	3.67	0.48
1.5	14.03	10.03	6.45	6.40	0
2	14.16	13.90	9.34	5.71	1.80
2.5	3.81	5.22	0.15	-0.97	-7.67
3	5.53	8.89	2.65	-0.29	-5.59
3.5	-2.94	-1.69	-11.42	-13.12	-22.04
4	10.90	8.39	9.85	3.90	-0.72
Control*	0.0256	0.018	0.1223	0.0815	0.0645
Std. Error					
0	1.35	1.78	1.01	1.29	1.78
0.5	1.94	0.53	0.93	1.58	2.47
1	1.03	0.79	0.55	0.32	1.44
1.5	0.78	1.55	0.73	1.17	2.19
2	1.23	2.12	0.73	0.86	0.94
2.5	1.87	1.59	1.28	2.60	2.55
3	1.05	1.67	0.57	1.28	1.40
3.5	2.34	4.38	4.06	4.07	5.59
4	1.02	0.83	1.29	1.56	1.65

*Same blank (control) used for both As^{III} and As^{V} treatment groups, and recorded as raw absorbance data.

Table D-2: Growth response of T-031 at all concentrations of As^V (0, 0.5, 1.0, 1.5, 2.0, 2.5, 3.0, 3.5, and 4.0 mM) and standard error of the mean (n = 3). Values represent %OD change from starting OD measurement (Day 0). Blank control values are shown in Table D-1.

%OD	1	2	4	5	8
0	3.70	10.13	35.21	40.04	37.80
0.5	13.82	31.20	40.45	42.58	52.27
1	21.35	34.09	36.53	36.37	43.31
1.5	18.82	31.77	34.29	33.86	40.46
2	16.62	24.70	30.84	29.58	34.90
2.5	25.46	30.52	35.27	36.10	41.98
14.70	5.53	31.48	33.05	32.44	39.71
3.5	-2.94	31.72	36.97	38.02	46.51
4	10.90	23.81	33.29	32.61	42.11
Std. Error					
0	1.35	1.78	1.01	1.29	1.78
0.5	1.07	1.61	0.29	0.47	1.18
1	1.55	1.24	0.84	0.80	0.70
1.5	1.01	1.13	0.13	0.42	0.38
2	0.80	1.76	1.02	0.81	1.25
2.5	1.61	1.35	0.88	1.46	1.44
3	0.89	1.40	1.22	1.92	1.57
3.5	0.51	1.47	0.50	0.60	1.31
4	1.71	1.40	2.12	1.57	2.46

References

Aizawa, K., and Miyachi, S. (1986) Carbonic anhydrase and CO_2 concentrating mechanisms in microalgae and cyanobacteria. *FEMS Microbiology Reviews* **39**: 215-233.

Allewalt, J.P., Bateson, M.M., Revsbech, N.P., Slack, K., and Ward, D.M. (2006) Effect of temperature and light on growth of and photosynthesis by Synechococcus isolates typical of those predominating in the octopus spring microbial mat community of Yellowstone National Park. *Applied and Environmental Microbiology* **72**: 544-550.

Alsina, M.A., Zanella, L., Hoel, C., Pizarro, G.E., Gaillard, J.-F., and Pasten, P.A. (2013) Arsenic speciation in sinter mineralization from a hydrothermal channel of El Tatio geothermal field, Chile. *Journal of Hydrology* **in press**.

Altschul, S.F., Gish, W., Miller, W., Myers, E.W., and Lipman, D.J. (1990) Basic Local Alignment Search Tool. *Journal of Molecular Biology* **215**: 403-410.

Amend, J.P., and Shock, E.L. (2001) Energetics of overall metabolic reactions of thermophilic and hyperthermophilic Archaea and Bacteria. *FEMS Microbiology Reviews* **25**: 175-243.

Amend, J.P., Rogers, K.L., Shock, E.L., Gurrieri, S., and Inguaggiato, S. (2003) Energetics of chemolithoautotrophy in the hydrothermal system of Vulcano Island, southern Italy. *Geobiology* **1**: 37-58.

Awramik, S.M., Schopf, J.W., and Walter, M.R. (1983) Filamentous fossil bacteria from the Archean of Western Australia. *Precambrian Research* **20**: 357-374.

Aziz, R.K., Bartels, D., Best, A.A., DeJongh, M., Disz, T., Edwards, R.A. et al. (2008) The RAST Server: rapid annotations using subsystems technology. *BMC Genomics* **9**: 75.

Azov, Y. (1982) Effect of pH on inorganic carbon uptake in algal cultures. *Applied and Environmental Microbiology* **43**: 1300-1306.

Badger, M.R. (1980) Kinetic properties of ribulose 1,5-bisphosphate carboxylase/oxygenase from Anabaena variabilis. *Archives of Biochemistry and Biophysics* **201**: 247-254.

Badger, M.R., and Price, G.D. (1992) The CO_2 concentrating mechanism in cyanobacteria and microalgae. *Physiologia Plantarum* **84**: 606-615.

Badger, M.R., and Price, G.D. (1994) The role of carbonic anhydrase in photosynthesis. *Annual Review of Plant Physiology and Plant Molecular Biology* **45**: 369-392.

Badger, M.R., and Price, G.D. (2003) CO_2 concentrating mechanisms in cyanobacteria: molecular components, their diversity and evolution. *Journal of Experimental Botany* **54**: 609-622.

Badger, M.R., Hanson, D., and Price, G.D. (2002) Evolution and diversity of CO_2 concentrating mechanisms in cyanobacteria. *Functional Plant Biology* **29**: 161-173.

Badger, M.R., Price, G.D., Long, B.M., and Woodger, F.J. (2006) The environmental plasticity and ecological genomics of the cyanobacterial CO_2 concentrating mechanism. *Journal of Experimental Botany* **57**: 249-265.

Ballantyne, J.M., and Moore, J.N. (1988) Arsenic geochemistry in geothermal systems. *Geochimica et Cosmochimica Acta* **52**: 475-483.

Baross, J.A., and Hoffman, S.E. (1985) Submarine hydrothermal vents and associated gradient environments as sites for the origin and evolution of life. *Origins of Life* **15**: 327-345.

Baross, J.A., Lilley, M.D., and Gordon, L.I. (1982) Is the CH_4, H_2 and CO venting from submarine hydrothermal systems produced by thermophilic bacteria? *Nature* **298**: 366-368.

Bazinet, A.L., Zwickl, D.J., and Cummings, M.P. (2014) A gateway for phylogenetic analysis powered by grid computing featuring GARLI 2.0. *Systematic Biology* **63**: 812-818.

Berkner, L.V., and Marshall, L.C. (1965) History of major atmospheric components. *Proceedings of the National Academy of Sciences of the United States of America* **53**: 1215-1226.

Bethke, C.M., Sanford, R.A., Kirk, M.F., Jin, Q., and Flynn, T.M. (2011) The thermodynamic ladder in geomicrobiology. *American Journal of Science* **311**: 183-210.

Bhattacharya, P., and Pal, R. (2010) Response of cyanobacteria to arsenic toxicity. *Journal of Applied Phycology* **23**: 293-299.

Boyd, E.S., Fecteau, K.M., Havig, J.R., Shock, E.L., and Peters, J.W. (2012) Modeling the habitat range of phototrophs in yellowstone national park: toward the development of a comprehensive fitness landscape. *Frontiers in Microbiology* **3**: 221.

Brock, T.D. (1978) Life at high temperatures. *Science* **158**: 1012-1019.

Brocks, J.J. (1999) Archean Molecular Fossils and the Early Rise of Eukaryotes. *Science* **285**: 1033-1036.

Budinoff, C.R., and Hollibaugh, J.T. (2008) Arsenite-dependent photoautotrophy by an Ectothiorhodospira-dominated consortium. *The ISME Journal* **2**: 340-343.

Buick, R. (2008) When did oxygenic photosynthesis evolve? *Philosophical Transactions of the Royal Society of London B Biological Sciences* **363**: 2731-2743.

Canfield, D.E., Rosing, M.T., and Bjerrum, C. (2006) Early anaerobic metabolisms. *Philosophical Transactions of the Royal Society of London B Biological Sciences* **361**: 1819-1836.

Caporaso, J.G., Kuczynski, J., Stombaugh, J., Bittinger, K., Bushman, F.D., Costello, E.K. et al. (2010) QIIME allows analysis of high-throughput community sequencing data. *Nature Methods* **7**: 335-336.

Carrasco, M., Mercado, J.M., and Niell, F.X. (2008) Diversity of inorganic carbon acquisition mechanisms by intact microbial mats of Microcoleus chthonoplastes (Cyanobacteriae, Oscillatoriaceae). *Physiologia Plantarum* **133**: 49-58.

Castenholz, R.W. (1973) The possible photosynthetic use of sulfide by the filamentous phototrophic bacteria of hot springs. *Limnology and Oceanography* **18**: 863-876.

Castenholz, R.W. (2001) Phylum BX. Cyanobacteria. In *Bergey's Manual*.

Cervantes, C., Ji, G., Ramirez, J.J., and Silver, S. (1994) Resistance to arsenic compounds in microorganisms. *FEMS Microbiology Ecology* **15**: 355-367.

Chenna, R. (2003) Multiple sequence alignment with the Clustal series of programs. *Nucleic Acids Research* **31**: 3497-3500.

Clingenpeel, S., Macur, R.E., Kan, J., Inskeep, W.P., Lovalvo, D., Varley, J. et al. (2011) Yellowstone Lake: high-energy geochemistry and rich bacterial diversity. *Environmental Microbiology* **13**: 2172-2185.

Cloud, P. (1965) Significance of the Gunflint (Precambrian) Microflora. *Science* **148**: 27-35.

Connon, S.A., Koski, A.K., Neal, A.L., Wood, S.A., and Magnuson, T.S. (2008) Ecophysiology and geochemistry of microbial arsenic oxidation within a high arsenic, circumneutral hot spring system of the Alvord Desert. *FEMS Microbiology Ecology* **64**: 117-128.

Cortecci, G., Boschetti, T., Mussi, M., Lameli, C.H., Mucchino, C., and Barbieri, M. (2005) New chemical and original isotopic data on waters from El Tatio geothermal field, northern Chile. *Geochemical Journal* **39**: 547-571.

Cox, A., Shock, E.L., and Havig, J.R. (2011) The transition to microbial photosynthesis in hot spring ecosystems. *Chemical Geology* **280**: 344-351.

Cusicanqui, H., Mahon, W.A.J., and Ellis, A.J. (1976) The geochemistry of the El Tatio Geothermal Field, northern Chile. In *Second United Nations Geothermal Symposium Proceedings, Lawrence Berkeley Laboratory*. Univ. of California, Berkeley, CA.

de Silva, S.L. (1989) Altiplano-Puna volcanic complex of the central Andes. *Geology* **17**: 1102-1106.

de Silva, S.L., Self, S., Francis, P.W., Drake, R.E., and Carlos, R.R. (1994) Effusive silicic volcanism in the Central Andes: The Chao dacite and other young lavas of the Altiplano-Puna Volcanic Complex. *Journal of Geophysical Research* **99**: 17805.

Dean, W.E. (1974) Determination of carbonate and organic matter in calcareous sediments and sedimentary rocks by loss on ignition: comparison with other methods. *Journal of Sedimentary Petrology* **44**: 242-248.

Deckert, G., Warren, P.V., Gaasterland, T., Young, W.G., Lenox, A.L., Graham, D.E. et al. (1998) The complete genome of the hyperthermophilic bacterium Aquifex aeolicus. *Nature* **392**: 353-358.

Des Marais, D.J. (1998) Earth's Early Biosphere. *Gravitational and Space Biology Bulletin* **11**: 23-30.

DeSantis, T.Z., Hugenholtz, P., Larsen, N., Rojas, M., Brodie, E.L., Keller, K. et al. (2006) Greengenes, a chimera-checked 16S rRNA gene database and workbench compatible with ARB. *Applied and Environmental Microbiology* **72**: 5069-5072.

Donkor, V., and Hader, D.-P. (1991) Effects of solar and ultraviolet radiation on motility, photomovement, and pigmentation in filamentous gliding cyanobacteria. *FEMS Microbiology Ecology* **86**: 159-168.

Drever, J.I. (1988) *The Geochemistry of Natural Waters*. Engelwood Cliffs, NJ: Prentice-Hall.

Edgar, R.C., Haas, B.J., Clemente, J.C., Quince, C., and Knight, R. (2011) UCHIME improves sensitivity and speed of chimera detection. *Bioinformatics* **27**: 2194-2200.

Edwards, K.J., Rogers, D.R., Wirsen, C.O., and McCollom, T.M. (2003) Isolation and Characterization of Novel Psychrophilic, Neutrophilic, Fe-Oxidizing, Chemolithoautotrophic α- and γ-Proteobacteria from the Deep Sea. *Applied and Environmental Microbiology* **69**: 2906-2913.

Efron, B. (1979) Censored data and the bootstrap. *Journal of the American Statistical Association* **76**: 312-319.

Eisenhut, M., Kahlon, S., Hasse, D., Ewald, R., Lieman-Hurwitz, J., Ogawa, T. et al. (2006) The plant-like C2 glycolate cycle and the bacterial-like glycerate pathway cooperate in phosphoglycolate metabolism in cyanobacteria. *Plant Physiology* **142**: 333-342.

Ellis, A.J., and Mahon, W.A.J. (1964) Natural hydrothermal systems and experimental hot-water/rock interactions. *Geochimica et Cosmochimica Acta* **28**: 1323-1357.

Ellis, A.J., and Mahon, W.A.J. (1967) Natural hydrothermal systems and experimental hot water/rock interactions (Part II). *Geochimica et Cosmochimica Acta* **31**: 519-538.

Ellis, A.J., and Mahon, W.A.J. (1977) *Chemistry and Geothermal Systems*. New York: Academic Press.

Engel, A.S., Johnson, L.R., and Porter, M.L. (2013) Arsenite oxidase gene diversity among Chloroflexi and Proteobacteria from El Tatio Geyser Field, Chile. *FEMS Microbiology Ecology* **83**: 745-756.

Farmer, J.D. (2000) Hydrothermal systems: doorways to early biosphere evolution. *GSA Today* **10**: 1-9.

Felsenstein, J. (1981) Evolutionary trees from DNA sequences: a maximum likelihood approach. *Journal of Molecular Evolution* **17**: 368-376.

Fernandez-Turiel, J.L., Garcia-Valles, M., Gimeno-Torrente, D., Saavedra-Alonso, J., and Martinez-Manent, S. (2005) The hot spring and geyser sinters of El Tatio, Northern Chile. *Sedimentary Geology* **180**: 125-147.

Ferrari, S.G., Silva, P.G., González, D.M., Navoni, J.A., and Silva, H.J. (2013) Arsenic tolerance of cyanobacterial strains with potential use in biotechnology. *Revista Argentina de Microbiología* **45**: 174-179.

Finlay, B.J. (2002) Global dispersal of free-living microbial eukaryote species. *Science* **296**: 1061-1063.

Finsinger, K., Scholz, I., Serrano, A., Morales, S., Uribe-Lorio, L., Mora, M. et al. (2008) Characterization of true-branching cyanobacteria from geothermal sites and hot springs of Costa Rica. *Environmental Microbiology* **10**: 460-473.

Florenzano, G., Sili, C., Pelosi, E., and Vincenzini, M. (1985) Cyanospira rippkae and Cyanospira capsulata (gen. nov. and spp. nov.): new filamentous heterocystous cyanobacteria from Magadi lake (Kenya). *Archives of Microbiology* **140**: 301-306.

Fournier, R.O. (2005) Geochemistry and Dynamics of the Yellowstone National Park Hydrothermal System. In *Geothermal Biology and Geochemistry in Yellowstone National Park*. Inskeep, W.P., and McDermott, T.R. (eds). Bozeman, MT: Thermal Biology Institute, Montana State University, pp. 3-29.

Fournier, R.O., and Potter, R.W. (1982) An equation correlating the solubility of quartz in water from 25 to 900C at pressures up to 10,000 bars. *Geochimica et Cosmochimica Acta* **46**: 1969-1973.

Franks, M.A. (2012) Archaea at the El Tatio Geyser Field: community composition, diversity, and distribution across hydrothermal features and geochemical gradients (Ph.D. Dissertation) The University of Texas at Austin.

Fukuzawa, H., Suzuki, E., Komukai, Y., and Miyachi, S. (1992) A gene homologous to chloroplast carbonic anhydrase (icfA) is essential to photosynthetic carbon dioxide fixation by Synechococcus PCC7942. *Proceedings of the National Academy of Sciences of the United States of America* **89**: 4437-4441.

Garcia-Pichel, F. (1998) Solar ultraviolet and the evolutionary history of cyanobacteria. *Origins of Life and Evolution of the Biosphere* **28**: 321-347.

Garcia-Pichel, F., and Castenholz, R.W. (1990) Comparative anoxygenic photosynthetic capacity in 7 strains of a thermophilic cyanobacterium. *Archives of Microbiology* **153**: 344-351.

Garcia-Pichel, F., and Castenholz, R.W. (1991) Characterization and biological implications of scytonemin, a cyanobacterial sheath pigment. *Journal of Phycology* **27**: 395-409.

Garcia-Valles, M., Fernandez-Turiel, J.L., Gimeno-Torrente, D., Saavedra-Alonso, J., and Martinez-Manent, S. (2008) Mineralogical characterization of silica sinters from the El Tatio geothermal field, Chile. *American Mineralogist* **93**: 1373-1383.

Ghalambor, C.K., McKay, J.K., Carroll, S.P., and Reznick, D.N. (2007) Adaptive versus non-adaptive phenotypic plasticity and the potential for contemporary adaptation in new environments. *Functional Ecology* **21**: 394-407.

Giggenbach, W.F. (1978) The isotopic composition of waters from the El Tatio geothermal field, Northern Chile. *Geochimica et Cosmochimica Acta* **42**: 979-988.

Gihring, T.M., and Banfield, J.F. (2001) Arsenite oxidation and arsenate respiration by a new Thermus isolate. *FEMS Microbiology Letters* **204**: 335-340.

Giordano, M., Beardall, J., and Raven, J.A. (2005) CO_2 concentrating mechanisms in algae: mechanisms, environmental modulation, and evolution. *Annual Review of Plant Biology* **56**: 99-133.

Giovannoni, S.J., Revsbech, N.P., Ward, D.M., and Castenholz, R.W. (1987) Obligately phototrophic Chlororflexus: primary production in anaerobic hot spring microbial mats. *Archives of Microbiology* **147**: 80-87.

Giovannoni, S.J., Turner, S., Olsen, G.J., Barns, S., Lane, D.J., and Pace, N.R. (1988) Evolutionary relationships among cyanobacteria and green chloroplasts. *Journal of Bacteriology* **170**: 3584-3592.

Glennon, J.A., and Pfaff, R.M. (2003) The extraordinary thermal activity of El Tatio Geyser Field, Antofagasta Region, Chile. *The GOSA Transactions* **8**: 31-78.

Goldman, J.C., Dennett, M.R., and Riley, C.B. (1981) Inorganic carbon sources and biomass regulation in intensive microalgal cultures. *Biotechnology and Bioengineering* **23**: 995-1014.

Greenfield, R.E., and Baker, G.C. (1920) Relationship of hydrogen-ion concentration of natural waters to carbon dioxide content. *The Journal of Industrial and Engineering Chemistry* **12**: 989-991.

Haas, B.J., Gevers, D., Earl, A.M., Feldgarden, M., Ward, D.V., Giannoukos, G. et al. (2011) Chimeric 16S rRNA sequence formation and detection in Sanger and 454-pyrosequenced PCR amplicons. *Genome Research* **21**: 494-504.

Hamamura, N., Macur, R.E., Korf, S., Ackerman, G., Taylor, W.P., Kozubal, M. et al. (2009) Linking microbial oxidation of arsenic with detection and phylogenetic analysis of arsenite oxidase genes in diverse geothermal environments. *Environmental Microbiology* **11**: 421-431.

Hamilton, T.L., Vogl, K., Bryant, D.A., Boyd, E.S., and Peters, J.W. (2012) Environmental constraints defining the distribution, composition, and evolution of chlorophototrophs in thermal features of Yellowstone National Park. *Geobiology* **10**: 236-249.

Hasegawa, M., Kishino, H., and Yano, T. (1985) Dating of the Human-Ape splitting by a molecular clock of mitochondrial DNA. *Journal of Molecular Evolution* **22**: 160-174.

Healy, J., and Hochstein, M.P. (1973) Horizontal flow in hydrothermal systems. *Journal of Hydrology (NZ)* **12**: 71-82.

Hedges, S.B. (1992) The number of replications needed for accurate estimation of the Bootstrap P value in phylogenetic studies. *Molecular Biology and Evolution* **9**: 366-369.

Herdman, M., Janvier, M., Rippka, R., and Stanier, R.Y. (1979) Genome size of cyanobacteria. *Journal of General Microbiology* **111**: 73-85.

Hoeft, S.E., Kulp, T.R., Han, S., Lanoil, B., and Oremland, R.S. (2010) Coupled arsenotrophy in a hot spring photosynthetic biofilm at Mono Lake, California. *Applied and Environmental Microbiology* **76**: 4633-4639.

Inskeep, W.P., and McDermott, T.R. (2005) Geomicrobiology of Acid-Sulfate-Chloride Springs in Yellowstone National Park. In *Geothermal Biology and Geochemistry in Yellowstone National Park*. Inskeep, W.P., and McDermott, T.R. (eds). Bozeman, MT: Thermal Biology Institute, Montana State University, pp. 143-162.

Ionescu, D., Hindiyeh, M., Malkawi, H., and Oren, A. (2010) Biogeography of thermophilic cyanobacteria: insights from the Zerka Ma'in hot springs (Jordan). *FEMS Microbiology Ecology* **72**: 103-113.

Jeffery, W.H., Aas, P., Lyons, M.M., Coffin, R.B., Ralph, J.P., and Mitchell, D.L. (1996) Ambient solar radiation-induced photodamage in marine bacterioplankton. *Photochemistry and Photobiology* **64**: 419-427.

Jones, B., and Renaut, R.W. (1997) Formation of silica oncoids around geysers and hot springs at El Tatio, northern Chile. *Sedimentology* **44**: 287-304.

Jorgensen, B., and Nelson, D. (1988) Bacterial zonation, photosynthesis, and spectral light distribution in hot spring microbial mats of Iceland. *Microbial Ecology* **16**: 133-147.

Kaneko, T., Nakamura, Y., Wolk, C.P., Kuritz, T., Sasamoto, S., Watanabe, A. et al. (2001) Complete genomic sequence of the filamentous nitrogen-fixing cyanobacterium Anabaena sp. Strain PCC 7120. *DNA Research* **8**: 205-213.

Kaneko, T., Sako, S., Kotani, H., Tanaka, A., Asamizu, E., Nakamura, Y. et al. (1996) Sequence analysis of the genome of the unicellular cyanobacterium Synechocystis sp. Strain PCC6803. II. Sequence determination of the entire genome and assignment of potential protein-coding regions. *DNA Research* **3**: 109-136.

Kaplan, A., and Reinhold, L. (1999) CO_2 concentrating mechanisms in photosynthetic microorganisms. *Annual Review of Plant Physiology and Plant Molecular Biology* **50**: 539-570.

Kaplan, A., Badger, M.R., and Berry, J.A. (1980) Photosynthesis and the intracellular inorganic carbon pool in the bluegreen alga Anabaena variabilis: response to external CO_2 concentration. *Planta* **149**: 219-226.

Kaplan, A., Schwarz, R., Lieman-Hurwitz, J., Ronen-Tarazi, M., and Reinhold, L. (1994) Physiological and Molecular Studies on the Response of Cyanobacteria to Changes in the Ambient Inorganic Carbon Concentration. In *The Molecular Biology of Cyanobacteria*. Bryant, D.A. (ed): Kluwer Academic Publishers, pp. 469-485.

Kasting, J.F. (1987) Theoretical constraints on oxygen and carbon dioxide concentrations in the Precambrian atmosphere. *Precambrian Research* **34**: 205-229.

Komarek, J. (1976) Taxonomic review of the genera Synechocystis Sauv. 1892, Synechococcus Nag. 1849, and Cyanothece gen. nov. (Cyanophyceae). *Archiv fur Protistenkunde*: 119-179.

Kulp, T.R., Hoeft, S.E., Asao, M., Madigan, M.T., Hollibaugh, J.T., Fisher, J.C. et al. (2008) Arsenic(III) fuels anoxygenic photosynthesis in hot spring biofilms from Mono Lake, California. *Science* **321**: 967-970.

Lahsen, A. (1988) Chilean geothermal resources and their possible utilization. *Geothermics* **17**: 401-410.

Lahsen, A., and Trujillo, P. (1976) El Tatio geothermal field. In *Proceedings of the 2nd United Nations Symposium on Geothermal Fields*. Berkeley, CA: pp. 157-178.

Landrum, J.T. (2007) Fate and Transport of Arsenic and Antimony in the El Tatio Geyser Field, Chile (Masters Thesis) The University of Texas at Austin.

Landrum, J.T., Bennett, P.C., Engel, A.S., Alsina, M.A., Pastén, P.A., and Milliken, K. (2009) Partitioning geochemistry of arsenic and antimony, El Tatio Geyser Field, Chile. *Applied Geochemistry* **24**: 664-676.

Langner, H.W., Jackson, C.R., McDermott, T.R., and Inskeep, W.P. (2001) Rapid oxidation of arsenite in a hot spring ecosystem, Yellowstone National Park. *Environmental Science and Technology* **35**: 3302-3309.

Larkin, M.A., Blackshields, G., Brown, N.P., Chenna, R., McGettigan, P.A., McWilliam, H. et al. (2007) Clustal W and Clustal X version 2.0. *Bioinformatics* **23**: 2947-2948.

Leiva, E.D., Ramila, C., Vargas, I.T., Escauriaza, C.R., Bonilla, C.A., Pizarro, G.E. et al. (2014) Natural attenuation process via microbial oxidation of arsenic in a high Andean watershed. *Science of the Total Environment* **466-467**: 490-502.

Lieutaud, A., van Lis, R., Duval, S., Capowiez, L., Muller, D., Lebrun, R. et al. (2010) Arsenite oxidase from Ralstonia sp. 22: characterization of the enzyme and its interaction with soluble cytochromes. *The Journal of Biological Chemistry* **285**: 20433-20441.

Lindskog, S., and Coleman, J.E. (1973) The catalytic mechanism of carbonic anhydrase. *Proceedings of the National Academy of Sciences of the United States of America* **70**: 2505-2508.

Liu, Z., DeSantis, T.Z., Andersen, G.L., and Knight, R. (2008) Accurate taxonomy assignments from 16S rRNA sequences produced by highly parallel pyrosequencers. *Nucleic Acids Research* **36**: e120.

Lloyd, J.R., and Oremland, R.S. (2006) Microbial transformations of arsenic in the environment: from soda lakes to aquifers. *Elements* **2**: 85-90.

Lopez-Maury, L., Florencio, F.J., and Reyes, J.C. (2003) Arsenic Sensing and Resistance System in the Cyanobacterium Synechocystis sp. Strain PCC 6803. *Journal of Bacteriology* **185**: 5363-5371.

Lowe, D.R. (1983) Restricted shallow-water sedimentation of early Archean stromatolitic and evaporitic strata of the Strelley Pool Chert, Pilbara Block, Western Australia. *Precambrian Research* **19**: 239-283.

Lyra, C., Laamanen, M., Lehtimaki, J.M., Surakka, A., and Sivonen, K. (2005) Benthic cyanobacteria of the genus Nodularia are non-toxic, without gas vacuoles, able to glide and genetically more diverse than planktonic Nodularia. *International Journal of Systematic and Evolutionary Microbiology* **55**: 555-568.

MacArthur, R.H., and Wilson, E.O. (1967) *The Theory of Island Biogeography*. Princeton, New Jersey: Princeton University Press.

Maeda, S., Badger, M.R., and Price, G.D. (2002) Novel gene products associated with NdhD3/D4-containing NDH-1 complexes are involved in photosynthetic CO2 hydration in the cyanobacterium, Synechococcus sp. PCC7942. *Molecular Microbiology* **43**: 425-435.

Maeda, S., Wada, H., Kumeda, K., Onoue, M., Ohki, A., Higashi, S., and Takeshita, T. (1987) Methylation of inorganic arsenic by arsenic-tolerant freshwater algae. *Applied Organometallic Chemistry* **1**: 465-472.

Maidak, B.L., Cole, J.R., Lilburn, T.G., Parker Jr., C.T., Saxman, P.R., Farris, R.J. et al. (2001) The RDP-II (Ribosomal Database Project). *Nucleic Acids Research* **29**: 173-174.

Martiny, J.B., Bohannan, B.J., Brown, J.H., Colwell, R.K., Fuhrman, J.A., Green, J.L. et al. (2006) Microbial biogeography: putting microorganisms on the map. *Nature Reviews Microbiology* **4**: 102-112.

McGinn, P.J., Price, G.D., and Badger, M.R. (2004) High light enhances the expression of low-CO_2-inducible transcripts involved in the CO_2-concentrating mechanisms in Synechocystis sp. PCC6803. *Plant, Cell and Environment* **27**: 615-626.

McGinn, P.J., Price, G.D., Maleszka, R., and Badger, M.R. (2003) Inorganic carbon limitation and light control the expression of transcripts related to the CO_2-concentrating mechanism in the cyanobacterium Synechocystis sp. strain PCC6803. *Plant Physiology* **132**: 218-229.

Miller, S.R. (2007) Diversity of the cosmopolitan thermophile Mastigocladus laminosus at global, regional and local scales. In *Algae and Cyanobacteria in Extreme Environments*. Seckbach, J. (ed): Springer, pp. 399-410.

Miller, S.R., and Castenholz, R.W. (2000) Evolution of thermotolerance in hot spring cyanobacteria of the genus Synechococcus. *Applied and Environmental Microbiology* **66**: 4222-4229.

Miller, S.R., and Bebout, B.M. (2004) Variation in Sulfide Tolerance of Photosystem II in Phylogenetically Diverse Cyanobacteria from Sulfidic Habitats. *Applied and Environmental Microbiology* **70**: 736-744.

Miller, S.R., Castenholz, R.W., and Pedersen, D. (2007) Phylogeography of the thermophilic cyanobacterium Mastigocladus laminosus. *Applied and Environmental Microbiology* **73**: 4751-4759.

Milligan, A.J., and Morel, F.M.M. (2002) A proton buffering role for silica in diatoms. *Science* **297**: 1848-1850.

Moffitt, M.C., Blackburn, S.I., and Neilan, B.A. (2001) rRNA sequences reflect the ecophysiology and define the toxic cyanobacteria of the genus Nodularia. *International Journal of Systematic and Evolutionary Microbiology* **51**: 505-512.

Moro, I., Di Bella, M., Rascio, N., La Rocca, N., and Andreoli, C. (2007) Conferva duplisecta Pollini: rediscovery in Euganean Thermal Springs (Italy) and new assignment to the Oscillatoria genus. *Caryologia* **60**: 133-136.

Mukhopadhyay, R., Rosen, B.P., Pung, L.T., and Silver, S. (2002) Microbial arsenic: from geocycles to genes and enzymes. *FEMS Microbiology Reviews* **26**: 311-325.

Nakamura, K., Kaneko, T., Sato, S., Mimuro, M., Miyashita, H., Tsuchiya, T. et al. (2003) Complete genome structure of Gloeobacter violaceus PCC 7421, a cyanobacterium that lacks thylakoids. *DNA Research* **10**: 137-145.

Nordstrom, D.K., and Archer, D.G. (2003) Arsenic thermodynamic data and environmental geochemistry. In *Arsenic in Groundwater: Geochemistry and Occurrence*. Welch, A.H., and Stollenwerk, K.G. (eds). Boston: Kluwer Academic Publishers, pp. 1-25.

Nordstrom, D.K., Ball, J.W., and McCleskey, R.B. (2005) Ground Water to Surface Water: Chemistry of Thermal Outflows in Yellowstone National Park. In *Geothermal Biology and Geochemistry in Yellowstone National Park*. Inskeep, W.P., and McDermott, T.R. (eds). Bozeman, MT: Thermal Biology Institute, Montana State University, pp. 73-94.

Nubel, U., Garcia-Pichel, F., and Muyzer, G. (1997) PCR primers to amplify 16S rRNA genes from cyanobacteria. *Applied and Environmental Microbiology* **63**: 3327-3332.

Omata, T., Price, G.D., Badger, M.R., Okamura, M., Gohta, S., and Ogawa, T. (1999) Identification of an ATP-binding cassette transporter involved in bicarbonate uptake in the cyanobacterium Synechococcus sp. strain PCC 7942. *Proceedings of the National Academy of Sciences of the United States of America* **96**: 13571-13576.

Oremland, R.S., and Stolz, J.F. (2003) The ecology of arsenic. *Science* **300**: 939-944.

Oremland, R.S., Stolz, J.F., and Hollibaugh, J.T. (2004) The microbial arsenic cycle in Mono Lake, California. *FEMS Microbiology Ecology* **48**: 15-27.

Oremland, R.S., Saltikov, C.W., Wolfe-Simon, F., and Stolz, J.F. (2009) Arsenic in the evolution of earth and extraterrestrial ecosystems. *Geomicrobiology Journal* **26**: 522-536.

Oren, A. (2012) Salts and Brines. In *Ecology of Cyanobacteria II: Their Diversity in Space and Time*. Whitton, B.A. (ed): Springer Science+Business Media, pp. 401-426.

Overbeek, R., Olson, R., Pusch, G.D., Olsen, G.J., Davis, J.J., Disz, T. et al. (2014) The SEED and the Rapid Annotation of microbial genomes using Subsystems Technology (RAST). *Nucleic Acids Research* **42**: D206-214.

Paerl, H. (1996) Microscale physiological and ecological studies of aquatic cyanobacteria: macroscale implications. *Microscopy Research and Technique* **33**: 47-72.

Paerl, H.W., Pinckney, J.L., and Steppe, T.F. (2000) Cyanobacterial-bacterial mat consortia: examining the functional unit of microbial survival and growth in extreme environments. *Environmental Microbiology* **2**: 11-26.

Paez-Espino, D., Tamames, J., de Lorenzo, V., and Canovas, D. (2009) Microbial responses to environmental arsenic. *Biometals* **22**: 117-130.

Palinska, K.A., Liesack, W., Rhiel, E., and Krumbein, W.E. (1996) Phenotype variability of identical genotypes: the need for a combined approach in cyanobacterial taxonomy demonstrated on Merismopedia-like isolates. *Archives of Microbiology* **166**: 224-233.

Papke, R.T., Ramsing, N.B., Bateson, M.M., and Ward, D.M. (2003) Geographical isolation in hot spring cyanobacteria. *Environmental Microbiology* **5**: 650-659.

Phoenix, V.R., Bennett, P.C., Engel, A.S., Tyler, S.W., and Ferris, F.G. (2006) Chilean high-altitude hot-spring sinters: a model system for UV screening mechanisms by early Precambrian cyanobacteria. *Geobiology* **4**: 15-28.

Pierson, B.K., Mitchell, H.K., and Ruff-Roberts, A.L. (1993) Chloroflexus aurantiacus and ultraviolet radiation: implications for Archean shallow-water stromatolites. *Origins of Life and Evolution of the Biosphere* **23**: 243-260.

Price, G.D., Coleman, J.R., and Badger, M.R. (1992) Association of carbonic anhydrase activity with carboxysomes isolated from the cyanobacterium Synechococcus PCC7942. *Plant Physiology* **100**: 784-793.

Price, G.D., Maeda, S., Omata, T., and Badger, M.R. (2002) Modes of active inorganic carbon uptake in the cyanobacterium, Synechococcus sp. PCC7942. *Functional Plant Biology* **29**: 131-149.

Price, G.D., Badger, M.R., Woodger, F.J., and Long, B.M. (2008) Advances in understanding the cyanobacterial CO_2-concentrating-mechanism (CCM): functional components, Ci transporters, diversity, genetic regulation and prospects for engineering into plants. *Journal of Experimental Botany* **59**: 1441-1461.

Price, G.D., Sultemeyer, D., Klughammer, B., Ludwig, M., and Badger, M.R. (1998) The functioning of the CO_2 concentrating mechanism in several cyanobacterial strains: a review of general physiological characteristics, genes, proteins, and recent advances. *Canadian Journal of Botany* **76**: 973-1002.

Price, G.D., Woodger, F.J., Badger, M.R., Howitt, S.M., and Tucker, L. (2004) Identification of a SulP-type bicarbonate transporter in marine cyanobacteria. *Proceedings of the National Academy of Sciences of the United States of America* **101**: 18228-18233.

Purcell, E. (1977) Life at low Reynolds number. *American Journal of Physics* **45**: 3-11.

R Core Team (2013) R: A language and environment for statistical computing. Vienna, Austria: R Foundation for Statistical Computing.

Rambler, M.B., and Margulis, L. (1980) Bacterial resistance to ultraviolet irradiation under anaerobiosis: implications for pre-Phanerozoic evolution. *Science* **210**: 638-640.

Rasmussen, B. (2000) Filamentous microfossils in a 3,235-million-year-old volcanogenic massive sulphide deposit. *Nature* **405**: 676-679.

Raven, J.A. (2003) Inorganic carbon concentrating mechanisms in relation to the biology of algae. *Photosynthesis Research* **77**: 155-171.

Raven, J.A. (2012) Carbon. In *The Ecology of Cyanobacteria II: Their Diversity in Time and Space*. Whitton, B.A. (ed). New York, NY: Springer Science+Business Media, pp. 443-460.

Reumann, S., and Weber, A.P. (2006) Plant peroxisomes respire in the light: some gaps of the photorespiratory C2 cycle have become filled--others remain. *Biochimica et Biophysica Acta* **1763**: 1496-1510.

Revsbech, N., and Ward, D. (1984) Microelectrode studies of interstitial water chemistry and photosynthetic activity in a hot spring microbial mat. *Applied and Environmental Microbiology* **48**: 270-275.

Reysenbach, A.L., and Cady, S.L. (2001) Microbiology of ancient and modern hydrothermal systems. *TRENDS in Microbiology* **9**: 79-86.

Reysenbach, A.L., and Shock, E.L. (2002) Merging genomes with geochemistry in hydrothermal ecosystems. *Science* **296**: 1077-1082.

Reysenbach, A.L., Longnecker, K., and Kirshtein, J. (2000) Novel Bacterial and Archaeal lineages from an in situ growth chamber deployed at a Mid-Atlantic Ridge hydrothermal vent. *Applied and Environmental Microbiology* **66**: 3798-3806.

Reysenbach, A.L., Gotz, D., Banta, A., Jeanthon, C., and Fouquet, Y. (2002) Expanding the distribution of the Aquificales to the deep-sea vents on Mid-Atlantic Ridge and Central Indian Ridge. *Cahiers de Biologie Marine* **43**: 425-428.

Rippka, R., Deruelles, J., Waterbury, J.B., Herdman, M., and Stainer, R.Y. (1979) Generic assignments, strain histories and properties of pure cultures of cyanobacteria. *Journal of General Microbiology* **111**: 1-61.

Rodgers, K.A., Greatrex, R., Hyland, M., Simmons, S.F., and Browne, P.R.L. (2002) A modern evaporitic occurrence of teruggite, $Ca_4MgB_{12}As_2O_{28}$.18H2O, and nobleite,

CaB_6O_{10}.4H2O, from the El Tatio geothermal field, Antofagasta Province, Chile. *Mineralogical Magazine* **66**: 253-259.

Roeselers, G., Norris, T.B., Castenholz, R.W., Rysgaard, S., Glud, R.N., Kuhl, M., and Muyzer, G. (2007) Diversity of phototrophic bacteria in microbial mats from Arctic hot springs (Greenland). *Environmental Microbiology* **9**: 26-38.

Romero, L., Alonso, H., Campano, P., Fanfani, L., Cidu, R., Dadea, C. et al. (2003) Arsenic enrichment in waters and sediments of the Rio Loa (Second Region, Chile). *Applied Geochemistry* **18**: 1399-1416.

Schirrmeister, B.E., Antonelli, A., and Bagheri, H.C. (2011) The origin of multicellularity in cyanobacteria. *BMC Evolutionary Biology* **11**: 45.

Shibata, M., Ohkawa, H., Katoh, H., Shimoyama, M., and Ogawa, T. (2002) Two CO_2 uptake systems in cyanobacteria: four systems for inorganic carbon acquisition in Synechocystis sp. strain PCC6803. *Functional Plant Biology* **29**: 123-129.

Silver, S., and Phung, L.T. (2005) Genes and enzymes involved in bacterial oxidation and reduction of inorganic arsenic. *Applied and Environmental Microbiology* **71**: 599-608.

Smedley, P.L., and Kinniburgh, D.G. (2002) A review of the source, behaviour and distribution of arsenic in natural waters. *Applied Geochemistry* **17**: 517-568.

Sompong, U., Hawkins, P.R., Besley, C., and Peerapornpisal, Y. (2005) The distribution of cyanobacteria across physical and chemical gradients in hot springs in northern Thailand. *FEMS Microbiology Ecology* **52**: 365-376.

Stal, L. (2012) Cyanobacterial Mats and Stromatolites. In *Ecology of Cyanobacteria II: Their Diversity in Space and Time*. Whitton, B.A. (ed): Springer Science+Business Media, pp. 65-125.

Stal, L.J., van Gemerden, H., and Krumbein, W.E. (1985) Structure and development of a benthic marine microbial mat. *FEMS Microbiology Ecology* **31**: 111-125.

Stanier, R.Y., Kunisawa, R., Mandel, M., and Cohen-Bazire, G. (1971) Purification and properties of unicellular blue-green algae (Order Chroococcales). *Bacteriological Reviews* **35**: 171-205.

Stauffer, R.E., and Thompson, J.M. (1984) Arsenic and antimony in geothermal waters of Yellowstone National Park, Wyoming, USA. *Geochimica et Cosmochimica Acta* **48**: 2547-2561.

Stauffer, R.E., Jenne, E.A., and Ball, J.W. (1980) Chemical studies of selected trace elements in hot-spring drainages of Yellowstone National Park. In. United States Department of the Interior, G.S. (ed). Washington: United States Government Printing Office, pp. 1-20.

Tajima, N., Sato, S., Maruyama, F., Kaneko, T., Sasaki, N.V., Kurokawa, K. et al. (2011) Genomic structure of the cyanobacterium Synechocystis sp. PCC 6803 strain GT-S. *DNA Research* **18**: 393-399.

Tassi, F., Martinez, C., Vaselli, O., Capaccioni, B., and Viramonte, J. (2005) Light hydrocarbons as redox and temperature indicators in the geothermal field of El Tatio (northern Chile). *Applied Geochemistry* **20**: 2049-2062.

Tassi, F., Aguilera, F., Darrah, T., Vaselli, O., Capaccioni, B., Poreda, R.J., and Delgado Huertas, A. (2010) Fluid geochemistry of hydrothermal systems in the Arica-Parinacota, Tarapacá and Antofagasta regions (northern Chile). *Journal of Volcanology and Geothermal Research* **192**: 1-15.

Taton, A., Grubisic, S., Brambilla, E., De Wit, R., and Wilmotte, A. (2003) Cyanobacterial Diversity in Natural and Artificial Microbial Mats of Lake Fryxell (McMurdo Dry Valleys, Antarctica): a Morphological and Molecular Approach. *Applied and Environmental Microbiology* **69**: 5157-5169.

Taton, A., Grubisic, S., Balthasart, P., Hodgson, D.A., Laybourn-Parry, J., and Wilmotte, A. (2006) Biogeographical distribution and ecological ranges of benthic cyanobacteria in East Antarctic lakes. *FEMS Microbiology Ecology* **57**: 272-289.

Templeton, A.S. (2011) Geomicrobiology of Iron in Extreme Environments. *Elements* **7**: 95-100.

Thiel, T. (1988) Phosphate transport and arsenate resistance in the cyanobacterium Anabaena variabilis. *Journal of Bacteriology* **170**: 1143-1147.

Thompson, J.M. (1979) Arsenic and fluoride in the Upper Madison River System: Firehole and Gibbon Rivers and Their Tributaries, Yellowstone National Park, Wyoming, and Southeast Montana. *Environmental Geology* **3**: 13-21.

Tomitani, A., Knoll, A.H., Cavanaugh, C.M., and Ohno, T. (2006) The evolutionary diversification of cyanobacteria: molecular-phylogenetic and paleontological perspectives. *Proceedings of the National Academy of Sciences of the United States of America* **103**: 5442-5447.

Turner, S., Pryer, K.M., Miao, V.P.W., and Palmer, J.D. (1999) Investigating deep phylogenetic relationships among Cyanobacteria and Plastids by small subunit rRNA sequence analysis. *Journal of Eukaryotic Microbiology* **46**: 327-338.

van der Leun, J.C., and de Gruijl, F.R. (1993) Influences of ozone depletion on human and animal health. In *UV-B radiation and ozone depletion: Effects on humans, animals, plants, microorganisms, and materials*. Tevini, M. (ed). Ann Arbor, MI: Lewis Publishers.

van der Meer, M.T., Schouten, S., de Leeuw, J.W., and Ward, D.M. (2000) Autotrophy of green non-sulphur bacteria in hot spring microbial mats: biological explanations for isotopically heavy organic carbon in the geological record. *Environmental Microbiology* **2**: 428-435.

Waddell, P.J., and Steel, M.A. (1997) General time-reversible distances with unequal rates across sites: mixing gamma and inverse Gaussian distributions with invariant sites. *Molecular Phylogenetics and Evolution* **8**: 398-414.

Walker, J.C.G., Klein, C., Schidlowski, M., Schopf, J.W., Stevenson, D.J., and Walter, M.R. (1983) Environmental evolution of the Archean-Early Proterozoic earth. In *Earth's earliest biosphere: Its origin and evolution*. Princeton, NJ: Princeton University Press, pp. 260-290.

Walter, M.R. (1983) Archean stromatolites: evidence of the Earth's earliest benthos. In *Earth's earliest biosphere: Its origin and evolution*. Schopf, J.W. (ed). Princeton, NJ: Princeton University Press, pp. 187-213.

Wang, Q., Garrity, G.M., Tiedje, J.M., and Cole, J.R. (2007) Naive Bayesian classifier for rapid assignment of rRNA sequences into the new bacterial taxonomy. *Applied and Environmental Microbiology* **73**: 5261-5267.

Wang, S., Zhang, D., and Pan, X. (2012) Effects of arsenic on growth and photosystem II (PSII) activity of Microcystis aeruginosa. *Ecotoxicology and Environmental Safety* **84**: 104-111.

Ward, D.M., and Castenholz, R.W. (2000) Cyanobacteria in Geothermal Habitats. In *The Ecology of Cyanobacteria*. Whitton, B.A., and Potts, M. (eds). Netherlands: Kluwer Academic Publishers, pp. 37-59.

Ward, D.M., and Cohan, F.M. (2005) Microbial Diversity in Hot Spring Cyanobacterial Mats: Pattern and Prediction. In *Geothermal Biology and Geochemistry in Yellowstone National Park*. Inskeep, W.P., and McDermott, T.R. (eds). Bozeman, MT: Montana State University Publications, pp. 185-201.

Ward, D.M., Castenholz, R.W., and Miller, S.R. (2012) Cyanobacteria in Geothermal Habitats. In *Ecology of Cyanobacteria II: Their Diversity in Space and Time*. Whitton, B.A. (ed): Springer Science + Business Media, pp. 39-63.

Ward, D.M., Ferris, M.J., Nold, S.C., and Bateson, M.M. (1998) A natural view of microbial biodiversity within hot spring cyanobacterial mat communities. *Microbiology and Molecular Biology Reviews* **62**: 1353-1370.

Webster, J., and Nordstrom, D. (2003) Geothermal arsenic. In *Arsenic in Ground Water: Geochemistry and Occurence* Welch, A.H., and Stollenwerk, K.G. (eds). Boston: Kluwer Academic Publishers, pp. 101-126.

Webster-Brown, J.G. (2000) Chemical contaminants and their effects. In *World Geothermal Congress*. Kizuno, Japan.

Weisburg, W.G., Barns, S.M., Pelletier, D.A., and Lane, D.J. (1991) 16S ribosomal DNA amplification for phylogenetic study. *Journal of Bacteriology* **173**: 697-703.

Whitton, B.A. (2012) *Ecology of Cyanobacteria II: Their Diversity in Space and Time*: Springer.

Whitton, B.A., and Potts, M. (2000) Introduction to the Cyanobacteria. In *The Ecology of Cyanobacteria: Their Diversity in Time and Space*. Whitton, B.A., and Potts, M. (eds). Dordrecht, Netherlands: Kluwer Academic Publishers, pp. 1-11.

Widdel (1993) Ferrous iron oxidation by anoxygenic phototrophic bacteria. *Nature* **362**: 835-836.

Wilmotte, A. (1994) Molecular evolution and taxonomy of the Cyanobacteria. In *The Molecular Biology of Cyanobacteria*. Bryant, D.A. (ed). Dordrecht, Netherlands: Springer Science + Business Media, pp. 1-25.

Woese, C.R. (1987) Bacterial evolution. *Microbiological Reviews* **51**: 221-271.

Wolery, T.J., and Sleep, N.H. (1976) Hydrothermal circulation and geochemical flux at mid-ocean ridges. *The Journal of Geology* **84**: 249-275.

Woodger, F.J., Badger, M.R., and Price, G.D. (2003) Inorganic carbon limitation induces transcripts encoding components of the CO_2-concentrating mechanism in Synechococcus sp. PCC7942 through a redox-independent pathway. *Plant Physiology* **133**: 2069-2080.

Yin, X.X., Chen, J., Qin, J., Sun, G.X., Rosen, B.P., and Zhu, Y.G. (2011) Biotransformation and volatilization of arsenic by three photosynthetic cyanobacteria. *Plant Physiology* **156**: 1631-1638.

Yu, J., Price, G.D., Song, L., and Badger, M.R. (1992) Isolation of a putative carboxysomal carbonic anhydrase gene from the cyanobacterium Synechococcus PCC7942. *Plant Physiology* **100**: 794-800.

Zhang, P., Battchikova, N., Jansen, T., Appel, J., Ogawa, T., and Aro, E.M. (2004) Expression and functional roles of the two distinct NDH-1 complexes and the carbon acquisition complex NdhD3/NdhF3/CupA/Sll1735 in Synechocystis sp PCC 6803. *The Plant Cell* **16**: 3326-3340.

Zwickl, D.J. (2006) Genetic algorithm approaches for the phylogenetic analysis of large biological datasets under the maximum likelihood criterion (Ph.D. Dissertation) The University of Texas at Austin.

Vita

Kimberly Dawn Myers spent her early childhood exploring the outdoors and fostering a lifelong passion for nature and biology. When young Kimberly spent countless hours perusing her parents' college texts on anthropology, chemistry, and zoology. For her mother and father the texts were merely artifacts from a previous stage in their lives, but for Kimberly they spurred an insatiable interest in life sciences.

She loved school, especially writing, science, and art, but never experienced any success or enjoyment from math. During the later stages of high school this frustration led her to shy away from calculus and physics and to take more art classes. When she received recognition for her painting skills she decided to leave science behind. Kimberly went to Cornell University in 2003 to pursue an undergraduate degree in fine arts. She reveled in painting, life drawing, printmaking, and above all the meditative darkroom of the photography studio. By her second year she had amassed a developing portfolio, but she no longer felt challenged by art and decided to pursue a degree in biology. On her first visit to the undergraduate biology program office she walked in with a solid plan of attack to fulfill the degree requirements. The office staff all but laughed and told her it would never work out. She graduated three years later with a Bachelor's Degree in ecology and evolutionary biology.

During her final year at Cornell she attended a lecture by the famous biologist Dr. Lynn Margulis, who talked about the wisdom of the marriage of biology and geoscience. Greatly inspired, Kimberly accepted an invitation to the Jackson School of Geosciences graduate program, where she began working towards a Ph.D. in geomicrobiology and aqueous geochemistry in August 2008. Kimberly was awarded an NSF postdoctoral fellowship and will continue to pursue her interests in microbiology and geochemistry on completing her graduate studies in 2015.

Permanent email address: myers.kd@gmail.com

This dissertation was typed by Kimberly Dawn Myers.